ARMY RESEARCH LABORATORY

Measurement of Pressure From Explosives in a Closed Chamber and the Free Field

Richard D. Dick
John D. Williams
Xiang Jun Wang
UNIVERSITY OF MARYLAND

Chapman Young III
SUNBURST RECOVERY, INC.

ARL-CR-309 October 1996

prepared by

University of Maryland
Department of Mechanical Engineering
College Park, MD 20742

under contracts

19961031 045

DAAD05-89-M-L426
and
DAAA15-89-C-0031

NOTICES

Destroy this report when it is no longer needed. DO NOT return it to the originator.

Additional copies of this report may be obtained from the National Technical Information Service, U.S. Department of Commerce, 5285 Port Royal Road, Springfield, VA 22161.

The findings of this report are not to be construed as an official Department of the Army position, unless so designated by other authorized documents.

The use of trade names or manufacturers' names in this report does not constitute indorsement of any commercial product.

REPORT DOCUMENTATION PAGE

Form Approved
OMB No. 0704-0188

1. AGENCY USE ONLY *(Leave blank)*	2. REPORT DATE	3. REPORT TYPE AND DATES COVERED
	October 1996	Final, Jul 89 - Dec 91

4. TITLE AND SUBTITLE
Measurement of Pressure From Explosives in a Closed Chamber and the Free Field

5. FUNDING NUMBERS
C: DAAD05-89-M-L426
C: DAAA15-89-C-0031

6. AUTHOR(S)
Richard D. Dick, John D. Williams, Xiang Jun Wang, and Chapman Young III*

7. PERFORMING ORGANIZATION NAME(S) AND ADDRESS(ES)
University of Maryland
Department of Mechanical Engineering
College Park, MD 20742

*Sunburst Recovery, Inc.
Steamboat Springs, CO 80477

8. PERFORMING ORGANIZATION REPORT NUMBER
01-5-28541
01-5-28546

9. SPONSORING/MONITORING AGENCY NAMES(S) AND ADDRESS(ES)
U.S. Army Research Laboratory
ATTN: AMSRL-WT-TB
Aberdeen Proving Ground, MD 21005-5066

10.SPONSORING/MONITORING AGENCY REPORT NUMBER
ARL-CR-309

11. SUPPLEMENTARY NOTES
Technical monitor was Richard Lottero, U.S. Army Research Laboratory.

12a. DISTRIBUTION/AVAILABILITY STATEMENT
Approved for public release; distribution is unlimited.

12b. DISTRIBUTION CODE

13. ABSTRACT *(Maximum 200 words)*

The reflected blast overpressures in a closed vessel and stagnation blast overpressures in the free field environment were measured for Composition B (Comp B), LX-14, and Pentolite in three sets of experiments. In the first set of tests the reflected pressures were measured in a 64:1 chamber volume-to-explosive volume ratio for these explosives in nominally 10-g sizes. A second set of tests consisted of measuring the reflected pressures in a 40:1 volume ratio chamber for nominally 15-g Comp B and LX-14 explosive charges. For the final set of measurements, the stagnation pressures were recorded for Comp B and LX-14, nominally 900-g sizes in a series of free field experiments conducted in the Colorado School of Mines Experimental Mine at Idaho Springs, CO. The bar pressure gage was the primary sensor/transducer combination for performing the measurements for both the closed chamber tests and the free field tests. For the closed vessel tests the bar gages were positioned to measure pressure at the wall of the chamber at several locations relative to the center of the explosive, which also was at the center of the vessel. The bar gages for the free field tests were located around the charge at distances determined by cube root scaling of the explosive weight to the vessel test geometry. Measured blast pressures were compared with those predicted using the JWL equation of state and the HULL hydrocode. Reasonable correspondence was found among the various gage locations and the measured and predicted blast pressures.

14. SUBJECT TERMS
blast, reflected pressure, stagnation pressure, explosives

15. NUMBER OF PAGES
235

16. PRICE CODE

17. SECURITY CLASSIFICATION OF REPORT	18. SECURITY CLASSIFICATION OF THIS PAGE	19. SECURITY CLASSIFICATION OF ABSTRACT	20. LIMITATION OF ABSTRACT
UNCLASSIFIED	UNCLASSIFIED	UNCLASSIFIED	UL

INTENTIONALLY LEFT BLANK.

PREFACE

The U.S. Army Ballistic Research Laboratory was deactivated on 30 September 1992 and subsequently became a part of the U.S. Army Research Laboratory (ARL) on 1 October 1992.

INTENTIONALLY LEFT BLANK.

TABLE OF CONTENTS

INTENTIONALLY LEFT BLANK.

LIST OF FIGURES

LIST OF TABLES

INTENTIONALLY LEFT BLANK.

SUMMARY

The reflected blast overpressures in a closed vessel and stagnation blast overpressures in the free field environment were measured for Composition B, LX-14, and Pentolite in three sets of experiments. In the first set of tests the reflected pressures were measured in a 64:1 chamber volume-to-explosive volume ratio for Composition B, LX-14, and Pentolite in nominally 10 g sizes. A second set of tests consisted of measuring the reflected pressures in a 40:1 volume ratio chamber for nominally 15 g Composition B and LX-14 explosive charges. For the final set of measurements, the stagnation pressures were recorded for Composition B and LX-14, nominally 900 g sizes in a series of free field experiments conducted in the Colorado School of Mines Experimental Mine at Idaho Springs, Colorado. The bar pressure gage was the primary sensor/transducer combination for performing the measurements for both the closed chamber tests and the free field tests. For the closed vessel tests the bar gages were positioned to measure pressure at the wall of the chamber at several locations relative to the center of the explosive, which also was at the center of the vessel. The bar gages for the free field tests were located around the charge at distances determined by scaling (cube root scaling of the explosive weight) to the vessel test geometry. Measured peak reflected pressures for the 10 g charges in the 64:1 ratio vessel at explosive center of gravity (station 36) are: (1) Comp B, 283 MPa, (2) LX-14, 485 MPa and compared to 492 MPa calculated from the JWL explosive equation-of-state for LX-14 and the HULL code, and (3) Pentolite, 324 MPa. For the 15 g charges in the 40:1 volume ratio, the reflected pressures are: (1) Comp B, 725 MPa and (2) LX-14, 658 MPa. Average stagnation pressures from the free field measurements for Comp B was 450 MPa at the charge center (station 136) and for LX-14 was 500 MPa also at station 136. Station 136 scales to the 64:1 chamber distances between the vessel wall and the charge surface at station 36. Average stagnation pressures from station 236 for Comp B was 500 MPa where station 236 corresponds to station 36 in the 40:1 vessel. Thus, there is

reasonable correspondence among the various gage locations and the blast pressure.

1. INTRODUCTION

1.1 Research Objectives. The purpose was to provide data to the US Army Ballistic Research Laboratory (BRL) for their study to assess the blast loading at close range on light armored vehicles. This was accomplished by measuring close-in blast overpressures in a closed chamber from small scale explosives in laboratory experiments at the University of Maryland, College Park, MD. In addition close-in blast pressures were measured in the free field from large size explosives. The explosives of interest were Pentolite, Composition B (Comp B), and LX-14, all military explosives.

1.2 Approach. A diagram of the simulation (Lottero and Wortman, 1988) for determining the blast loading by measuring the overpressure is shown in Figure 1. The experiment consists of a mass of condensed military explosive in the shape of a right circular cylinder at a standoff, S, above a plate. The explosive is initiated at the top center as indicated. The plate is assumed rigid so the armor plate does not move. In the work reported here, the experimental approach is based on the above simulation in which the overpressure is the reflected pressure at the explosive gas/plate interface. That is, the reflected blast pressure is measured at several close-in standoff distances inside a vessel from small scale charges. In addition the stagnation blast pressure is measured at a few close-in standoff distances from larger unconfined explosives. The reflected pressures were measured in the closed chamber tests primarily by bar gages. The small scale explosives had masses nominally 10 g and 15 g and had a cylindrical shape with a diameter-to-height ratio of one. All the small scale test charges were supplied by the (BRL). For the tests using the 10 g charges the volume of undetonated explosive to the volume of the confinement vessel was 64:1 and 40:1 for the tests using 15 g charges. The overpressures were measured on the interior of the confining vessel as a

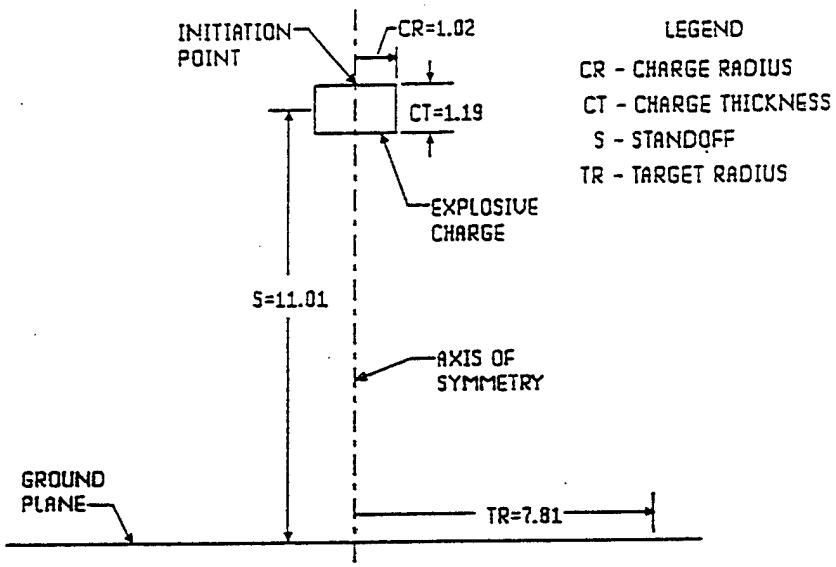

Figure 1. Diagram of blast loading simulation.

function of time at various locations relative to the center of the explosive. The 10 g explosives included Pentolite, Comp B, and LX-14. A few tests were performed using DuPont Detasheet to prove out the experimental system. Comp B and LX-14 were the explosives of interest for the 15 g charges.

In the free field experiments the stagnation blast pressure was measured after detonating the Comp B and LX-14 charges. The nominal mass of each charge was 900 g which were also supplied by BRL. The larger scale explosives were scaled from the charges used for the closed vessel tests. These explosives were also cylindrical in shape with a diameter-to-height ratio of one and were not confined when detonated. The pressure measurement positions were scaled to match the locations for the small scale experiments by means of bar gages positioned around the charges. Because of the size of the explosive the tests were conducted in the Colorado School of Mines Experimental Mine at Idaho Springs, CO.

2. GENERAL DISCUSSION

2.1 HULL Calculations. BRL conducted an extensive series of HULL calculations using the Jones-Wilkens-Lee (JWL) explosive equation-of-state to predict the overpressure on the wall of the confinement vessel. The calculations included a determination of the pressure on the top, bottom, and side on the inside of the 64:1 volume ratio containment vessel for the 10 g explosives (Lottero, 1988 and 1989) and were applied to the 15 g explosives in the 40:1 volume-ratio vessel. Three explosive placement configurations were computed. In one the charge was centered in the chamber, in the second the explosive was located a half charge height above the chamber center, and finally the explosive was placed one charge length above the center of the vessel. For all three cases the axis of the cylindrical charge was collocated with the axis of the chamber. From these predictions, the type of pressure gages and the locations within the chamber were selected

to ensure the transducers were not overranged. The HULL calculations for the small scale tests indicated the best charge positioning was to collocate the charge center with the vessel center. Initiation of the explosive in the computations was at the end of the charge and on-axis. The test configuration, hydrocode station number, and explosive type and mass are shown in Figure 2. Pressures for various stations from the calculations on 11.53 g of LX-14 are presented in Table 1. This is the only calculation performed because LX-14 is considered the most energetic explosive of the three. Figure 3 is a calculated curve showing the pressures as a function of time including reverberations that occur in the chamber. The average peak pressures at the chamber wall are listed in Table 2.

2.2 Vessel Stress Analysis. The blast loading calculations were the starting point for designing the confinement vessel. An extensive series of stress analysis calculations for the vessel were performed using several methods. The techniques are (1) assuming an infinitely long thick walled cylinder (Timoshenko, 1959), (2) assuming an infinitely long thin walled cylinder (Timoshenko, 1959), (3) assuming an infinitely long cylinder (ASME, 1974), (4) assuming a flat circular plate, edge clamped (Timoshenko, 1959), (5) assuming a finite length thin cylinder with the ends clamped (Allison, 1989), and (6) stress concentration at the fillets (Timoshenko,1959). In addition calculations were done to study loading cycles until fatigue failure for a vessel subjected to repeated blast loading. As a result 180 cycles to fatigue failure were predicted based on a 200 MPa design pressure and 4340 steel with a flow stress of 930 MPa. Since less than 100 tests were expected the 180 cycle value was an adequate safety margin. The specifics of the vessel design are discussed in Chapter 3.

2.3 Blast Pressures. In the fluid flow corresponding to this study, there are three pressures amenable to measurement. They are static pressure, stagnation pressure, and reflected pressure.

Table 1. Computed Pressure on Interior of Vessel Wall, 11.53 g LX-14.

HULL Station	Radial, Axial (mm,mm)	Pressure (MPa)
1	0.0, 0.0	1900
5	10.0, 0.0	1090
8	20.0, 0.0	465
10	30.0, 0.0	181
12	40.0, 0.0	434
13	10.0, 0.0	1030
17	10.0, 80.0	572
20	20.0, 80.0	173
22	30.0, 80.0	327
24	40.0, 80.0	302
36	40.0, 40.0	492
38	40.0, 10.0	165
40	40.0, 20.0	413
42	40.0, 30.0	635
45	40.0, 50.0	211
47	40.0, 60.0	69
49	40.0, 70.0	130

Table 2. Average Peak Pressure on Interior Vessel Wall, 11.53 g LX-14.

Pressure Peak Number	Average Pressure (MPa) Bottom	Top	Side
1	92.2	71.1	78.2
2	75.2	99.0	21.6
3	29.0	26.7	17.4
4	17.2	19.9	15.4
5	11.1		
250 microseconds	8.5	9.3	12.4

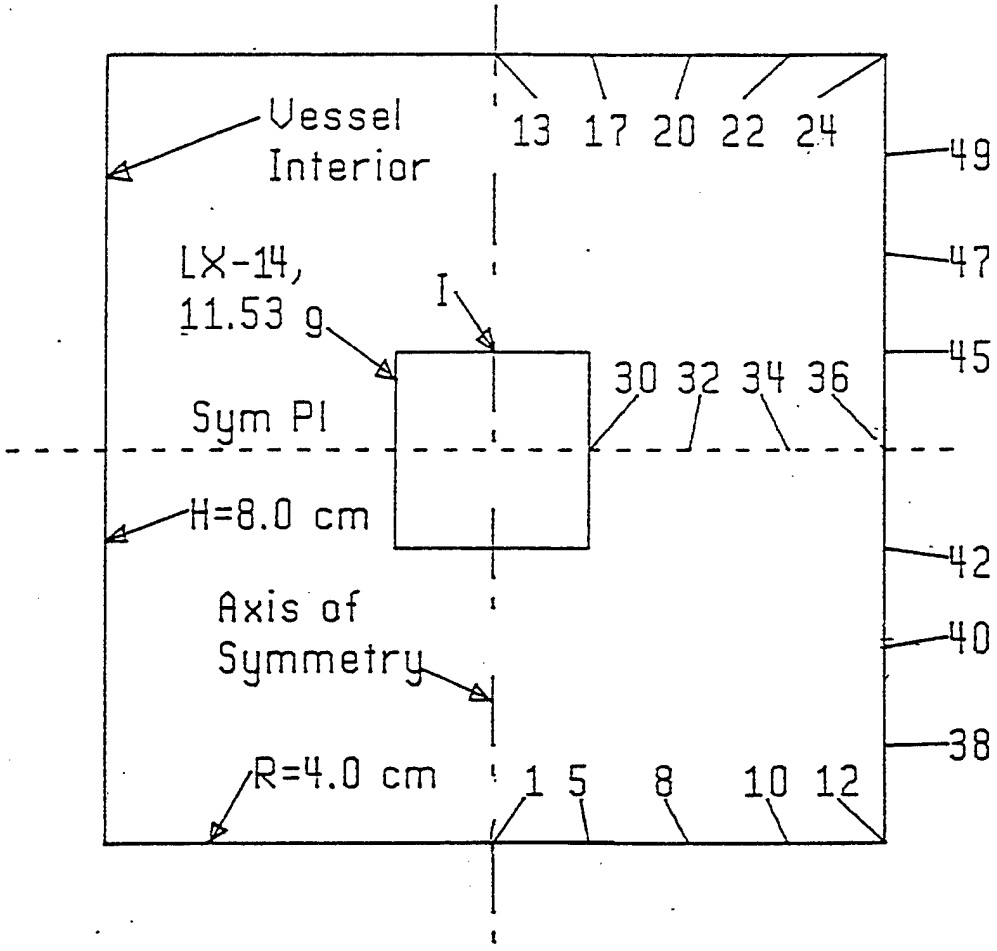

Figure 2. Test configuration for the HULL calculations.

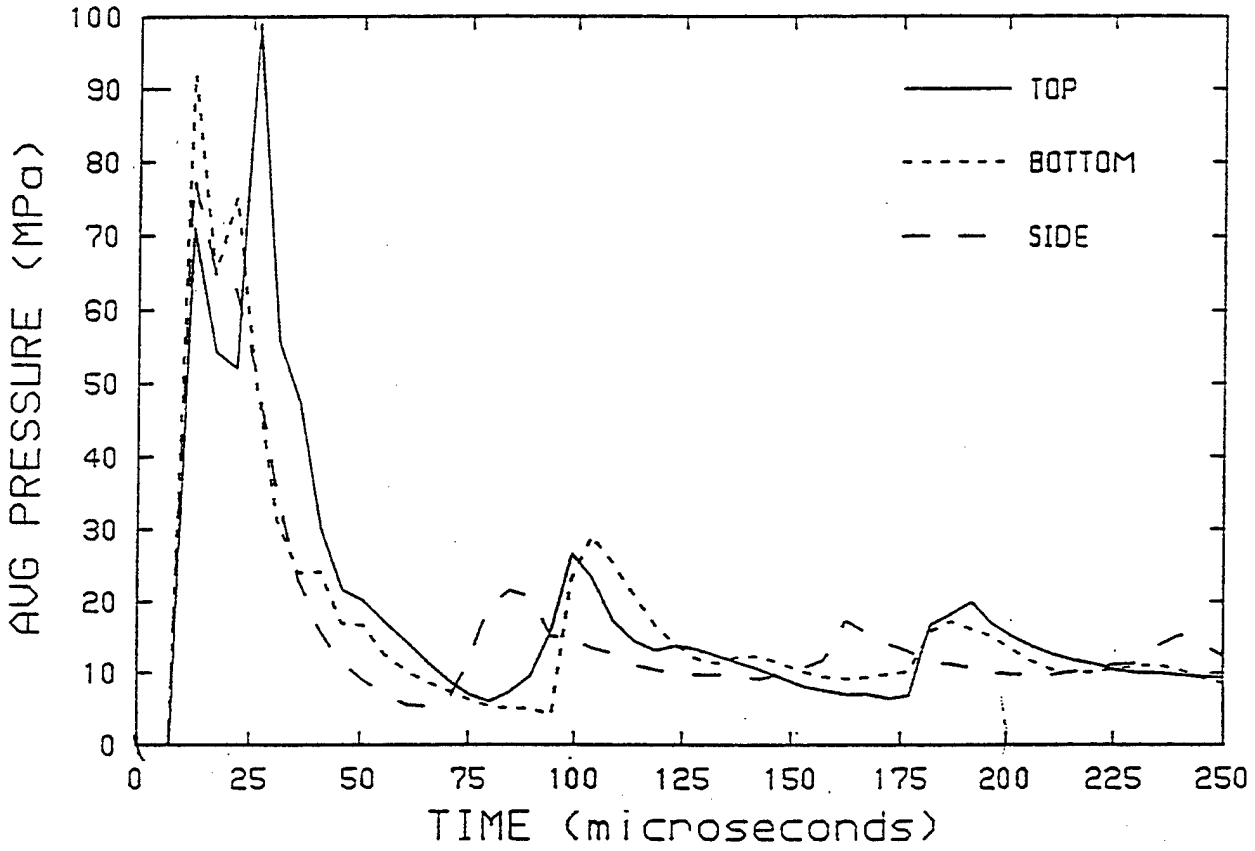

Figure 3. Calculated pressures versus time.

The overpressures from explosive shocks in air at the walls of the confinement vessel are considered reflected pressure. In this case a pressure gage is mounted flush with the wall and the pressure history is recorded as the air shock/detonation gas front strikes the rigid chamber surface and then reflects. There is a complication, however. The shock wave sweeping across the gage produces a pressure front that results in a combination of normal and oblique reflection because of the manner in which the explosive is initiated. For both the 10 and 15 g explosive charges, the measured pressures are regarded as reflected pressures in the closed vessel tests.

The orientation of the pressure gages for the free field blast tests were such that the stagnation pressure was the quantity measured. Strictly speaking, the stagnation pressure is the pressure indicated when bringing the flow to rest isentropically. A pitot tube, an open-ended tube facing the flow direction for air speed measurement for aircraft, is an example of the instrument to measure stagnation pressure. This concept is applied to the measurement of the stagnation pressure associated with explosive shocks in air.

The measurement of the static pressure from the blast wave was also considered, but was later abandoned because the experimental setup was too complicated for the benefit produced.

Figure 4 is a diagram (Groethe) of the gage orientation relative to the flow (left to right) for the three basic pressure measurements. The gage shown in this diagram is a bar gage, but the type of pressure gage is irrelevant to the measurement scheme.

2.4 Explosive Charges and Assembly. 10 and 15 g charges were selected for the blast overpressure measurements in the closed vessels. Nominally 900 g explosive charges were used for the free field blast measurements. The 10 g charges under study were Comp

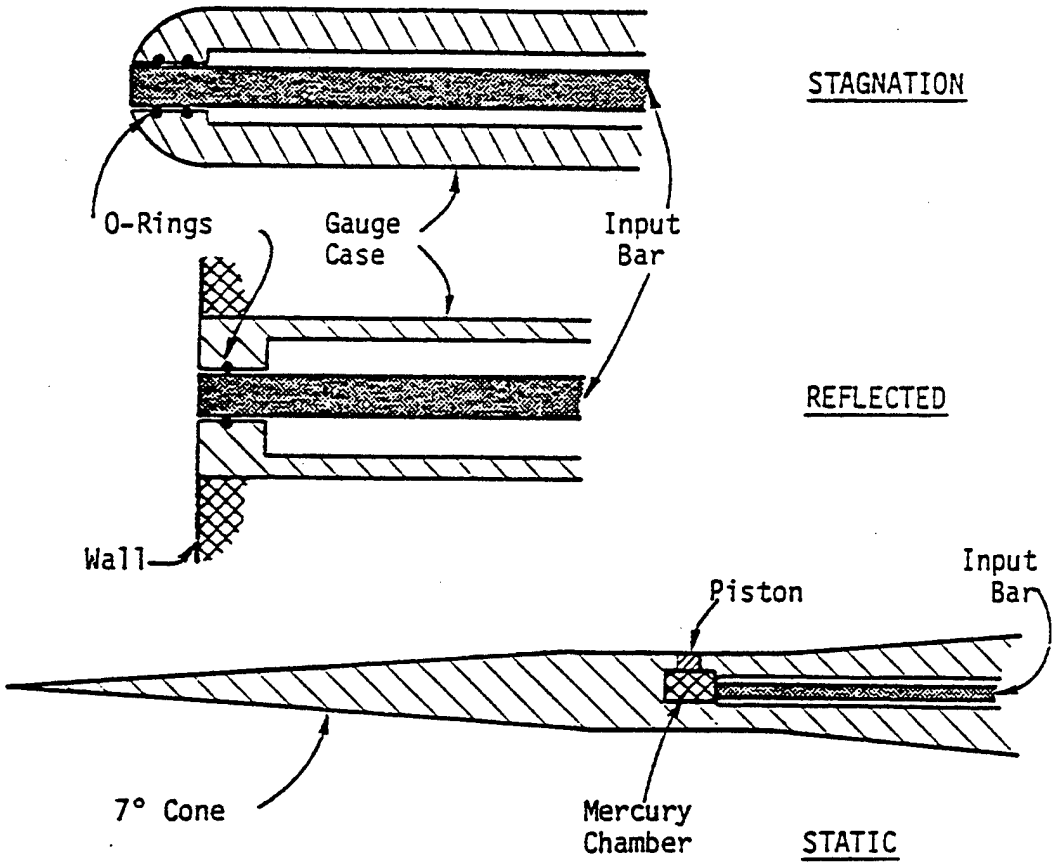

Figure 4. Gage orientation in the gas flow stream.

B, LX-14, and Pentolite. These explosives were cast (rather than pressed) and resulted in solid cylinders nominally 20 mm in diameter and 20 mm in length (1:1 diameter-to-length ratio). The tests using 15 g explosives were Composition B and LX-14. Again the explosives were cast into cylinders 22 mm in diameter and 22 mm in length for a 1:1 diameter-to-length ratio. The 900 g Comp B and LX-14 charges were also cast into solid cylinders 88 mm in diameter by 88 mm in length. The actual dimensions and masses for each of the 10, 15, and 900 g charges were measured and recorded. Table 3 is a list of these measurements and the identification numbers that correlates with the test numbers. The 900 g explosive charges are discussed in Section 4.1.

The explosive assembly consisted of a RP-80(Delrin) exploding bridgewire (EPW) detonator attached directly to the center of the end of the explosive by a thin epoxy bead around the Delrin sleeve and the charge. This detonator attachment worked well except for the 15 g and 900 g Comp B explosive cylinders. For the Comp B tests, a 2.5 g Detasheet booster explosive between the detonator and the test cylinder was necessary for prompt initiation. Careful assembly techniques included accurately centering the detonator and having good contact between the detonator and the explosive. The conditions for the 10 and 15 g tests along with the identification are listed in Table 4.

3. CONFINEMENT CHAMBERS

3.1 64:1 Ratio Chamber. This chamber was fabricated for use in measuring the reflected blast pressure in a closed vessel from 10 g explosive charges. The design is straight forward as indicated in Figure 5. The hollow cylinder chamber and the top and bottom plates were 4340 steel. This steel has high strength, excellent fracture toughness, and good ductility, all the ingredients necessary to contain an explosive charge. To preserve the ductility the steel was not heat treated after fabrication. When assembled the chamber was placed between the top and bottom

Table 3. 10 and 15 g Explosive Charge Data.

Main Charge I.D.	Main Charge HE Type	Main Charge Mass (g)	Main Charge Diam (mm)	Main Charge Length (mm)	Detonator Prime/Boost HE Type	Detonator Prime/Boost HE Mass (g)
1	Comp B	10.6	19.9	20.0	PETN/RDX	0.201
2	Comp B	10.6	19.9	20.0	PETN/RDX	0.201
3	Comp B	10.6	19.9	20.0	PETN/RDX	0.201
4	Comp B	10.7	20.0	20.1	PETN/RDX	0.201
5	Comp B	10.6	19.9	20.1	PETN/RDX	0.201
6	Comp B	10.6	19.9	20.0	PETN/RDX	0.201
1	LX-14	11.3	20.1	20.1	PETN/RDX	0.201
2	LX-14	11.3	20.0	19.9	PETN/RDX	0.201
3	LX-14	11.4	20.0	20.0	PETN/RDX	0.201
4	LX-14	11.4	20.0	20.0	PETN/RDX	0.201
5	LX-14	11.3	20.0	19.9	PETN/RDX	0.201
3	Pentolite	10.4	19.9	20.1	PETN/RDX	0.201
4	Pentolite	10.4	19.9	20.1	PETN/RDX	0.201
5	Pentolite	10.2	19.9	20.1	PETN/RDX	0.201
6	Pentolite	10.3	19.9	20.1	PETN/RDX	0.201
7	Pentolite	10.6	19.9	20.1	PETN/RDX	0.201
9	Pentolite	10.4	20.0	20.1	PETN/RDX	0.201
1	Comp B	14.4	22.0	22.2	PETN/RDX	0.201
2	Comp B	14.3	22.0	22.0	PETN/RDX	0.201
3	Comp B	14.4	22.0	22.3	PETN/RDX	0.201
4	Comp B	14.3	22.1	22.1	PETN/RDX	0.201
5	Comp B	14.3	22.1	22.1	PETN/RDX	0.201
6	Comp B	14.3	22.1	22.1	PETN/RDX	0.201
7	Comp B	14.4	22.1	22.1	PETN/RDX	0.201
1	LX-14	15.1	22.0	22.0	PETN/RDX	0.201
2	LX-14	15.1	22.1	22.2	PETN/RDX	0.201
3	LX-14	15.2	22.0	22.3	PETN/RDX	0.201
4	LX-14	15.1	22.0	22.1	PETN/RDX	0.201

Table 4. Test Conditions for 10 g Blast Measurements.

Test i.d.	Charge i.d.	Test Date	Ambient Temp (K)	Ambient Pressure (kPa)	Detonator Explo Weight (g)	Detonator Type	Detasheet Booster Charge (g)
10 g							
CB.1	1	7/26/90	298	102.2	0.200	RP-80	
CB.2	2	7/26/90	299	102.1	0.200	RP-80	
CB.3	3	7/27/90	298	102.0	0.200	RP-80	
CB.4	4	7/27/90	298	101.9	0.200	RP-80	
CB.5	5	9/10/90	295	101.1	0.200	RP-80	
CB.6	6	9/21/90	295	101.3	0.200	RP-80	
LX.1	1	7/24/90	300	101.5	0.200	RP-80	
LX.2	2	7/24/90	299	101.4	0.200	RP-80	
LX.3	3	7/25/90	298	101.8	0.200	RP-80	
LX.4	4	7/25/90	298	101.7	0.200	RP-80	
LX.5	5	9/4/90	297	102.6	0.200	RP-80	
P.3	3	7/20/90	300	101.3	0.200	RP-80	
P.4	4	7/23/90	299	100.9	0.200	RP-80	
P.5	5	6/15/90	298	101.8	0.200	RP-80	
P.6	6	7/19/90	300	101.5	0.200	RP-80	
P.7	7	5/10/90	298	98.9	0.200	RP-80	
P.9	9	7/18/90	299	101.3	0.200	RP-80	
15 g							
CB.1	1	1/17/91	-	-	0.203	RP-80	0.0
CB.2	2	1/29/91	289	100.6	0.203	RP-80	0.0
CB.3	3	2/12/91	287	101.9	0.203	RP-80	0.0
CB.4	4	12/3/91	296	99.4	0.203	RP-80	2.4
CB.5	5	12/10/91	295	100.9	0.203	RP-80	2.4
CB.6	6	12/24/91	296	101.4	0.203	RP-80	2.4
CB.7	7	12/27/91	295	101.7	0.203	RP-80	2.4
LX.1	1	2/11/91	289	101.0	0.203	RP-80	0.0
LX.2	2	2/20/91	290	102.1	0.203	RP-80	0.0
LX.3	3	11/4/910	288	101.2	0.203	RP-80	0.0
LX.4	4	11/27/910	296	101.6	0.203	RP-80	0.0

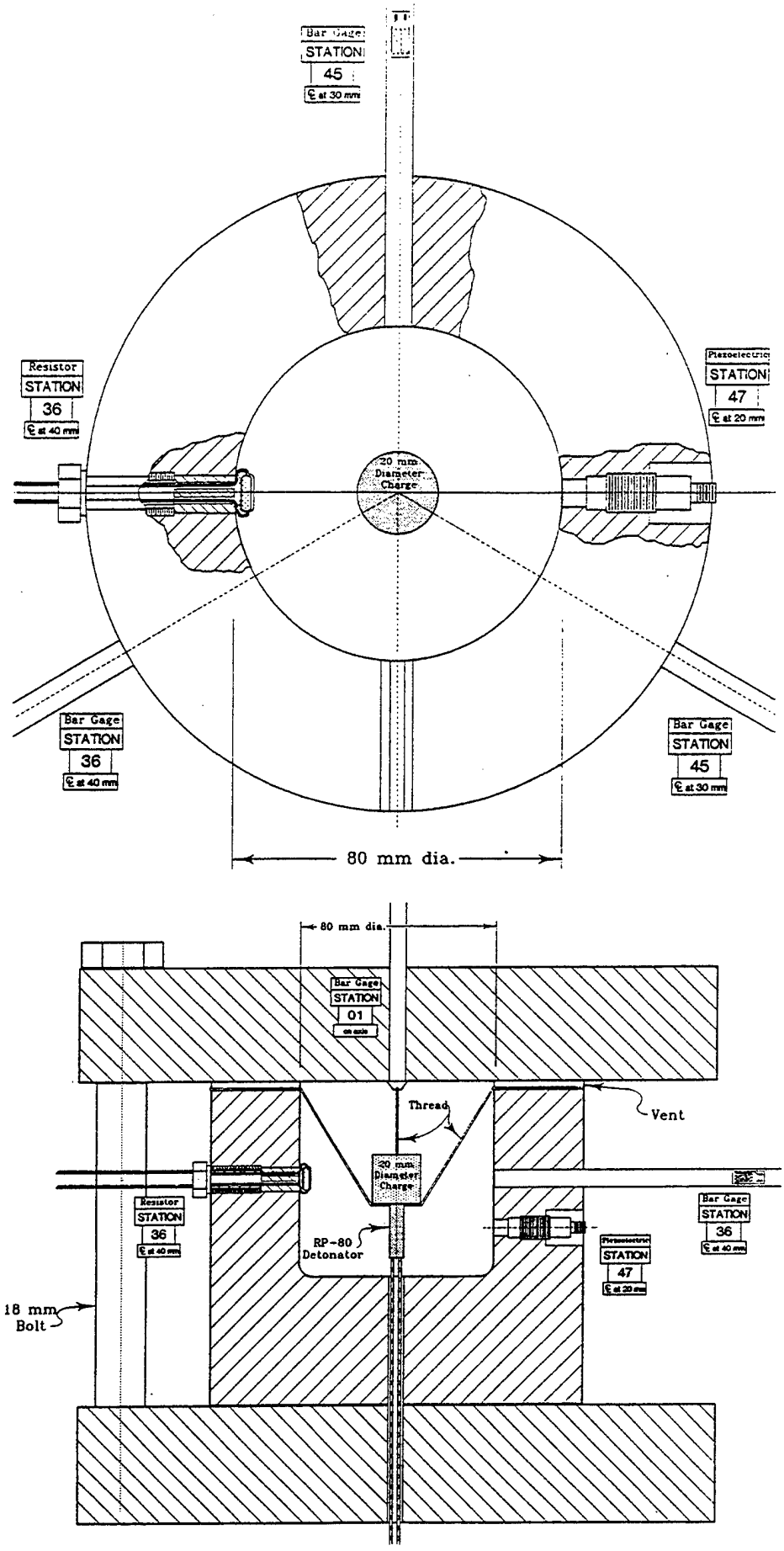

Figure 5. Design of the 64:1 volume ratio confinement chamber.

plates and secured with 18 high strength bolts which were 12.7-mm in diameter by 254-mm long and were spaced equally on a 190.5-mm diameter circle. As indicated in the figure, the chamber was 127-mm high and bored to a depth of 80 mm and a diameter of 80 mm. Holes were drilled through the wall for gage ports and also a hole was also drilled through the bottom of the chamber for the detonator wires. Two 3.0-mm deep vent grooves in the top surface of the chamber provided a an escape path for the explosive gases. The conditions for the 10 and 15 g tests along with the identification are listed in Table 4.

The top and bottom plates have square dimensions of 228.6 mm by 38.1-mm thick and the plates contain holes for 18 bolts. In the center of the top plate, a 6.6-mm diameter through-hole is located for a bar pressure gage. The bottom plate contains a 6.35-mm diameter hole in the center that coincides with the hole in the center of the chamber through which to pass the detonator wires. Two 6.35 diameter pins extend below the bottom surface of the top plate to mate with alignment holes in the chamber.

3.1.1 Sensor Locations. Six sensor ports were in the closed vessel, five in the cylindrical chamber and one through the top plate. Table 5 is a list of the port locations and the sensor type for all tests. Figure 6 is a schematic of the ports. At the beginning of the testing four sensor ports were machined in the chamber including the one through the top plate, but later, two more ports were drilled to accommodate other sensors. Specifically, one sensor was at Station 1, two at Station 36, one at Station 42, and two at Station 45. This arrangement covered blast pressures at the top and bottom edge of the explosive, at the explosive center, and on the axis of the cylinder or Z-axis. Bar pressure gages were located at Stations 1, 36, and 45 while the PCB piezoelectric gage and the 470 ohm carbon resistor gage were at Stations 42 and 36, respectively. A discussion of the sensors is in Section 4 of this report.

Table 5. Gage/Station Correlation Chamber 1 (64:1).

Test	Gage	Location	Position	Port #	R(mm)	Z(mm)	Station
CB.1	Bar 1	top	on-axis	1	00.0	00.0	1
	Bar 2	rear	below	3	40.0	50.0	45
	Bar 3	lt rear	center	2	40.0	40.0	36
	Bar 4	front	below	4	40.0	50.0	45
	470ohm		center	5	40.0	40.0	36
	PCB		below	6	40.0	60.0	47
CB.2	Bar 1	top	on-axis	1	00.0	00.0	1
	Bar 2	rear	below	3	40.0	50.0	45
	Bar 3	lt rear	center	2	40.0	40.0	36
	Bar 4	front	below	4	40.0	50.0	45
	470ohm		center	5	40.0	40.0	36
	PCB		below	6	40.0	60.0	47
CB.3	Bar 1	top	on-axis	1	00.0	00.0	1
	Bar 2	rear	below	3	40.0	50.0	45
	Bar 3	lt rear	center	2	40.0	40.0	36
	Bar 4	front	below	4	40.0	50.0	45
	470ohm		center	5	40.0	40.0	36
	PCB		below	6	40.0	60.0	47
CB.4	Bar 1	top	on-axis	1	00.0	00.0	1
	Bar 2	rear	below	3	40.0	50.0	45
	Bar 3	lt rear	center	2	40.0	40.0	36
	Bar 4	front	below	4	40.0	50.0	45
	470ohm		center	5	40.0	40.0	36
	PCB		below	6	40.0	60.0	47
CB.5	Bar 1	lt rear	center	2	40.0	40.0	36
	Bar 2	rear	below	3	40.0	50.0	45
	Bar 3	top	on-axis	1	00.0	00.0	1
	Bar 4	front	below	4	40.0	50.0	45
	470ohm		center	5	40.0	40.0	36
	PCB		below	6	40.0	60.0	47
CB.6	Bar 1	lt rear	center	2	40.0	40.0	36
	Bar 2	rear	below	3	40.0	50.0	45
	Bar 3	top	on-axis	1	00.0	00.0	1
	Bar 4	front	below	4	40.0	50.0	45
	470ohm		center	5	40.0	40.0	36
	PCB		below	6	40.0	60.0	47
LX.1	Bar 1	top	on-axis	1	00.0	00.0	1
	Bar 2	rear	below	3	40.0	50.0	45
	Bar 3	lt rear	center	2	40.0	40.0	36
	Bar 4	front	below	4	40.0	50.0	45
	470ohm		center	5	40.0	40.0	36
	PCB		below	6	40.0	60.0	47
LX.2	Bar 1	top	on-axis	1	00.0	00.0	1
	Bar 2	rear	below	3	40.0	50.0	45
	Bar 3	lt rear	center	2	40.0	40.0	36
	Bar 4	front	below	4	40.0	50.0	45
	470ohm		center	5	40.0	40.0	36
	PCB		below	6	40.0	60.0	47

LX.3	Bar 1	top	on-axis	1	00.0	00.0	1
	Bar 2	rear	below	3	40.0	50.0	45
	Bar 3	lt rear	center	2	40.0	40.0	36
	Bar 4	front	below	4	40.0	50.0	45
	470ohm		center	5	40.0	40.0	36
	PCB		below	6	40.0	60.0	47
LX.4	Bar 1	top	on-axis	1	00.0	00.0	1
	Bar 2	rear	below	3	40.0	50.0	45
	Bar 3	lt rear	center	2	40.0	40.0	36
	Bar 4	front	below	4	40.0	50.0	45
	470ohm		center	5	40.0	40.0	36
	PCB		below	6	40.0	60.0	47
LX-5	Bar 1	lt rear	center	2	40.0	40.0	36
	Bar 2	rear	below	3	40.0	50.0	45
	Bar 3	top	on-axis	1	00.0	00.0	1
	Bar 4	front	below	4	40.0	50.0	45
	470ohm		center	5	40.0	40.0	36
	PCB		below	6	40.0	60.0	47
P.3	Bar 1	top	on-axis	1	00.0	00.0	1
	Bar 2	rear	below	3	40.0	50.0	45
	Bar 3	lt rear	center	2	40.0	40.0	36
	Bar 4	front	below	4	40.0	50.0	45
	470ohm		center	5	40.0	40.0	36
	PCB		below	6	40.0	60.0	47
P.4	Bar 1	top	on-axis	1	00.0	00.0	1
	Bar 2	rear	below	3	40.0	50.0	45
	Bar 3	lt rear	center	2	40.0	40.0	36
	Bar 4	front	below	4	40.0	50.0	45
	470ohm		center	5	40.0	40.0	36
	PCB		below	6	40.0	60.0	47
P.5	Bar 1	top	on-axis	1	00.0	00.0	1
	Bar 2	rear	below	3	40.0	50.0	45
	Bar 3	lt rear	center	2	40.0	40.0	36
	Bar 4	front	below	4	40.0	50.0	45
	470ohm-1		center	5	40.0	40.0	36
	470ohm-2		below	6	40.0	60.0	47
P.7	Bar 1		below		40.0	50.0	45
	Bar 2		center		40.0	40.0	36
	50ohm		above		30.0	00.0	22
	PCB-1		above		30.0	00.0	22
	PCB-2		center		40.0	40.0	36
	PCB-3		below		40.0	60.0	47
P.9	Bar 1	top	on-axis	1	00.0	00.0	1
	Bar 2	rear	below	3	40.0	50.0	45
	Bar 3	lt rear	center	2	40.0	40.0	36
	Bar 4	front	below	4	40.0	50.0	45
	470ohm		center	5	40.0	40.0	36
	PCB		below	6	40.0	60.0	47

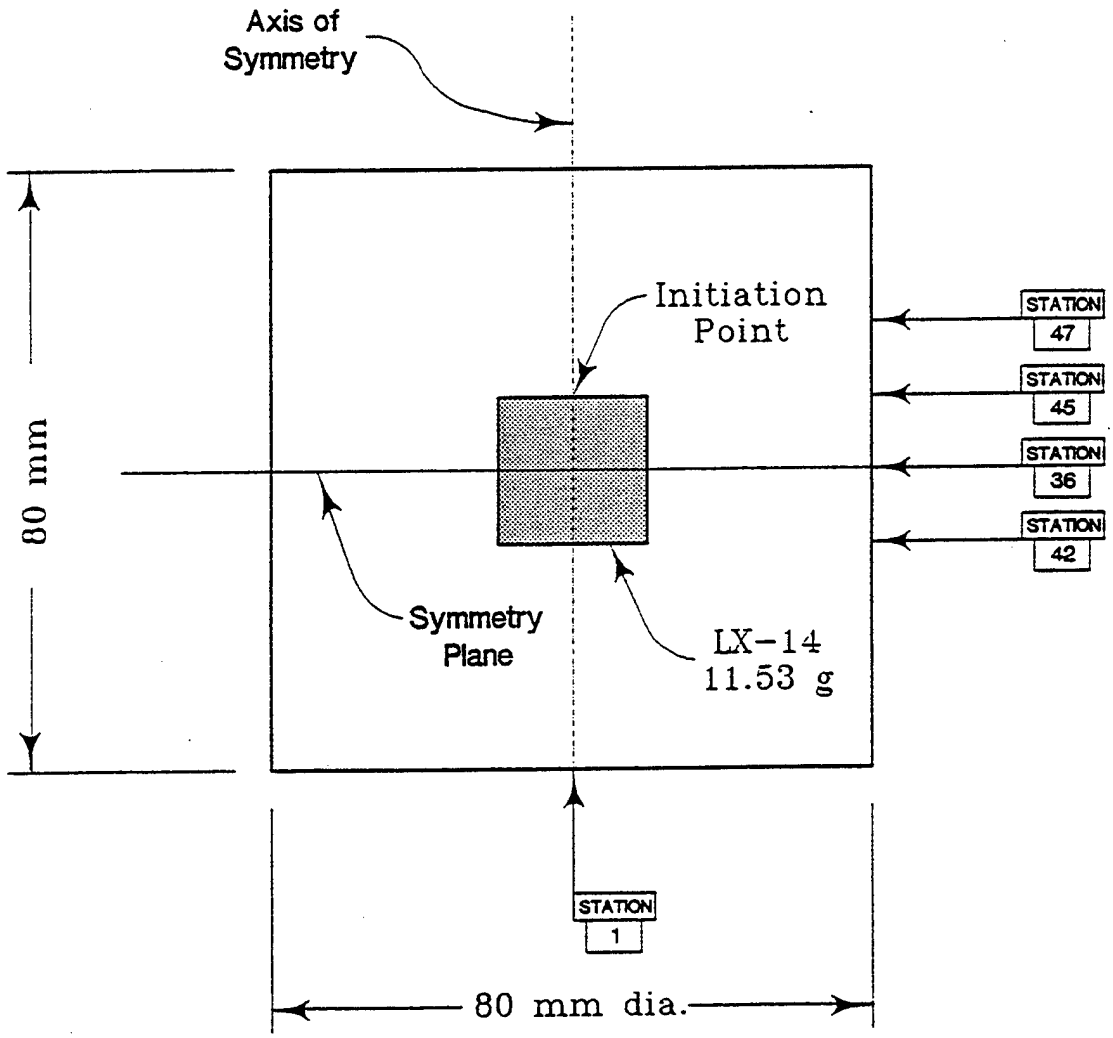

Figure 6. Sensor and explosive locations for 64:1 chamber.

The station identification corresponds to the data shown in Figure 2. Two pairs of sensor ports had identical locations which provided redundancy in the pressure measurement around the symmetry axis. The ports were drilled to a diameter of 7 mm and a depth of 45.0 mm and then finished to a diameter of 6.6 mm for the remaining 5.0 mm to the inside surface of the chamber. This shoulder provided support for the end of the bar, but slightly decoupled the bar from the thick wall of the chamber. The PCB gauge port was threaded according to the manufacturers specifications.

3.1.2 Test Assembly. As shown in Figures 5a and 6, the explosive charge was centered in the 80-mm diameter by 80-mm high inner chamber. Attached to the explosive cylinder was a RP-80 EPW detonator to initiate the charge. The wires exited through the hole in the bottom of the chamber and the base plate and then connected to the "fire set". Four cotton threads supported and positioned the explosive at the center of the vessel. The setup for a test had ten steps: (1) Position the confinement vessel on the base plate so that the center holes coincide. (2) Mount the gages in the sensor ports. (3) Connect the sensors to their respective signal conditioning circuits and in turn connect to the recording oscilloscope via amplifiers. (4) Calibrate the recording system. (5) Calibrate the pressure bar gages. (6) Connect the Reynolds FS-10 fire set to the firing module. (7) Perform a dry run of the detonator firing system with a dummy detonator. (8) Attach the RP-80 detonator directly to the center of the bottom of the explosive charge, then place the explosive assembly at the center of the chamber with cotton thread and extend the detonator wires through the bottom plate after adjusting the final position. (9) Place the top plate over the chamber, bolt the top and bottom plates together, and then insert the bar gage in the sensor hole in the top plate. (10) Connect the detonator wires to the firing module, arm the oscilloscopes, and finally activate the FS-10 to initiate the explosive.

The experiment is straight forward, but each step was checked several times to maintain safety, to minimize misfires, and to prevent signal recording problems.

3.2 40:1 Ratio Chamber. This chamber was fabricated to measure the reflected blast pressure in closed vessel from the 15 g charges, simulating a closer standoff distance than the 64:1 vessel. The design is similar to the 64:1 chamber, but with some differences. As with the 64:1 vessel, the cylindrical chamber and the top plate were 4340 high strength steel, but the bottom plate was 1018 steel. The steel was not heat treated to preserve ductility. The vessel was clamped together with 12 high strength bolts that were 19.05 mm in diameter by 254-mm long and the bolts were equally spaced on a 209.6-mm diameter circle. The cylindrical section of the vessel was 127-mm high and bored to a depth of 75 mm and a diameter of 75 mm. Ports were drilled through the wall for the various gages at known locations. Also a hole was drilled through the bottom of the cylinder to accommodate the detonator wires. Figure 7 is a diagram of the confinement vessel.

The top plate had square dimensions of 254.0 mm and a thickness of 50.8 mm. In the center of the top plate was a hole 9.65 mm in diameter hole by 38.1-mm deep and then finished with a 6.6-mm diameter hole for the bar gage. Also, two 6.35 diameter pins extended below the bottom surface to mate with alignment holes in the cylindrical chamber.

The bottom plate was also 254-mm square but 38.1-mm thick. A 9.5-mm diameter hole in the center coincided with the hole in the cylindrical chamber to accept the detonator wires.

3.2.1 Sensor Locations. The vessel contained five sensor ports, four in the cylindrical section and one in the top plate. Table 6 is a list of the port locations and the type of gage for all the tests. Figure 8 is a schematic of the port locations. Four

Table 6. Gage/Station Correlation Chamber 2 (40:1).

Test	Gage	Location	Position	Port #	R(mm)	Z(mm)	Station
CB.1	Bar 1	top	on-axis	4	00.0	00.0	1
	Bar 2	rt front	above	1	37.5	26.5	42
	Bar 3	rear	below	3	37.5	57.5	47
	Bar 4	lt front	center	2	37.5	37.5	36
CB.2	Bar 1	rt front	above	1	37.5	26.5	42
	Bar 2	top	on-axis	4	00.0	00.0	1
	Bar 3	rear	below	3	37.5	57.5	47
	Bar 4	lt front	center	2	37.5	37.7	36
CB.3	Bar 1	top	on-axis	4	00.0	00.0	1
	Bar 2	rt front	above	1	37.5	26.5	42
	Bar 3	rear	below	3	37.5	57.5	47
	Bar 4	lt front	center	2	37.5	37.5	36
CB.4	Bar 1	right	center	2	37.5	37.5	36
	Bar 2	top	on-axis	4	00.0	00.0	1
	Bar 3	front	below	3	37.5	57.5	47
	Bar 4	left	above	1	37.5	26.5	42
	PVDF	right	center	2	37.5	37.5	36
	PCB		center	2'	37.5	37.5	36
CB.5	Bar 1	right	center	2	37.5	37.5	36
	Bar 2	top	on-axis	4	00.0	00.0	1
	Bar 3	front	below	3	37.5	57.5	47
	Bar 4	left	above	1	37.5	26.5	42
	PVDF	right	center	2	37.5	37.5	36
	PCB		center	2'	37.5	37.5	36
CB.6	Bar 1	right	center	2	37.5	37.5	36
	Bar 2	top	on-axis	4	00.0	00.0	1
	Bar 3	front	below	3	37.5	57.5	47
	Bar 4	left	above	1	37.5	26.5	42
	PVDF	right	center	2	37.5	37.5	36
	PCB		center	2'	37.5	37.5	36
CB.7	Bar 1	right	center	2	37.5	37.5	36
	Bar 2	top	on-axis	4	00.0	00.0	1
	Bar 3	front	below	3	37.5	57.5	47
	Bar 4	left	above	1	37.5	26.5	42
	PVDF	right	center	2	37.5	37.5	36
	PCB		center	2'	37.5	37.5	36
LX.1	Bar 1	top	on-axis	4	00.0	00.0	1
	Bar 2	rt front	above	1	37.5	26.5	42
	Bar 3	rear	below	3	37.5	57.5	47
	Bar 4	lt front	center	2	37.5	37.5	36
LX.2	Bar 1	top	on-axis	4	00.0	00.0	1
	Bar 2	rt front	above	1	37.5	26.5	42
	Bar 3	rear	below	3	37.5	57.5	47
	Bar 4	lt front	center	2	37.5	37.5	36
LX.3	Bar 1	top	on-axis	4	00.0	00.0	1
	Bar 2	rt front	above	1	37.5	26.5	42
	Bar 3	rear	below	3	37.5	57.5	47
	Bar 4	lt front	center	2	37.5	37.5	36
LX.4	Bar 1	right	center	2	37.5	37.5	36
	Bar 2	top	on-axis	4	00.0	00.0	1
	Bar 3	front	below	3	37.5	57.5	47
	Bar 4	left	above	1	37.5	26.5	42
	PCB	-	center	2'	37.5	37.5	36

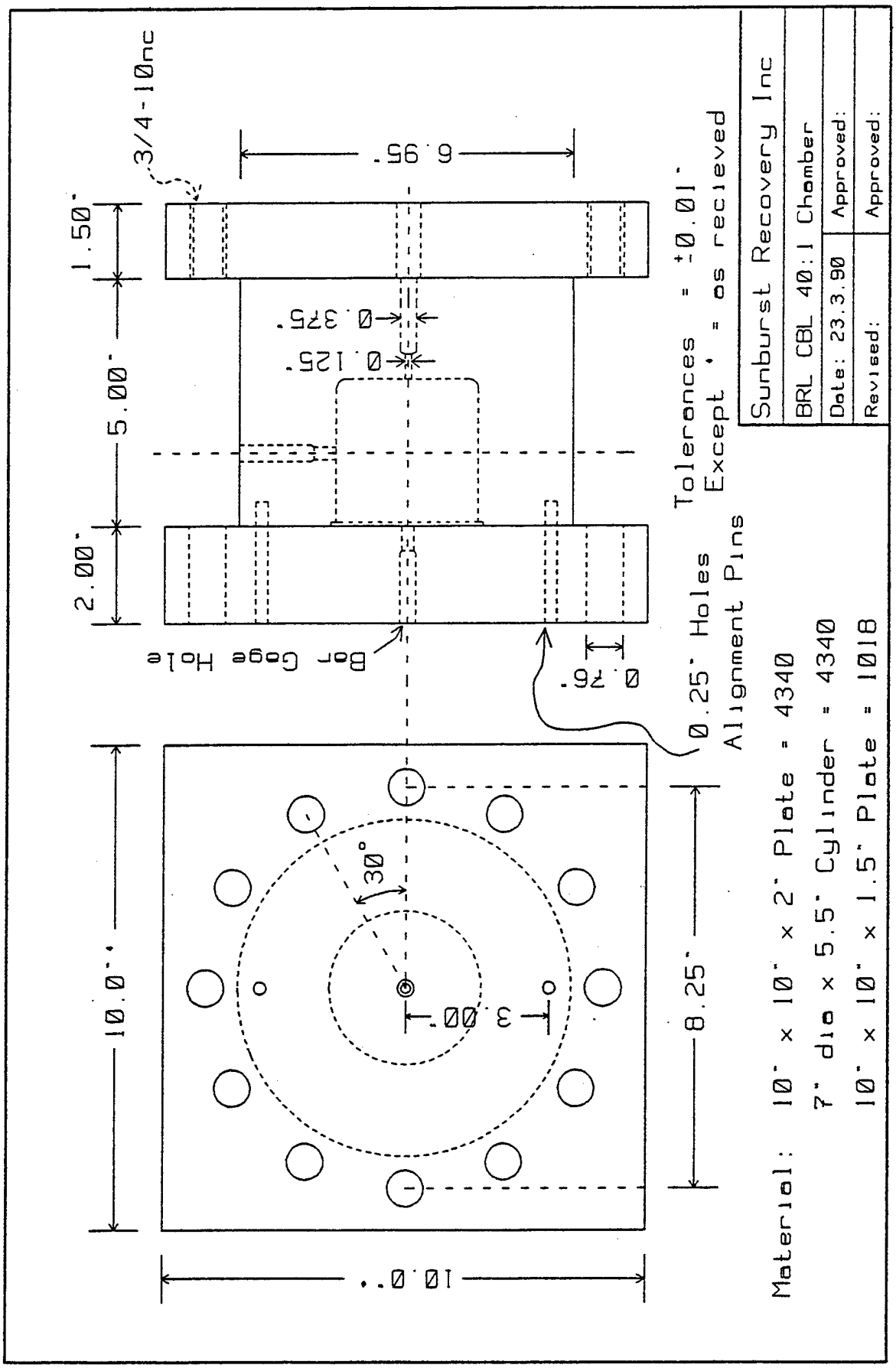

Figure 7. Design of the 40:1 volume ratio confinement chamber.

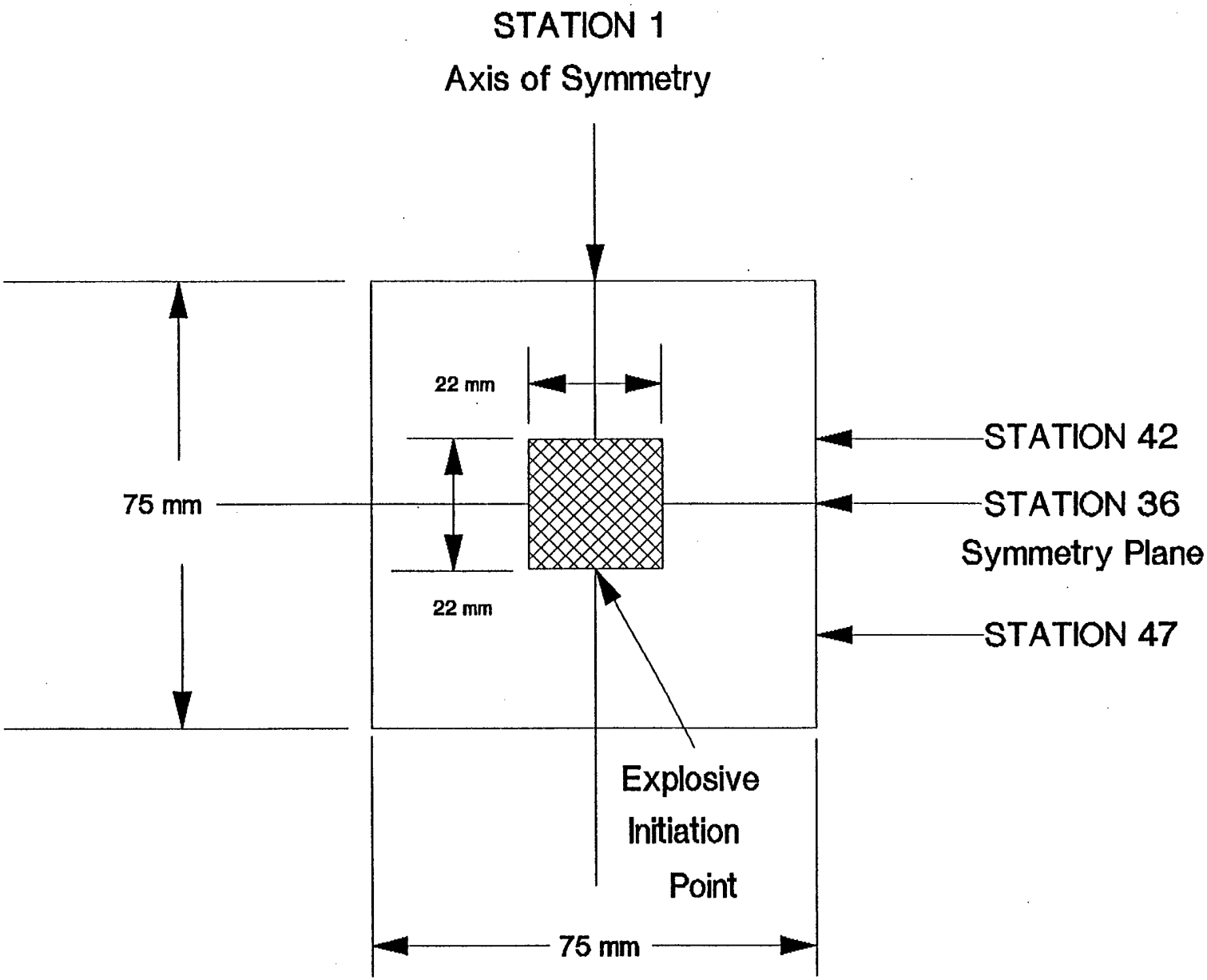

Figure 8. Sensor and explosive locations for the 40:1 chamber.

sensors were bar gages and one gage was a PCB pressure transducer. One port/sensor was at Station 1, two at Station 36, one at Station 42, and one at Station 47. This arrangement covered the measurement of blast pressures at the top edge of the explosive, the center of the explosive, below the charge, and on the axis of the cylindrical explosive. As indicated in Table 6 bar gages were at Stations 1, 36, 42, and 47 while the PCB gage was at Station 36.

The station numbering corresponds to that shown in Figure 2. As discussed in Section 3.1.2 the port holes were drilled to provide support for the end of the bar extending to the inner surface of the vessel. The PCB gage port was threaded according to the manufacturer's specifications.

3.2.2. Test Assembly. As shown in Figure 8, the explosive charge was centered in the 75-mm diameter by 75-mm high inner chamber and initiated by a RP-80 EPW detonator attached to the bottom end of the explosive. The wires exited through the holes in the bottom of the vessel and then connected to the FS-10 fire set. The explosive was supported by a very low density polystyrene cylinder cut to a height to accurately position the explosive at the center of the chamber. Because each explosive charge had slightly different dimensions, each foam support had to be adjusted to provide the exact height to center the charge.

The setup for a test using the 15 g charges was the same procedure as described in Section 3.1.3.

3.2.3 Comp B Initiation Difficulties. The 15 g Comp B charges failed to initiate for the first two tests in which the RP-80 EPW detonator was attached directly to the explosive in contrast to the test series using 10 g charges. After some thought and guessing, analysis of the gage signals, and consulting with colleagues at the Naval Surface Warfare Center in Silver Spring, MD, the conclusion was that the RP-80 did not have sufficient

energy to promptly initiate cast Comp B. It is much more difficult to initiate cast Comp B than the pressed material because the pressed material has a large number of voids which act as hot spots for prompt detonation. By contrast cast Comp B usually has a small number of hot spots and hence, initiation is difficult. Prompt initiation was achieved when 2.5 g of Detasheet explosive booster was placed between the EBW detonator and the Comp B charge. Figure 9 is a diagram of the assembly using the Detasheet booster charge, the RP-80 detonator, and the polystyrene support. Initiation was not a problem for the 15 g LX-14 explosive nor was initiation of the 10 g Comp B explosive. The difference in behavior between the two explosive weights is not understood since the 10 g Comp B explosives were also cast, but were from a different Lot Number.

A similar initiation problem occurred when attempting to the 900 g Comp B explosives at the Experimental Mine in Colorado. The solution was to place a four gram Detasheet booster between the charge and the RP-80 detonator. This permitted prompt initiation of the Comp B.

4. FREE FIELD BLAST PRESSURE EXPERIMENTAL SETUP.

4.1 Explosive Charges and Test Location for Free-Field Tests. For the free-field tests conducted in support of the close-in blast loading program, it was desired to use the largest explosive charges practicable. Based upon cost, charge manufacturing constraints and the desire to use the large charges in various types of test (eg. manganin gage tests as conducted by SRI International and plate loading tests conducted by FMC), a cylindrical charge size of 88 mm in diameter by 88 mm long was chosen. Charges of this dimension were manufactured by BRL of both LX-14 and Comp-B explosive. The LX-14 charges had a nominal weight of 965 g giving a nominal density of 1810 kg/m^3. The Comp-B charges had a nominal weight of 903 g giving a nominal

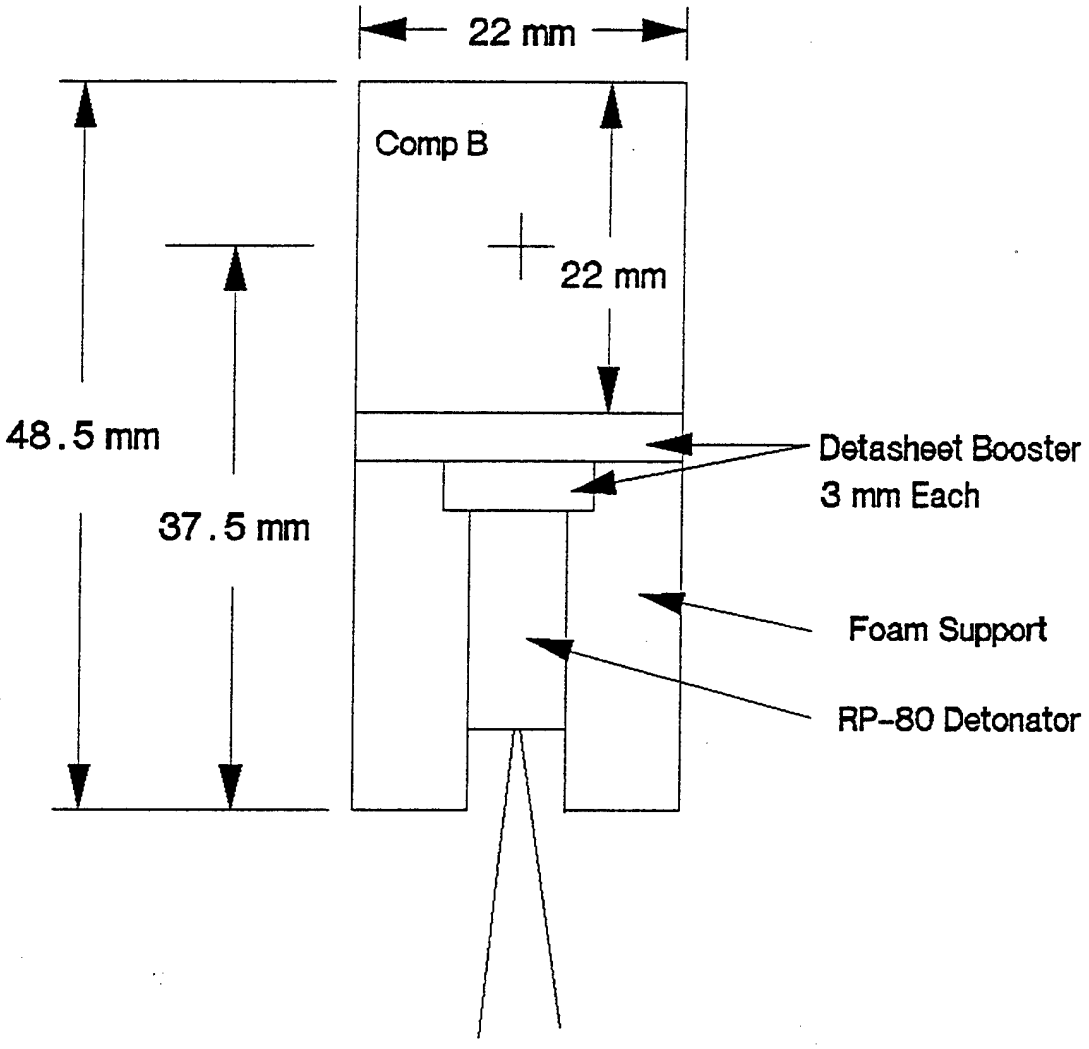

Figure 9. 15 g Comp B tests explosive assembly.

density of 1704 kg/m^3. The actual weight of each charge as determined by BRL after manufacture and as weighed at the CSM Mine just before test execution are given in Table 7.

As the very large airblast which would be generated by the free-field (unconfined) detonation of approximately 1.0 kg charges, precluded conducting the tests in the available University of Maryland facilities, the execution of the large-charge tests was carried out in the Colorado School of Mines Experimental Mine located in Idaho Springs Colorado. This research mine offered an ideal location for conducting the required tests as the mine had many underground test drifts in which the charges could be detonated without concern for shock and airblast and to which the required instrumentation could be easily provided and supported. The execution of the tests was carried out by Sunburst Recovery, Inc. under subcontract to the University of Maryland.

4.2 Free-Field Gage Location and Scaled Distance. For the free-field large-charge tests it was desired to use gage locations and distances which could be directly comparable to gage locations used in the small-scale confined-volume tests conducted at the University of Maryland. As nearly all the confined volume tests were carried out with charges and confined-volume chambers giving nominal charge to volume ratios of 64:1 and 40:1, it was desired to use gage distances corresponding to the scaled dimensions of the confined-volume chambers. For comparison with the 64:1 confined-volume tests a scaled gage location radius of 4.0 would be required. For the large cylindrical charges of LX-14 and Comp-B, with a length of 88 mm and a radius of 44 mm, gage locations at 176 mm from the charge center are indicated. For comparison with the 40:1 confined-volume tests a scaled gage location radius of 3.42, at a distance of 150.5 mm, would be required.

The general test geometry utilized for all of the tests

Table 7. Nominal 900 g explosive charge data.

	Main Charge			Primary Explosive		Booster Explosive	
Charge Number	Provided by	Type	Mass (gm)	Type	Mass (gm)	Type	Mass (gm)
CB.1	BRL	Comp B	905.0	PETN+RDX	0.2	NONE	0.0
CB.2	BRL	Comp B	903.0	PETN+RDX	0.2	PETN+DP	2.5
CB.3	BRL	Comp B	904.0	PETN+RDX	0.2	PETN+DP	2.5
CB.4	BRL	Comp B	907.0	PETN+RDX	0.2	PETN+DP	2.5
LX.1	BRL	LX-14	964.0	PETN+RDX	0.2	PETN+DP	2.5
LX.2	BRL	LX-14	971.0	PETN+RDX	0.2	PETN+DP	2.5
LX.3	BRL	LX-14	964.0	PETN+RDX	0.2	PETN+DP	2.5
LX.4	BRL	LX-14	968.0	PETN+RDX	0.2	PETN+DP	2.5
Key: PETN+RDX = RP-80 Charge PETN+DP = PETN in Detaprime Tube							

conducted on the large LX-14 and Comp-B charges at the CSM mine is illustrated in Figure 10. All the tests incorporated at least four stagnation pressure bar gages (as described in Section 4.3, below). In every test, one stagnation pressure gage was located radially out on the midplane of the charge at a distance of four charge radii (Position 136) from the charge center and one gage was located on the axis of the cylindrical charge opposite the detonator end at a distance of four charge radii from the center of the charge (Position 101). Most tests included three or four additional stagnation pressure gages usually located at Positions 120, 108, 140, and/or 236. Gage positions identified with a 1XX number (Figure 10) corresponded to positions of interest in the confined volume laboratory tests with a volume-to-charge ratio of 64:1. Gage position 236 (Figure 10) with a reference distance of 3.42 charge radii corresponding to confined volume tests with a 40:1 ratio. All these gage locations are summarized in Table 8, which gives the radial and axial locations in both relative-to-charge radius and centimeters.

4.3 Stagnation Pressure Bar Design, Construction and Calibration. Based upon the difficulties realized in obtaining good pressure data with standard piezoelectric pressure gages in the laboratory confined volume tests (as discussed in Section 5.2, below, it was decided to use a simple bar gage instrumented with standard strain gages for the large-scale free-field tests. Both the good quality data obtained with strain gage instrumented pressure bars in the laboratory tests and the greater ease with which such bars could be fielded in the adverse free-field environment indicated that the pressure bar approach was preferred for the tests in the CSM mine. The general construction of the pressure bars built for and used in the CSM tests is illustrated in Figure 11. The bar assembly included a standard pressure bar instrumented with strain gages, which was enclosed within a protective support tube and had an obdurating nose piece with a 10 degree included angle to transition from the bar diameter to the protective tube diameter. Pressure bars of

Table 8. Gage locations for the free field tests.

BRL-CSM Free-Field Gage Positions		
Gage Position Number	Radial Position R (r_o)	Axial Position Y (r_o)
64:1 Equivalent		
101	**0**	**4**
108	2	4
113	0	-4
120	2	-4
136	**4**	**0**
140	4	2
147	4	-2
40:1 Equivalent		
201	0	3.42
208	1.71	3.42
213	0	-3.42
220	1.71	-3.42
236	3.42	0
240	3.42	1.71
247	3.42	-1.71

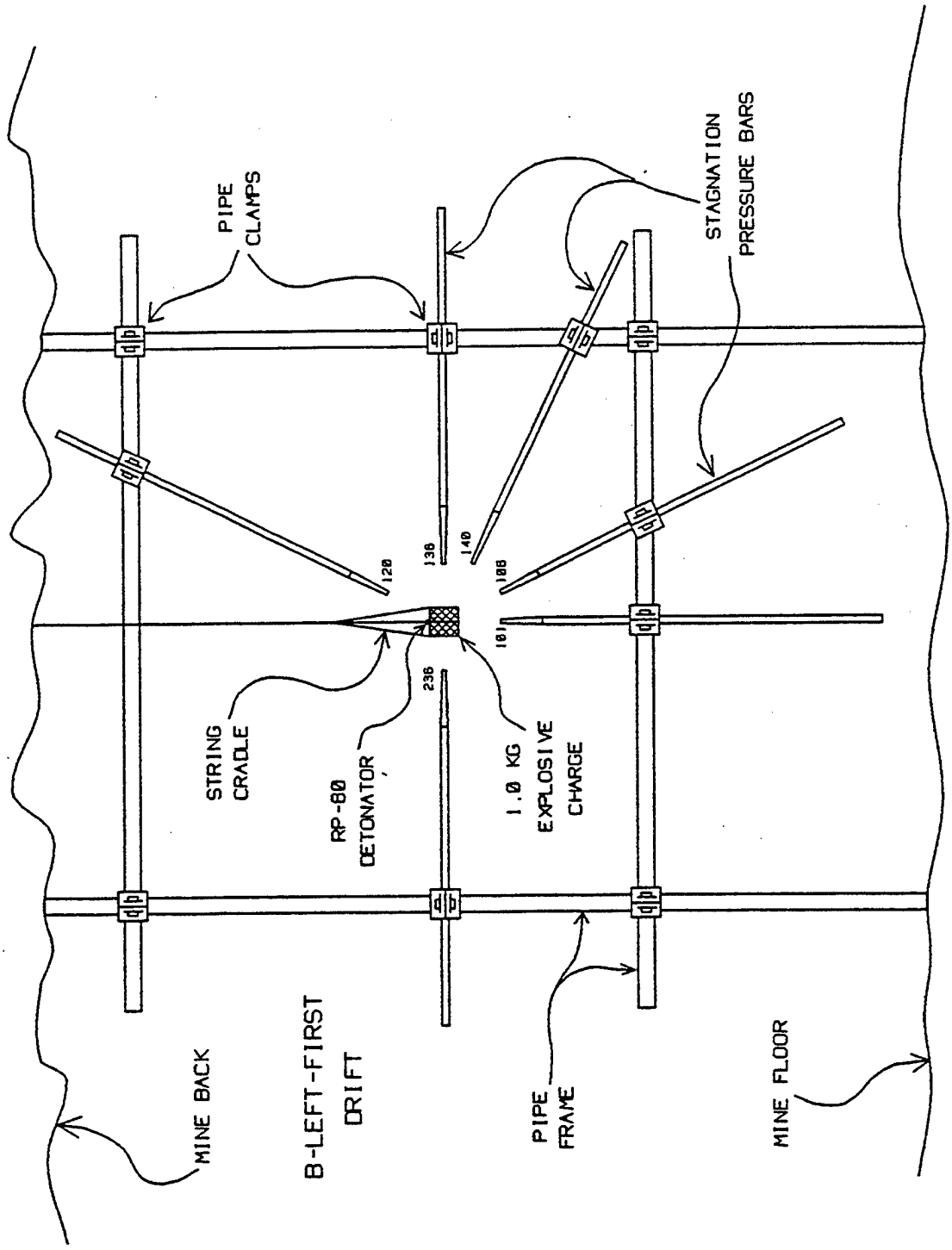

Figure 10. Diagram for the stagnation pressure bars.

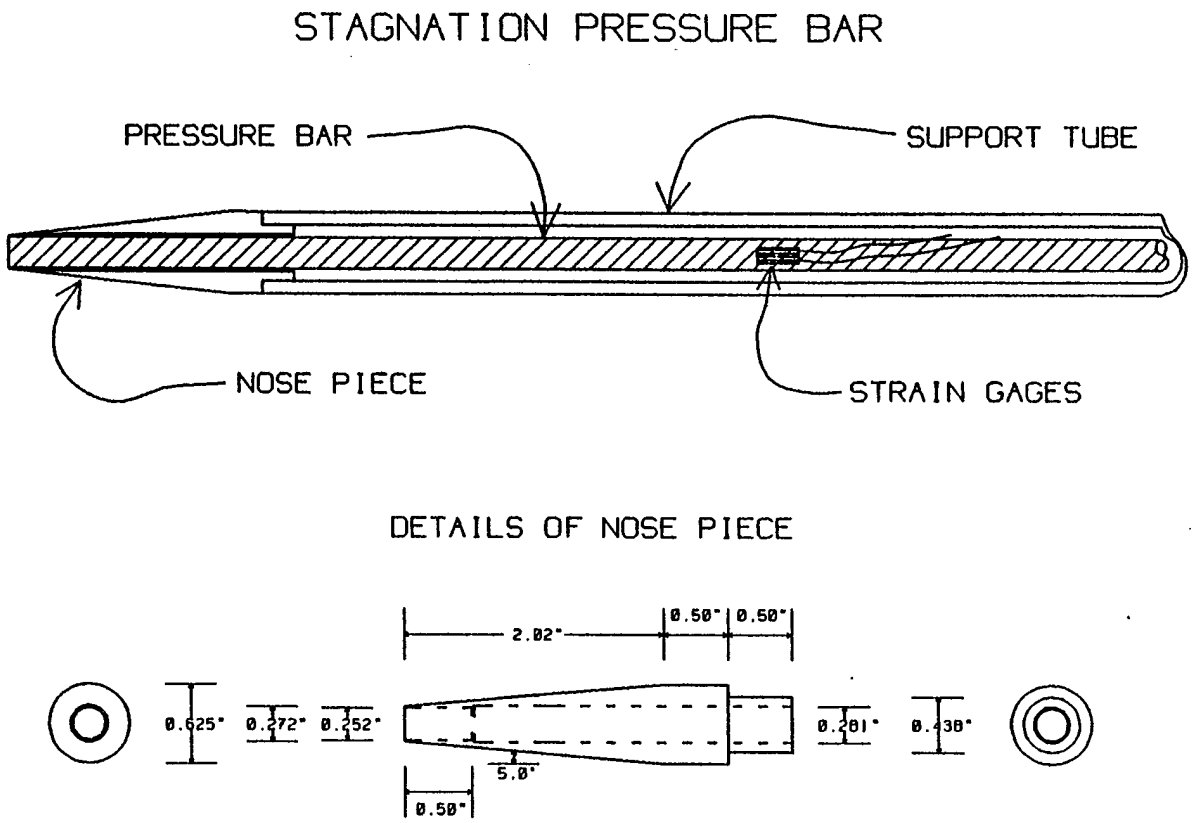

Figure 11. Pressure bar construction.

both 6.35 mm (0.25 inch) and 7.94 mm (0.3125 inch) diameters were built and used. The 6.35 mm bars were carried inside a steel tube with an inside diameter of 9.53 mm (0.375 inch) and an outside diameter of 15.88 mm (0.625 inch). The 7.94 mm bars were carried inside a steel tube with an inside diameter of 12.7 mm (0.50 inch) and an outside diameter of 19.05 mm (0.75 inch). Details of both the 6.35 mm and 7.94 mm conical obdurating nose pieces are shown in Figure 12. The ends of the bar towards the charge were carried in the obdurating nose piece while the tail or far end of the bars were carried on a small O-ring with a snug fit between the bar and the inside of the guide tube. A lubricating grease, containing molybdenum disulfide was used to seal and lubricate a 0.03 mm annulus between the bar and the inside of the nose piece.

The bars were instrumented with Micro-Measurement 350 Ohm strain gages in a half-bridge configuration. On each bar, two gages were carefully fastened to the bar with epoxy at a distance of 150.0 (±0.1) mm from the charge end and at exactly opposing positions within 0.1 mm. The balancing half of the strain gage bridge was provided by precision 350 ohm resistors in a gage box located within 4.0 m (13 ft) of the bar. The gages were mounted to the bars by first cleaning and lightly roughening the bar with 600 grit emery paper, then removing any residual dirt and oil with trichlorethylene and finally by pressing the gage into position with Hysol 608 epoxy. The gages were oriented with the active elements aligned with the axis of the bar, such that the gages measured bar shortening rather than Poisson bulging. The connection tabs on the gages were soldered to 26 gage teflon coated wires which were carried inside the guide tubes. At the far end of the bars and guide tubes the gage leads were soldered to two conductors inside a shielded cable. The far end of this cable was connected by screw connectors to the gage box containing the two 350 ohm resistors to complete the bridge circuit and a balancing resistor to enable the box output to be set to a desired null or offset voltage.

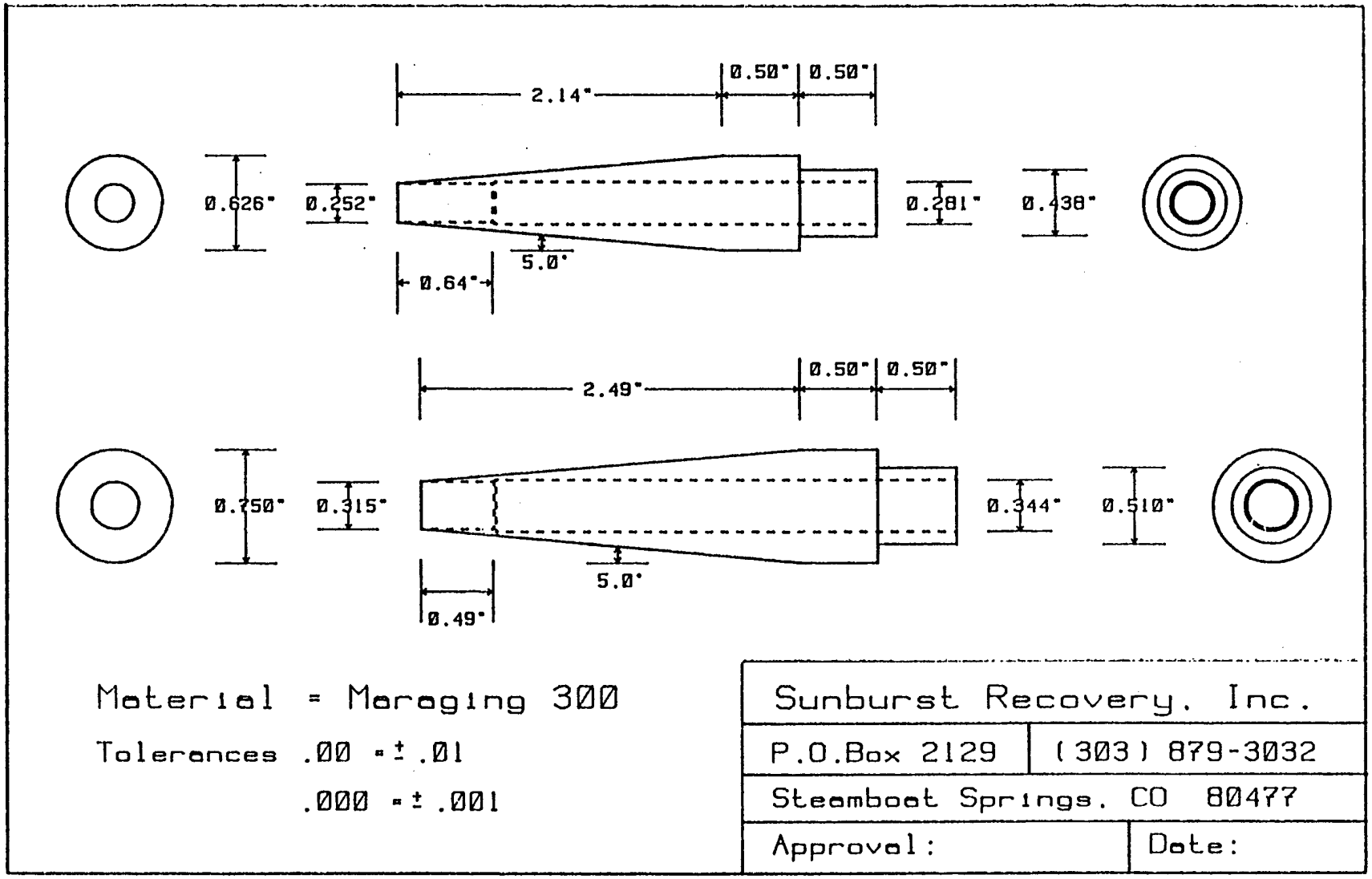

Figure 12. Nose cone details for the pressure bars.

The bars were constructed of two different steels, one being a polished and ground rod of H-13 (Latrobe Steel MM-66) and the other being V-44 (Latrobe Steel Carpenter Technology Viscount 44). The hardened and ground H-13 bars were only available in a 6.35 mm diameter at a maximum length of 0.61 m (2.0 ft). All longer 6.35 mm bars and all 7.94 mm bars were constructed from the V-44 steel. Details on the bars used at each gage location in each test are given in Table 9.

At the beginning of the program, the bars were calibrated utilizing a small gas gun in the University of Maryland laboratories to provide for a precise velocity symmetric impact on the end of a bar. The symmetric impact was realized by launching a 6.35 mm "piston" made of the same steel as the bar and with a length of 152.4 mm (6.0 in). By carefully measuring the bar wave velocity and with the assumption that particle velocity was one half of the impact piston velocity it was possible to calculate both stress and strain in the bar according to the equations presented in Section 5.1. After numerous calibration tests with both MM-66 and Viscount 44 bars, it was established that strain gage bridge output agreed with theoretically calculated output within 0.5 percent. As this degree accuracy was significantly better than required for measurements in the adverse environment of the free-filed tests, it was not necessary to perform precision symmetric-impact calibrations of all bars prior to the free-field tests. Less sophisticated impact tests were conducted on each bar with a simple compressed air gun prior the field tests in order to verify proper gage bonding and performance and functioning of the bridge and recording circuits.

4.4 Free-Field Test Setup and Procedures. All eight free-field tests were carried out in the Colorado School of Mines (CSM) Experimental Mine located in Idaho Springs, Colorado. This mine is a old gold and silver mine in gneissic and schistose rocks which has been used by CSM as an experimental facility for

Table 9. Steel bar data for the free field tests.

Charge Number	Shot Date	Gage Location 101	Gage Location 108	Gage Location 120	Gage Location 136-A	Gage Location 136-B	Gage Location 140	Gage Location 142	Gage Location 236	Notes and Remarks
CB.1	16-Aug-90	B-6-44		B-8-44	B-6-44		B-6-44			Low-Order Detonation
CB.2	20-Sep-90	B-6-44	B-6-44	B-8-44	B-6-44	B-8-44	B-6-44			Gage 120 Anomalous
CB.3	02-Oct-91	B-6-66	B-6-44	B-8-44	B-8-44		B-6-44		B-6-44	Bad Noise - esp. 236
CB.4	17-Oct-91	B-6-66	B-6-44	B-8-44	B-8-44		B-6-44		B-6-44	Bad Noise 136 & 236
LX.1	24-Aug-90	B-6-44			B-6-44	B-8-44	B-6-44	B-6-44		101 Amp Saturated
LX.2	30-Aug-90	B-6-44		B-8-44	B-6-44	B-8-44	B-6-44			Lost 136B
LX.3	25-Sep-91	B-6-66	B-6-44	B-8-44	B-8-44		B-6-44		B-6-44	Scopes Out of Range
LX.4	16-Oct-91	B-6-66	B-6-44	B-8-44	B-8-44		B-6-44		B-6-44	Bad Noise 108, 120 &140

several years. The mine environment, providing for complete protection from large air blasts and explosion debris, combined with the instrumentation and facility support available, made this an ideal location for conducting the free-field experiments. The experiments were carried out in two series, with four charges (two of Comp-B and two of LX-14) tested in August and September of 1990 and with four charges (also two of Comp-B and two of LX-14) tested in September and October of 1991. The details for each test are given in Table 10.

All the tests were conducted by utilizing a pipe frame constructed in the B-Left-First drift of the CSM mine to both carry up to six pressure bar gages in their protective tubes and to support the explosive charge. The pipe frame setup is illustrated schematically in Figure 13. The frame provided adequate support for the bars while neither interfering with the free-field conditions of interest nor being subject to damage by the tests. The explosive charge was suspended at the desired location by carrying the charge in a yoke made of 1.0 mm diameter cotton cord which was held in place on the charge with 12.7 mm wide fiber reinforced tape. The tape was wrapped around the top and bottom of the cylindrical charge at positions which were not in line with the various gage positions of interest. Except for the first test (CB.1 on Comp-B), the charges were detonated with a 1.0 g charge of pressed PETN held in a 2.0 g tube of Detaprime, a commercial blasting product made of PETN and a plasticizing binder. The Detaprime tubes were 12.7 mm long with a 6.35 mm inside diameter and a 12.7 mm outside diameter. The tubes were held to the top of the large charge with a strip of 12.7 mm wide fiber reinforced tape placed across the end of the tube and across the top of the charge. The 1.0 g PETN charge (and, consequently the main charge) were detonated by a Reynolds RP-80 exploding bridgewire detonator, in all except the last two tests. The outside diameter of the RP-80 fit snugly into the end of the Detaprime tube which was not packed with PETN so as to be in excellent contact with the packed PETN.

Table 10. Free field test data.

Charge Number	Shot Date	Ambient Pressure (kPa)	Ambient Temperature (K)	Notes and Remarks
CB.1	16-Aug-90	1135.8	283.6	Low Order Detonation - No Data
CB.2	20-Sep-90	1092.5	283.6	Good Detonation - 6 of 6 Gages
CB.3	02-Oct-91	1106.4	283.6	Good Detonation - 4 of 6 Gages
CB.4	17-Oct-91	1073.0	283.6	Good Detonation - 4 of 6 Gages
LX.1	24-Aug-90	1089.9	283.6	Good Detonation - 4 of 5 Gages
LX.2	30-Aug-90	1091.5	283.6	Good Detonation - 4 of 5 Gages
LX.3	25-Sep-91	1100.6	283.6	Good Detonation - Data Truncated
LX.4	16-Oct-91	1085.1	283.6	Good Detonation - 3 of 6 Gages

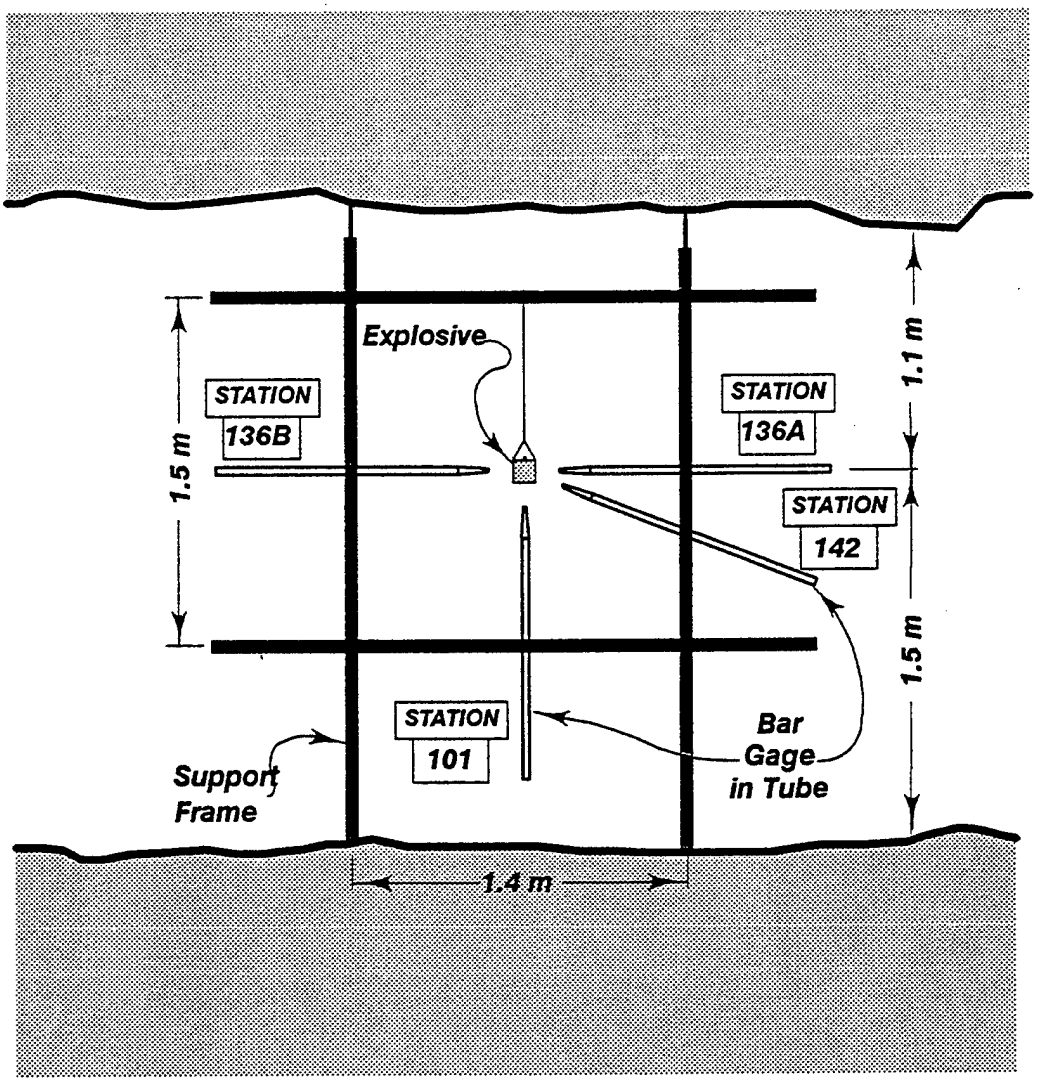

Figure 13. Experimental setup in the mine tests.

For the first test, CB.1 on a Comp-B charge did not employ the PETN/Detaprime booster and had the RP-80 in direct contact with the top center of the charge. This initiation system failed to initiate a high order detonation in the Comp-B but did cause enough low-order detonation to completely pulverize the Comp-B. A post test inspection indicated that most of the Comp-B did not burn but was highly pulverized and spread as a fine powder all over the B-Left-First drift. For the last two tests, LX.4 on LX-14 and CB.4 on Comp-B, a 1.0 m long detonating delay line of 7 grain/foot mild detonating cord was used between the RP-80 and the PETN/Detaprime booster. This delay line was implemented to increase the time between the firing of the RP-80 and the detonation of the charge so as to allow severe electrical noise associated with RP-80 initiation to decay to a more acceptable level.

For the first series of tests, conducted in 1990, data recording included four channels of 16 megasample/second digital recording utilized for the gages with the most rapid rise time and four channels of 0.5 megasample/second digital recording for gages with slower rise times and/or as backup channels. For the second series of tests, conducted in 1991, data recording included eight channels of 16 megasample/second digital recording, which gave the higher recording rate for all six gages utilized in these tests. In addition, four channels of 0.5 megasample/second digital recording was used as backup. All digital data was reduced to pressure time records and filtered as necessary to provide the best quality data. Atmospheric pressure and temperature were recorded for all tests.

5. MEASUREMENT SYSTEM FOR THE CLOSED VESSEL AND FREE FIELD

5.1 Closed Vessel. During the course of the project five different sensors were used to measure blast pressure in the closed vessel tests. They were bar gages, the PCB piezoelectric pressure gages, flatpack of carbon pressure gages in a protective

sleeve, 1/8 watt carbon resistor gages, and PVDF piezoelectric pressure gage. The results from the flatpack gages were not satisfactory and abandoned after only a few tests (all using 10 g explosives). The most reliable and easiest transducer to use was the bar gage and most of the blast pressure data resulted from records from this gage. Each of the sensors and the measurement systems are discussed in next several sections.

5.1.1 Bar Pressure Gage. The bar pressure gages used for these measurements is a application of the propagation of stress waves in a cylindrical bar (Kolsky, 1963; Edwards, Hooper, and Tasker, 1978; Edwards, Thomas, and Tasker, 1980). If one end of a long steel bar is struck by another steel bar, an elastic stress wave propagates along the bar and at the same time an elastic wave is sent back into the striker bar. The velocity of the steel striker bar controls the stress level attained in the bar and hence the strain. To guarantee elastic conditions the stress in the bar must be less than the yield strength of the bar steel and is an upper limit on the velocity of the striker bar. The equations that govern the stress and strain achieved in the bar are given by

$$\sigma = E\ \epsilon \qquad (1)$$

$$\epsilon = V_0 / 2C_1 \qquad (2)$$

$$C_l = (E / d_0)^{0.5} \qquad (3)$$

where σ = stress in Pa, $\epsilon = \Delta L/L_0$, E = Young's modulus in Pa, C_1 = elastic wave speed in the steel in m/s, V_0 = striker bar velocity in m/s, and d_0 = density of the steel in kg/m^3. By measuring the strain in the bar as a function of time as the stress wave propagates and knowing Young's modulus, the stress wave amplitude can be calculated using Eq.(1). Another method is to measure the striker bar velocity and then calculate the strain from Eq. (2) knowing the elastic wave speed in the bar. The stress is then calculated from Eq. (1). The elastic wave speed is determined from a knowledge of Young's modulus and the material density or the velocity is measured experimentally.

In the blast overpressure measurement using the bar gage, hardened and ground steel bars [Ref. Latrobe] 6.35-mm diameter by either 0.609-m or 0.914-m long were used. The mechanical properties for the steel bars are a density of 7800 kg/m^3, a Young's modulus of 212.3 GPa, an elastic wave speed of 5217 m/s, hardness of RC-66, and a yield strength of 2.0 GPa (290 ksi). The ends were ground flat. Two strain gages oriented 180 degrees apart were attached to the bars 125 mm from one end to monitor strain as a function of time. The gages were purchased from Measurements Group, Inc. whose catalogue number is EA-06-062AQ-350. These gages have a small active element of 1.588 by 1.588 mm (1/16 inch square) and a nominal resistance of 350 ohms. In addition 25-mm lead wire extensions were furnished with each gage to simplify soldering to the connecting circuits. Mounting techniques suggested by Measurements Group were followed for intimate contact to the bar surface and long term attachment under dynamic conditions.

5.1.2. PCB Pressure Gage. One port in the cylindrical chamber contained a piezoelectric pressure gage manufactured by PCB Piezotronics, Inc. One of two basic gage models were used, Models 109A02 or 109A12 and 119M39/003A05/402M99. The sensing element for both gages was quartz and both gages had a maximum pressure range of 125,000 psi (860 MPa). Table 11 is a specification list for the gages. The difference between the two gage types is that the 100 series gages have a charge amplifier built into the gage body while the 110 series gage requires an external charge amplifier. The 100 series gage were used in many of the blast pressure tests with very little success, that is, the signal traces contained very high frequency and high amplitude noise that swamped the pressure pulse. The source of the noise was believed to be a combination of shocking the built-in integrated circuit in the gage, the cable connection rattling from the blast impact, and the one piece transducer body configuration. This conclusion was arrived at when the 100 series gage was replaced by the 119M39 gage and resulted in credible blast pressure

Table 11. PCB Pressure Gage Specifications From The Catalogue.

	Model 109A12	Model 119M39
Sensitivity (mV/psi) (pC/psi)	0.07	0.25
Resolution (psi)	2	2
Resonant Frequency (kHz)	500	500
Rise Time (us)	1	1
Linearity (% FS)	2	2
Range For 5V out (psi)	1.0×10^5	
Maximum Pressure (psi)	1.25×10^5	1.25×10^5
Capacitance (pF)		20
Impedance (ohms)	100	1.0×10^{13}
Weight (g)		11

signals. This gage has an external charge amplifier in the cable line between the gage and the power supply, a two piece gage body for isolation, and very tight connection between the cable nut and the gage to minimize rattling and hence, high frequency noise.

Each model had a ceramic ablative coating on the end to protect the diaphragm and housing from the blast environment in this application.

5.1.3. Piezoresistive Pressure Gages. Two types of piezoresistive gages, foil and eighth watt standard resistor, were used to measure the blast pressure on several tests. In both instances carbon was the sensor material. Carbon has a negative coefficient of resistivity, that is, the resistance of the carbon element decreases as the pressure increases. Carbon has high sensitivity at low pressures (100 to 2000 MPa) and low sensitivity at high pressures. A foil type carbon pressure gages manufactured by Dynasen Inc., model C300-50-EKRTE, was sandwiched between mica and mylar sheets to form a flatpack gage which was placed at the desired location in the chamber. The mica and mylar protected the gage against abrasion from the blast long enough to record a signal. The carbon sensing element is 3.81 by 5.08 mm and the gage has a nominal resistance of 50 ohms to match 50 ohm coaxial signal cable. The gage was connected to one arm of a Wheatstone bridge network and energized by a special pulsed power supply. This circuitry minimized Joule heating of the gage causing baseline shift over long energizing periods. As it turned out these gages were difficult to use and did not produce credible signals. As a consequence this gage type was abandoned in favor of the carbon resistor gage technique.

The sensing element for this second piezoresistive gage is a one eighth watt standard carbon composition resistor placed (Watson, 1967 ; Wilson, 1987) placed in the path of the blast wave inside the confinement chamber. A 470 ohm resistor and the

lead wires were encased in epoxy to protect and insulate the gage long enough to extract a signal. No special pulsed circuitry was used to connect and power the gage. Pressure gages constructed in this manner had high sensitivity at low pressures similar to the carbon foil gages. Generally the gages survived the blast environment long enough to produce credible signals. An accurate calibration curve prevented continuous usage. This pressure gage technique, however, is on firm ground.

5.1.4. PVDF Pressure Gages with the Bar Gage. The final pressure gage technique combines the use of a PVDF gage (Bauer, 1988) to measure the stress in a steel bar from the blast wave, similar to the bar pressure gage described above. PVDF (polyvinylidene difluoride polymer) gages are piezoelectric pressure gages which generate electrical charge proportional to the applied deformation. The sensitivity of this material, that is, the charge/unit pressure, is very large (much greater than quartz by comparison) resulting in the production large voltages from small stresses. For this application, a PVDF gage is placed between the ends of two 0.3-m long steel bars of which the free end of one bar is inserted in the chamber. Figure 14 shows the arrangement. In this configuration the PVDF gage provides a direct measure of the stress induced in the bar by the blast wave. A strain gage pair was also mounted on the bar exposed to the blast (first bar) as an independent measurement of the stress and as a means to calibrate the PVDF gage.

6. SIGNAL RECORDING

6.1. Closed Chamber Tests. The following sections describe some of the signal recording steps taken for the closed vessel tests such as signal conditioning, electrical grounding, and calibration.

6.1.1. Recording Strain Gage Signals from the Bar Pressure Gages. The strain gage pairs on each of the steel pressure bars

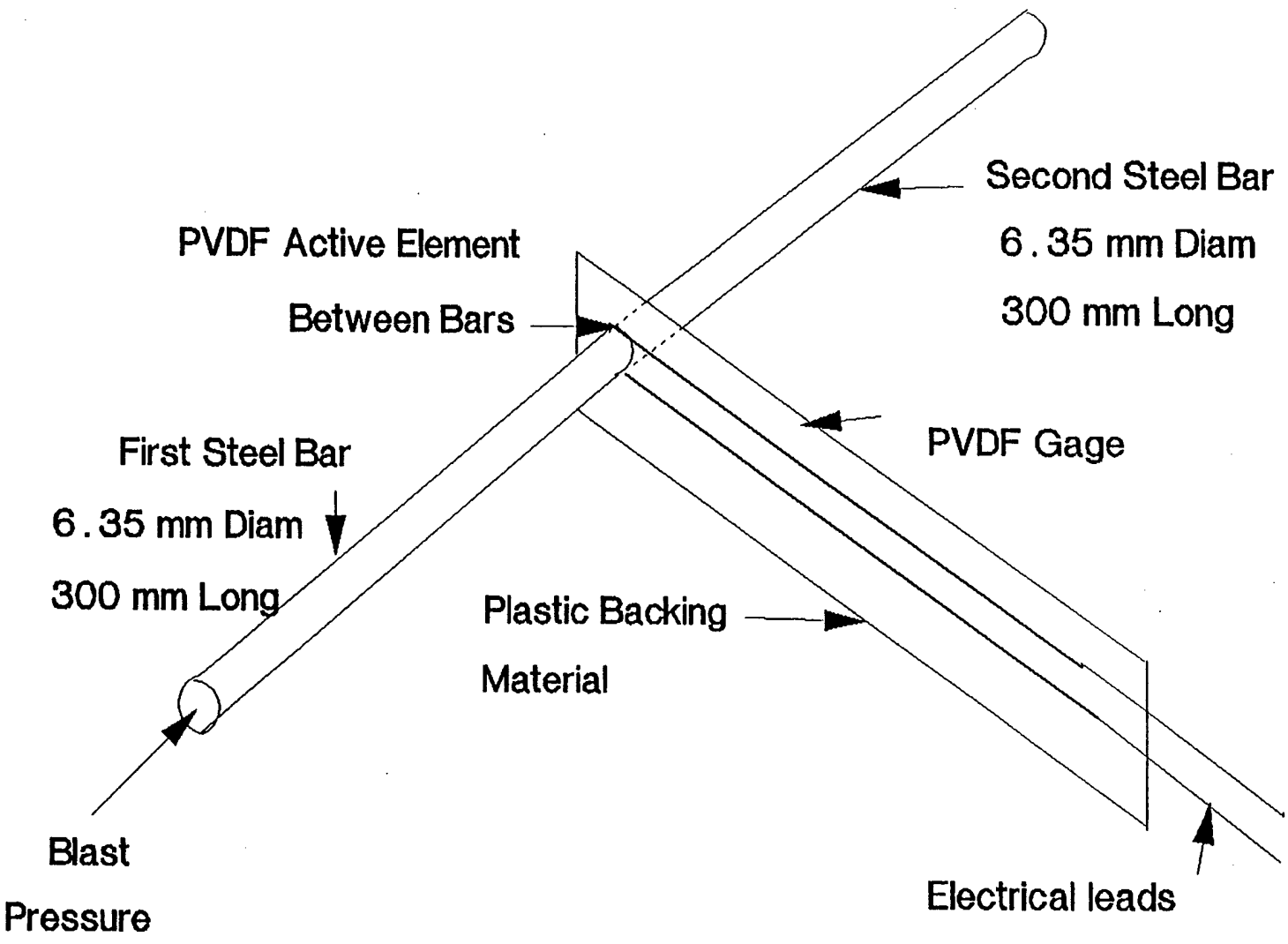

Figure 14. PVDF - bar gage arrangement.

were connected to a constant voltage, voltage sensitive Wheatstone bridge circuit. The circuit was powered by a 15 V DC supply and the output voltage amplified by Tektronics amplifiers, either model AM501 Op-Amp or model AM502 differential amplifiers. The signal is then recorded on Nicolet digital storage oscilloscopes model 320 and the signal data are stored in a bubble memory device for processing by computer later. Figure 15 is a schematic diagram of the circuitry and measurement system. Generally, the AM501 and AM502 amplifiers were set at a gain of 100 which provided sufficient voltage for the Nicolet scopes voltage range. In addition the amplifiers were operated in the DC to 1.0 MHz response range to record the signal at the widest bandwidth available. Even though the gage-bridge-amplifier-scope system was powered continuously for long periods during test setup, calibration, and execution, a stable baseline trace was observed on the Nicolet scopes. The bridge completion circuit for each set of bar strain gages was housed in a small aluminum box placed within 200 mm of the gages to keep the lead wires as short as possible to minimize noise pickup.

The first half of the total number of tests performed utilized approximately 15 m of twisted shielded wire pairs between the bridge box and the amplifiers in order to conduct the test remotely for safety considerations. However, bursts of high frequency noise were common on the signal traces and at times interfered with the gage response signal. To attack the noise problem for the other half of the tests, an attempt was made to encase the entire system - chamber, bars, bridge circuits, signal wires, amplifiers, and scope - in a "Faraday cage" to minimize noise pickup such as detonator firing noise and current loops. First, all the twisted pair signal wire was replaced with RG-223 50 ohm coaxial cable (RG-223 has a double shield). Then the bars were shielded by mounting them inside steel tubes and even the bridge boxes attached to the tube. Next the chamber and bar shields were connected to a 15-m long heavy ground wire strap to the recorder end of the system. There the amplifiers and the

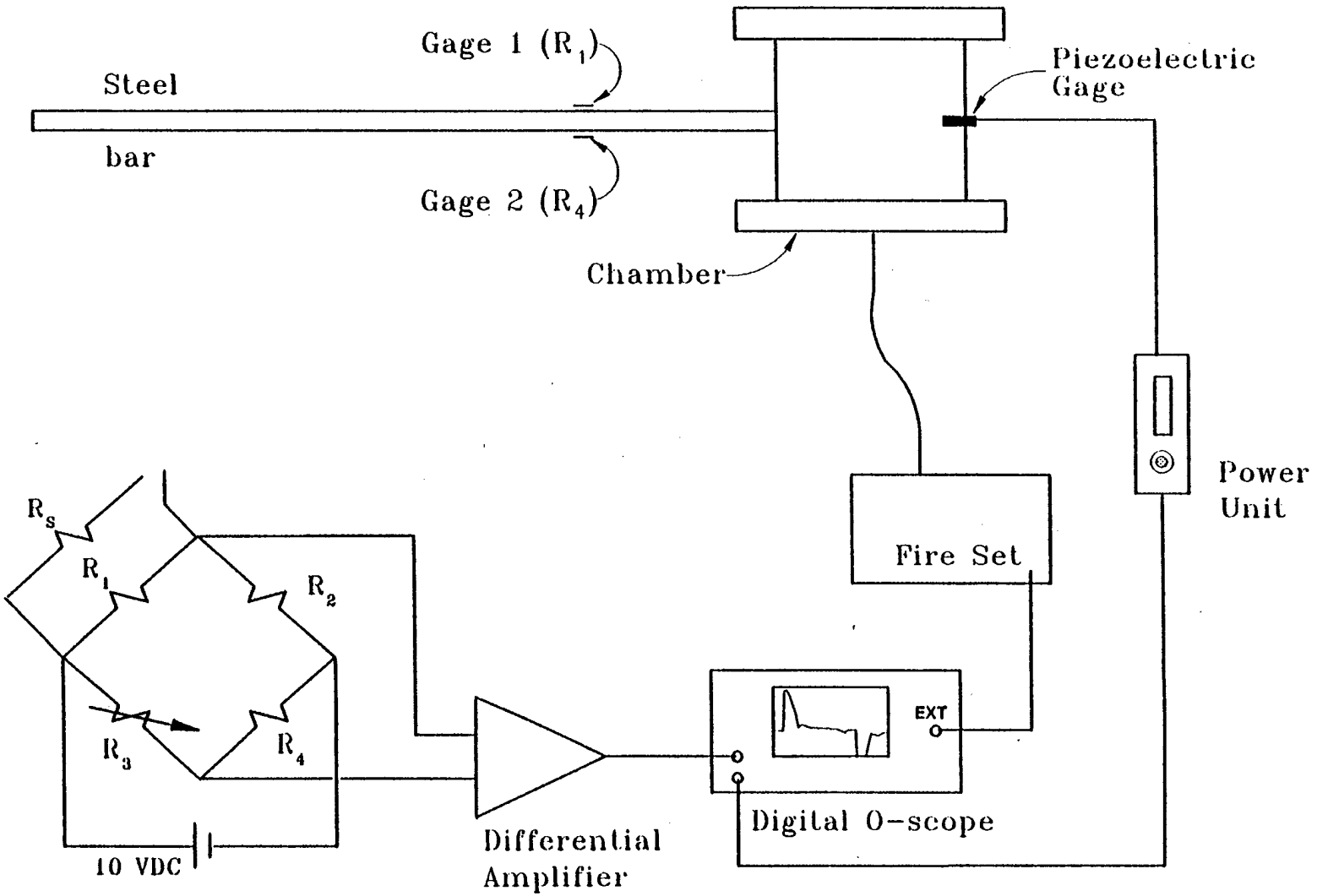

Figure 15. Bar pressure gage signal map and recording system.

Nicolet scopes were securely grounded to the strap and the strap in turn was grounded to an "Earth ground". This scheme provided only one grounding point in the system, that is, at the recorders. The objective was to eliminate current paths through ground loops that may have existed between the recorders and the chamber and/or experiment end. The bursts of noise were not eliminated completely, but the resulting signal traces were much quieter and cleaner than with the previous system. The source of the high frequency bursts is still unknown.

Calibration of the bar gage was accomplished by two methods. One technique consists of striking the end of the bar with a projectile of the same diameter and steel as the bar with a known velocity and then use Eq. (2) to calculate the strain. Meanwhile the bar is instrumented with stain gages to measure strain directly as a function of time. The strain gages are connected to the identical signal conditioning and recording circuitry via the same signal paths used for the blast tests. The velocity of the projectile is accurately measured by the laser intercept method and the bar wave velocity is determined from the measurement of the length of the bar, the measurement of the distance between the strain gage location and the end of the bar, and the measurement of the wave reflection times between the ends of the bar from the signals. A comparison of the measured and calculated strains for several projectile impact velocities resulted in values that matched to within 0.5 %. Results from this calibration exercise provided confidence in the bar gage as a method to measure the blast pressure. Each steel bar and strain gage combination was calibrated in this manner before use in a test. This calibration method was not used each time a test was performed, but occasionally a performance test was done to verify the system accuracy.

The second calibration procedure was used for each blast measurement test as well as for each verification test described in the previous paragraph. This method consists of switching an

accurately known shunt resistance across the two arms of the Wheatstone bridge containing the strain gages (see Figure 15). After balancing the bridge, the shunt resistors are connected in the circuit and the voltage read. The calibrated strain, ϵ_c, is then computed from the following relationship,

$$\epsilon_c = (1/S_g)(R_g/R_s+R_g) \qquad (4)$$

where S_g is the gage factor provided by the manufacturer and R_g and R_s are the nominal strain gage resistance and the known shunt resistance, respectively. In practice the calibration voltages were recorded via the same paths as the signal voltages from the tests for each bar gage system on every test. The actual values for the parameters in Eq. (4) are S_g = 2.09, R_g = 350 ohms, and R_s = 174650 ohms. These values produced a calibration strain of 957 microstrain. The shunt resistance was a permanent part of the Wheatstone bridge circuit box. Each bar gage has a complete strain versus output voltage calibration curve for the 15.0 V bridge input.

6.1.2. PCB Gage Signal Recording. Signal recording from these gages followed the methods suggested by the manufacturer. The output was sufficient that the signal voltages were run directly to the Nicolet oscilloscopes. The only signal conditioning was the unity gain charge amplifier between the gage and the power supply, either as a built-in integrated circuit or as an external charge converter. Figure 16 is a diagram of the recording circuit and the signal path to the recorder.

PCB provided the calibration curve for the gages (in this case a linear curve) which afforded easy conversion from voltage to pressure. A note of caution. These gages experienced many high pressure blast waves which may have significantly altered the calibration curve. Occasional calibration over the course of the testing is necessary to ensure confidence in the measurements.

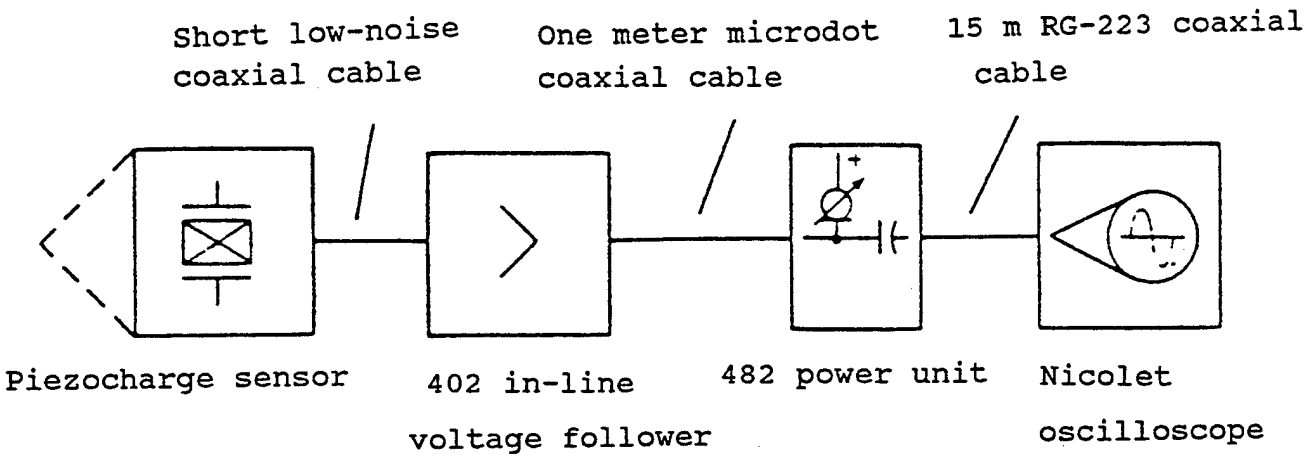

Figure 16. PCB pressure gage signal map and recording circuit.

6.1.3. PVDF Gage Signal Recording from a Bar Gage. Figure 17 is the basic circuit diagram for recording the signal voltage. A determination of the stress, $\sigma(t)$, from the voltage is by means of the following relationship,

$$\sigma(t) = [V(t)/10.025]^{1.654} \qquad (5)$$

where V(t) is the measured voltage and the stress is in gigaPascals. The coefficients are for a specific PVDF gage model whose calibration is supplied by the manufacturer. The output voltage from the PVDF gage in this configuration was several volts and hence, no amplification was necessary. RG-223 coaxial cable 15-m long provided the conduit between the gage and the Nicolet digital oscilloscope.

6.2 Recording Instrumentation for Free-Field Tests in CSM Mine. Due to the severe air blast occurring in the immediate vicinity of the free-field tests with explosive charges approaching 1 kg in weight, it was necessary to locate the recording instrumentation at an adequate distance from the test frame discussed in Section 4.4, above. The multiple drift layout of the CSM mine allowed an instrumentation alcove to be located 76 m (250 ft) from the test frame with two 90 degree drift intersections between the frame and the alcove serving to attenuate the air blast. Eight 50-Ohm coaxial cables were strung from the test frame to the alcove for data transmission during each test. In addition, a three conductor shielded cable was strung to provide charging and fire control for the Reynolds FS-10 EBW (Exploding Bridge Wire) firing system. Each of the coaxial cables was calibrated for signal loss from the test area to the alcove and was checked for loss and noise prior to each test. The signal loss for the coaxial lines was found to be a fairly uniform 16 percent.

Due to the long coaxial cable lengths it was necessary to amplify the gage output signals at a location near the test

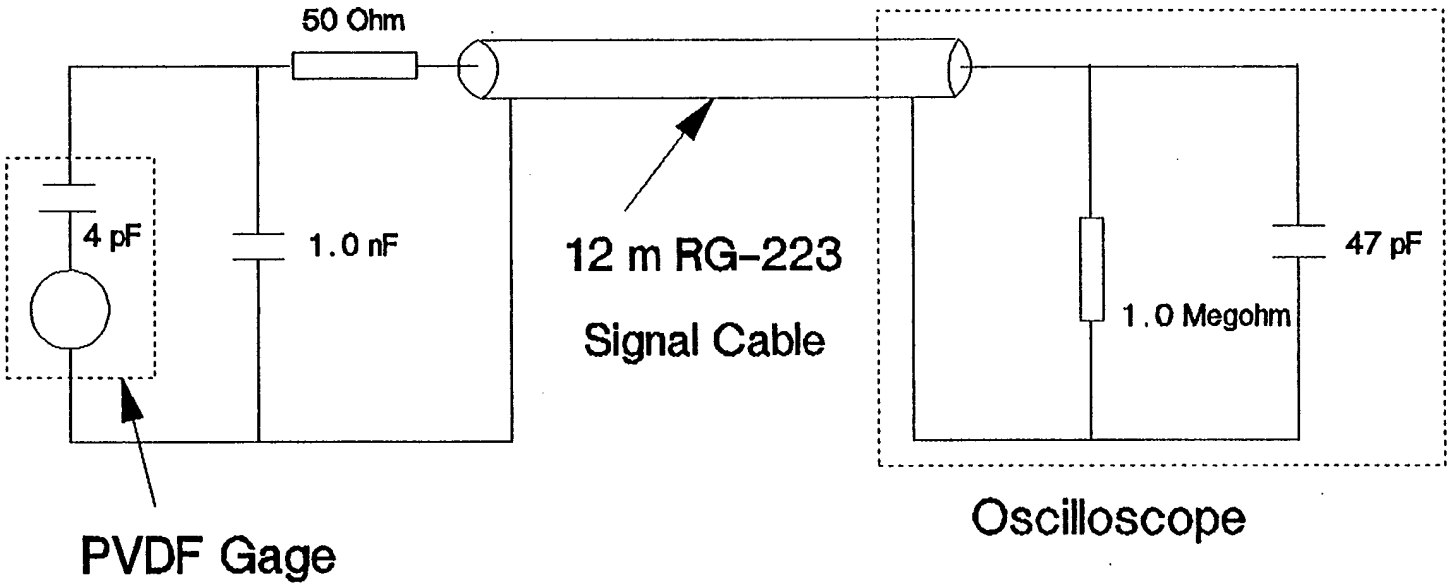

Figure 17. PVDF pressure gage signal map and recording circuit.

frame. Both Tektronix 501 operational amplifiers and Tektronix 502 differential amplifiers were employed. While the 502 units gave precise gains, they would only provide a satisfactory signal to noise ratio at a minimum gain of 100 and their peak voltage limitation of 5 volts precluded their being used for the ground zero gages at position 101. The gain of the Tektronix 501 amplifiers could be set by an appropriate resistor selection for their op-amp functioning but their effective gain was found to be highly affected by the coaxial lines, any 50 Ohm termination used at the alcove end of the lines, the absolute value of the resistors used to set their gain and the impedance of the strain gage circuit providing input for the 501s. Consequently it was necessary to calibrate carefully the complete circuit when 501s were used. Conversely, the Tektronix 502 differential amplifiers gave a signal gain that was independent of the above factors and circuit calibration or verification for each test was considerably simpler.

For the first series of tests, conducted in 1990, data recording included four channels of 16 megasample/second digital recording utilized for the gages with the most rapid rise time and four channels of 0.5 megasample/second digital recording utilized for gages with slower rise times and/or as backup channels. A Tektronix 2214 digital oscilloscope with four channels of 16,000 8-bit words was used for the 16 MHz data sampling. The 2214 had the provision for digital data transfer to a microcomputer so that the data could be reduced, filtered, analyzed and plotted as desired. A Rapid Systems 4x4, R-1000 microcomputer based digital data acquisition system was used for the 0.5 MHz data sampling. The Rapid Systems unit had four channels of 32,000 8-bit words with the data being directly transferred to the host microcomputer after each test. For the second series of tests, conducted in 1991, data recording included two Tektronix 2214 units giving eight channels of 16 MHz digital recording, which gave the higher recording rate for all six gages utilized in each of these tests. In addition, the Rapid Systems 4x4 unit was used to provide four backup channels

at 0.5 MHz. All digital data was reduced to pressure-time records, filtered as necessary to provide the best quality data and plotted for presentation. Atmospheric pressure and temperature were recorded for all tests.

7. DATA ANALYSIS AND RESULTS FROM THE CLOSED VESSEL TESTS

7.1. Typical Signals. There are hundreds of signal records from approximately 50 blast pressure tests. Only representative records are presented from the various gage types. Records for all tests are contained in an Appendix and on the floppy disks submitted with this report. The records show gage pressure as a function of time and most are from the bar gages since the bulk of the pressure measurements were using this method.

7.1.1. Bar Gage Records. Typical bar gage signal records are shown in Figures 18 to 29 and represent tests using 10 and 15 g charges of Comp B, LX-14, and Pentolite. The records also represent measurements from several pressure measurement stations described in Section 2.1, Table 1, and Figure 2. Figures 18 and 19 are records from a 15 g test on Comp B from stations 1 and 36 which are, respectively, locations on-axis with the charge and at the center-of-gravity (CG) of the charge. Figures 20 and 21 are records from a 15 g test on LX-14 at the same stations as the Comp B test. Figures 22 and 23 are records from a 10 g test on Pentolite also from stations 1 and 36. Figures 24 and 25 are signals from a 15 g Comp B charge from stations 42 and 47 and Figures 26 and 27 are signals from a 15 g LX-14 charge also from stations 42 and 47. These station numbers represent locations that are above and below the CG for the explosives. Figure 28 is a signal from a 10 g Pentolite charge from station 45. This number also represents the positions above the CG of the Pentolite charge. Refer to the Appendix for all the records.

7.1.2. PCB Gage Records. There are only a few PCB gage signals that proved to be credible and two records are shown in Figures 29 and 30. The record in Figure 29 is from a Pentolite test with

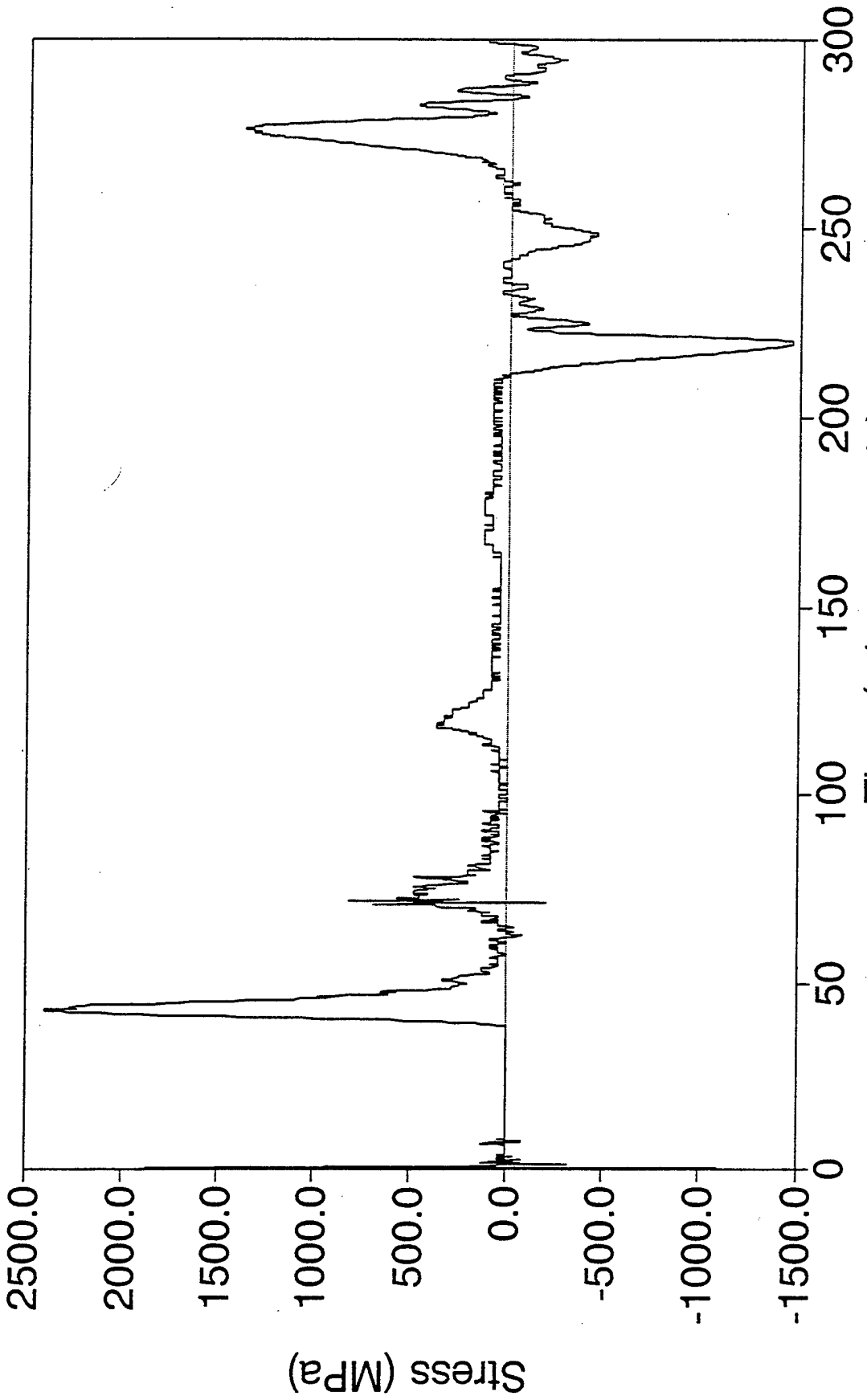

Figure 18. Station 1 bar gage signal, 15 g Comp B in chamber 2.

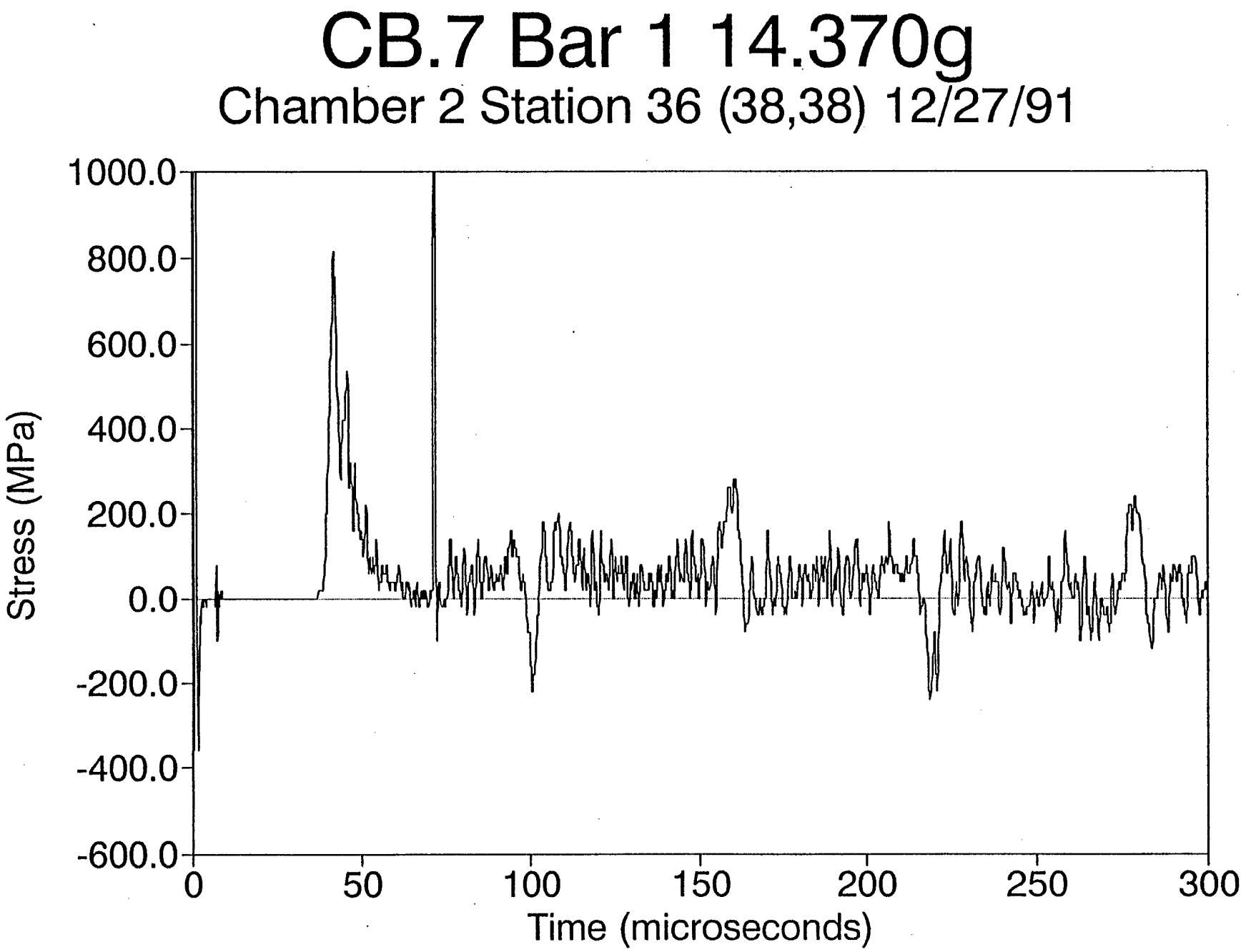

Figure 19. Station 36 bar gage signal, 15 g Comp B in chamber 2.

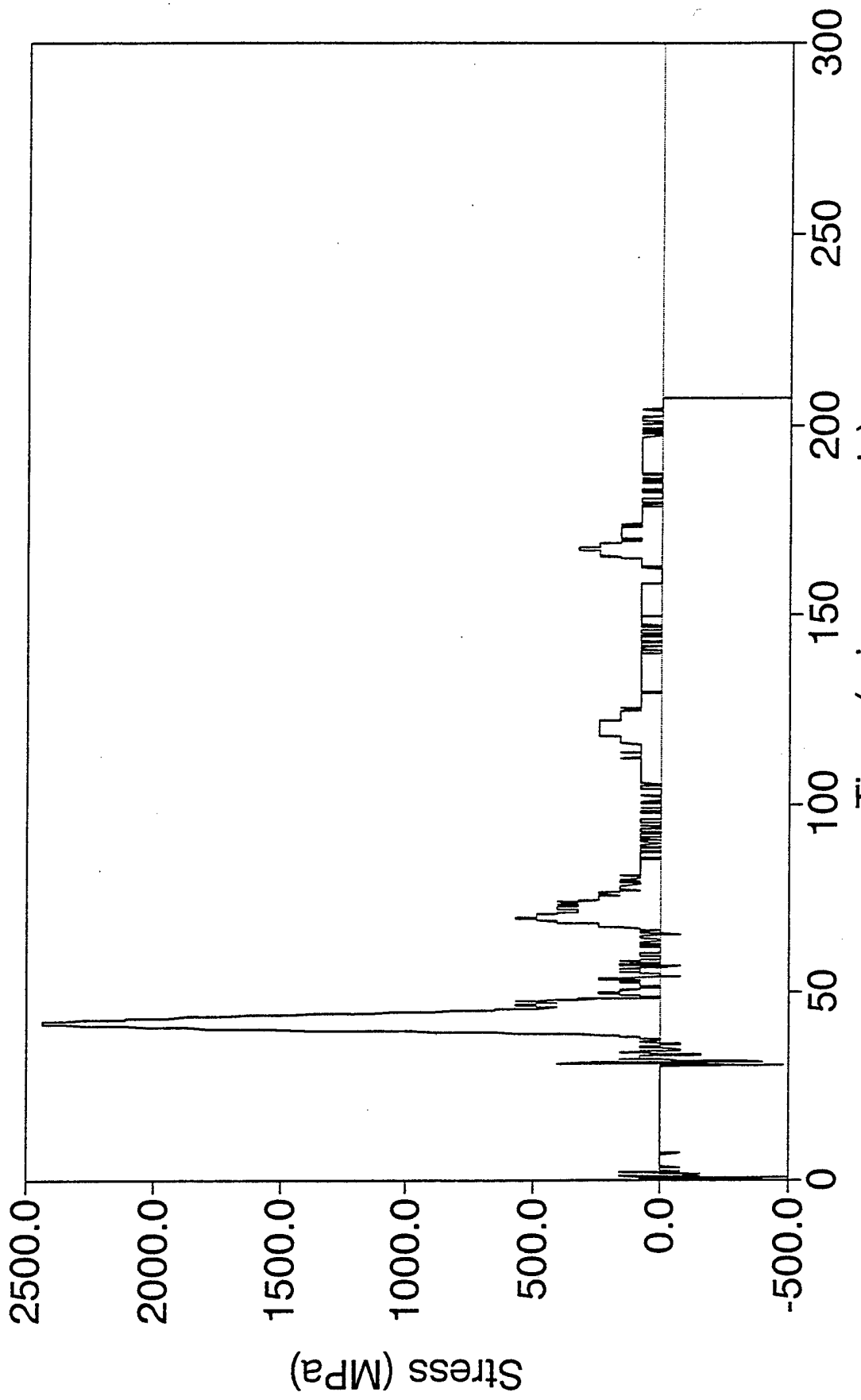

Figure 20. Station 1 bar gage signal, 15 g LX-14 in chamber 2.

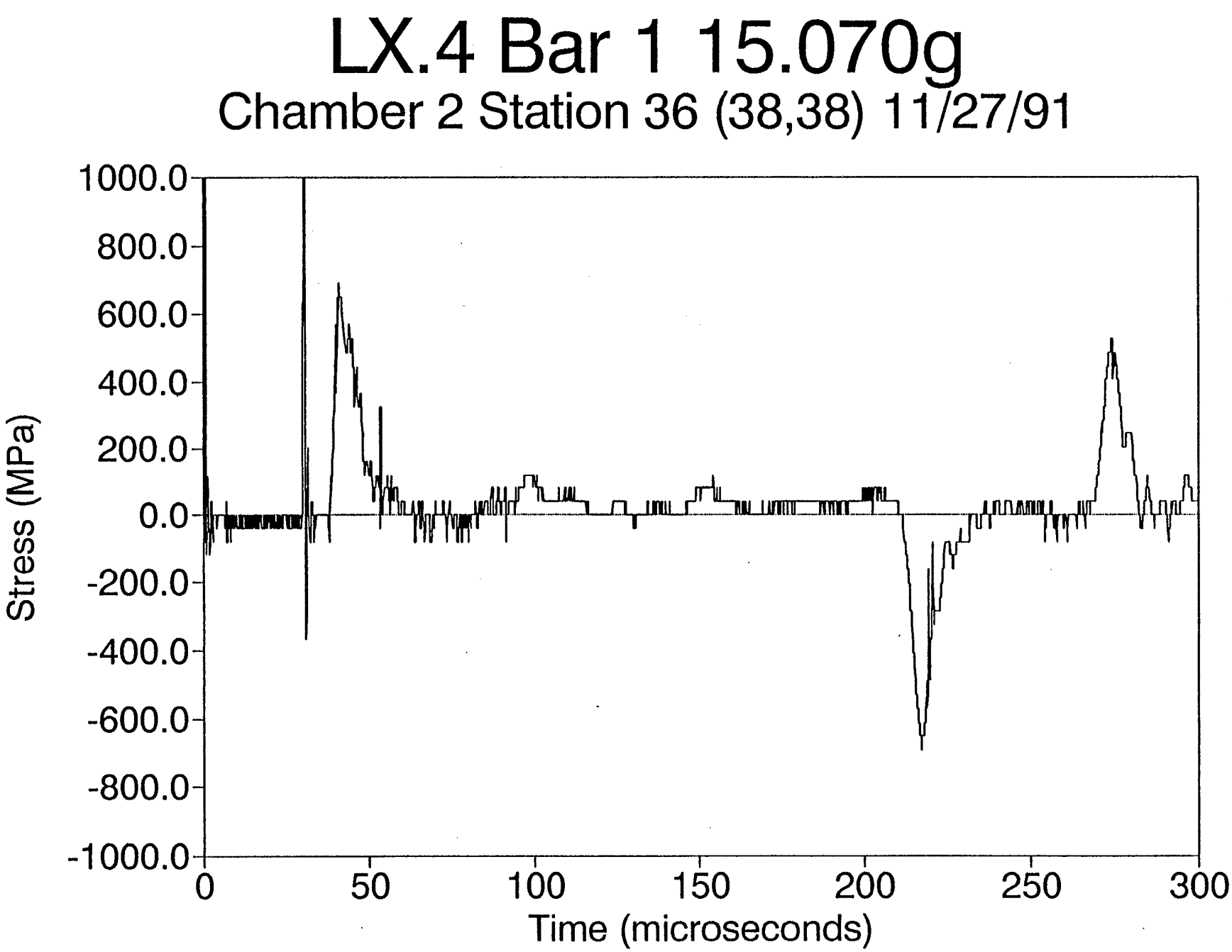

Figure 21. Station 36 bar gage signal, 15 g LX-14 in chamber 2.

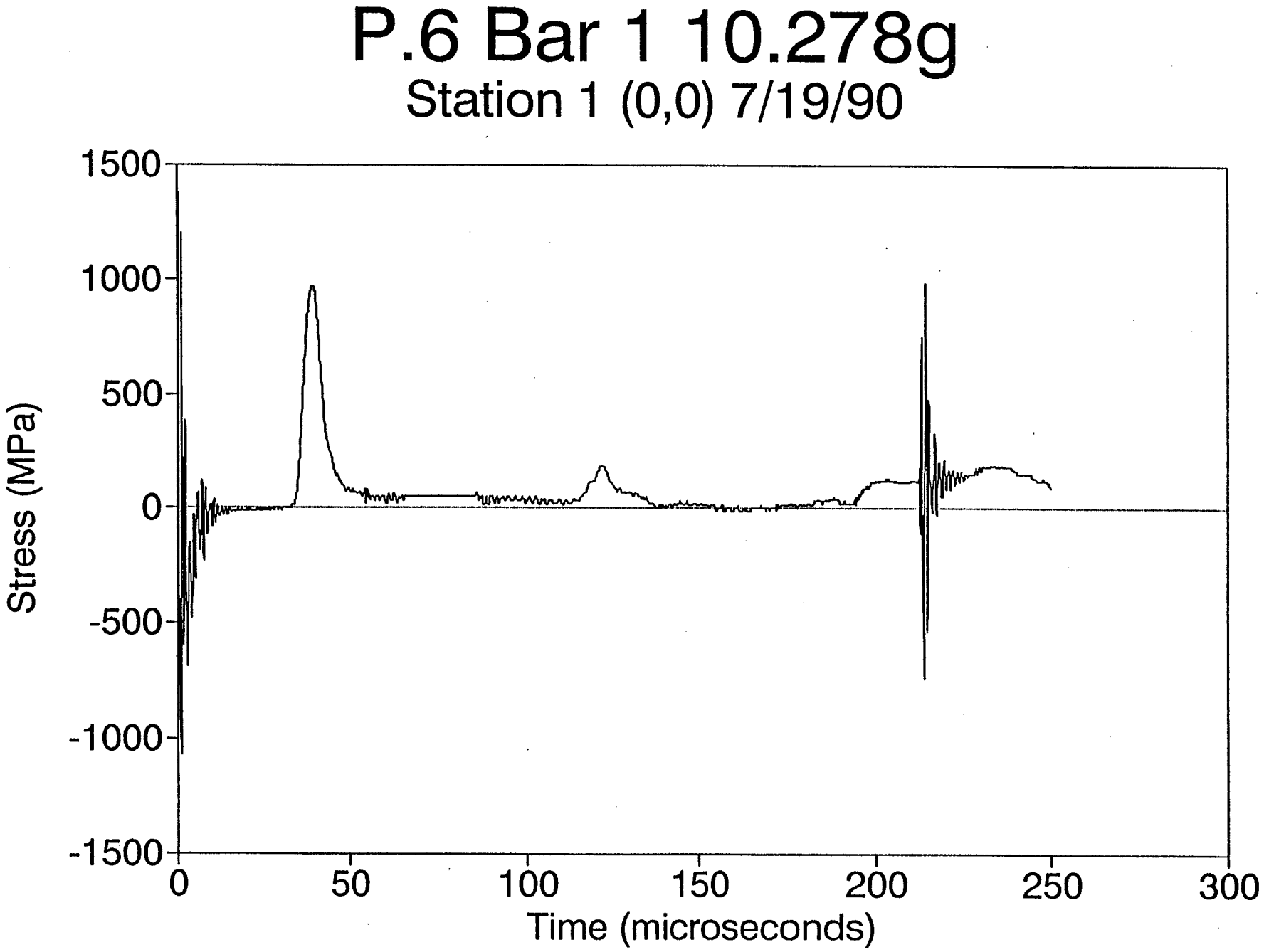

Figure 22. Station 1 bar gage signal, 10 g Pentolite in chamber 1.

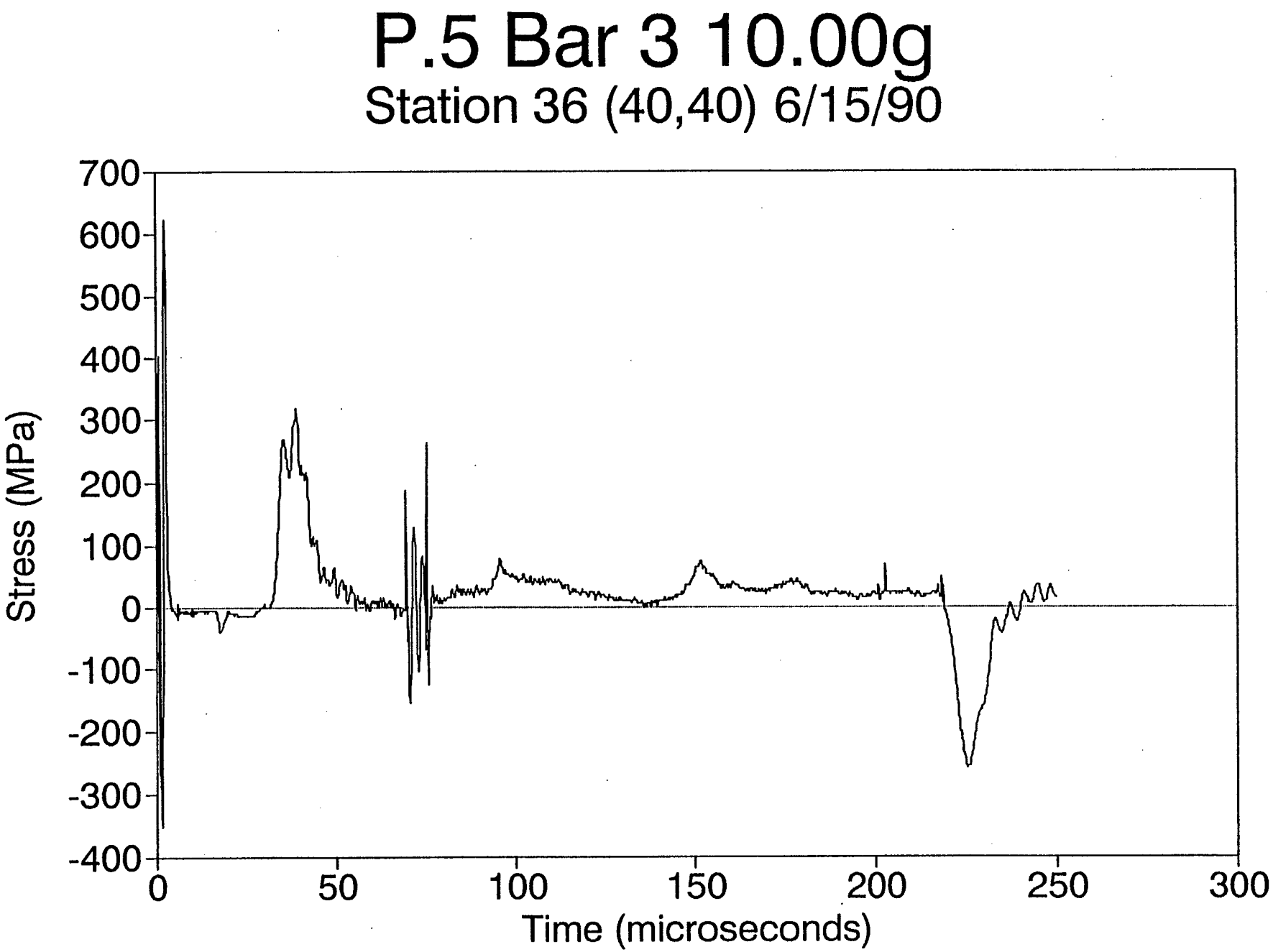

Figure 23. Station 36 bar gage signal, 10 g Pentolite in chamber 1.

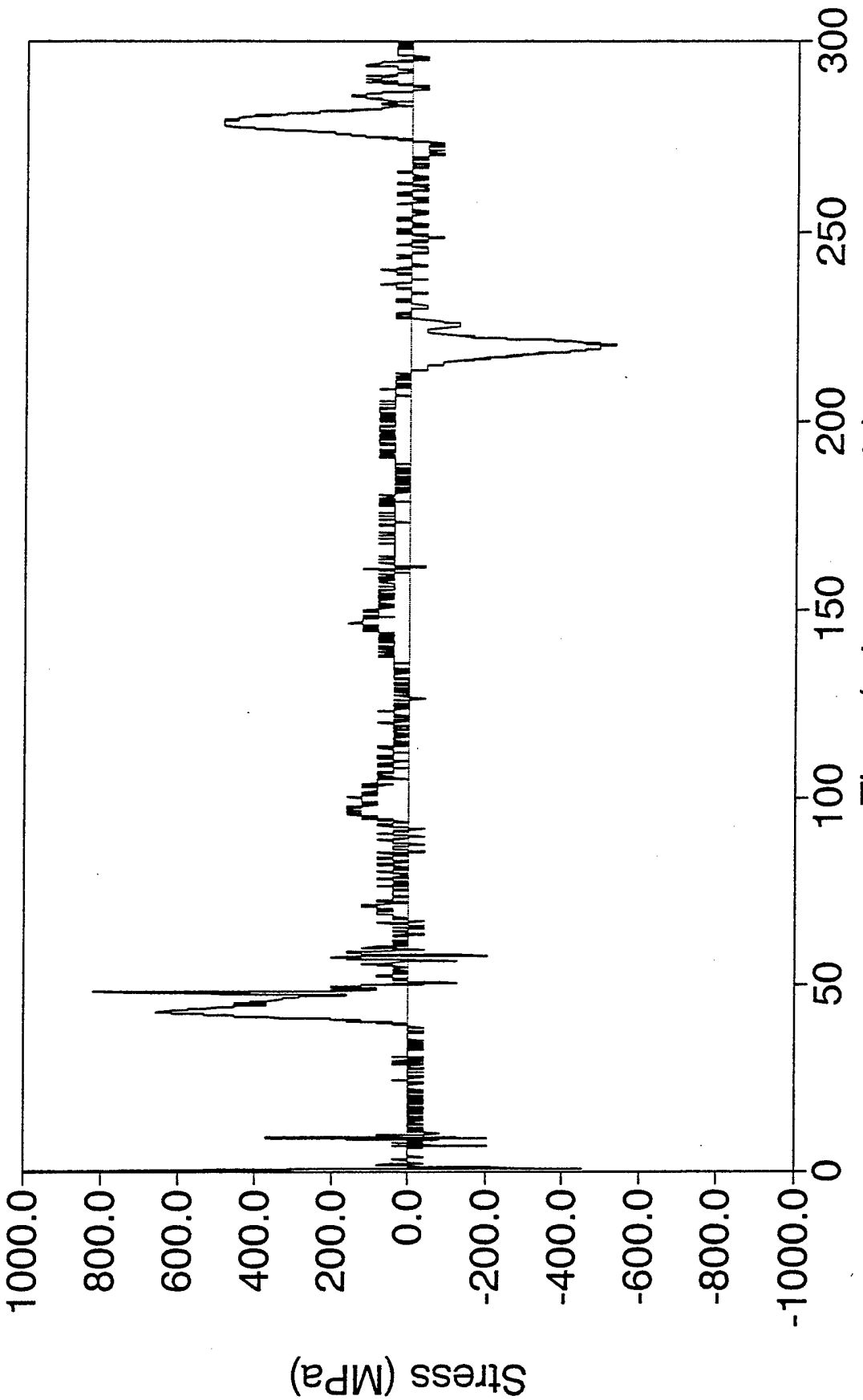

Figure 24. Station 42 bar gage signal, 15 g Comp B in chamber 2.

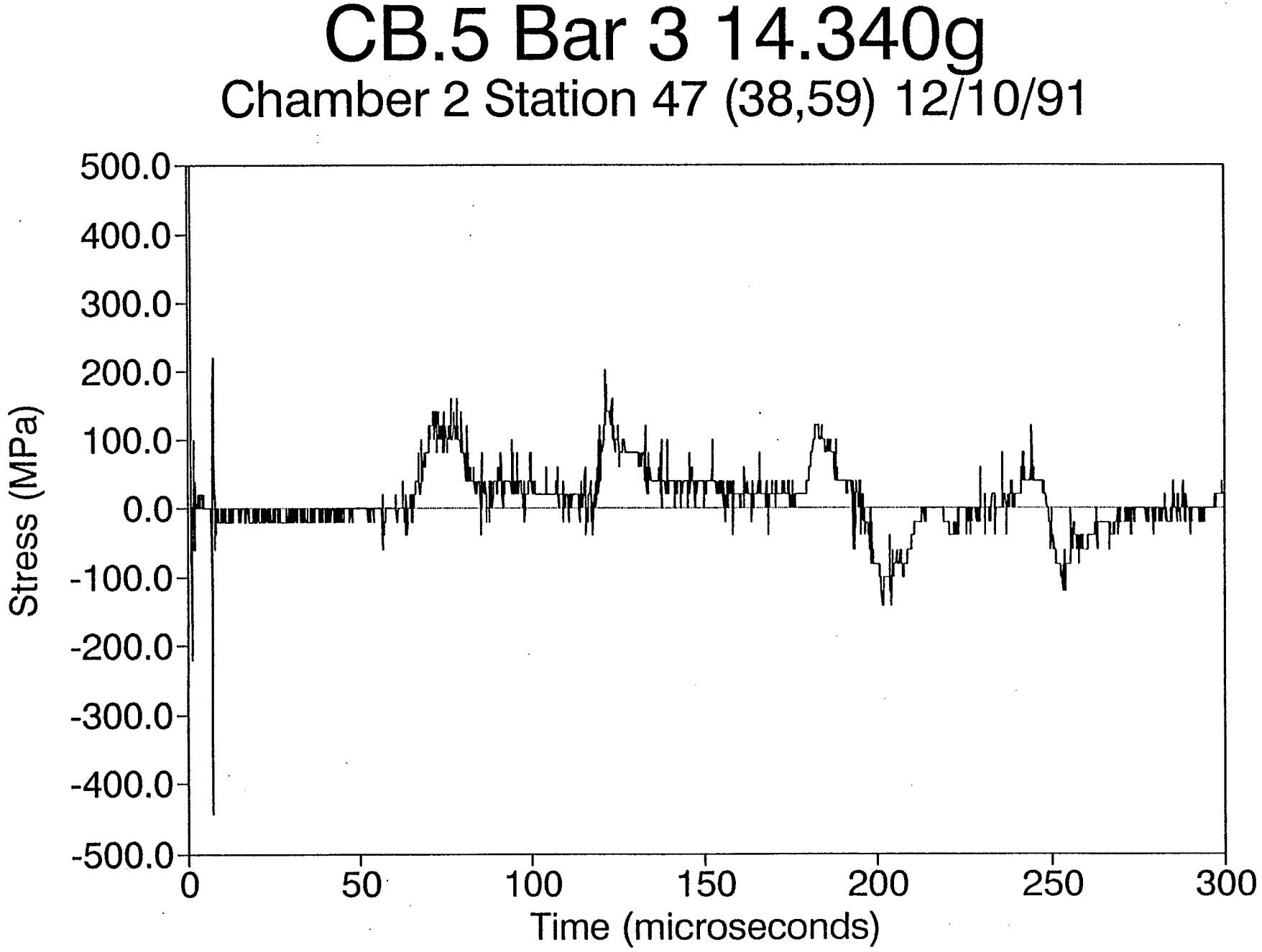

Figure 25. Station 47 bar gage signal, 15 g Comp B in chamber 2.

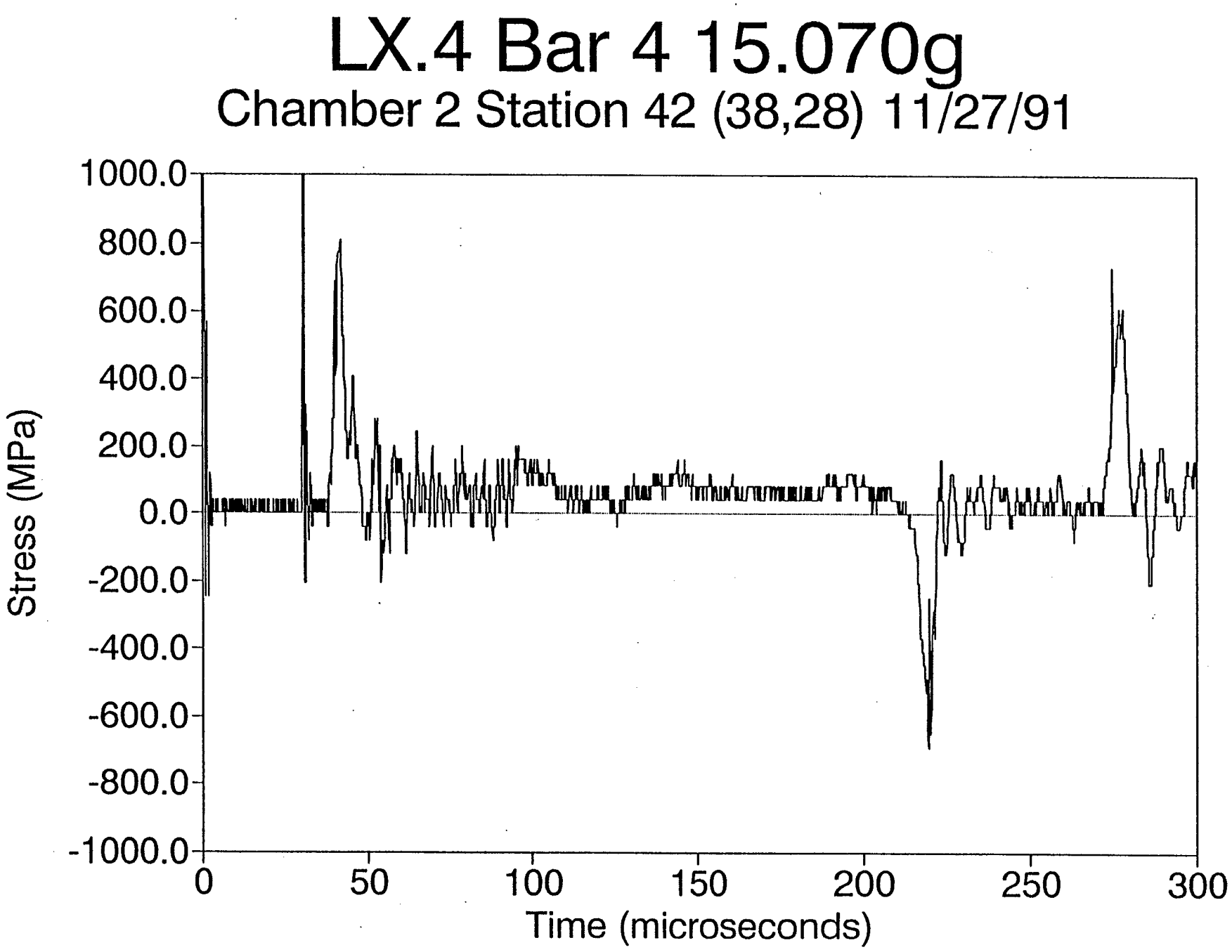

Figure 26. Station 42 bar gage signal, 15 g LX-14 in chamber 2.

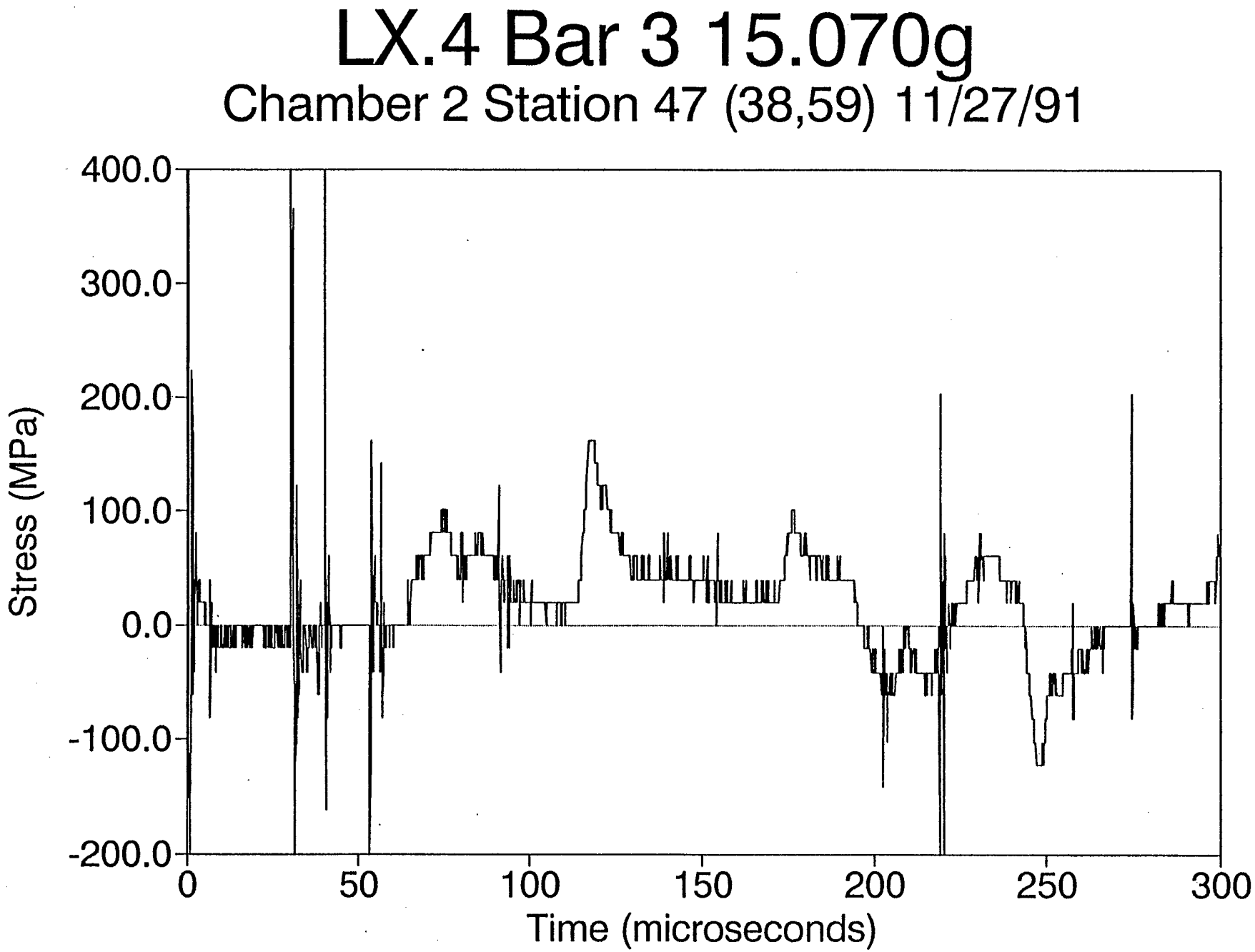

Figure 27. Station 47 bar gage signal, 15 g LX-14 in chamber 2.

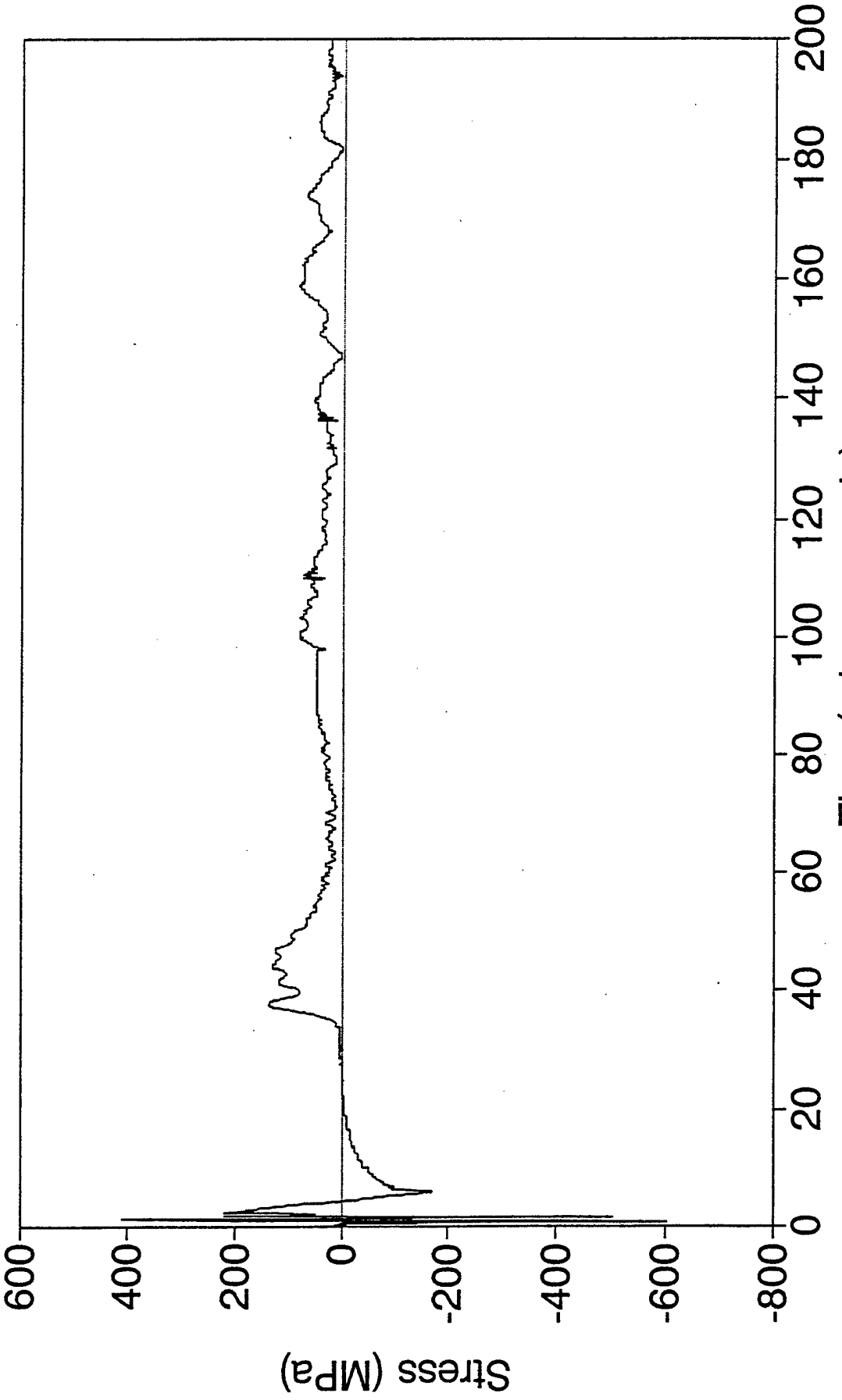

Figure 28. Station 45 bar gage signal, 10 g Pentolite in chamber 1.

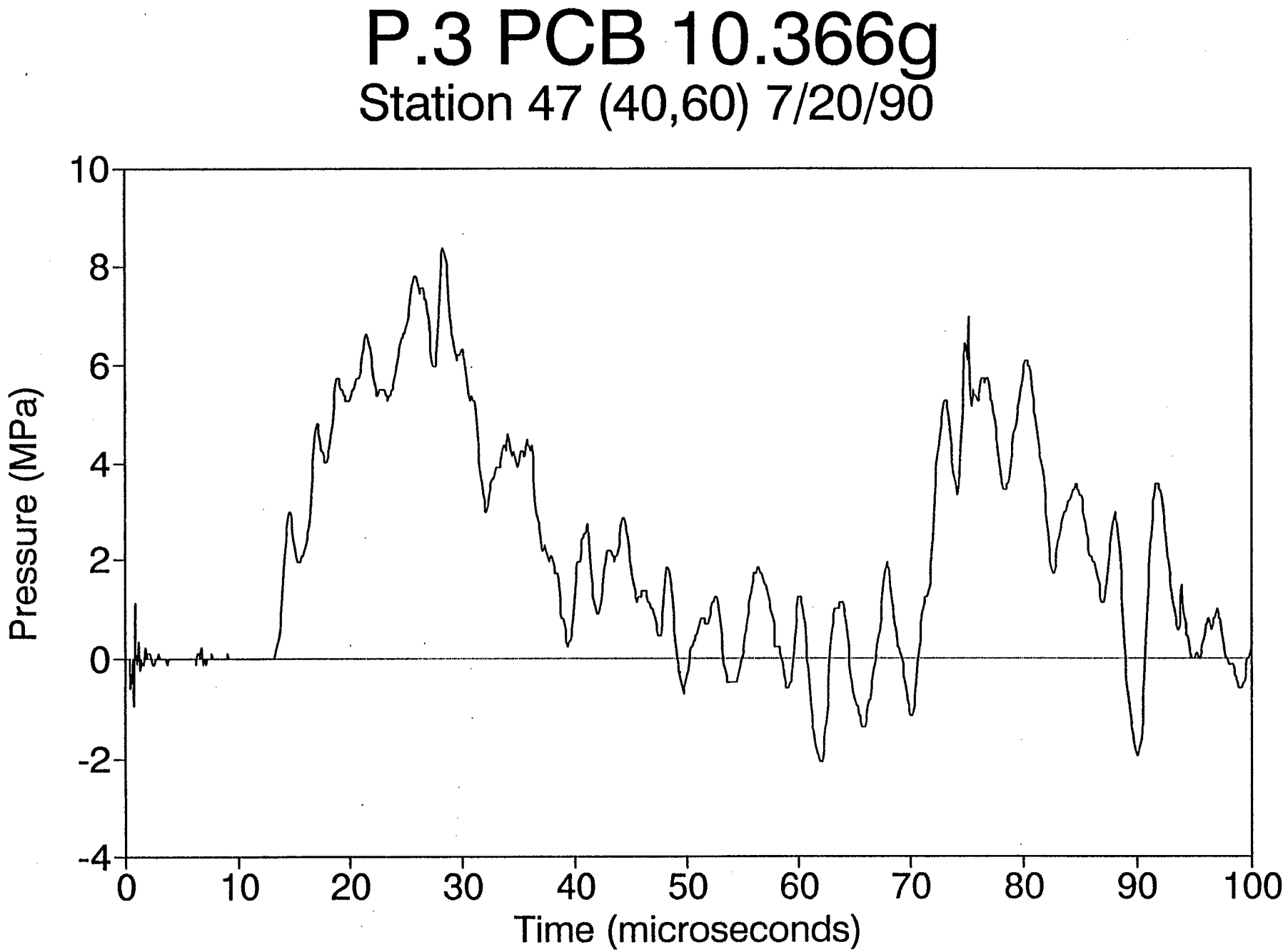

Figure 29. Station 47 PCB gage signal, 10 g Pentolite in chamber 1.

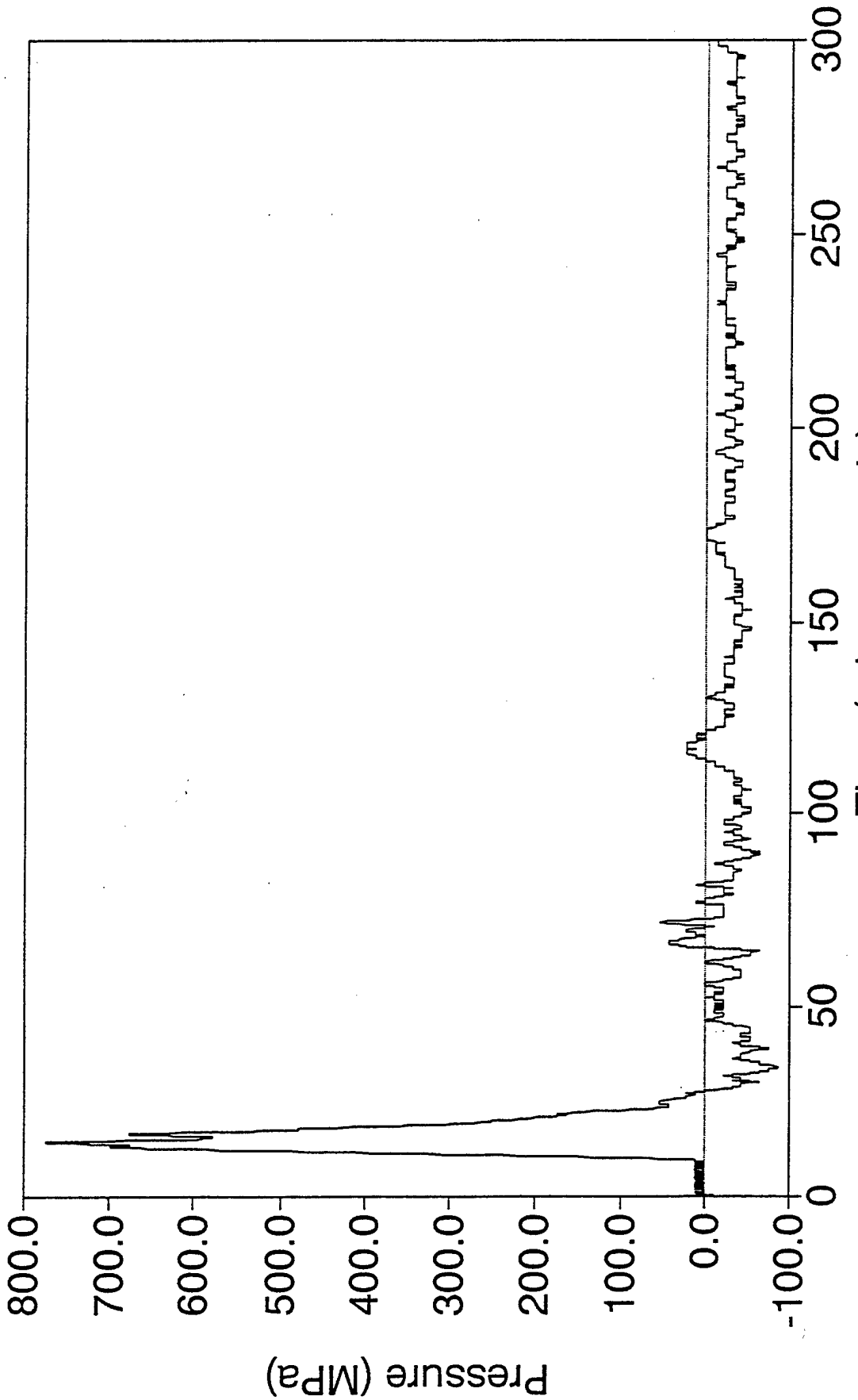

Figure 30. Station 36 PCB gage signal, 15 g LX-14 in chamber 2.

the PCB gage located at station 47. The voltage mode PCB gage was used for the measurement. Figure 30 is a record from a 15 g LX-14 explosive test in which the gage was located at station 36 (CG of the charge). The charge mode PCB gage was used for this pressure measurement.

7.1.3. PVDF Gage Records. Figure 31 is a signal from a PVDF gage combined with a bar gage on a 15 g Comp B explosive test. A total of three PVDF gage records from three different tests were acquired. The record shown in Figure 31 was from a gage calibrated by the manufacturer, but no calibration was available for the other two gages. However, since the same manufacturer supplied the gages, the same calibration constants were also used to analyze these voltage signals. Further, the active area of the gage was the area of the bar. This required that the entire area of the ends of both bars be in intimate contact with the gage strip.

7.2. Comments on the Signals.

7.2.1.Bar Gage Records. In almost every instance the bar gage signals exhibited features common to all sensor locations for the 10 and 15 g charge tests. Each exhibited the following: (1) A zero time noise spike from the fire set. (2) A positive voltage pulse (interpreted as the blast wave signal) from the strain gages at 30 - 60 μs after zero time due to the compressive stress wave propagating towards the free end of the bar. (3) The signal returns to the base line for approximately 150 μs. (4) A negative voltage pulse at about 200 μs from the strain gages corresponding to the tensile wave formed by reflection of the wave from the end of the bar. and (5) A positive voltage pulse at 275 μs from the strain gages which is the second compressive wave after reflecting from the chamber end of the bar. There are differences in the timing and amplitude of the various signal features that correspond to the position of the bar gage relative to the center of the charge. Bursts of high frequency noise of varying amplitude are also present on the many of the signal traces.

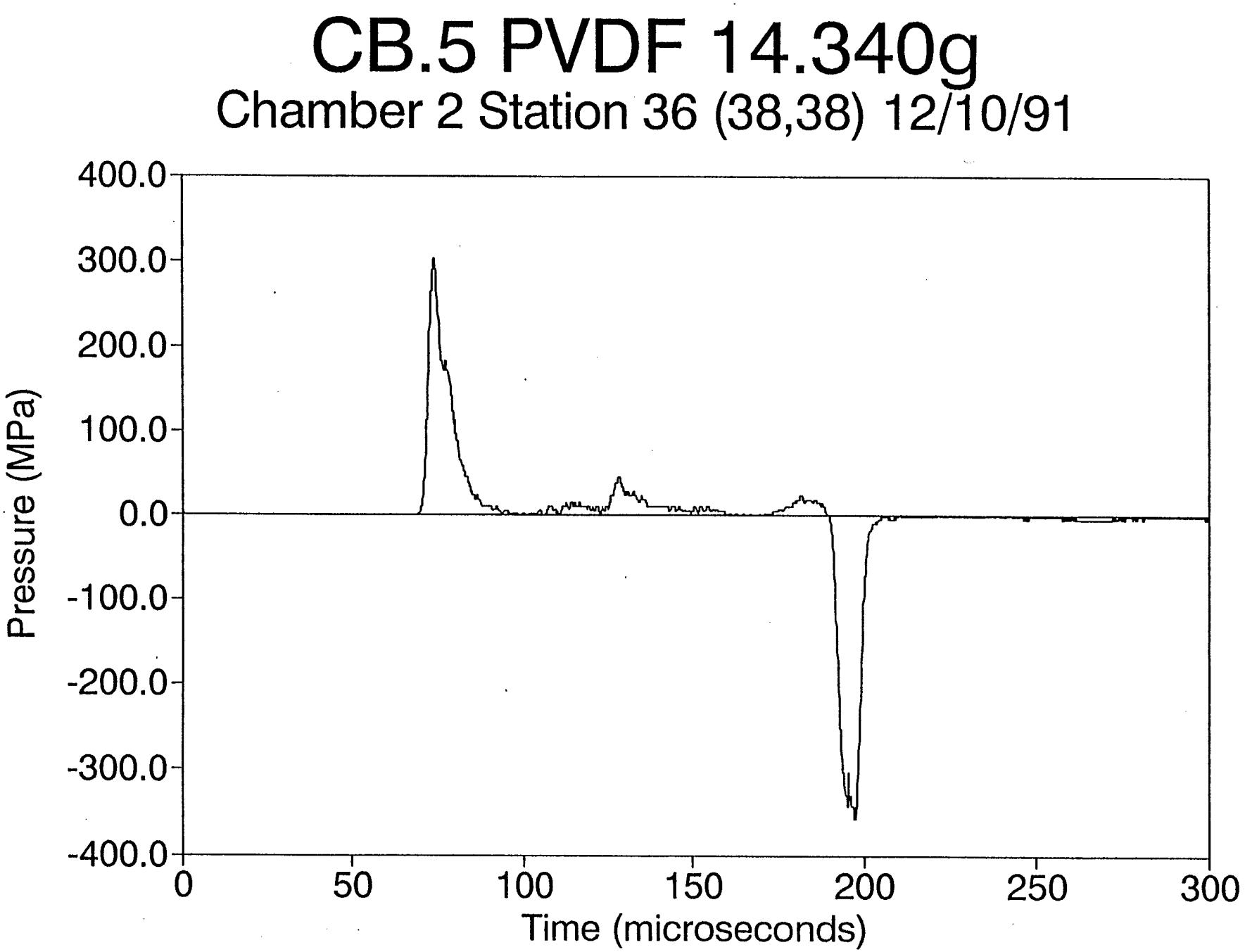

Figure 31. Station 36 PVDF/bar gage signal, 15 g Comp B in chamber 2.

Occasionally these noise bursts interfered with the blast wave signal.

Signal amplitudes are largest from the bar gage at station 1 (1200 to 2500 MPa) which is the port collocated with the charge and chamber cylindrical axes. For the 10 and 15 g charge tests, the average time-of-arrival (TOA) of the compressive wave is about 33 μs and about 200 μs for the reflected wave. The strain gage was mounted 25 mm farther from the end of the bar for some tests so the first and reflected pulse TOA readings are slightly longer than the other series of blast measurements

The signals from station 36 located at the center of gravity of the charges have a sharp first pulse of 300 to 700 MPa depending on the explosive with a TOA of 34 μs, followed by a reflected pulse at about 285 μs with nearly equal amplitude. Again the TOA depends on the length of the bar and the location of the strain gages relative to the end.

The blast signals from station 42, which is the sensor port located at the top edge of the explosive, signify a compressive stress pulse at approximately 40 μs with an amplitude of about 600 MPa. 200 μs later a 600 MPa tension wave is observed.

Signals from the bar gages below the charge center (station 47 for the 15 g tests and station 45 for the 10 g tests) were lower amplitude than from the other stations (100 MPa). The first compressive pulses arrive at about 65 μs, later than the other stations. The reflected pulses were sometimes obscure, but with some interpretation they were recognizable.

7.2.2. PCB Gage Records. Usually a single PCB pressure gage signal corresponding to the blast wave occurred about 10 μs after the zero time fire set noise fiducial. Some records show a series of small amplitude pulses which indicate reverberations within the chamber. The high frequency noise bursts were not observed in the PCB gage signal records.

7.2.3. PVDF Gage Records. The PVDF gage signal records show a compressive stress pulse at about 65 μs after zero time and a negative voltage signal from the reflected tensile wave at about 200 μs. Smaller amplitude reverberations signal features were also observed. The 60 μs time of the first pulse corresponds closely to the expected arrival time computed from the wave speed of the steel. Also, the time at which the reflected signal occurs agrees with the travel time for twice the length of the steel bar backing the gage. The noise bursts observed on the bar gage signal records were not present on the PVDF gage records.

7.3. Reflections within the Chamber. Several smaller amplitude pulses with a period of 50 to 75 μs were observed on most of the records from the bar and PCB gages. The period depends on the explosive charge,vessel size, and the location of the gage. These signals are the result of shock waves reflecting between the line of convergence along the cylindrical axis and the walls of the confinement chamber in the high pressure explosive gas products. These reverberations have sufficient strength (100 MPa in some tests) to activate the gages. After about 200 μs the reverberations die out.

7.4. Tables of Measured Values.

7.4.1. 64:1 Chamber. Table 12 is list of values measured for TOA, peak stress amplitude, and reverberation period at the gage stations for the 10 g explosive blast tests in the 64:1 volume ratio chamber.

7.4.2. 40:1 Chamber. Table 13 is the list of values measured for TOA, peak stress amplitude, and reverberation period at the gage stations for the 15 g charge tests in the 40:1 volume ratio chamber.

8. DATA ANALYSIS AND RESULTS FROM THE FREE FIELD TESTS

8.1 Data and Analysis of Free-Field Tests. Relatively

Table 12. 64:1 volume ratio test results.

Pressure in MPa
TOA in microseconds
Period in microseconds

Test No.	Sta 1	Sta 36	Sta 45	Sta 45	PCB Sta 47
CB.1					
P	1058.0	219.0	115.0	160.0	
TOA	33.4	34.9	37.5	36.9	
Period			55.0	55.0	
CB.2					
P	1086.0	283.0	130.0	143.0	
TOA	33.2	34.8	35.4	36.2	
Period	55.0		66.0	62.0	
CB.3					
P	1093.0	285.0	120.0	140.0	
TOA	33.3	34.5	36.2	36.2	
Period	55.0		55.0	58.0	
CB.4					
P	1108.0	273.0	141.0	144.0	
TOA	38.7	34.1	33.9	36.1	
Period	55.0	45.0	55.0	55.0	
CB.5					
P	975.0	325.0	133.0	234.0	
TOA	38.7		31.1	35.8	
Period	56.0	45.0	55.0	55.0	
CB.6					
P	937.0	311.0	219.0	265.0	24.3
TOA	39.4	39.9	37.5	46.0	20.1
Period		58.0	59.0		58.0
LX.1					
P	1070.0	488.0	155.0	160.0	9.3
TOA	33.3	33.9	33.5	33.9	13.7
Period	53.0	53.0	58.0	53.0	
LX.2					
P	1071.0	565.0	163.0	171.0	7.6
TOA	32.9	32.9	33.5	34.9	12.9
Period	49.0				
LX.3					
P	1147.0	433.0	168.0	185.0	8.5
TOA	32.8	32.6	33.5	33.4	13.5
Peroid		55.0	60.0	58.0	

LX.4					
P	1153.0	509.0	132.0	193.0	8.9
TOA	32.6	33.1	33.7	34.8	13.1
Period	51.0		57.0	58.0	
LX.5					
P	1232.0	428.0	150.0	134.0	10.1
TOA	33.9	34.8	33.7	37.6	12.4
Period	53.0	55.0	58.0	55.0	
P.3					
P	1027.0	329.0	145.0		8.4
TOA	33.5	33.9	34.4		13.3
Period	60.0	55.0	55.0		
P.4					
P	1037.0	294.0	135.0	184.0	8.1
TOA	33.5	33.8	34.4	34.4	12.2
Period	51.0		58.0		
P.5					
P	638.0	309.0	135.0	135.0	
TOA	37.3	32.2	33.6	32.3	
Period	51.0	55.0	59.0	63.0	
P.6					
P	967.0	334.0	120.0	209.0	7.1
TOA	33.7	34.0	34.5	34.4	10.6
Period		57.0	59.0	59.0	
P.7					
P		278.0	147.0		
TOA		36.9	32.3		
Period					
P.9					
P	1077.0	399.0	135.0		8.0
TOA	33.8	34.3	34.0		12.8
Period	51.0	55.0			

Table 13. 40:1 volume ratio test results.

Pressure in MPa
TOA in microseconds
Period in microseconds

Test No.	Sta 1	Sta 36	Sta 42	Sta 47	PCB Sta 36	PVDF Sta 36
CB.4						
P		650.0	657.0	161.0	621.0	611.0
TOA		36.5	39.5	65.0	11.5	69.0
Period			53.0	56.0	10.0	
CB.5						
P	2681.0	724.0	649.0	141.0		289.0
TOA	39.5	35.2	39.3	65.5		68.4
Period			50.0	55.0		54.0
CB.6						
P	2436.0	731.0	657.0	154.0		694.0
TOA	39.3	39.0	40.0	66.5		69.0
Period	50.0	53.0		55.0		
CB.7						
P	2356.0	796.0	764.0			509.0
TOA	38.9	38.8	38.5			68.0
Period	45.0		47.0	54.0		
LX.1						
P	1303.0	558.0	513.0	120.0		
TOA	27.0	32.6	33.5	40.0		
Period	49.0	61.0	59.0	59.0		
LX.2						
P	1425.0	726.0	586.0	94.0		
TOA	26.7	33.0	33.5	40.0		
Period	49.0		49.0			
LX.3						
P	1343.0					
TOA	23.3					
Period	49.0					
LX.4						
P	2436.0	690.0	771.0	81.0	773.0	
TOA	37.6	38.3	38.2	65.0	9.5	
Period	46.0	54.0	44.0	50.0	53.0	

satisfactory data was obtained in six of the eight free-field tests conducted within the CSM mine. As indicated above the first test with Comp-B explosive failed to detonate properly and no data was obtained. Incomplete data was obtained on the first test conducted in the 1991 series. This test was conducted with an LX-14 charge (Test LX-3) and the peak amplitude of the majority of the gage signals was lost due to an error in setting the recording ranges on the Tektronix 2214 digital oscilloscopes. Data on the other six tests was of reasonable quality but persistent noise problems reduced the quality of many gage records. The pressure bar gages fielded in each of the eight free-field tests are indicated in Table 9. The type of bar at each gage location is indicated by the B-X-YY notation, where B indicates a pressure bar gage, X indicates the bar diameter and YY indicates the type of steel for the bar. An X equal to 6 refers to a 6.35 mm (0.25 inch) diameter and an X equal to 8 refers to a 7.94 mm (0.315 inch) diameter. A YY equal to 44 refers to the Viscount 44 steel and to 66 refers to the Double Six steel. Only four bar gages were used in the first test (CB.1), with five or six bar gages used in all subsequent tests. The position of each of the bar gages is illustrated in Figures 10 and 13, in Section 4. The pertinent features of the eight CSM free-field tests, along with the data considered of value to close-in blast loading analyses, are discussed in the following paragraphs on a test by test basis.

8.1.1 Test CB.1 - 16 August 1990. As indicated earlier this test did not yield any useful data due to the failure of the Comp-B charge to detonate properly. Although the charge did go low-order to some extent and generated a moderate air blast, the pressures acting on the four bar gages fielded in the test were so low that any pressure signal was lost in electrical noise. Due to failure of this charge to detonate, a revised booster charge was designed and used successfully in all subsequent tests.

8.1.2 Test CB.2 - 20 September 1990. As indicated in Table 9,

six pressure bar gages were fielded in Test CB.2. As only four channels of 16 MHz data acquisition were available it was necessary to record two gages (at locations 120 and 140) on the low sampling rate Rapid Systems 4x4 unit. All of the data recorded on the Tektronix 2214 (Gage locations 101, 108 and two at 136) was of satisfactory quality. Data for the gages at 120 and 140 were of poor quality. The reduced data for the second test with Comp-B (CB.2) are shown in Figure 32.

8.1.3 Test CB.3 - 02 October 1991. Six pressure bar gages were fielded in this test as indicated in Table 9. Although all bar gages performed perfectly in pre-shot tests, only three gage records of any value were recorded. Very high electrical noise during the primary signal time of the gage at position 236 precluded using this portion of the record. The pressure record associated with the stress wave reflected from the far end of the bar was free of electrical noise and consequently this data was time shifted to provide an approximate record for the 236 position. While the amplitude and duration of this reflected signal may be representative of the actual signal, the pressure rise time is certainly too low due to dispersion in the bar. The very high electrical noise on those data channel which did not give useful data indicated also that stray currents from the EBW detonator might be getting into the signal lines. Consequently, it was decided to fire the last Comp-B charge (as well as the last LX-14 charge) with a delay line of mild detonating cord. Pressure data from the two good gage records (positions 101 and 136) and from the time shifted reflected position 236 record are shown in Figure 33.

8.1.4 Test CB.4 - 17 October 1991. Six pressure bar gages were fielded in the last Comp-B test as indicated in Table 9. Due to the electrical noise noted in earlier Comp-B tests with the EBW detonator and 2.5 gm booster placed directly on the main charge, a detonating delay line made of 1.5 m of 7 gr/ft mild detonating cord was employed to isolate any electrical discharge from the EBW from the pressure bar gages. This 1.5 m line gave

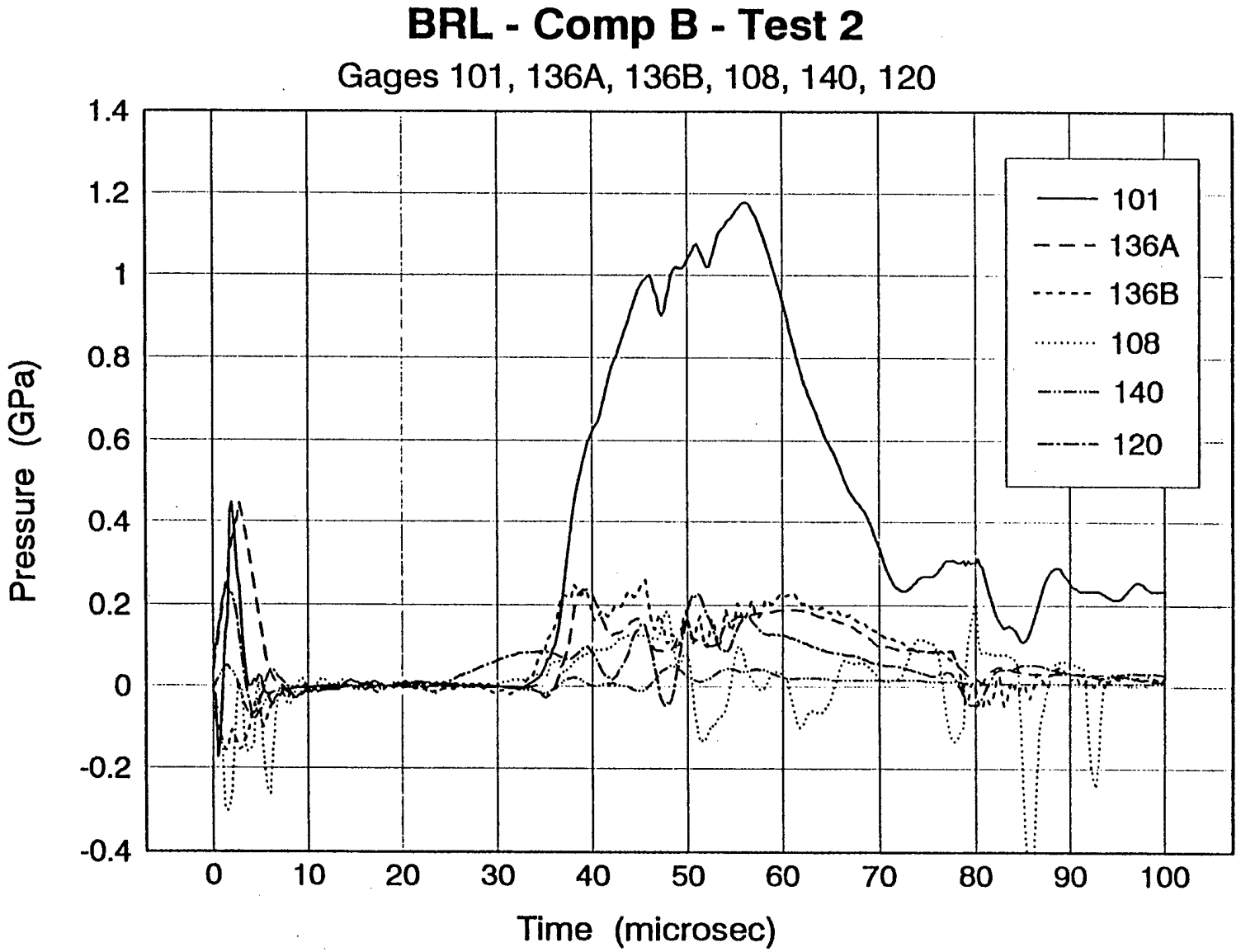

Figure 32. Bar gage records from free field test CB.2.

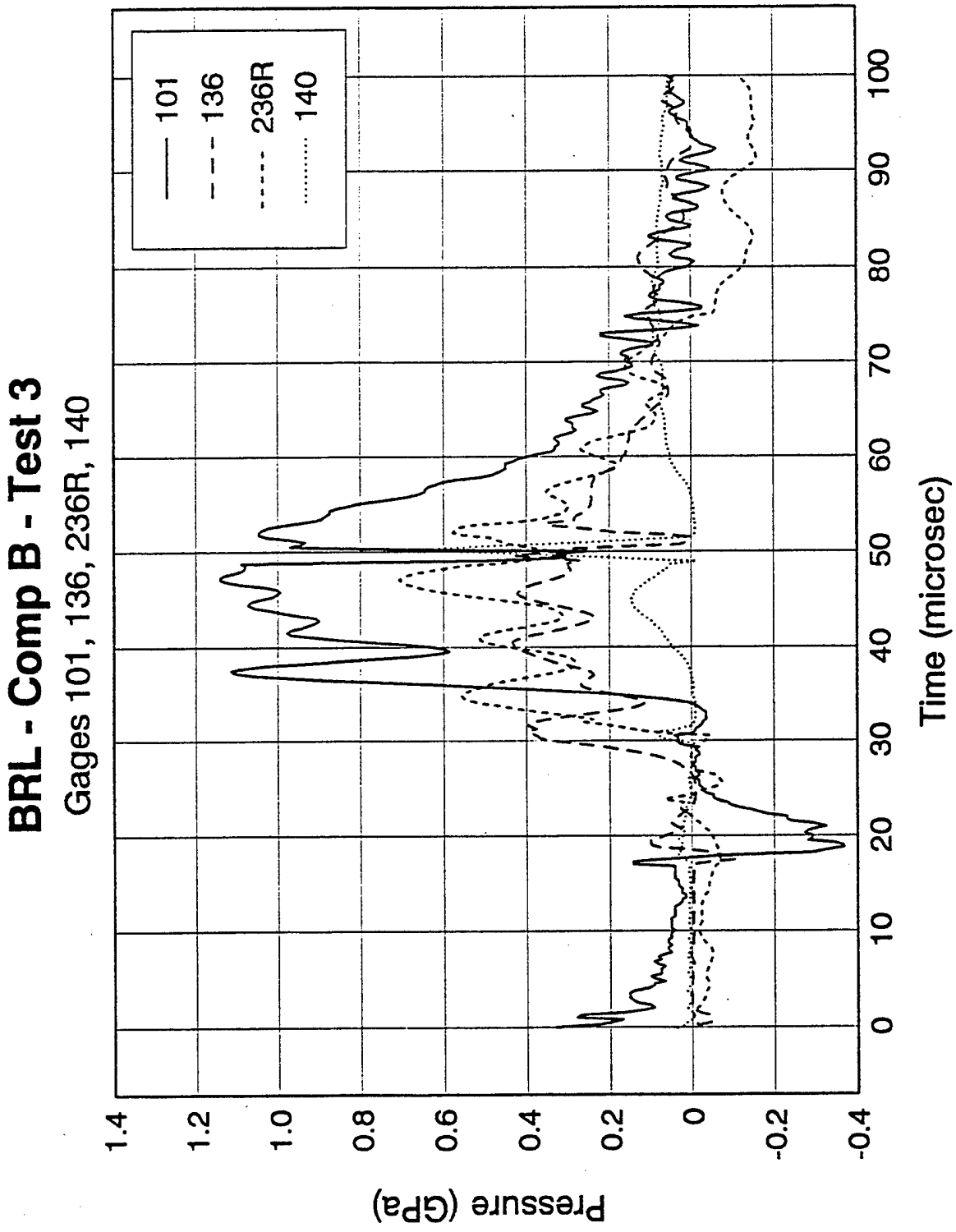

Figure 33. Bar gage records from free field test CB.3.

just over 200 microsec of delay. In order to establish the time of initiation of the main charge simple capacitor discharge pins were used to determine the time when the booster charge was initiated by the delay line. The data from the capacitor discharge pins was of excellent quality giving high confidence in the selection of a time for main charge imitation. Although all bar gages performed perfectly in pre-shot tests, only four gage records of any value were recorded and only the position 101 gage was of good quality. As for Test CB.3, very high electrical noise during the primary signal time of the 236 gage precluded using this portion of the record but the pressure record for the stress wave reflected from the far end of the bar was free of electrical noise and time shifted to provide an approximate record for the 236 position. Pressure data from the one good gage records (position 101), from the two poor gage records (positions 136 and 120) and from the time shifted reflected 236 record are shown in Figure 34.

8.1.5 Test LX.1 - 24 August 1990. As indicated in Table 9, five pressure bar gages were fielded in this test. Reduced data from this first test with an LX-14 charge are shown in Figure 35. The pressure versus time records shown in Figure 35 are for four of the five pressure bars fielded in the test. The pressure bar located at position 142 did not yield a meaningful signal. As anticipated the pressure at the 101 position, directly opposite the detonated end of the charge, was much higher than the pressure recorded at the other, off axis, positions. The very large amplitude oscillating signal beginning at 0 microsec and lasting for 25 microsec is very representative of the electrical noise generated by the EBW detonating system. The peculiar square peak for the portion of the 101 gage record over 1.6 GPa is probably due to amplifier problems that were corrected for in later tests. The highly oscillating records for the gages at positions 136 and 140 are probably due to flexural waves being introduced into the bars due to the fact that these bar gages were located off axis and could not be positioned at an angle such that they would be subject to axial loading only (see

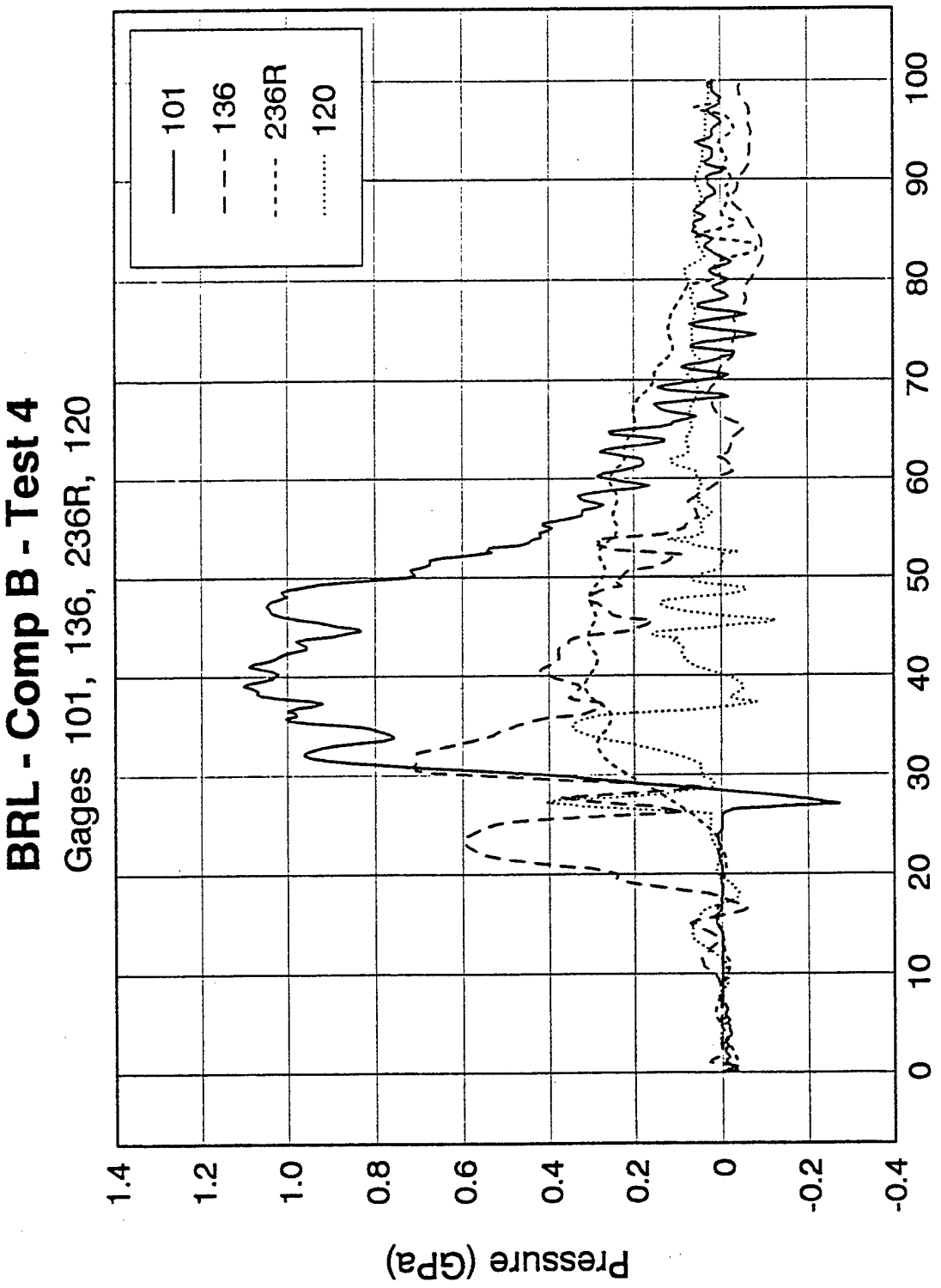

Figure 34. Bar gage records from free field test CB.4.

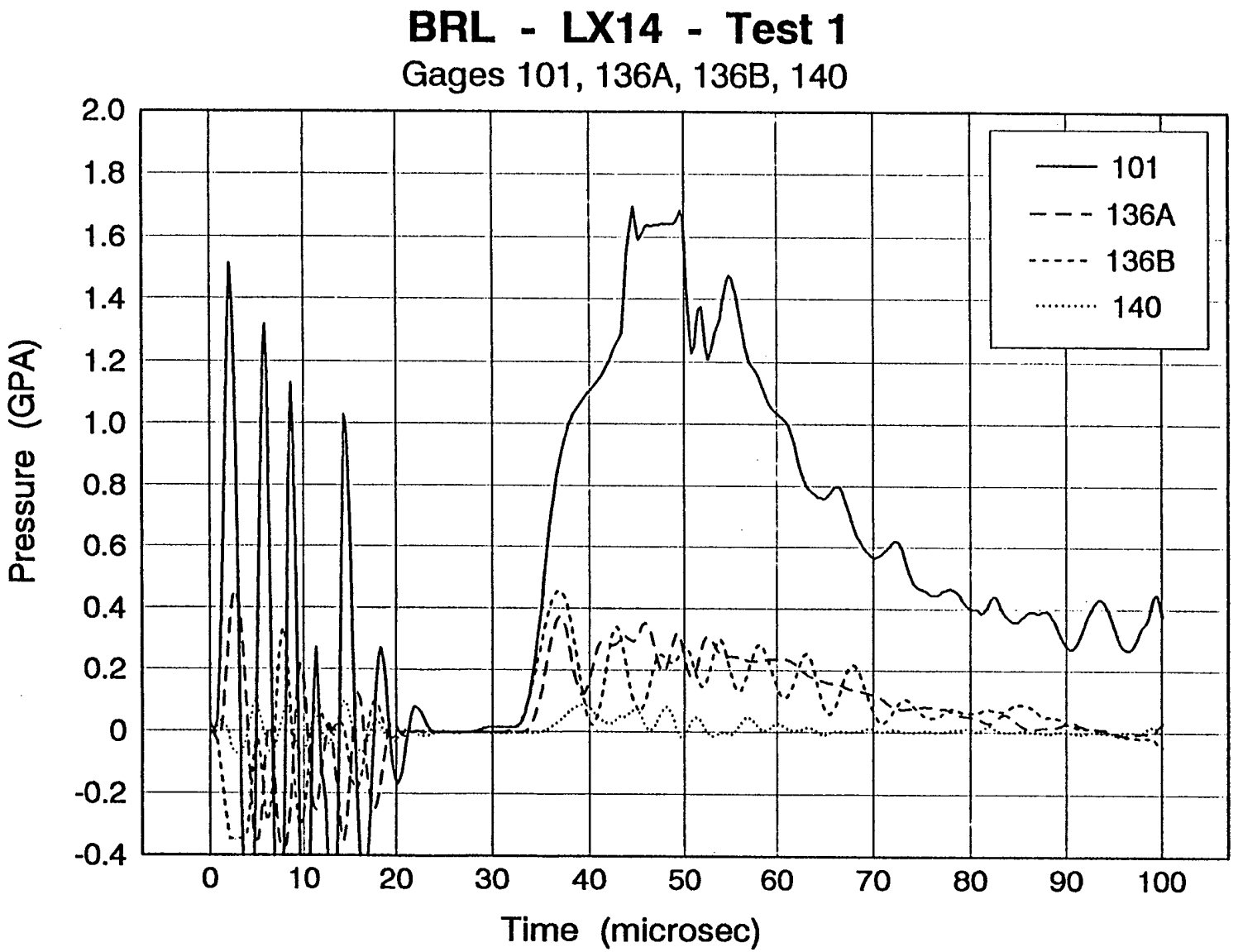

Figure 35. Bar gage records from free field test LX.1.

Figure 10). As the charge detonated the direction from which the explosive products loading the bar would change inducing flexural waves in the bar.

8.1.6 Test LX.2 - 30 August 1990. Five pressure bar gages were fielded in the second LX-14 test, also. The pressure versus time records shown in Figure 36 are for four of the five pressure bars fielded in the test. The record from the second position 136 gage was not usable. The records for the 120 and 140 gages are both late in arrival by approximately 5 microsec and the 120 gage is very low in amplitude. As three (101, 136 and 140) of these four records were recorded on the Tektronix 2214 with a common time base there is no ready explanation for the late gage 140 arrival.

8.1.7 Test LX.3 - 25 September 1991. As indicated in Table 9, six pressure bar gages were fielded in the first LX-14 test of the 1991 tests. This test was one of the more frustrating in that all gages appeared to perform quite well in terms of electrical and mechanical noise but four of the six records were truncated by having the Tektronix 2214 channels set to a too sensitive level. The pressure versus time records for all six gages are shown in Figure 37. Only gages at positions 120 and 140 did not have their peak values lost due to the improper scope settings. The low amplitude and late arrival of the gage 120 signal is consistent with the data obtained at this gage location in Test LX.3. The pressure data for position 140 is much lower in Test LX.3 than in Test LX.2, however.

8.1.8 Test LX.4 - 16 October 1991. Six pressure bar gages were fielded in the last LX-14 test. As was typical for the free-field tests, only three of the six bar gages gave useful data. As was also the usual case, the better records were for the position 101 and 136 gages. A very good primary record for a position 236 gage was also obtained in this test. The pressure versus time records for the three good gages are shown in Figure 38.

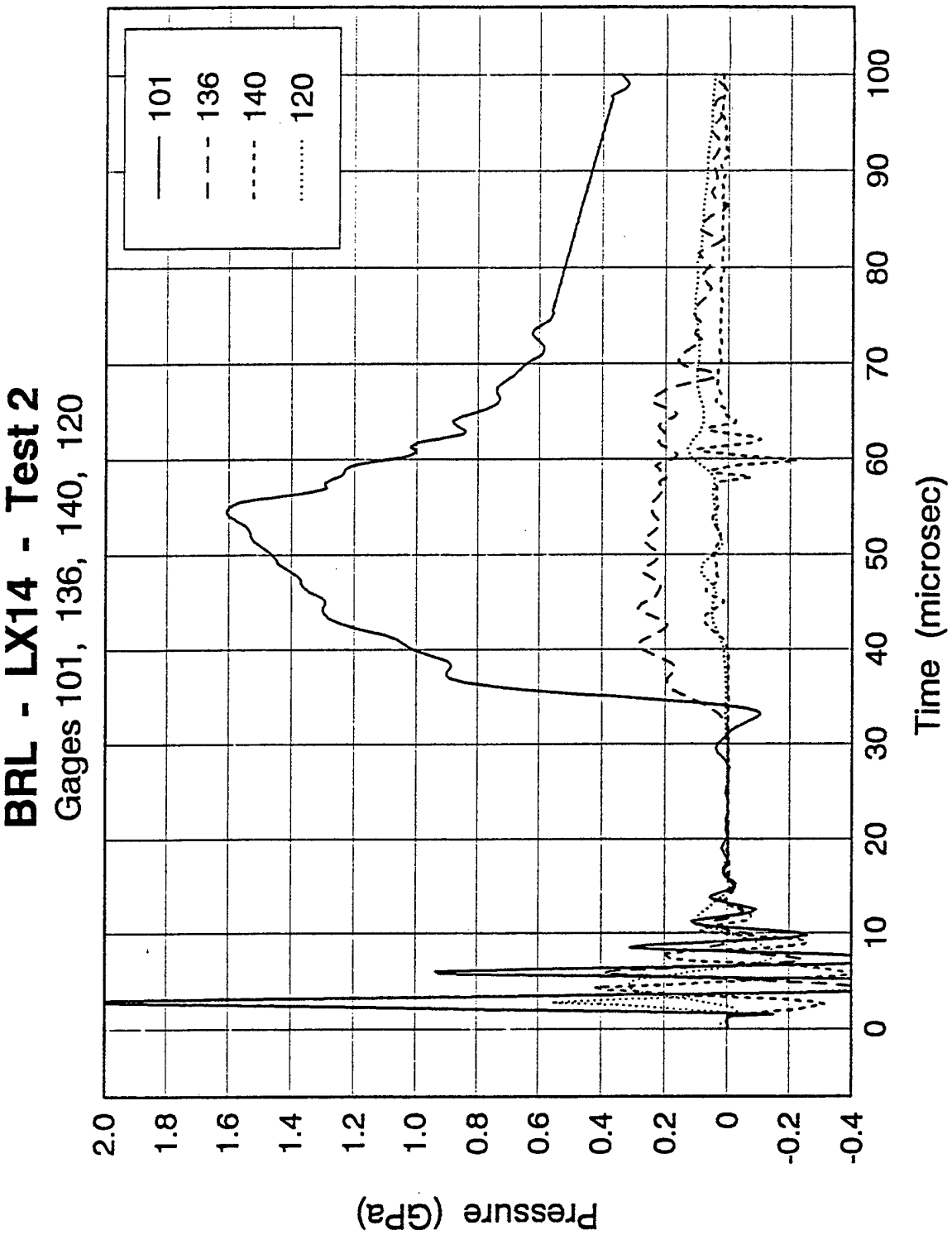

Figure 36. Bar gage records from free field test LX.2.

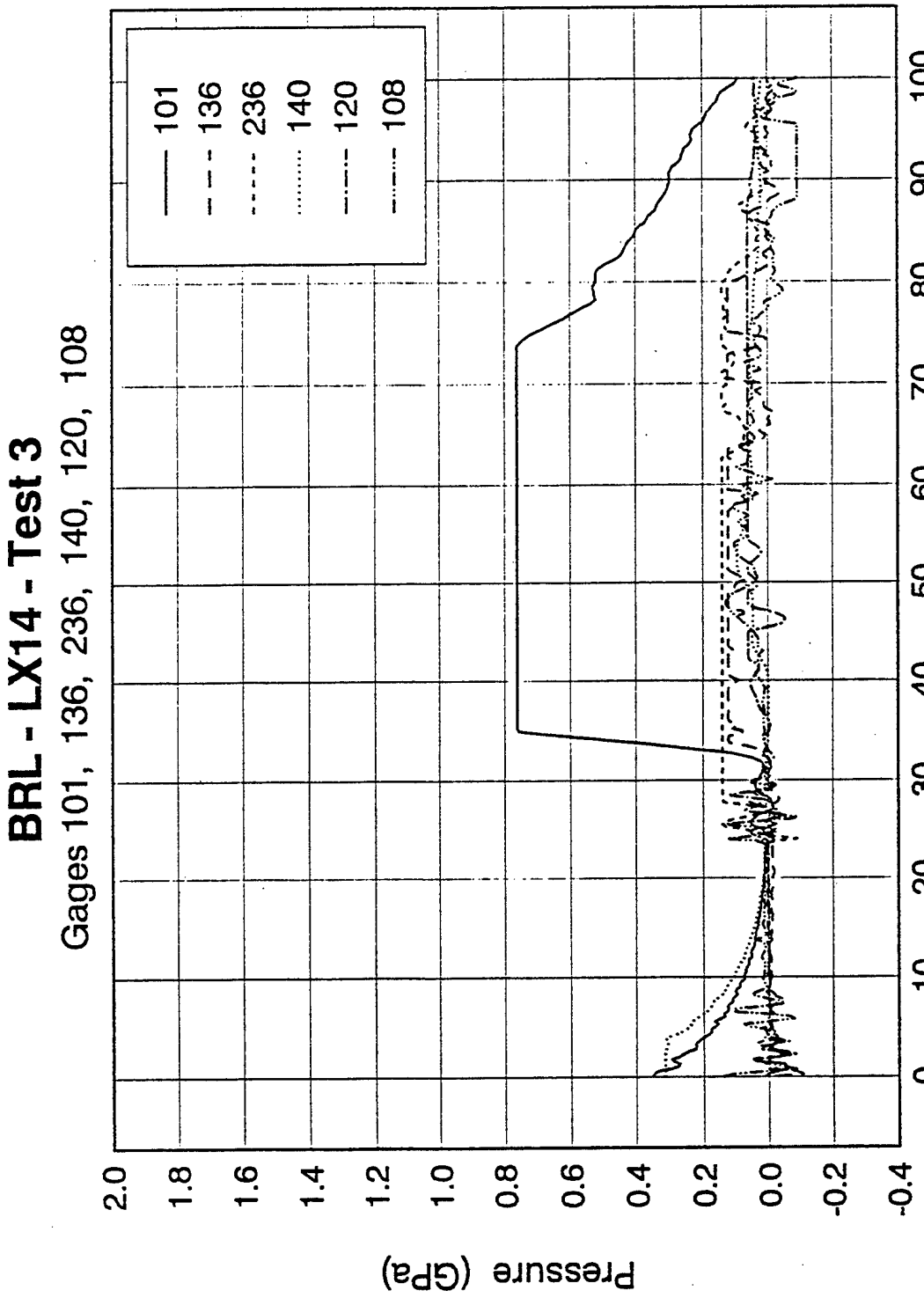

Figure 37. Bar gage records from free field test LX.3.

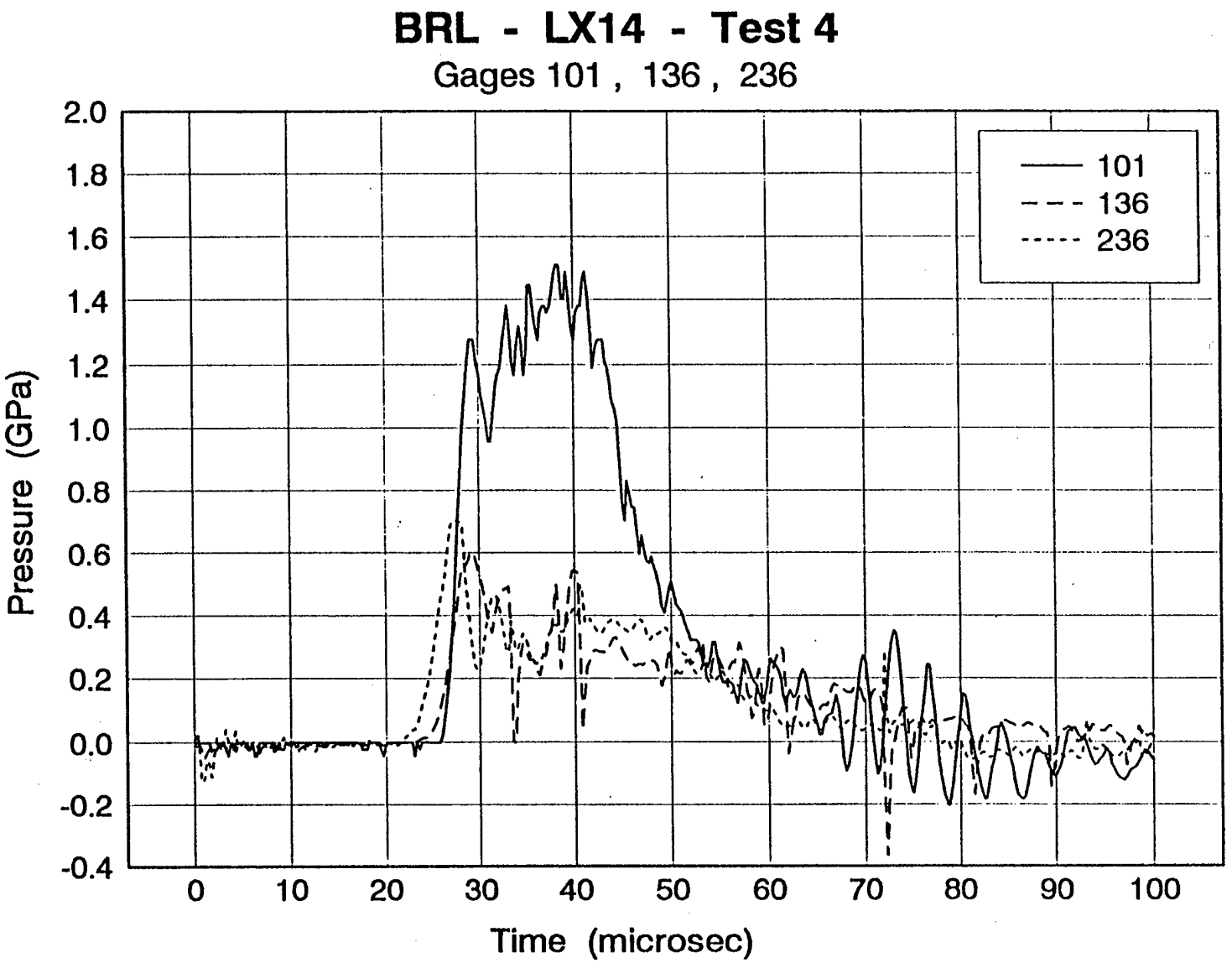

Figure 38. Bar gage records from free field test LX.4.

The four records obtained from the position 101 pressure bar gages in the four LX-14 tests are shown plotted together in Figure 39. Despite the many problems which plagued the tests, these four records display a considerable amount of consistency. Except for the amplifier induced square peak on the LX.1 data the three full records display very similar rise time and peak amplitude behavior. Only the LX.4 data indicate a significant variation in pressure duration, while the truncated data of LX.3 serves to confirm the pressure duration measured in tests LX.1 and LX.2.

Six pressure records for the position 136 gages in the LX-14 tests are shown together in Figure 40. Again these data show some consistency, with only the data from LX.2 indicating a slower pressure rise time. The truncated data of LX.3 is not at variance with the data of the other tests. The pressure oscillations in the gage 136 records, especially early in the pressure history, may be due to flexural wave loading of the bars because of their non-axial loading.

The average peak pressure for LX-14 at position 101 is about 30% larger than for Comp B as indicated in Figures 39 and 41 for the two explosives. Both sets of results display considerable variety in the shapes and peak pressures among each of the individual tests.

9. DISCUSSION OF RESULTS

9.1. Closed Vessel Experiments. Table 14 is a summary of all the 10 and 15 g closed vessel tests on Comp B, LX-14, and Pentolite. The data from Tables 12 and 13 provided the information for the summary. The measured blast pressures were consistent from tests to test for each station for a given explosive. However, Test LX.4, in which a 15 g charge was tested, is an exception to this statement where the blast pressure at station 1 is almost twice the pressure measured for the other three tests. The reason is not known. There are a couple of other

Table 14. Comparing experiment with calculation.

Explosive	Station	Pressure (MPa) Experiment	Pressure (MPa) Calculation
10 g Comp B	1	1042	
	36	283	
	45a	143	
	45b	181	
	47	24	
15 g Comp B	1	1357	
	36	725	
	42	682	
	47	152	
	36a	621	
	36b	604	
10 g LX-14	1	1134	1900
	36	485	492
	45a	154	211
	45b	167	211
	47	8.9	69
15 g LX-14	1	1627	
	36	658	
	42	623	
	47	98	
	36a	773	
10 g Pentolite	1	949	
	367	324	
	45a	136	
	45b	176	
	47	7.9	

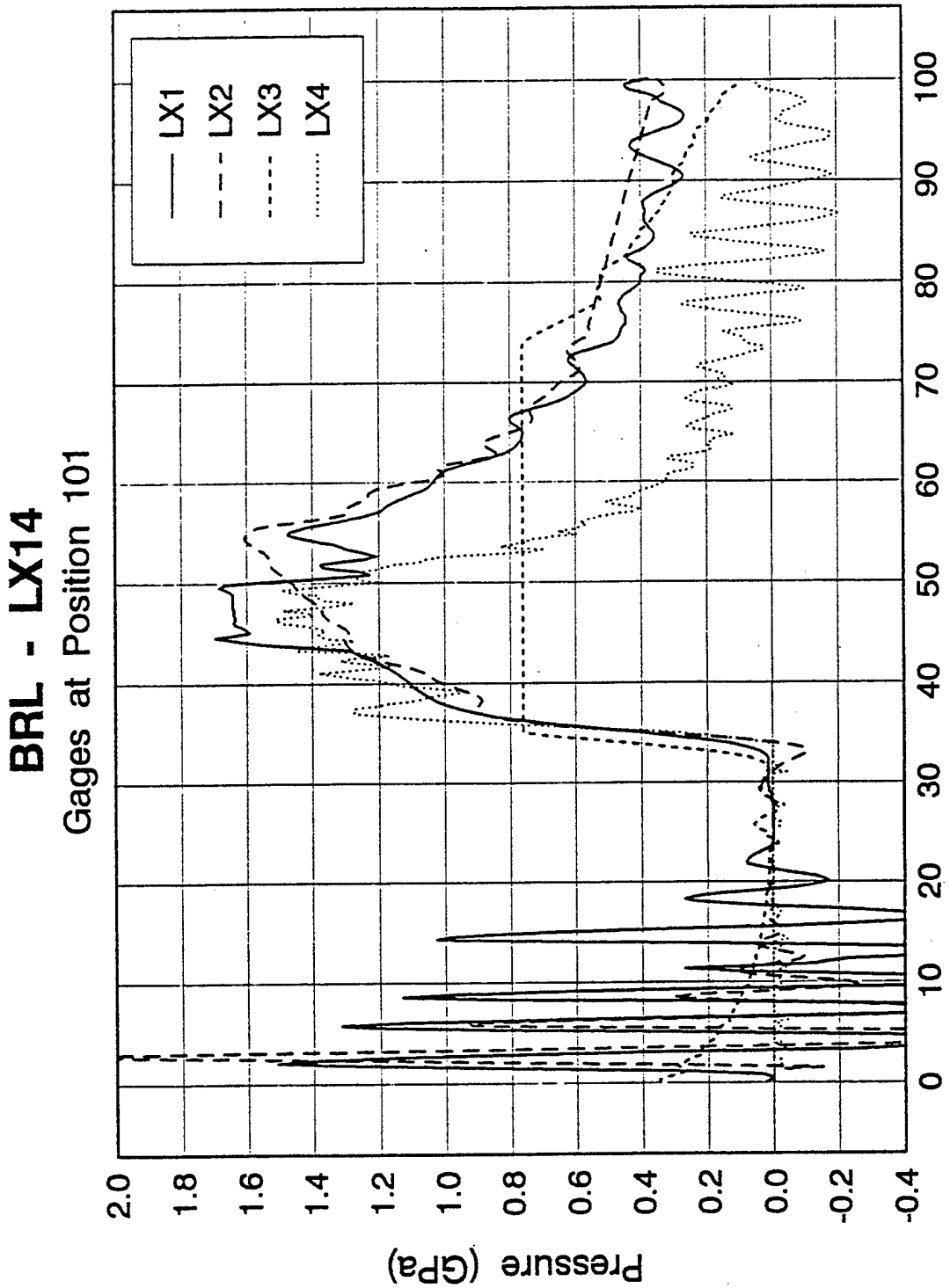

Figure 39. Position 101 gage records from all LX-14 field tests.

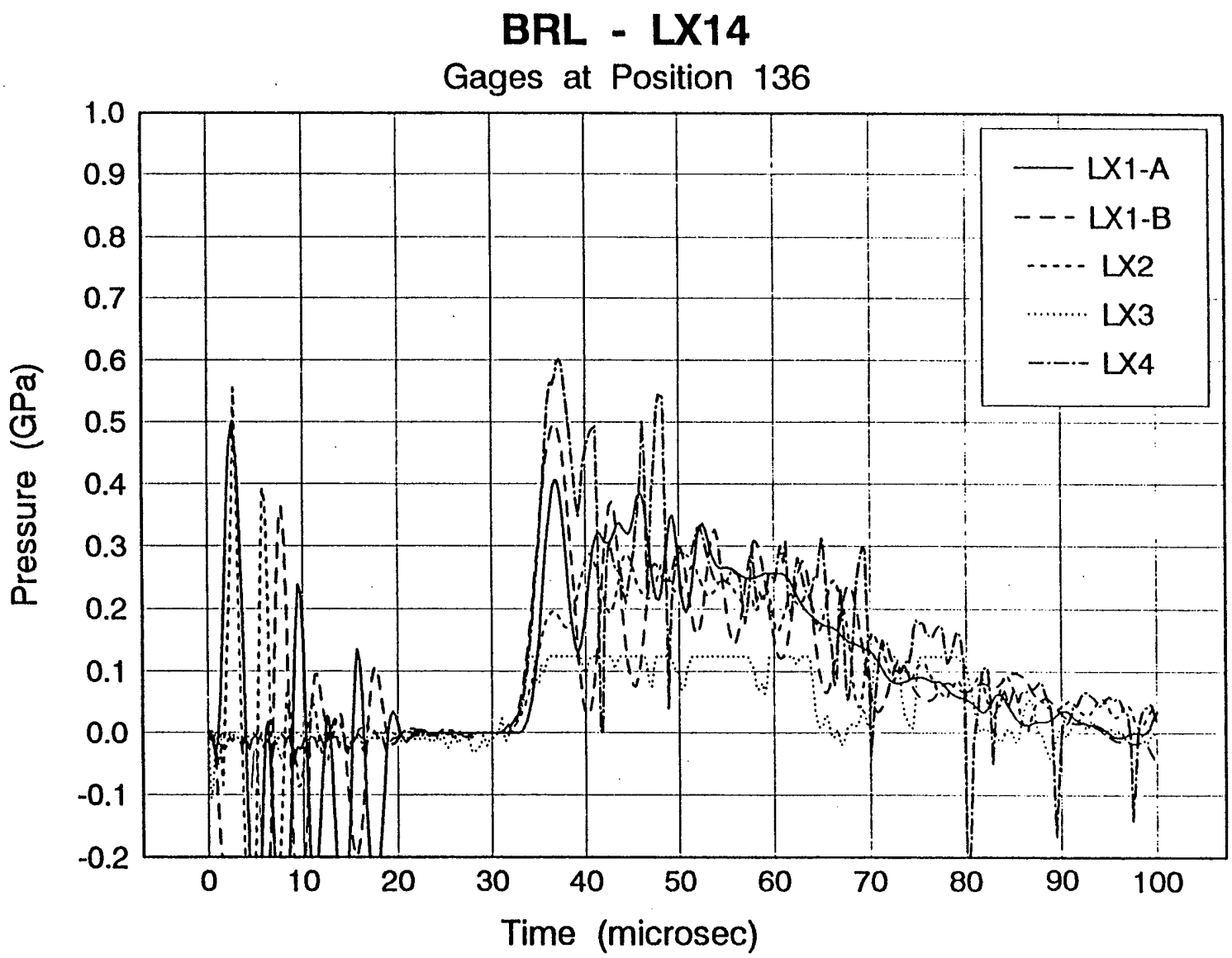

Figure 40. Position 136 gage records from all LX-14 field tests.

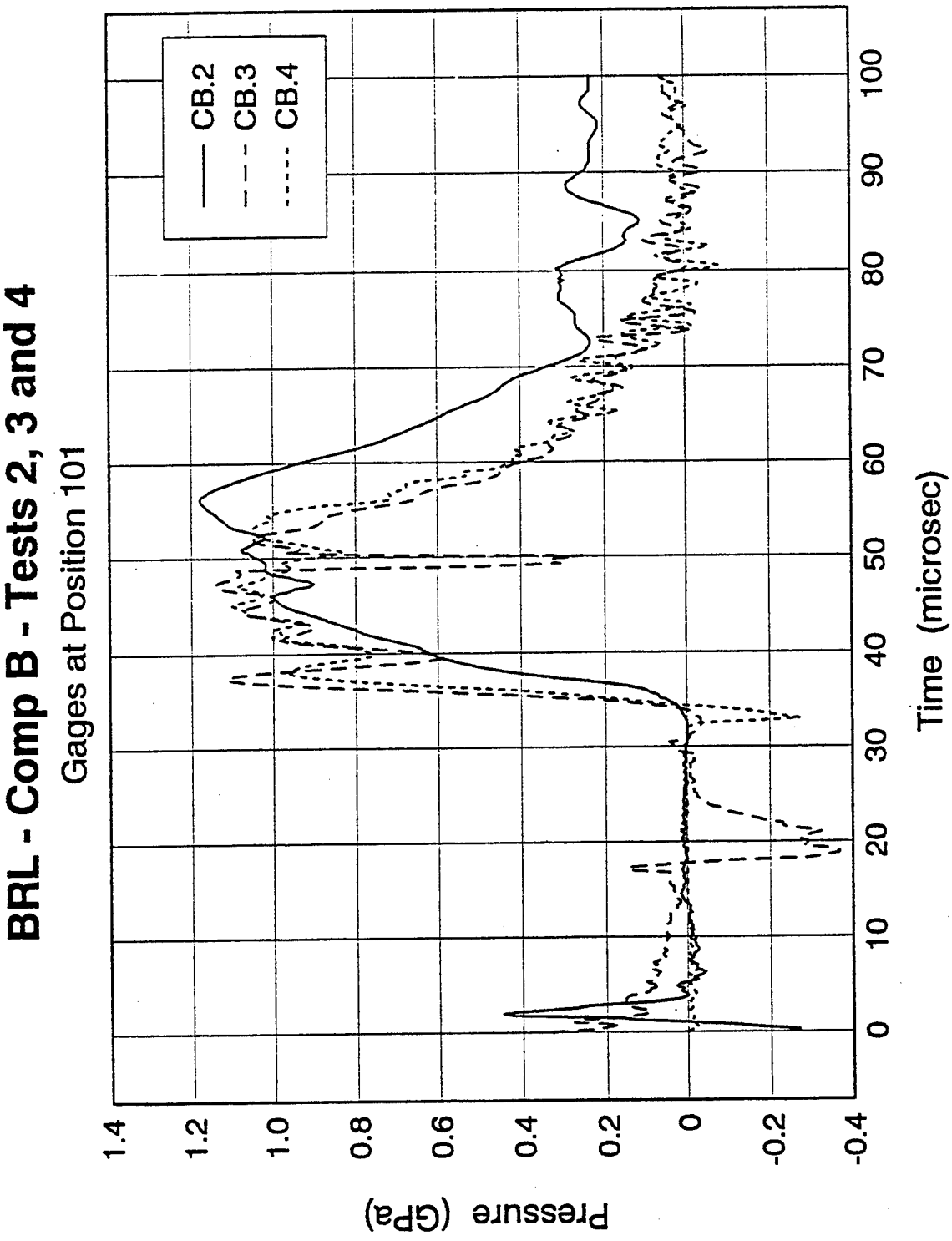

Figure 41. Position 101 gage records from all Comp B field tests.

exceptions, but are not as serious as LX.4. Based on the blast measurements the most energetic explosive is LX-14, followed by Comp B, and Pentolite is the least energetic.

The agreement between the measured and calculated blast pressures for 10 g of LX-14 in the 64:1 vessel is good for stations 36 and 45, but is poor for stations 1 and 47. Calculations for the other explosive types and weights and for the other confinement vessel are not available to compare with experiment.

For the 10 g LX-14 tests the average measured resonance time for the 64:1 vessel for station 1 is 52 μs, which is 24 μs shorter than the calculations. At station 36 the average period is 55 μs while the calculated value is 62 μs which is 10 % agreement rather than 30 % for station 1. Station 1 measurements from the 15 g LX-14 tests in the 40:1 vessel results in a measured period of 49 μs and calculated period of 60 μs. At station 36 the measured period is 58 μs and the calculated time is 70 μs. Finally at station 47 the measured period is 55 μs and the calculated period is 60 μs which is good agreement. Two further observations about the reverberation signals are (1) the period seemed to increase by 10 - 15 % with time and (2) after about 200 μs the reverberation signals have died out. The measurement of the period is difficult because there is evidence for more than one vessel resonance frequency, complicating the identification of like resonance signal peaks.

The bar gage proved to be the best transducer/sensor combination for measuring the blast pressure. The concept is uncomplicated, the technique direct, the signals generally easy to interpret, the gage is simple to calibrate, and the gage has good high frequency response. The source or sources of the high frequency noise bursts (approximately 0.8 - 1.0 MHz) that appeared on the signal records from the bar gages is still unknown. Grounding each part of the experimental apparatus to a heavy ground strap and then grounding the strap at a single point

did reduce the noise, but did not eliminate it.

The charge mode PCB pressure gage with an external charge amplifier used in these tests is an adequate gage for blast measurements in the range of shock pressures from 50 to 500 MPa. Even at the high pressure end the gage has sufficient frequency response to produce a readable signal. The PCB gages with the built-in charge amplifiers, however, do not have sufficient high frequency response at high shock pressures. Often the records were plagued by high frequency signals related to overdriving the gage and cable connection problems.

The 1/8th watt, 470 ohm carbon composition resistor has promise as a pressure gage, but the carbon flat pack gage is not useful in the experimental arrangement used for these tests.

10. **RECOMMENDATIONS**

10.1. Usage of PVDF Gages. Combining the PVDF gage with a steel bar should be pursued as a pressure gage. The PVDF material has high output under shock conditions and hence, the voltage signal can be connected directly to the recording device without signal conditioning and amplification. The gages are expensive, however, if calibrated by the manufacturer. A method for ensuring good contact between the ends of the bars and the active area of the gage needs working out. Because the PVDF material has high output a solution may be for the active gage area be only 5% of the area of the end of the bar. It would seem easier to ensure good contact over a very small gage area than over the large area of the bar.

10.2. Pressed Versus Cast Explosives. As stated earlier problems were encountered in initiating the Comp B explosives in the 15 and 900 g sizes (and maybe even the 10 g size) and required placing a small booster charge of Detasheet between the detonator and the main charge. The reason is the charges were cast rather than pressed to the desired shape and size. It is

recommended that in the future the charges be fabricated by pressing the explosive material to near crystal density. This ensures sufficient void volume for the creation of hot spots to support prompt detonation.

11. REFERENCES

Lottero, R.E. and J.D. Wortman. "Computation Predictions of Close-in Blast Loading from Bare Spherical Charges." Proceedings of the 1988 Army Science Conference, Fort Monroe, VA, 26 - 27 October, 1988.

Lottero, R.E. "Statement of Work: Measurement of Pressure from Explosives in a Low Volume Ratio Closed Chamber." BRL Report, 1988.

Lottero, R.E. "Statement of Work: Close-in Explosive Blast Loading Measurements and Analysis." BRL Report, 1989.

Timoshenko, S. Strength of Materials Part II, Advanced Theory and Problems. 3rd Ed. D. Van Nostrand Co., Inc. Princeton, NJ, 1959.

ASME, "Section VIII - Division 2 Pressure Vessels." ASME Boiler and Pressure Vessel Committee, Rules for Construction of Pressure Vessels, American Society of Mechanical Engineers, New York, NY, 1974.

Allison, W.D. BRL Communications, 1989.

Groethe, M. "Ground Motion and Airblast Gauges." S-CUBED Report SSS-DVR-89-1003, November 1988.

Steel bars were purchased from KONCOR Industries, Division of Latrobe Steel Co., Subsidiary of the Timken Co., Wauseon, OH.

Kolsky, H. Stress Waves in Solids. Dover Publications, Inc., New York, NY, 1963.

Edwards, D.H., G. Hooper, and D. Tasker. "Blast Wave Measurements Close to Explosive Charges." Report to R.A.R.D.E. Fort Halstead under Extra-Mural Contract ER3/9/4/2110/010/RAR, 1978.

Edwards, D.H., G.O. Thomas, and D. Tasker. "Blast Wave Measurements Close to Explosive Charges." Interim Report to R.A.R.D.E. Fort Halstead under Extra-Mural Contract

ER/9/4/2110/010/RAR, 1980.

Watson, R.W. "Gauge for Determining Shock Pressures," Review of Scientific Instruments, vol. 38, no. 7, pp.978-980, 1967.

Wilson, W.H., D.C. Holloway, and G. Bjarnholt. "Measurement of Pressure Loading from Explosively Loaded Boreholes Using Expendable Piezoelectric Transducers," Technology and Theory of Stress Measurements for Shock Applications, AMD, Vol 83, R.B. Stout, F.R. Norwood, and M. Fourney, Editors, American Society of Mechanical Engineers, pp 97-108, 1987.

Bauer, F., and A. Lichtenberger. "Use of PVDF Shock Gauges for Stress Measurements in Hopkinson Bar." Proceedings of the 1987 APS Topical Conference on Shock Compression of Condensed Matter. Elsevier Science Pub., 1988, pp 631-634.

INTENTIONALLY LEFT BLANK.

APPENDIX:

DATA PLOTS

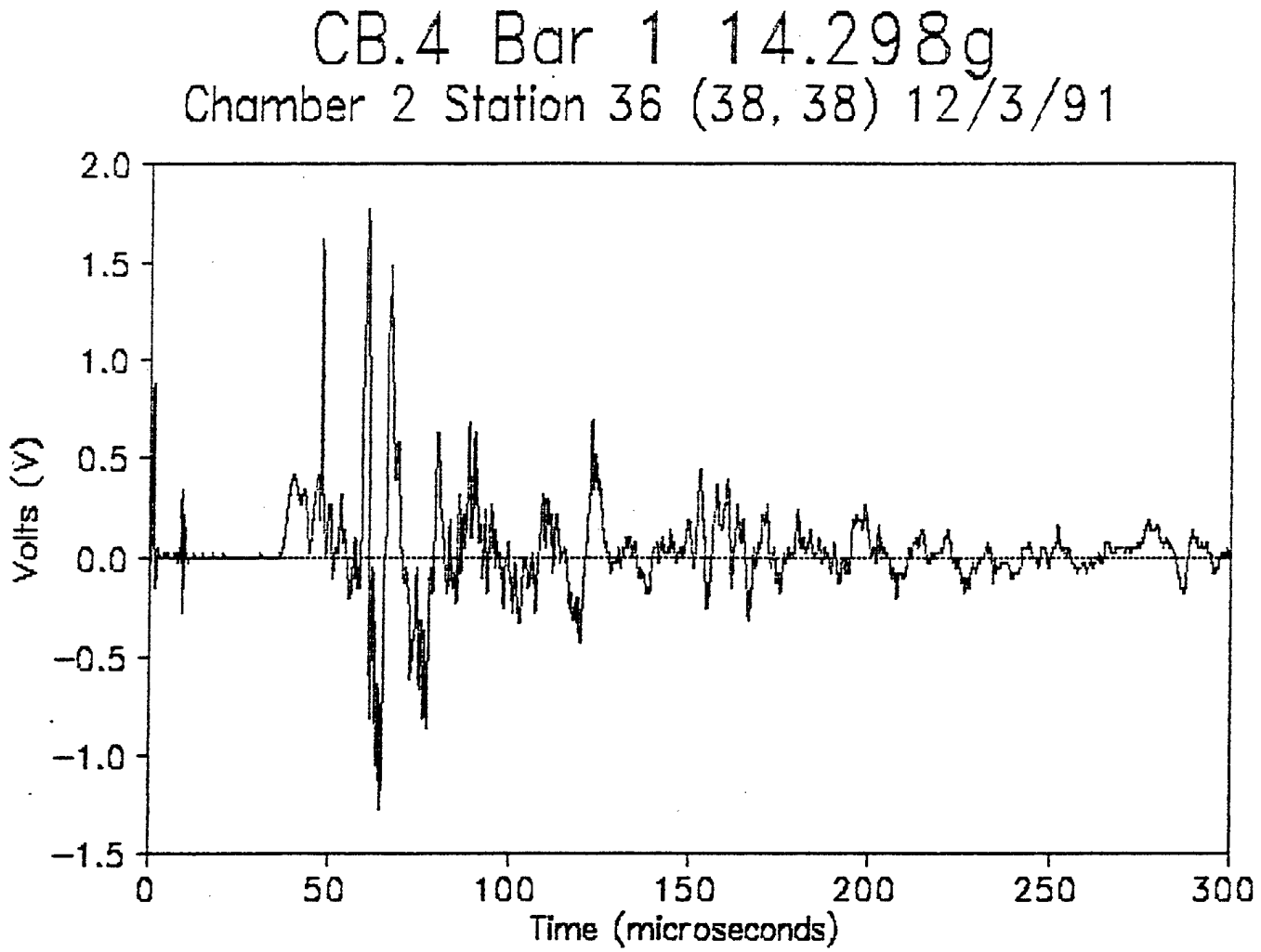
CB.4 Bar 1 14.298g
Chamber 2 Station 36 (38, 38) 12/3/91
2.0
1.5
1.0
0.5
0.0
−0.5
−1.0
−1.5
Volts (V)
0
50
100
150
200
250
300
Time (microseconds)

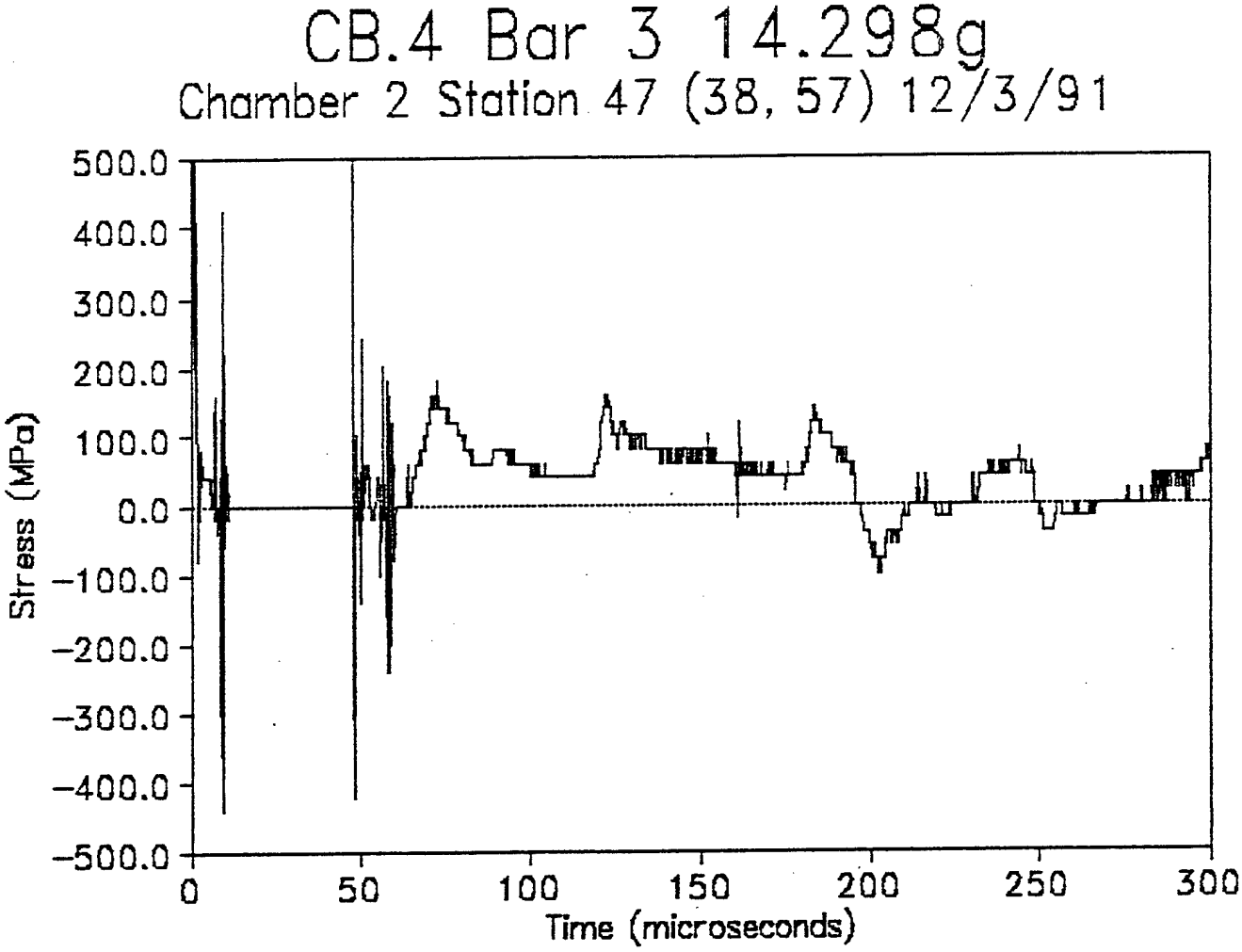
CB.4 Bar 3 14.298g
Chamber 2 Station 47 (38, 57) 12/3/91
500.0
400.0
300.0
200.0
100.0
0.0
-100.0
-200.0
-300.0
-400.0
-500.0
Stress (MPa)
0
50
100
150
200
250
300
Time (microseconds)

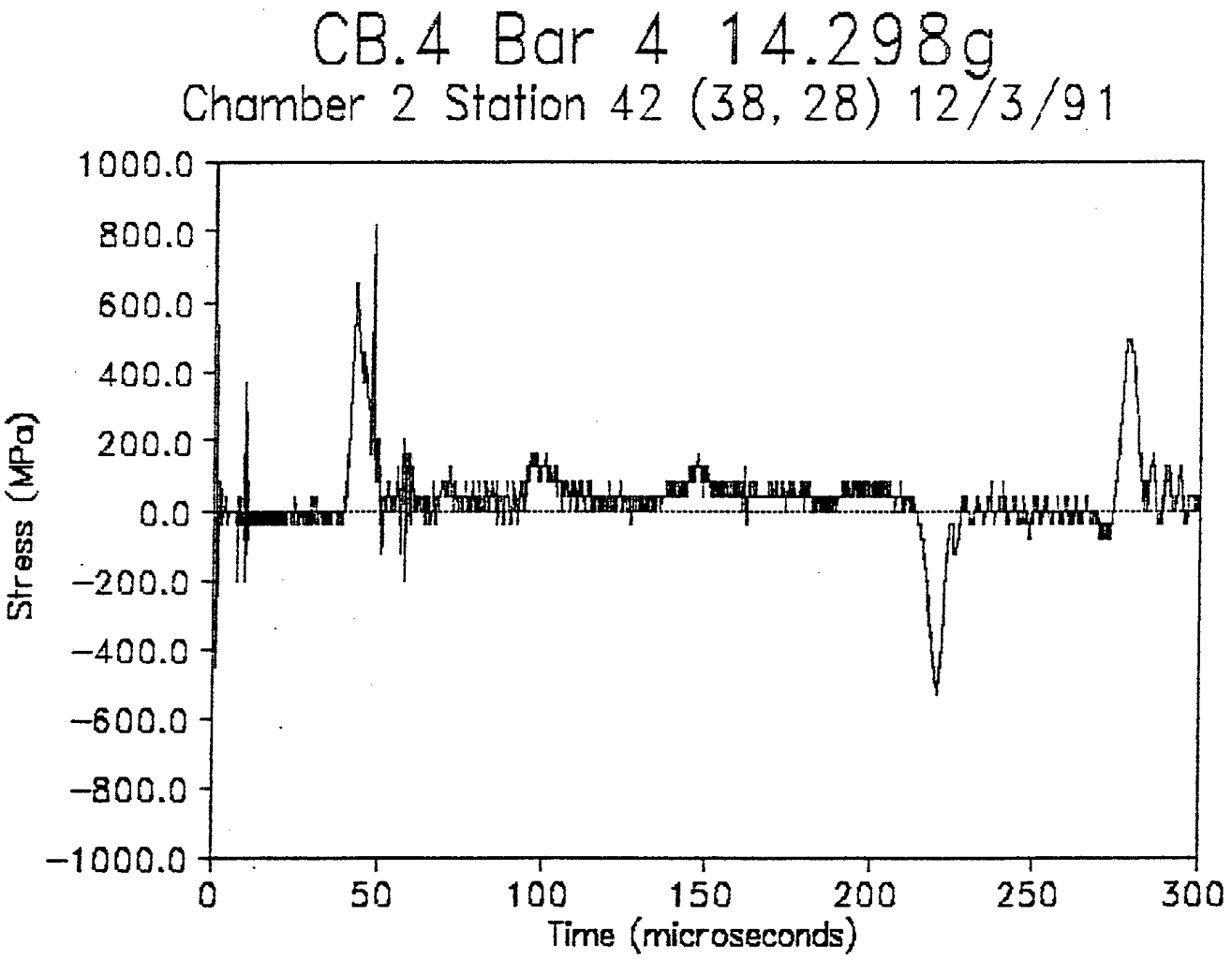
CB.4 Bar 4 14.298g
Chamber 2 Station 42 (38, 28) 12/3/91
1000.0
800.0
600.0
400.0
200.0
0.0
-200.0
-400.0
-600.0
-800.0
-1000.0
Stress (MPa)
0
50
100
150
200
250
300
Time (microseconds)

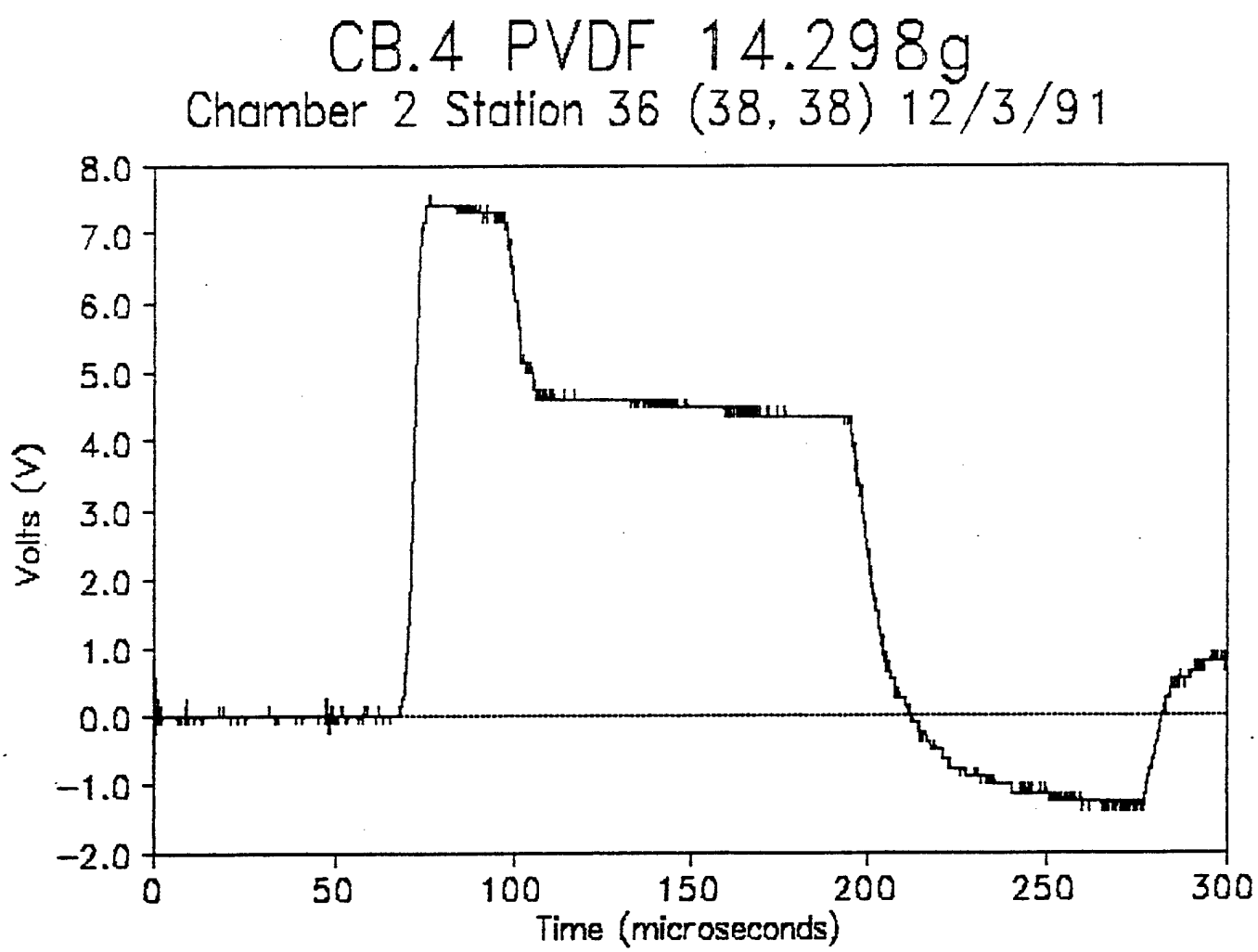
CB.4 PVDF 14.298g
Chamber 2 Station 36 (38, 38) 12/3/91
8.0
7.0
6.0
5.0
4.0
3.0
2.0
1.0
0.0
−1.0
−2.0
Volts (V)
0
50
100
150
200
250
300
Time (microseconds)

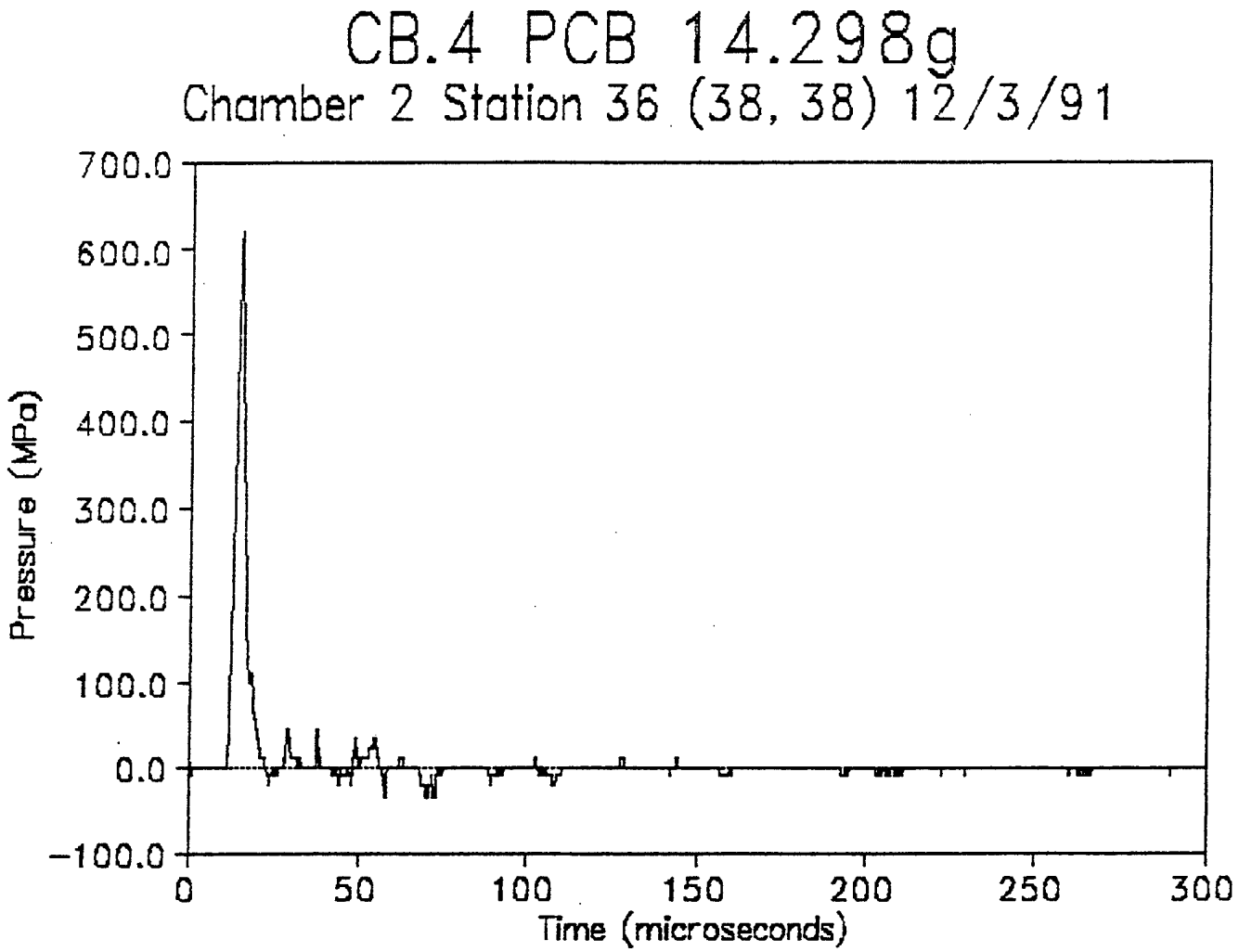
CB.4 PCB 14.298g
Chamber 2 Station 36 (38, 38) 12/3/91
700.0
600.0
500.0
400.0
300.0
200.0
100.0
0.0
-100.0
Pressure (MPa)
0
50
100
150
200
250
300
Time (microseconds)

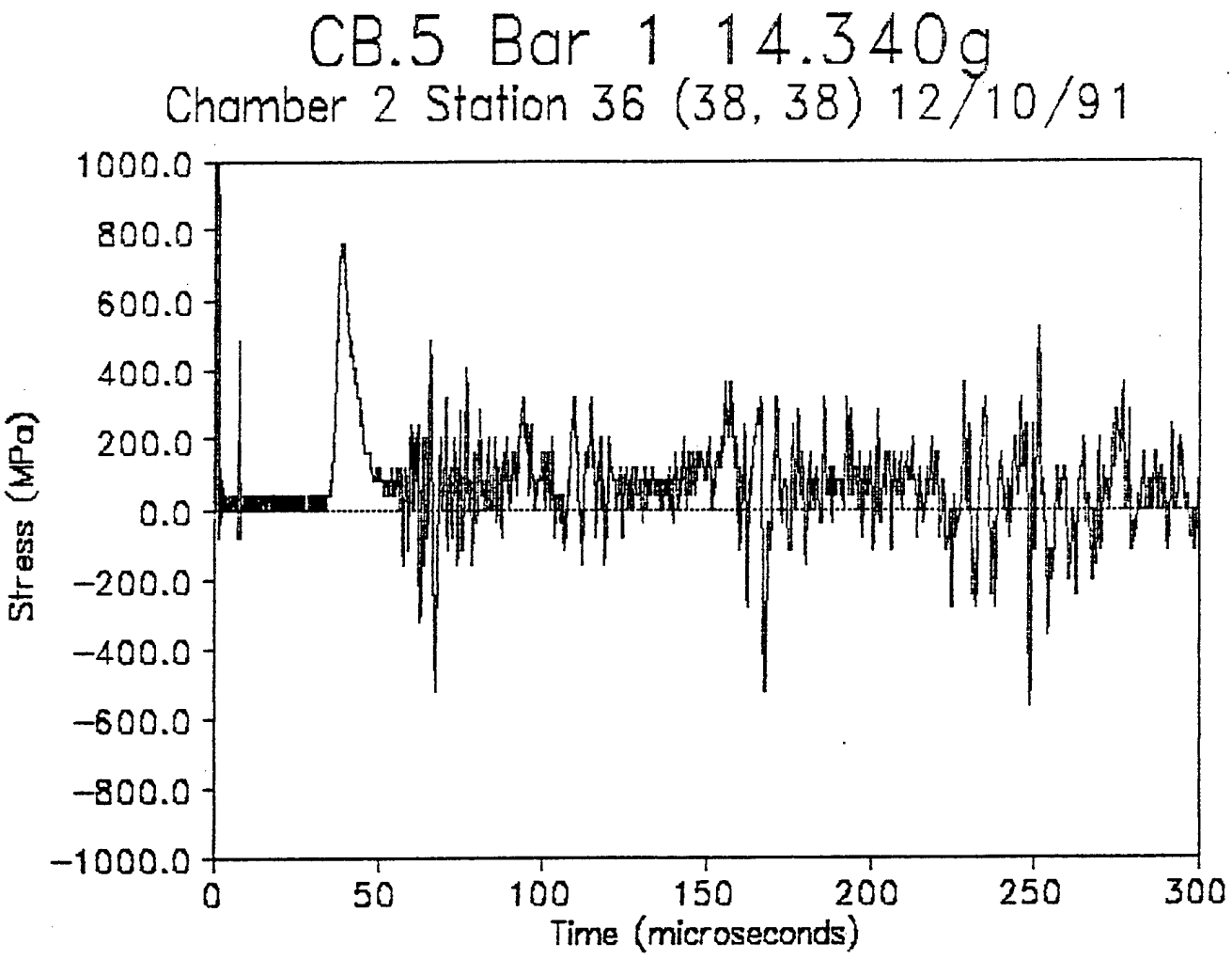
CB.5 Bar 1 14.340g
Chamber 2 Station 36 (38, 38) 12/10/91
1000.0
800.0
600.0
400.0
200.0
0.0
-200.0
-400.0
-600.0
-800.0
-1000.0
Stress (MPa)
0
50
100
150
200
250
300
Time (microseconds)

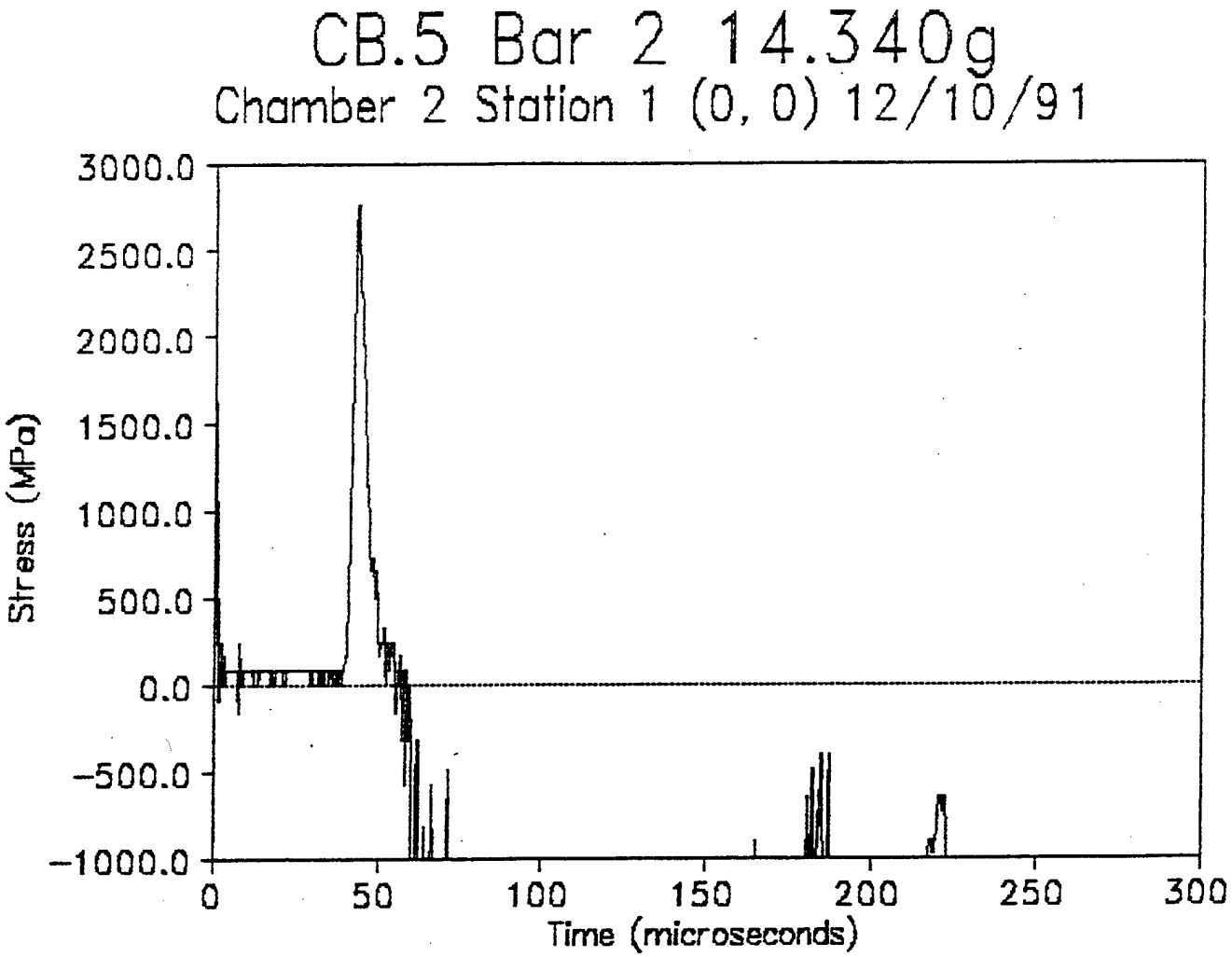
CB.5 Bar 2 14.340g
Chamber 2 Station 1 (0, 0) 12/10/91
3000.0
2500.0
2000.0
1500.0
1000.0
500.0
0.0
-500.0
-1000.0
Stress (MPa)
0
50
100
150
200
250
300
Time (microseconds)

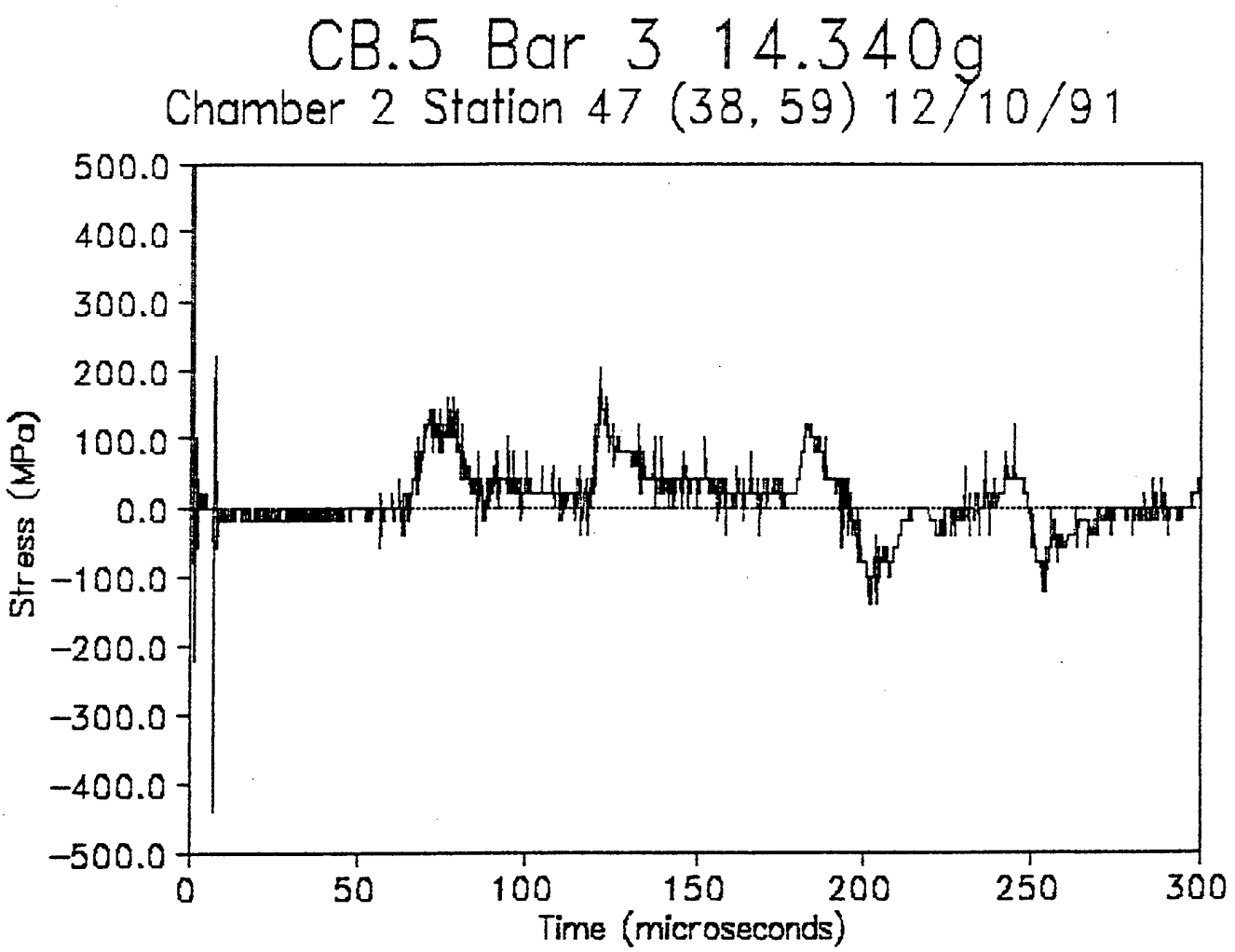
CB.5 Bar 3 14.340g
Chamber 2 Station 47 (38, 59) 12/10/91
500.0
400.0
300.0
200.0
100.0
0.0
-100.0
-200.0
-300.0
-400.0
-500.0
Stress (MPa)
0
50
100
150
200
250
300
Time (microseconds)

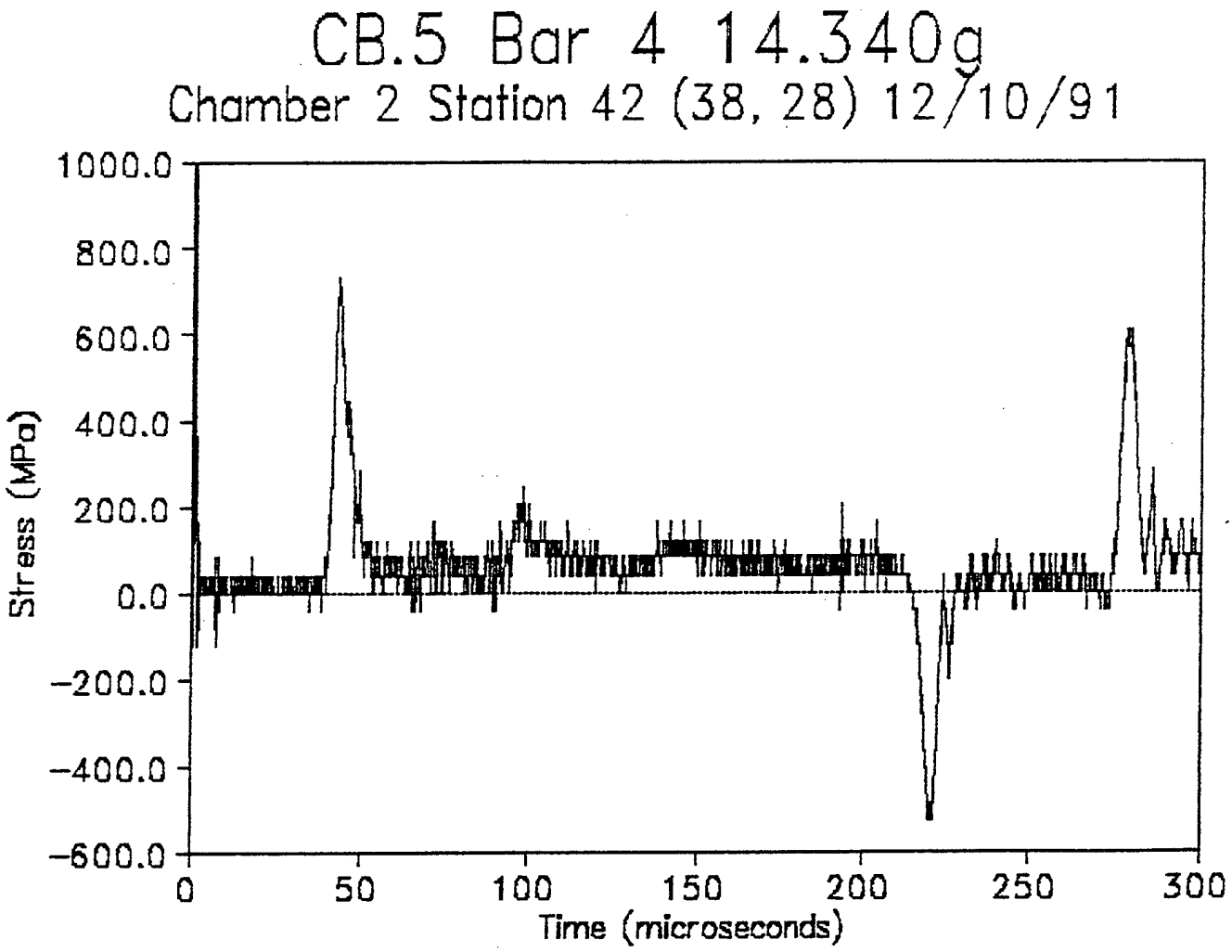
CB.5 Bar 4 14.340g
Chamber 2 Station 42 (38, 28) 12/10/91
1000.0
800.0
600.0
400.0
200.0
0.0
-200.0
-400.0
-600.0
Stress (MPa)
0
50
100
150
200
250
300
Time (microseconds)

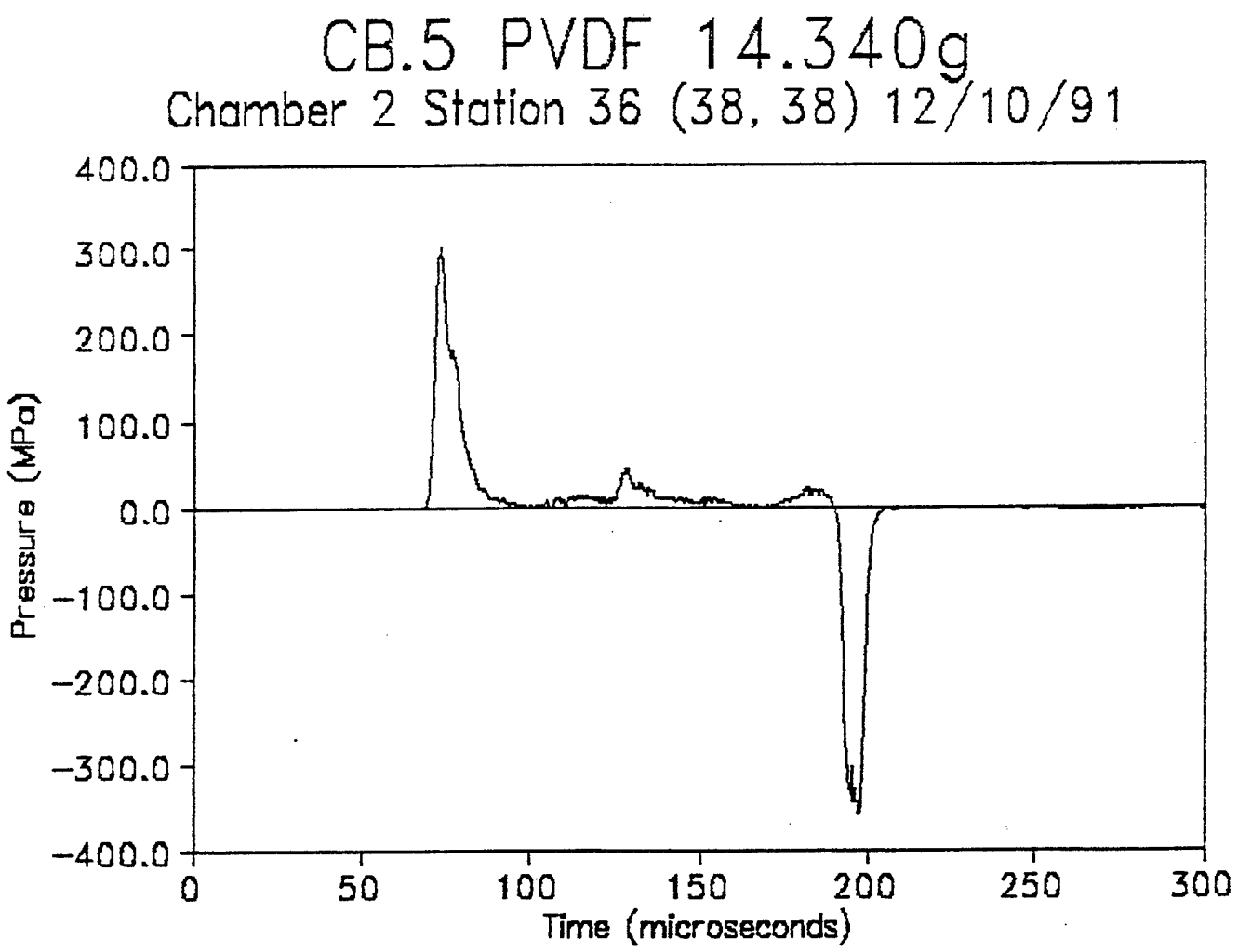
CB.5 PVDF 14.340g
Chamber 2 Station 36 (38, 38) 12/10/91
400.0
300.0
200.0
100.0
0.0
-100.0
-200.0
-300.0
-400.0
Pressure (MPa)
0
50
100
150
200
250
300
Time (microseconds)

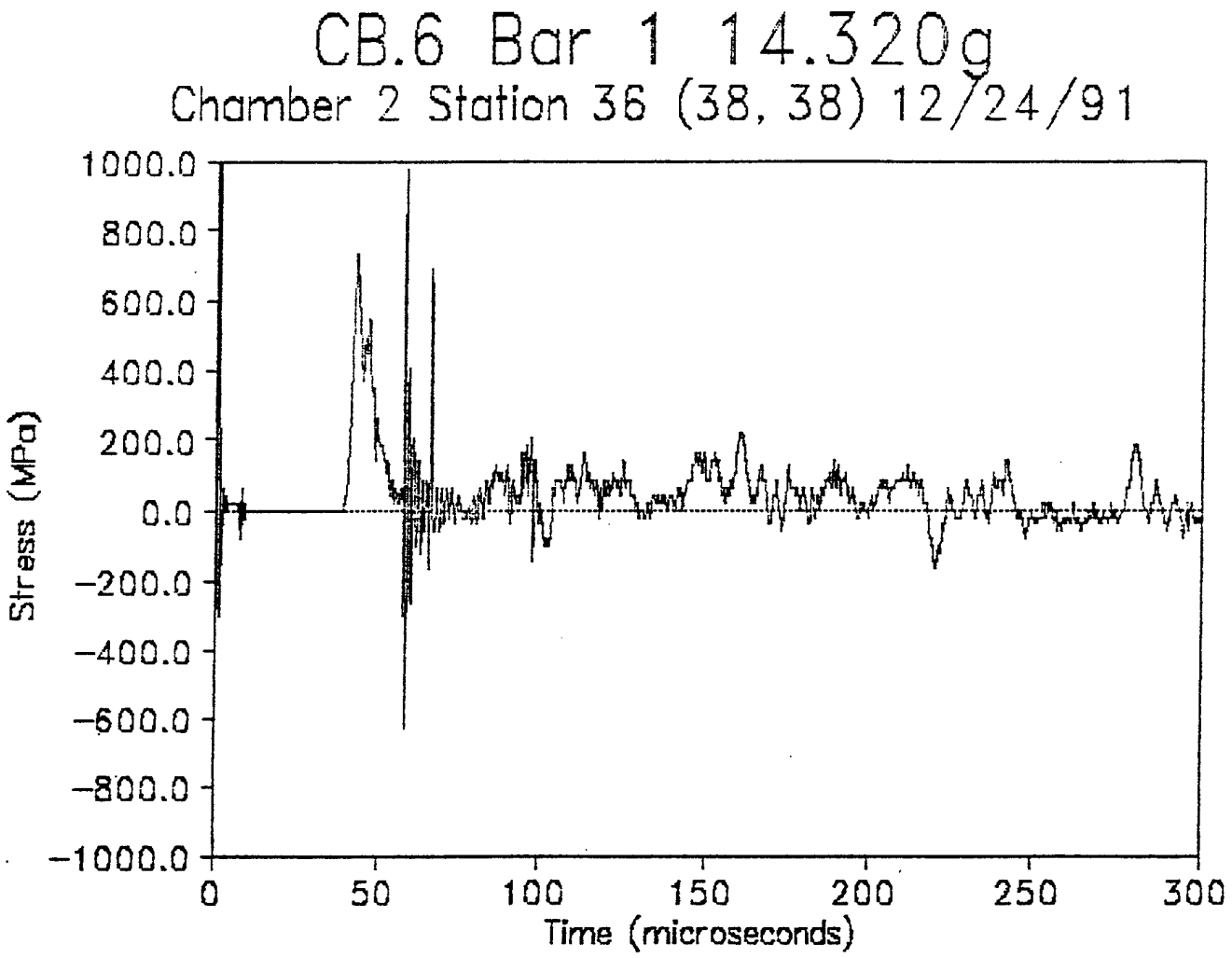
CB.6 Bar 1 14.320g
Chamber 2 Station 36 (38, 38) 12/24/91
1000.0
800.0
600.0
400.0
200.0
0.0
-200.0
-400.0
-600.0
-800.0
-1000.0
Stress (MPa)
0
50
100
150
200
250
300
Time (microseconds)

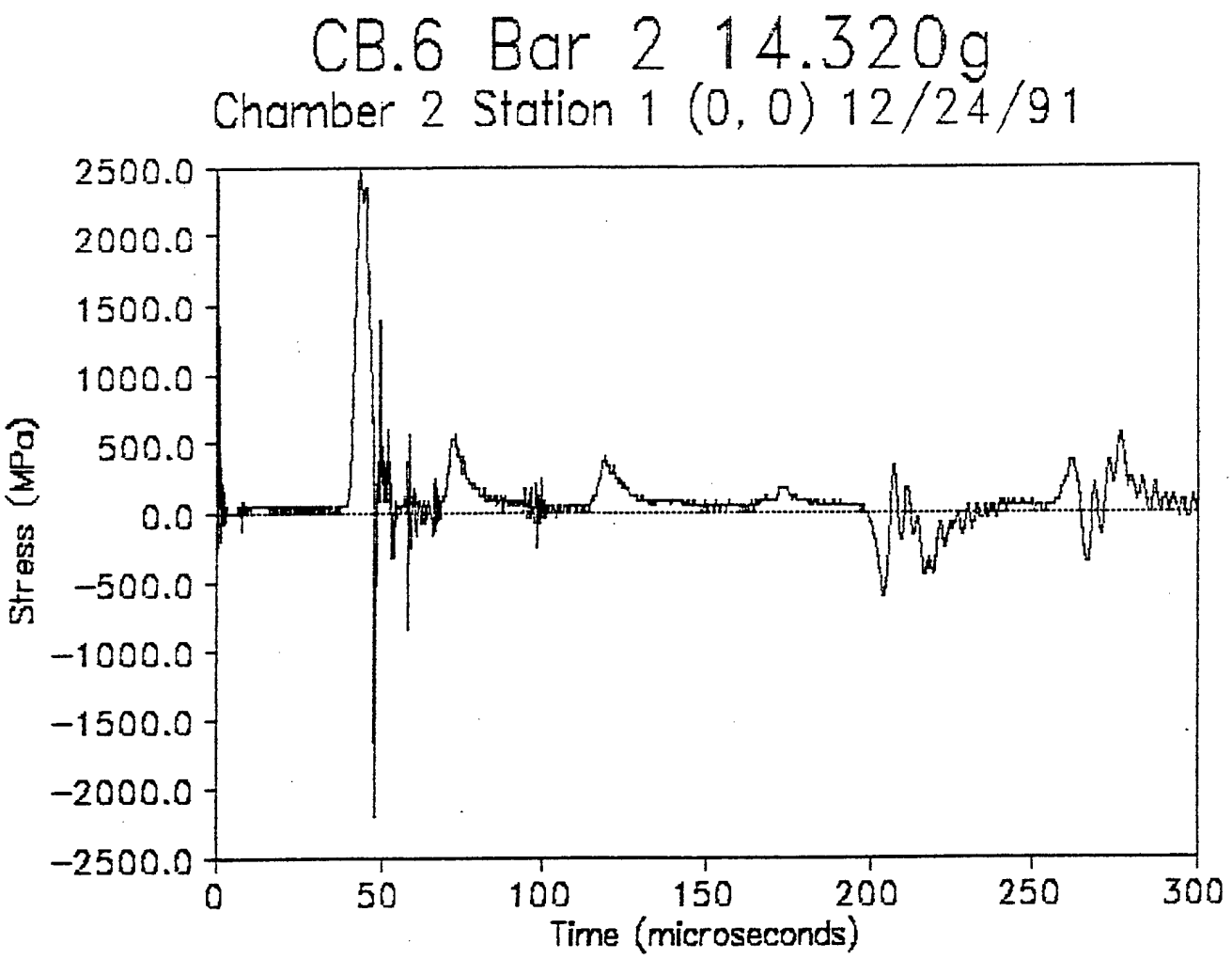
CB.6 Bar 2 14.320g
Chamber 2 Station 1 (0, 0) 12/24/91
2500.0
2000.0
1500.0
1000.0
500.0
0.0
-500.0
-1000.0
-1500.0
-2000.0
-2500.0
Stress (MPa)
0
50
100
150
200
250
300
Time (microseconds)

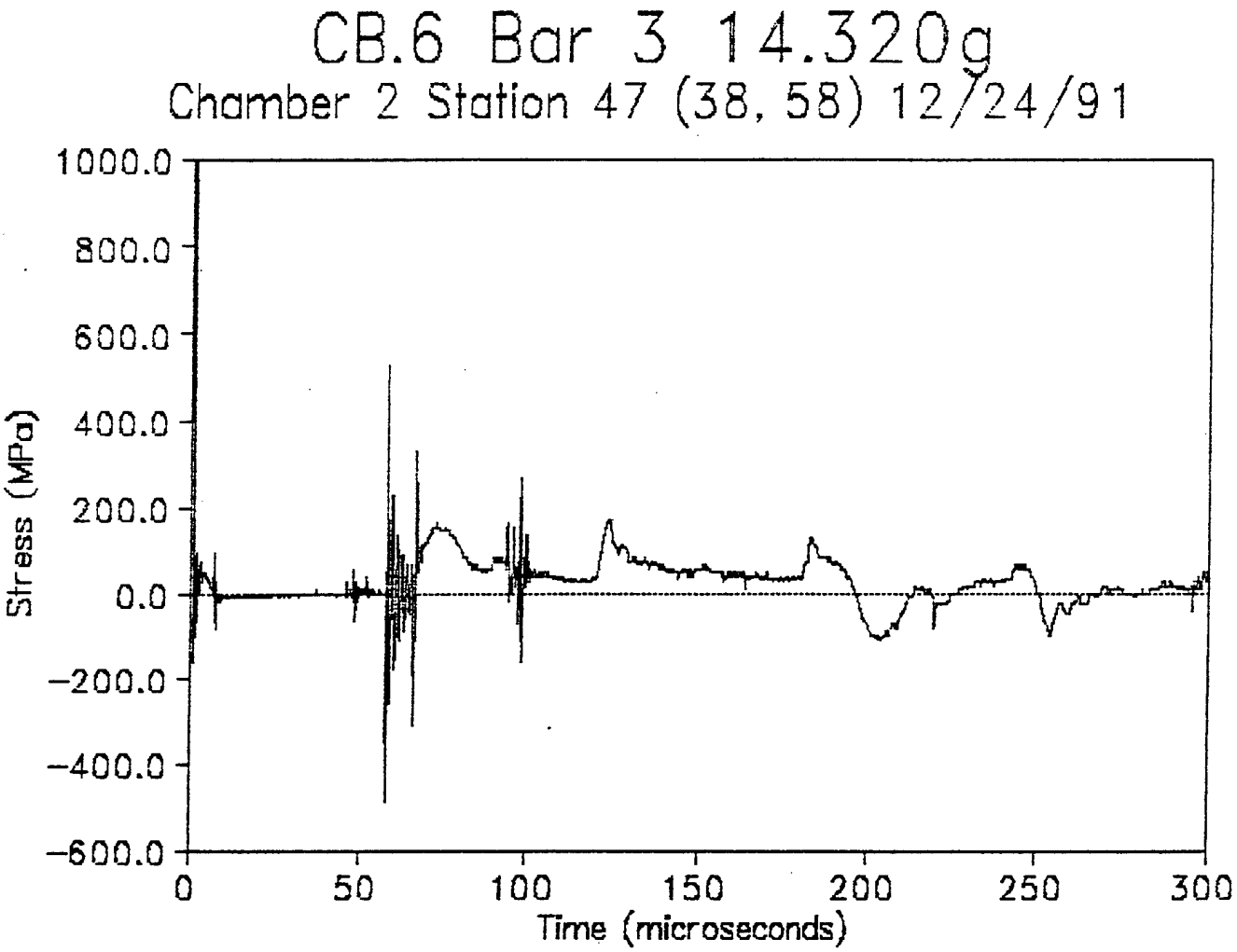
CB.6 Bar 3 14.320g
Chamber 2 Station 47 (38, 58) 12/24/91
1000.0
800.0
600.0
400.0
200.0
0.0
-200.0
-400.0
-600.0
Stress (MPa)
0
50
100
150
200
250
300
Time (microseconds)

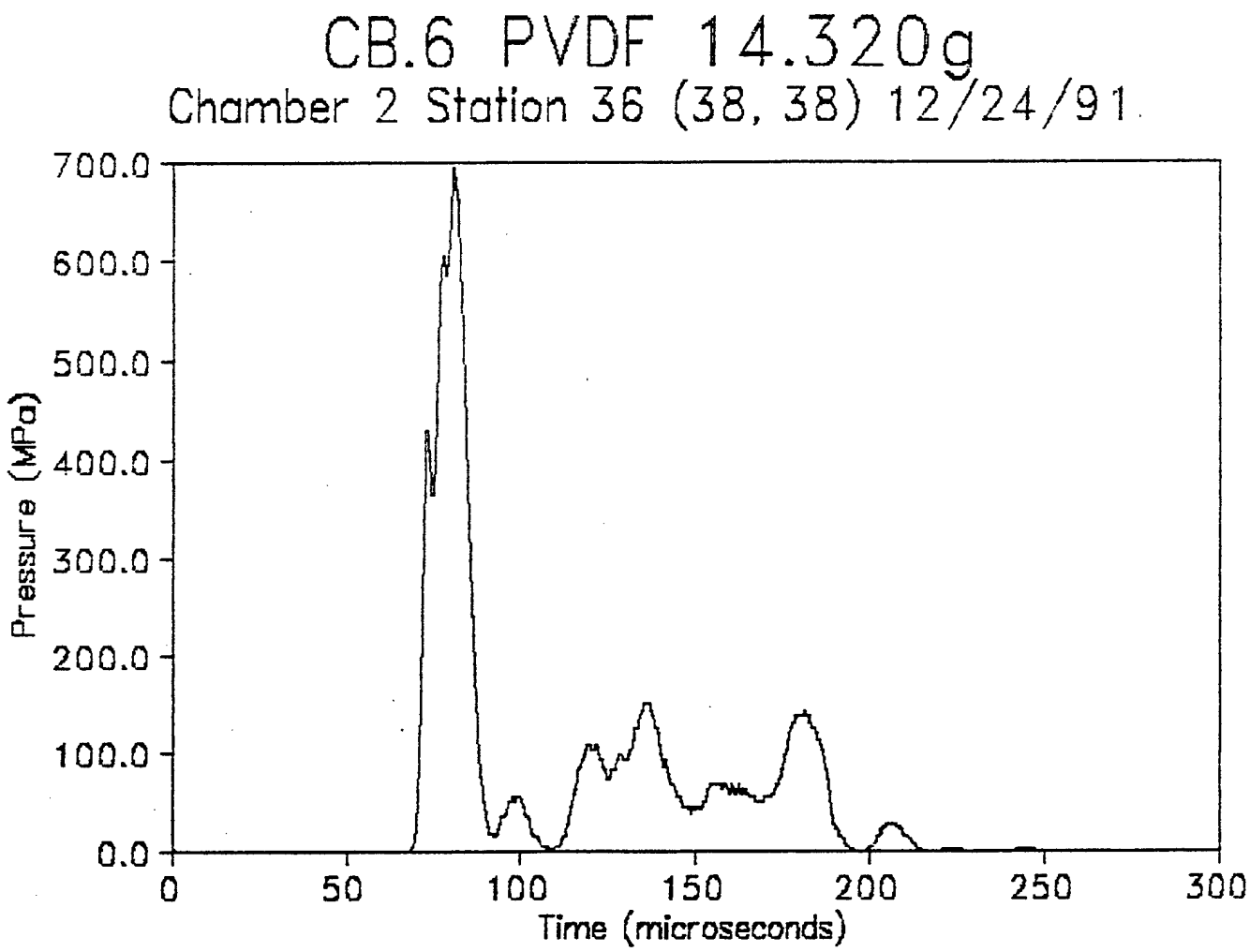
CB.6 PVDF 14.320g
Chamber 2 Station 36 (38, 38) 12/24/91
700.0
600.0
500.0
400.0
300.0
200.0
100.0
0.0
Pressure (MPa)
0
50
100
150
200
250
300
Time (microseconds)

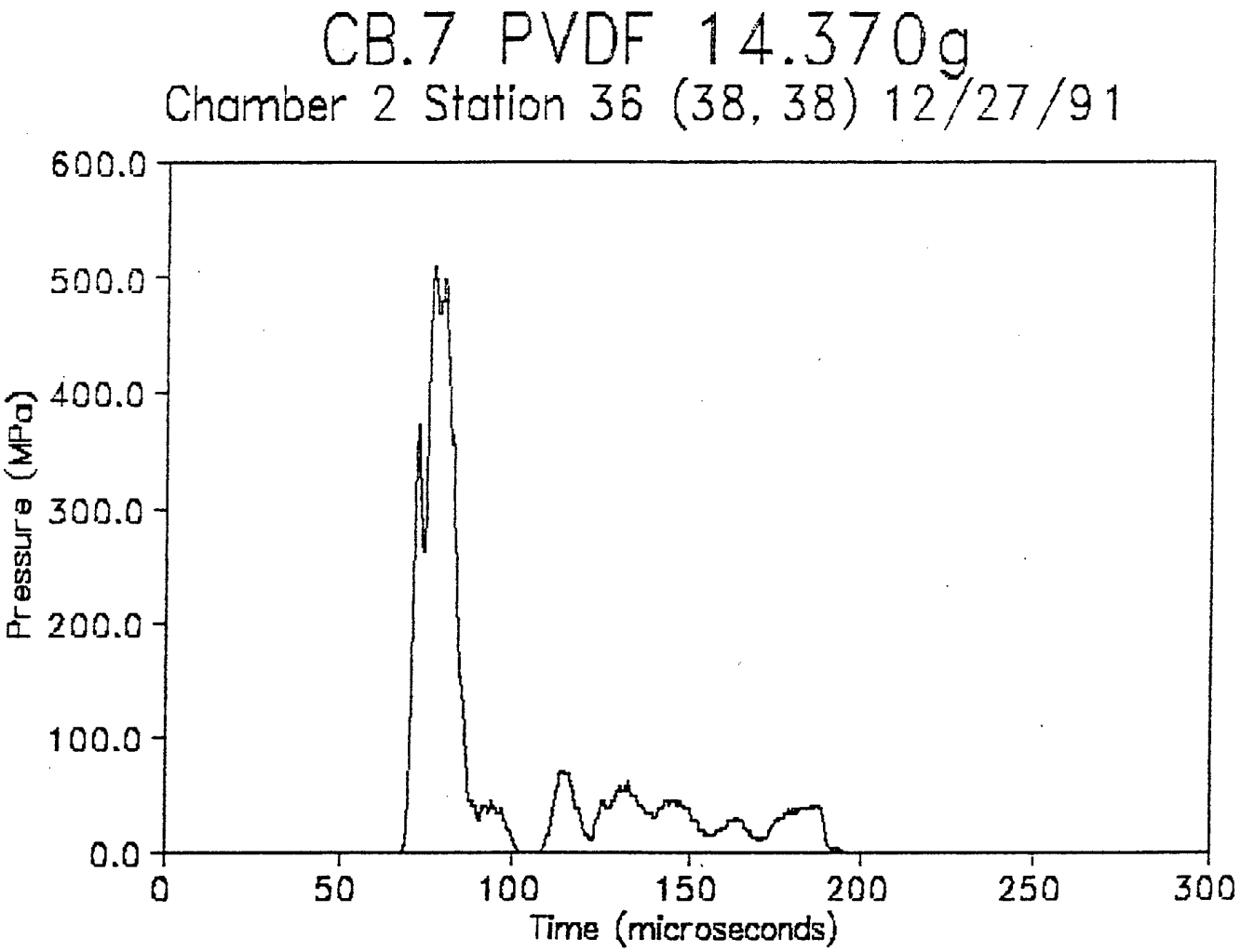
CB.7 PVDF 14.370g
Chamber 2 Station 36 (38, 38) 12/27/91
600.0
500.0
400.0
300.0
200.0
100.0
0.0
Pressure (MPa)
0
50
100
150
200
250
300
Time (microseconds)

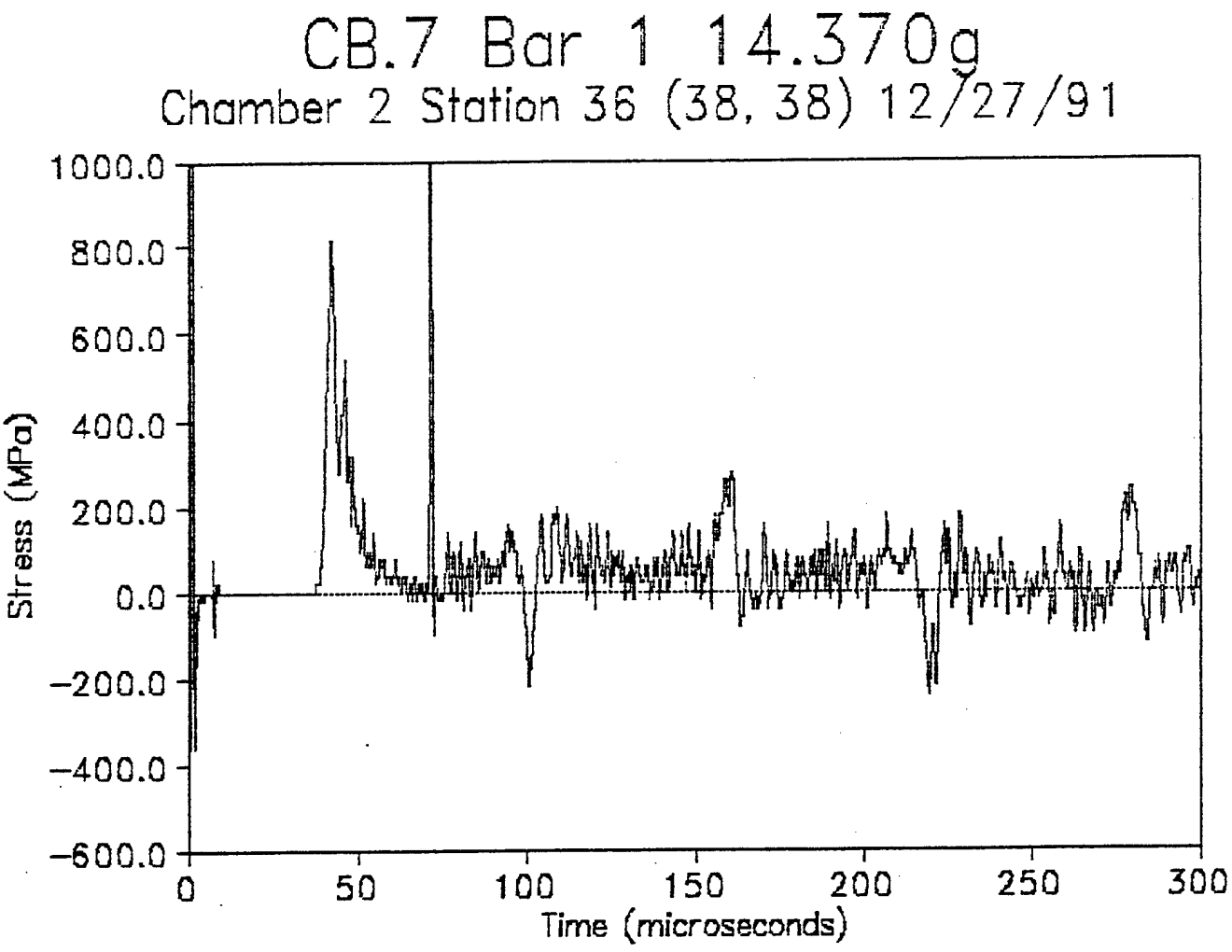
CB.7 Bar 1 14.370g
Chamber 2 Station 36 (38, 38) 12/27/91
1000.0
800.0
600.0
400.0
200.0
0.0
-200.0
-400.0
-600.0
Stress (MPa)
0
50
100
150
200
250
300
Time (microseconds)

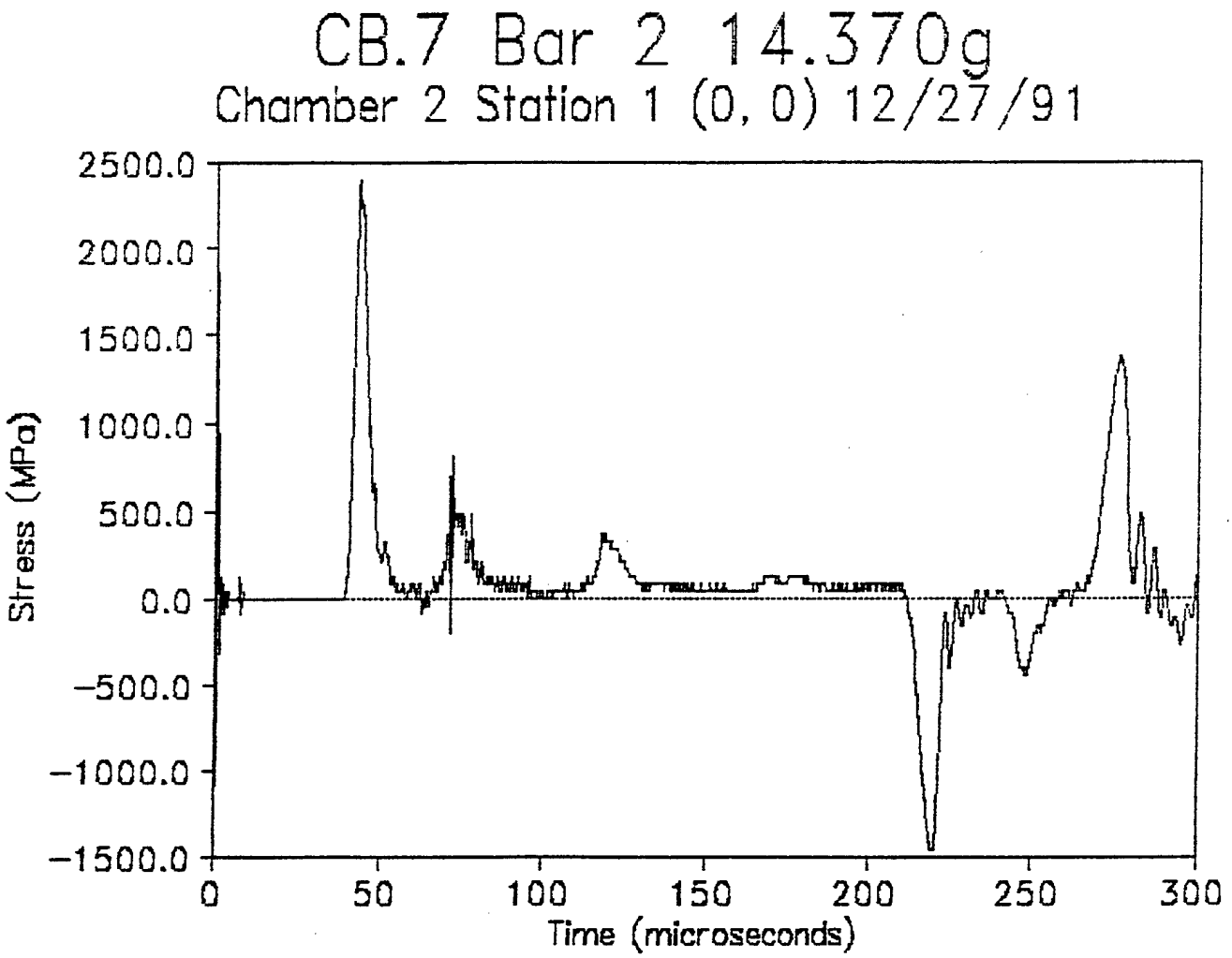
CB.7 Bar 2 14.370g
Chamber 2 Station 1 (0, 0) 12/27/91
2500.0
2000.0
1500.0
1000.0
500.0
0.0
−500.0
−1000.0
−1500.0
Stress (MPa)
0
50
100
150
200
250
300
Time (microseconds)

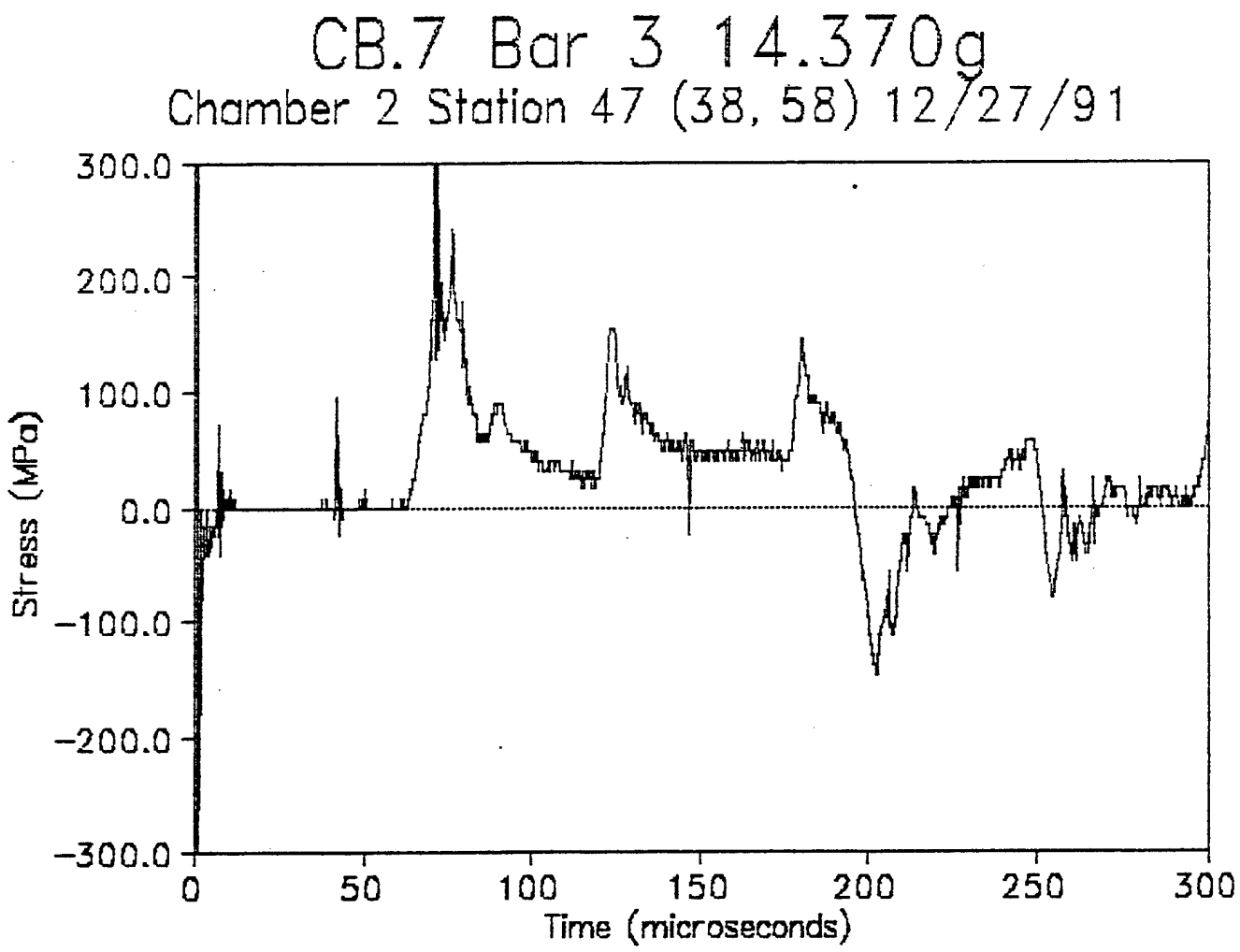
CB.7 Bar 3 14.370g
Chamber 2 Station 47 (38, 58) 12/27/91
300.0
200.0
100.0
0.0
-100.0
-200.0
-300.0
Stress (MPa)
0
50
100
150
200
250
300
Time (microseconds)

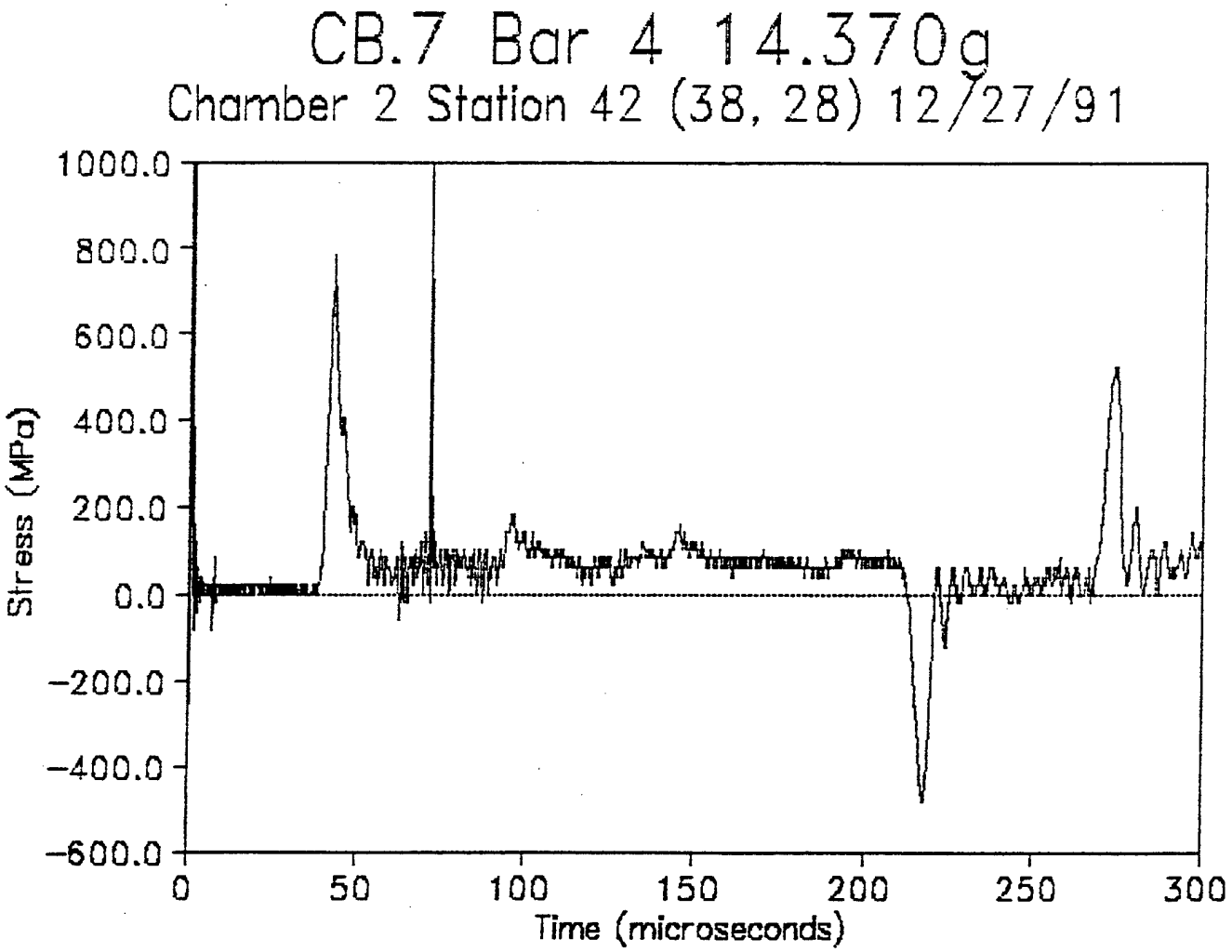
CB.7 Bar 4 14.370g
Chamber 2 Station 42 (38, 28) 12/27/91
1000.0
800.0
600.0
400.0
200.0
0.0
-200.0
-400.0
-600.0
Stress (MPa)
0
50
100
150
200
250
300
Time (microseconds)

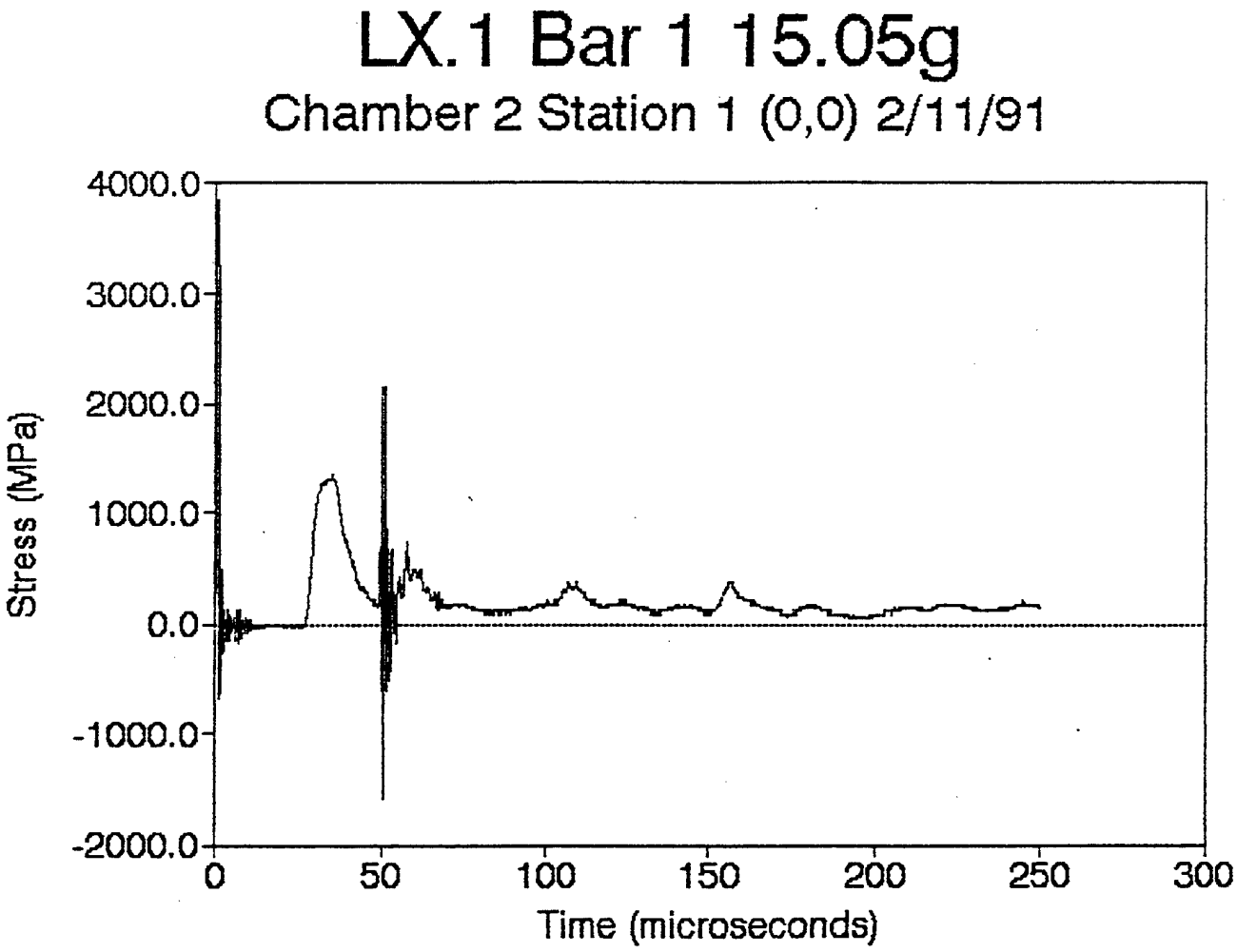
LX.1 Bar 1 15.05g
Chamber 2 Station 1 (0,0) 2/11/91
4000.0
3000.0
2000.0
1000.0
0.0
-1000.0
-2000.0
Stress (MPa)
0
50
100
150
200
250
300
Time (microseconds)

LX.1 Bar 2 15.05g

Chamber 2 Station 42 (38,28) 2/11/91

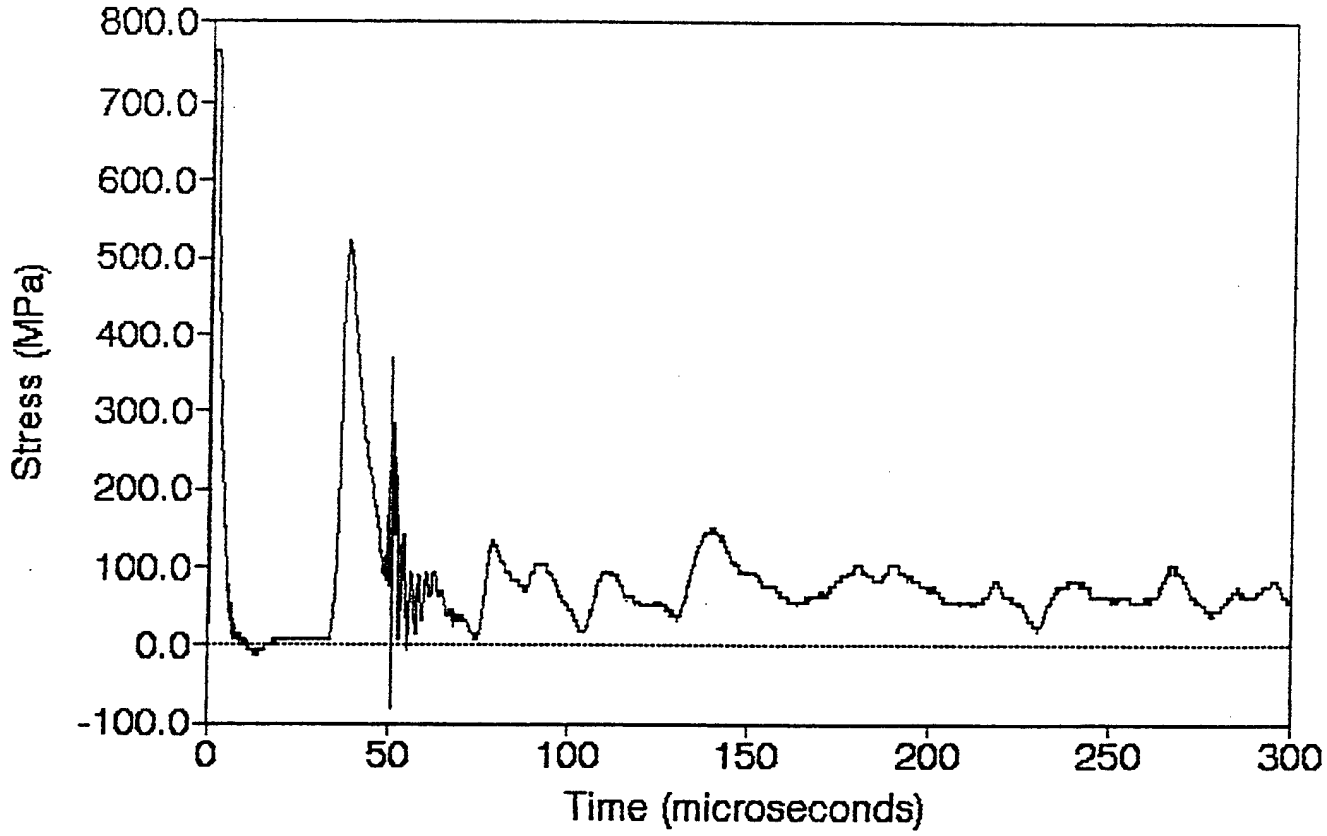

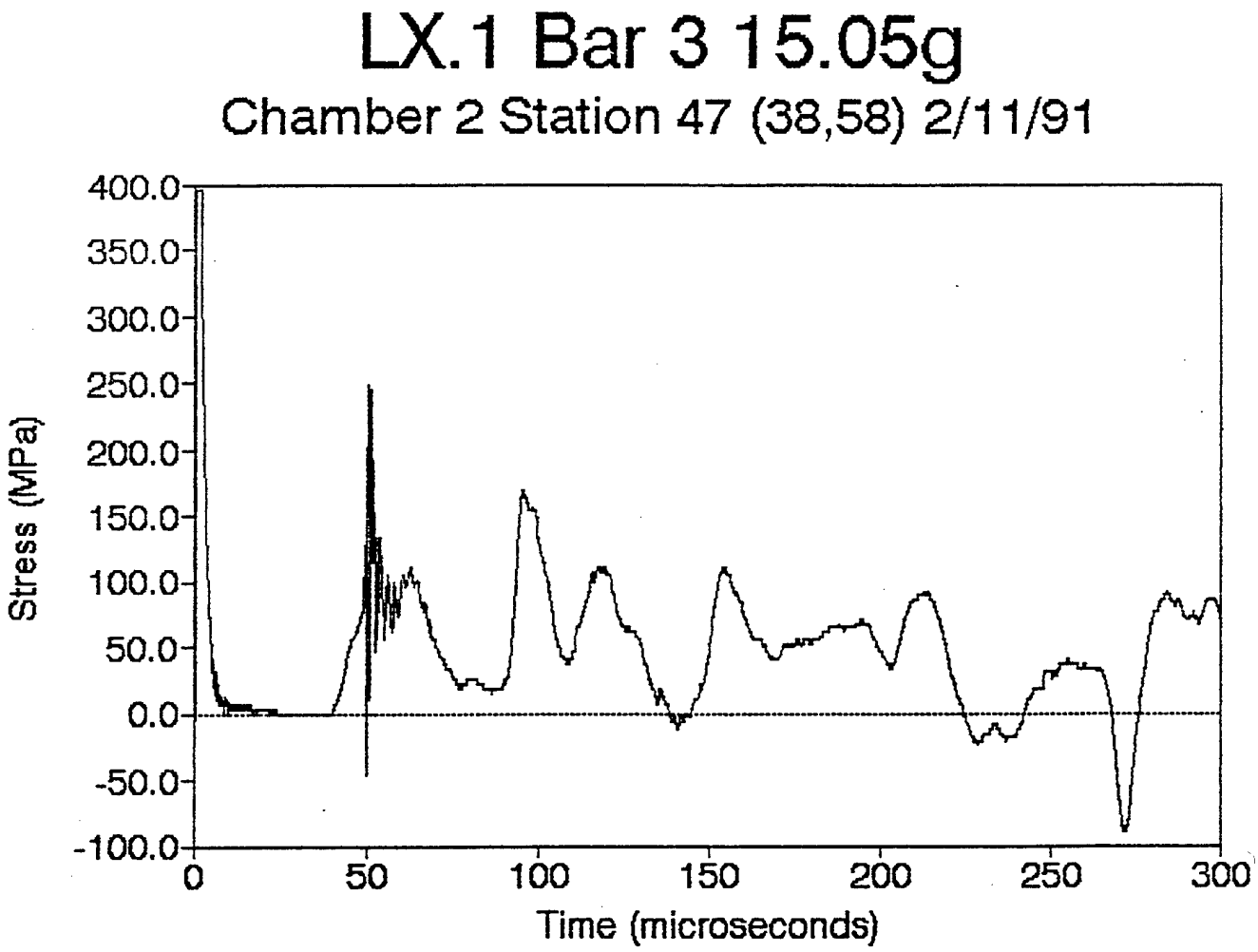
LX.1 Bar 3 15.05g
Chamber 2 Station 47 (38,58) 2/11/91
Stress (MPa)
400.0
350.0
300.0
250.0
200.0
150.0
100.0
50.0
0.0
-50.0
-100.0
0
50
100
150
200
250
300
Time (microseconds)

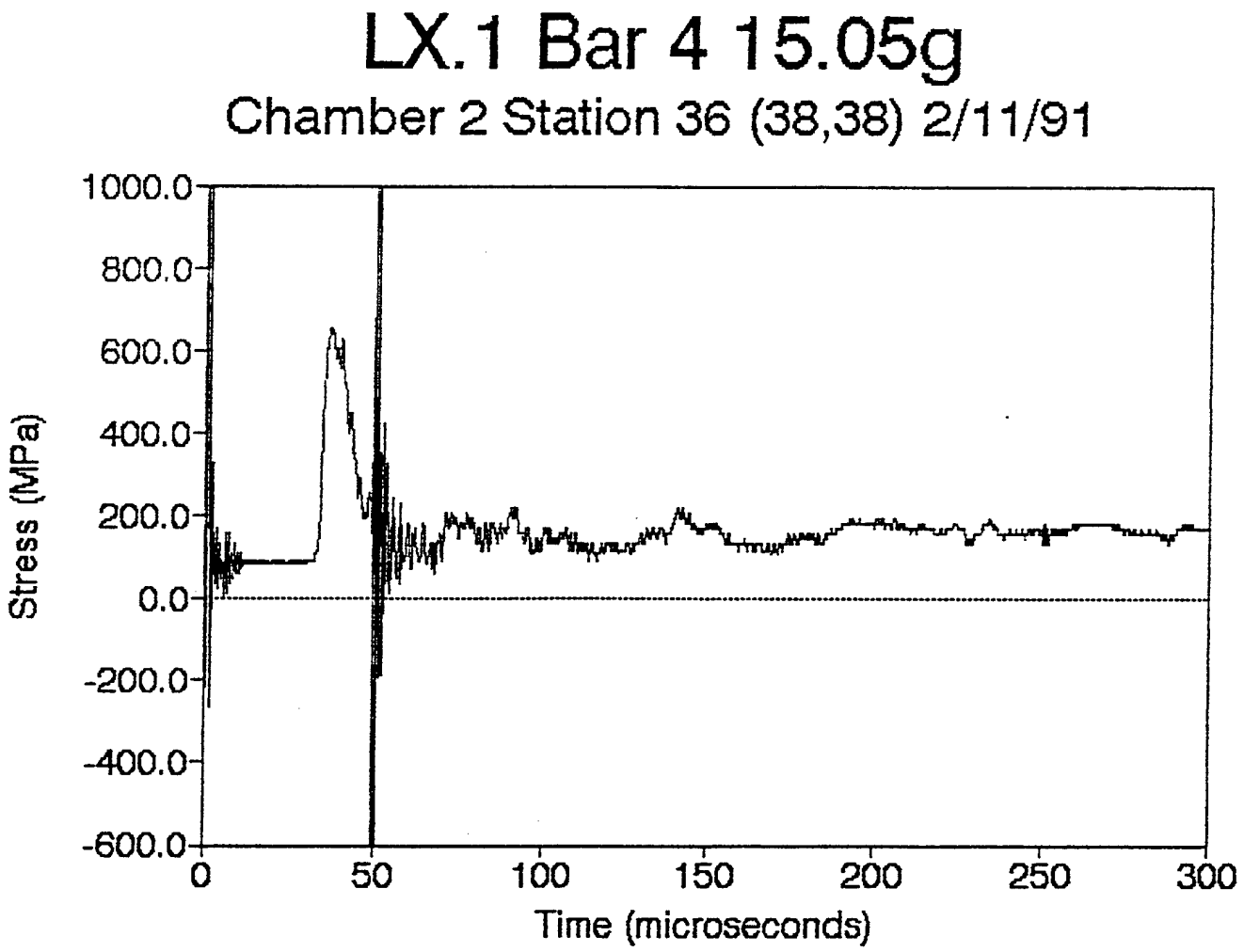
LX.1 Bar 4 15.05g
Chamber 2 Station 36 (38,38) 2/11/91
1000.0
800.0
600.0
400.0
200.0
0.0
-200.0
-400.0
-600.0
Stress (MPa)
0
50
100
150
200
250
300
Time (microseconds)

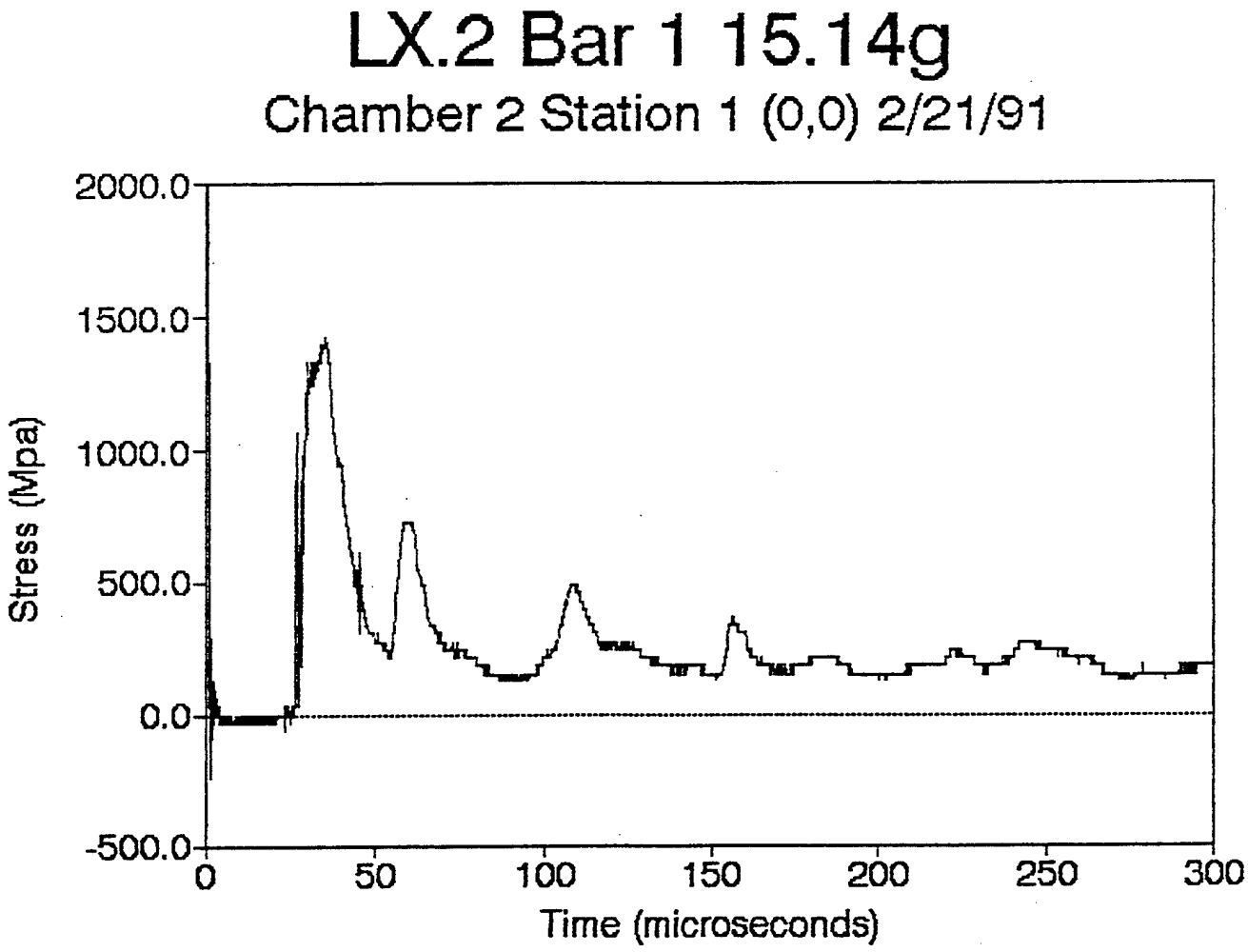
LX.2 Bar 1 15.14g
Chamber 2 Station 1 (0,0) 2/21/91
2000.0
1500.0
1000.0
500.0
0.0
-500.0
Stress (Mpa)
0
50
100
150
200
250
300
Time (microseconds)

LX.2 Bar 2 15.14g

Chamber 2 Station 42 (38.28) 2/21/91

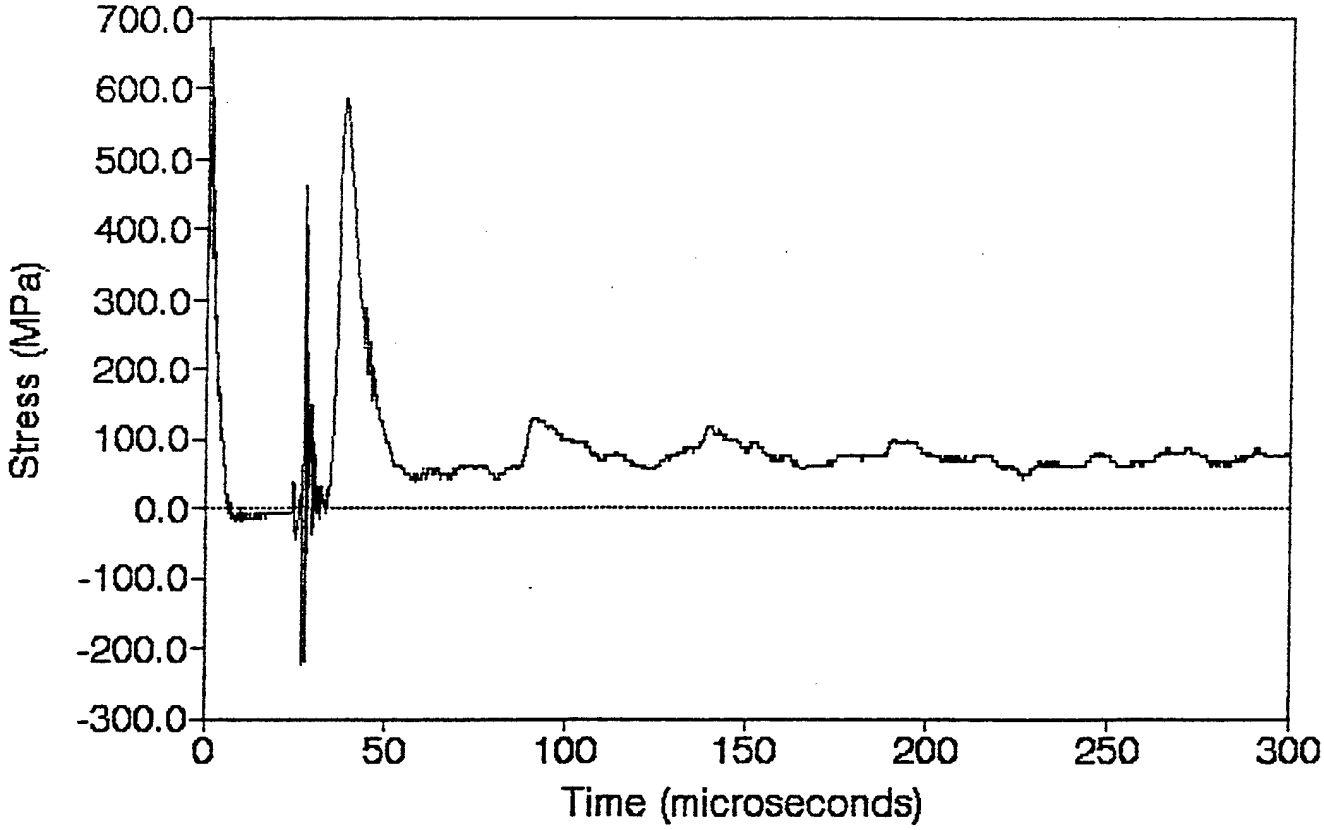

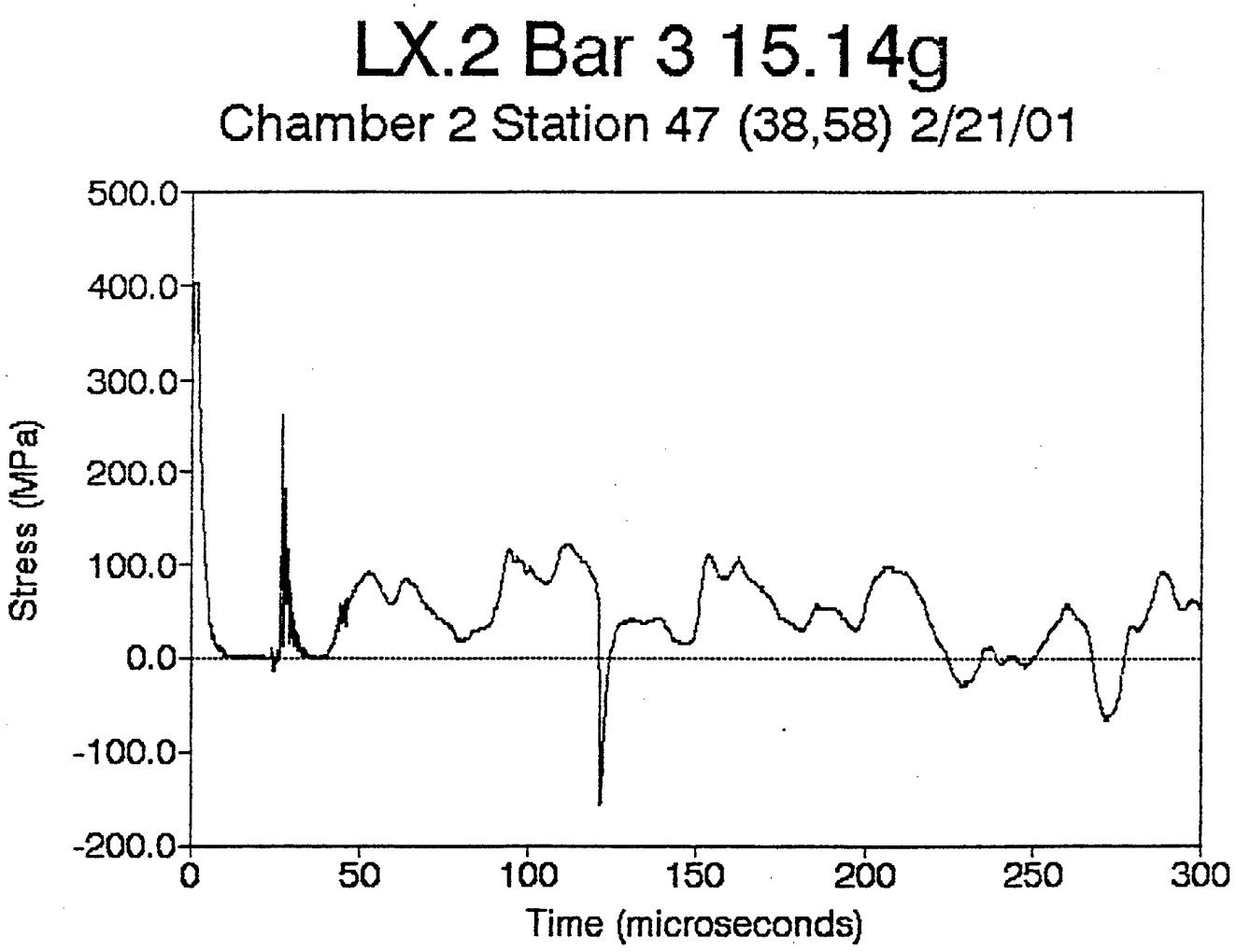
LX.2 Bar 3 15.14g
Chamber 2 Station 47 (38,58) 2/21/01
500.0
400.0
300.0
200.0
100.0
0.0
-100.0
-200.0
Stress (MPa)
0
50
100
150
200
250
300
Time (microseconds)

LX.2 Bar 4 15.14g

Chamber 2 Station 36 (38,38) 2/21/91

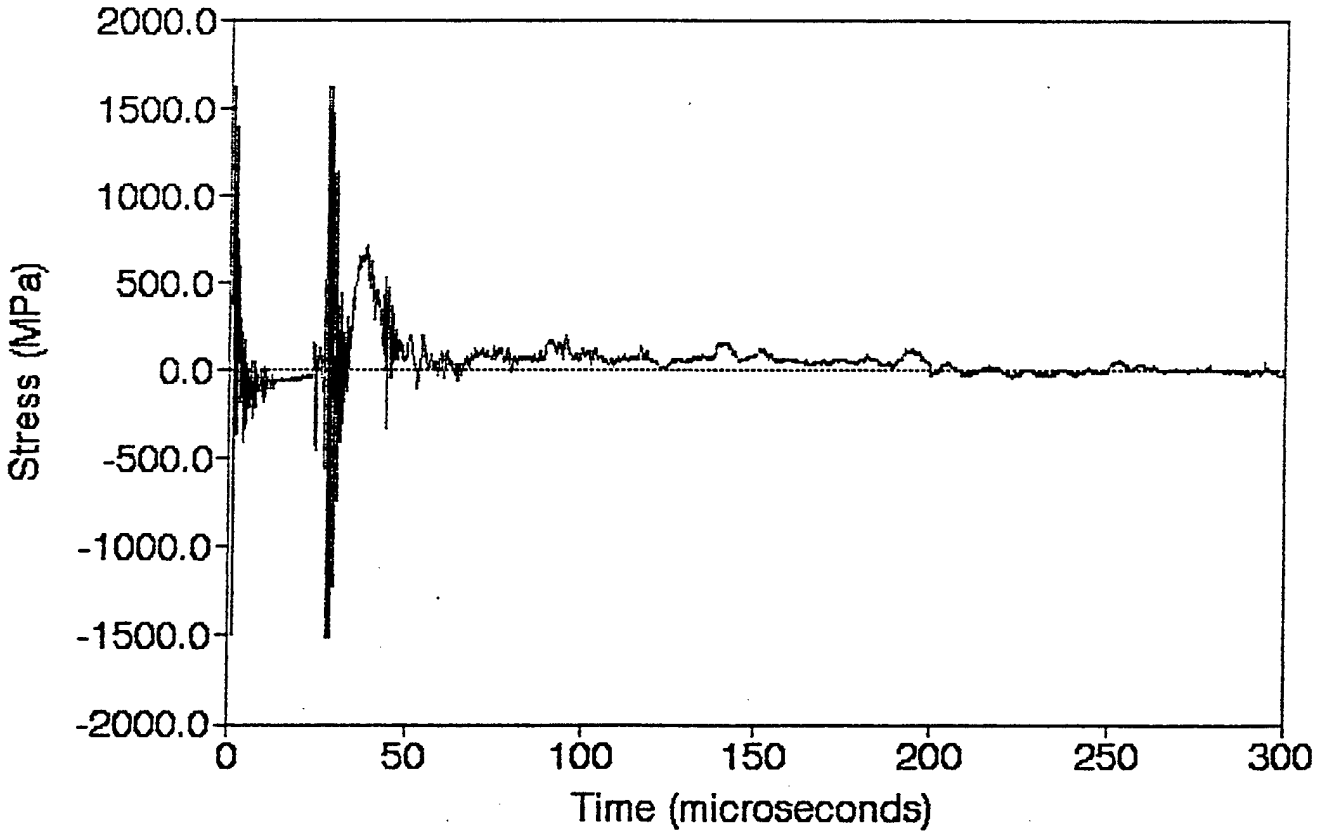

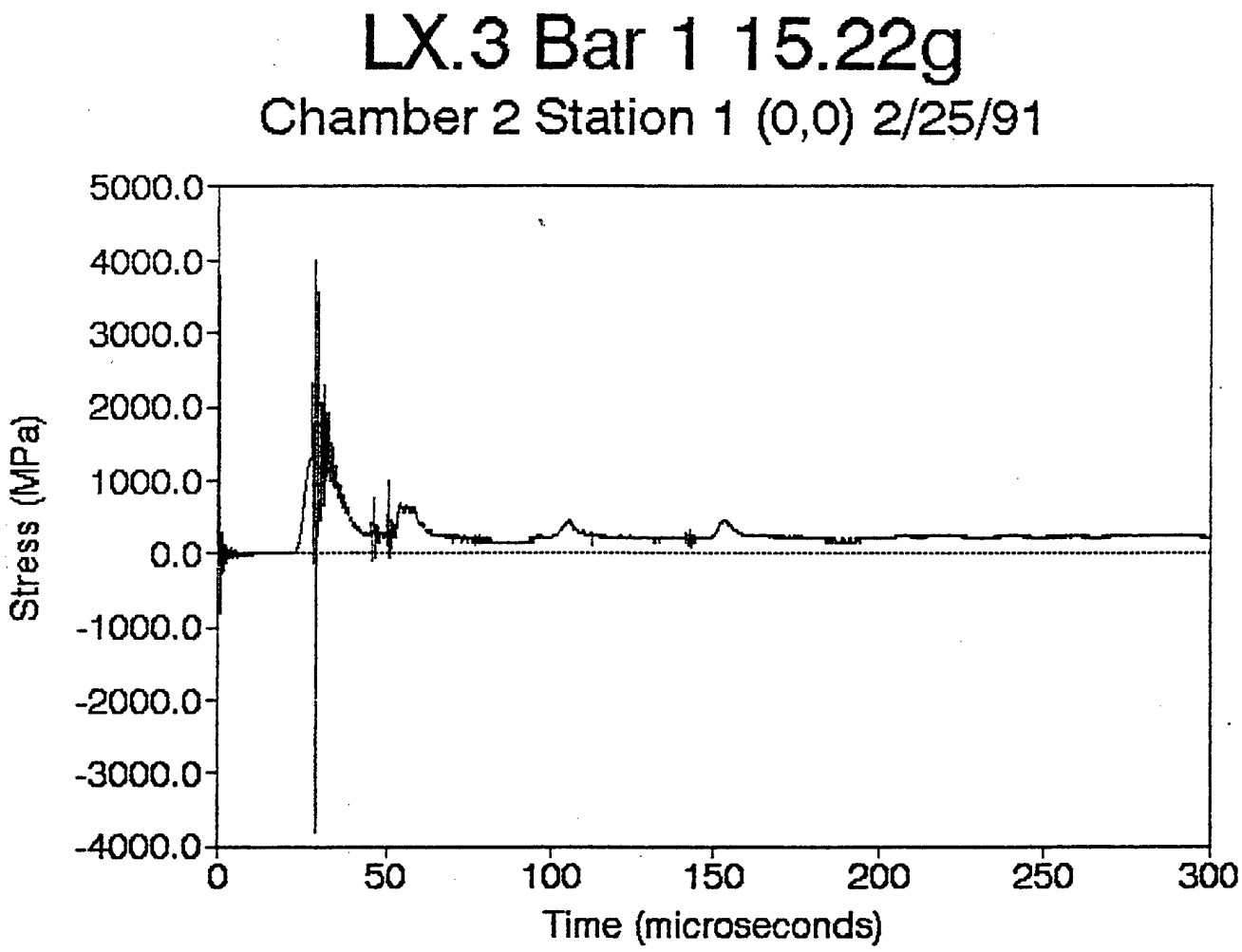
LX.3 Bar 1 15.22g
Chamber 2 Station 1 (0,0) 2/25/91
5000.0
4000.0
3000.0
2000.0
1000.0
0.0
-1000.0
-2000.0
-3000.0
-4000.0
Stress (MPa)
0
50
100
150
200
250
300
Time (microseconds)

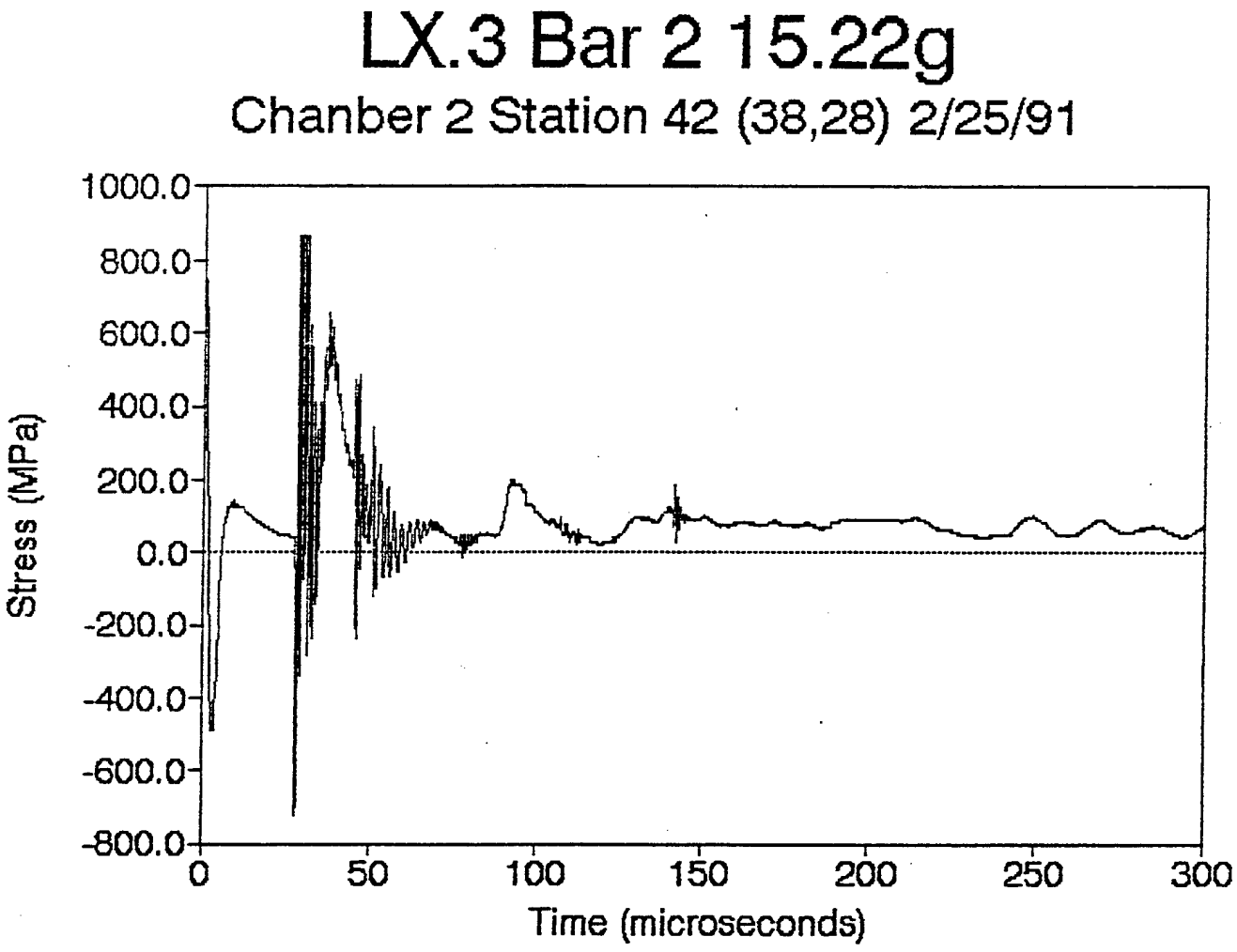
LX.3 Bar 2 15.22g
Chanber 2 Station 42 (38,28) 2/25/91
1000.0
800.0
600.0
400.0
200.0
0.0
-200.0
-400.0
-600.0
-800.0
Stress (MPa)
0
50
100
150
200
250
300
Time (microseconds)

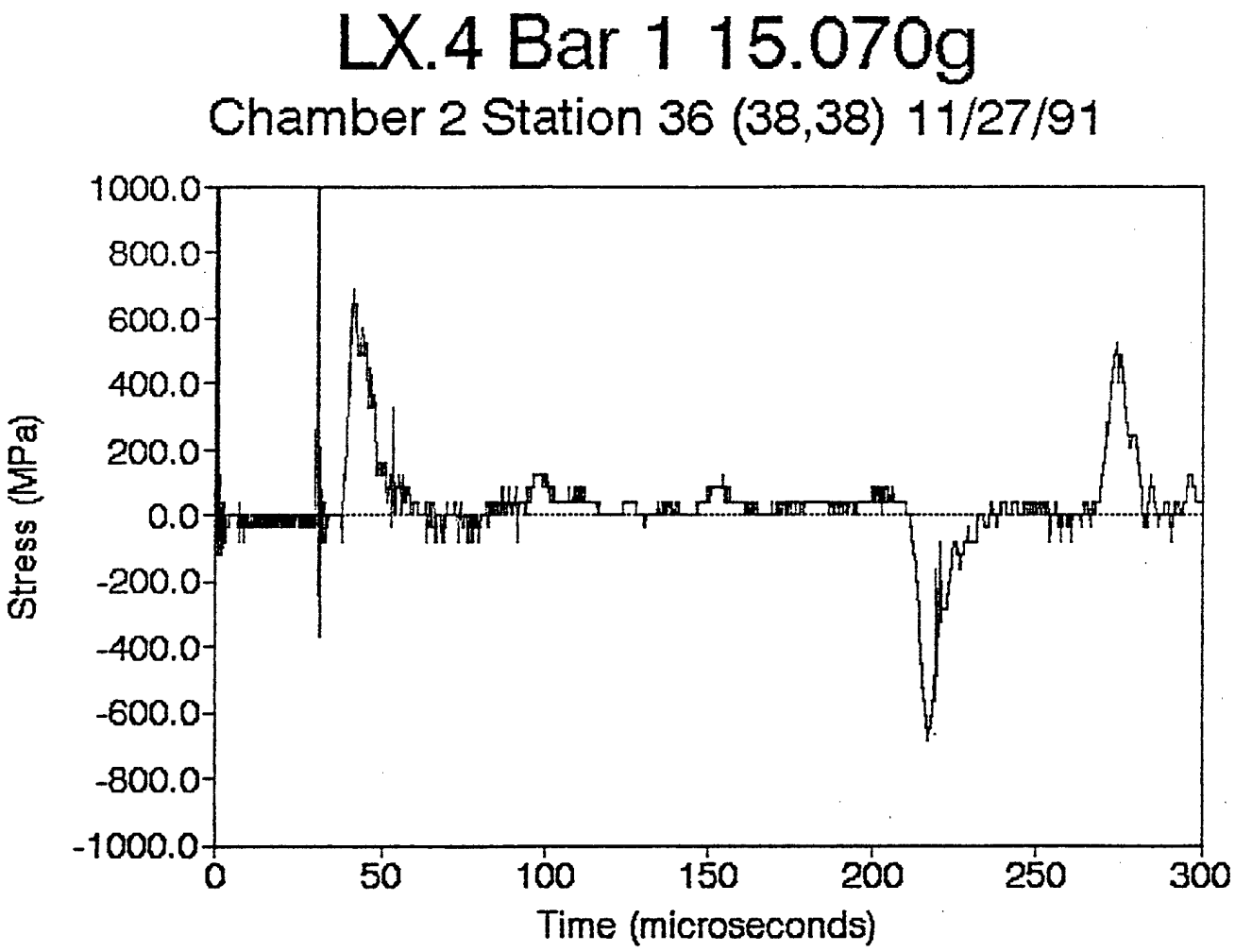
LX.4 Bar 1 15.070g
Chamber 2 Station 36 (38,38) 11/27/91
1000.0
800.0
600.0
400.0
200.0
0.0
-200.0
-400.0
-600.0
-800.0
-1000.0
Stress (MPa)
0
50
100
150
200
250
300
Time (microseconds)

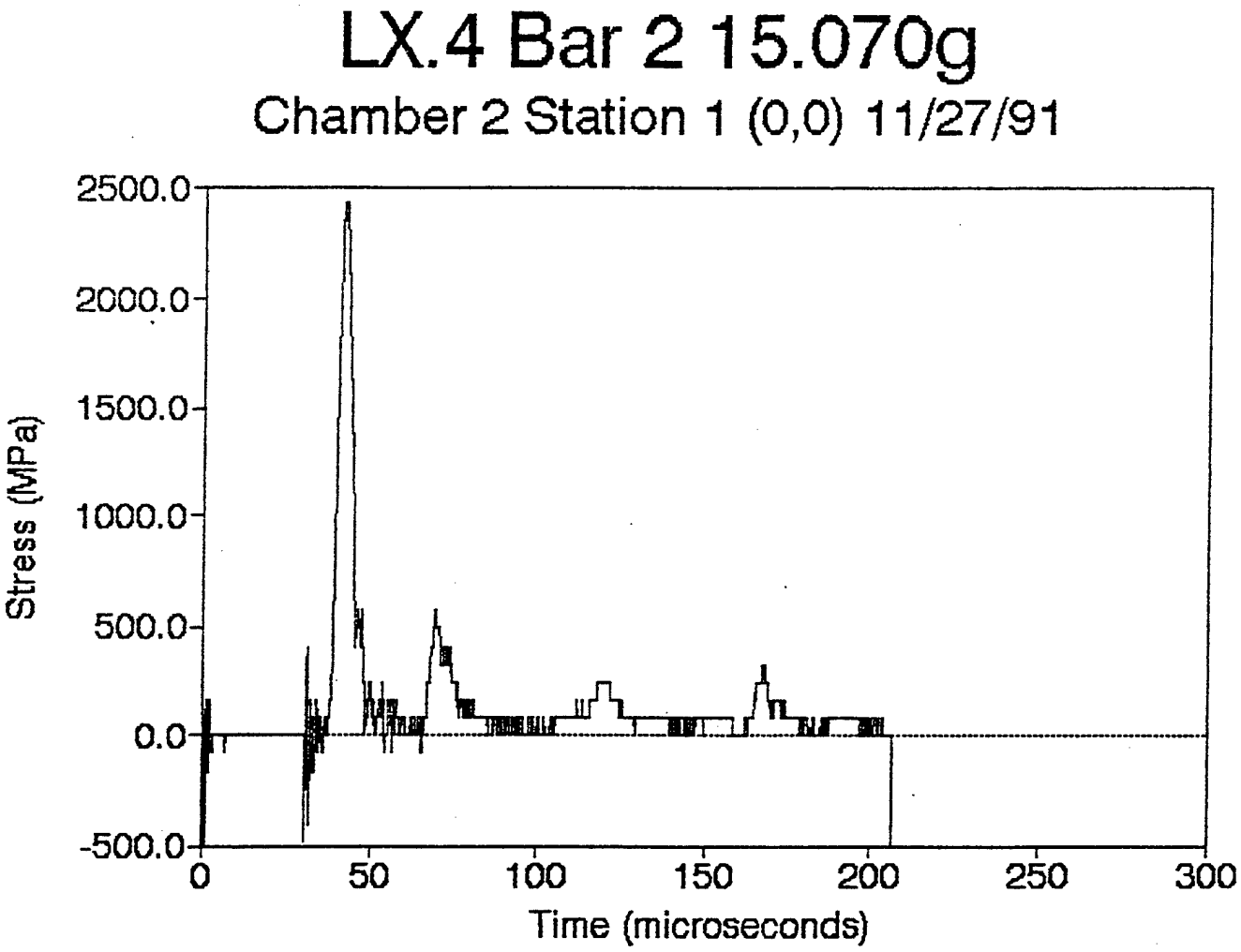
LX.4 Bar 2 15.070g
Chamber 2 Station 1 (0,0) 11/27/91
2500.0
2000.0
1500.0
1000.0
500.0
0.0
-500.0
Stress (MPa)
0
50
100
150
200
250
300
Time (microseconds)

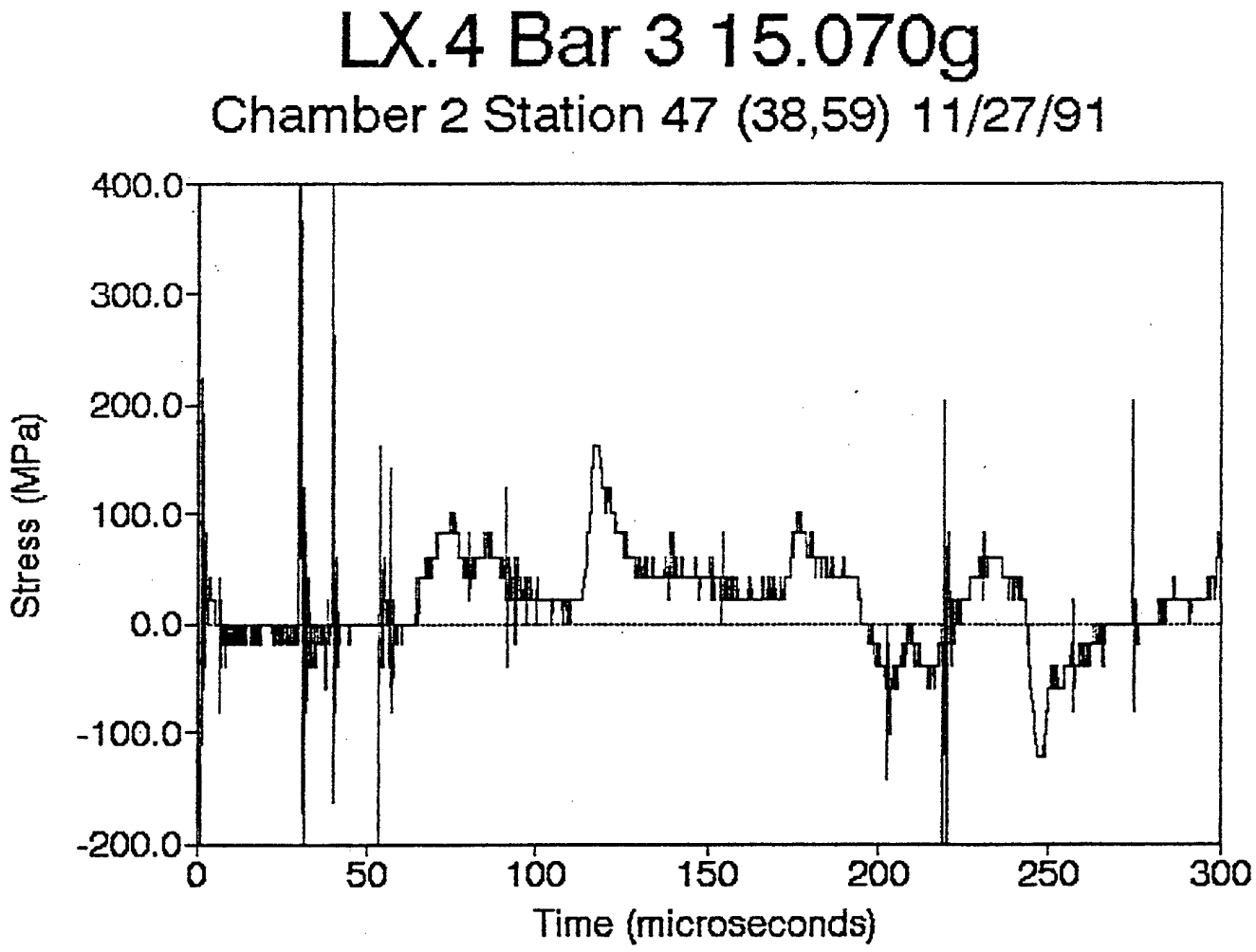
LX.4 Bar 3 15.070g
Chamber 2 Station 47 (38,59) 11/27/91
Stress (MPa)
400.0
300.0
200.0
100.0
0.0
-100.0
-200.0
0
50
100
150
200
250
300
Time (microseconds)

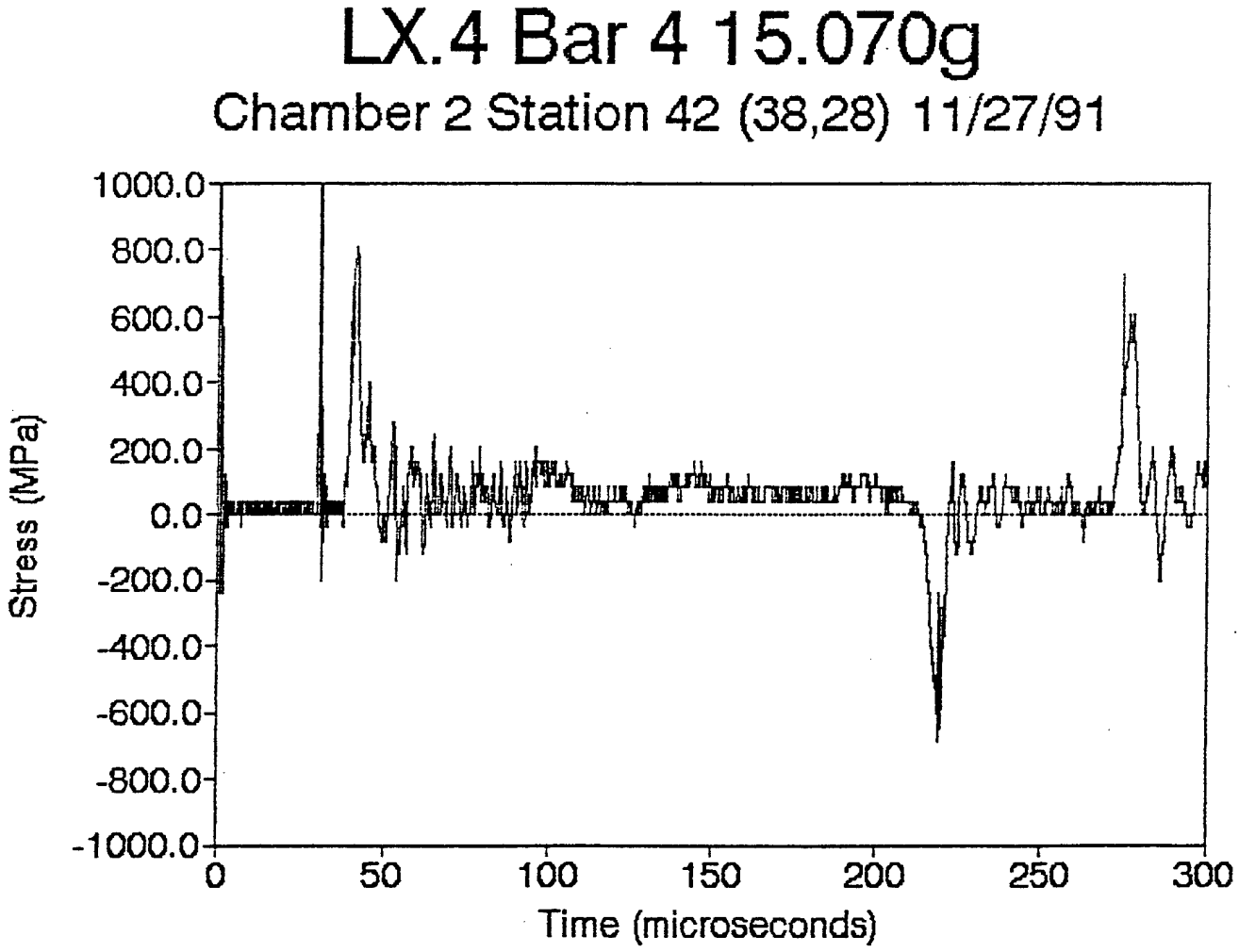
LX.4 Bar 4 15.070g
Chamber 2 Station 42 (38,28) 11/27/91
1000.0
800.0
600.0
400.0
200.0
0.0
-200.0
-400.0
-600.0
-800.0
-1000.0
Stress (MPa)
0
50
100
150
200
250
300
Time (microseconds)

LX.4 PCB 15.070g

Chamber 2 Station 36 (38,38) 11/27/91

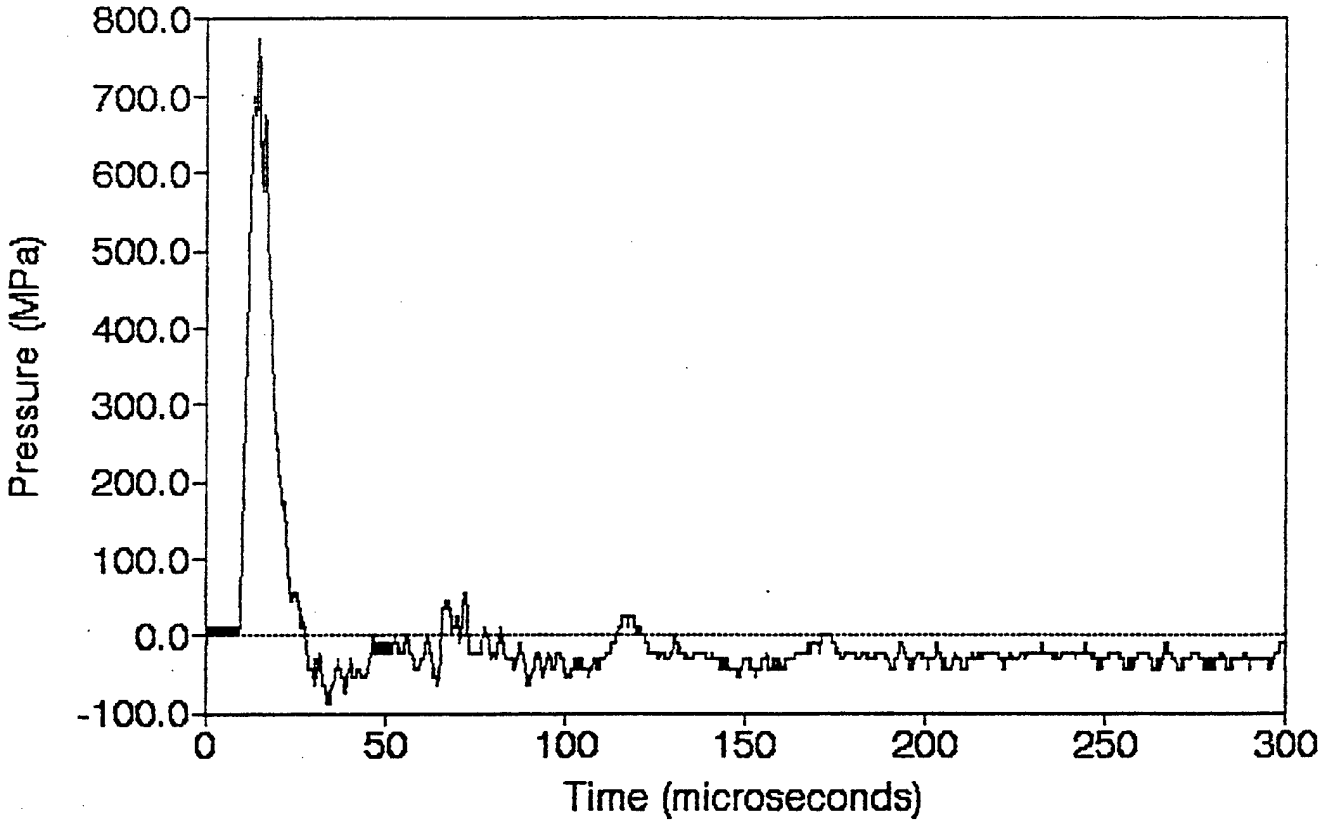

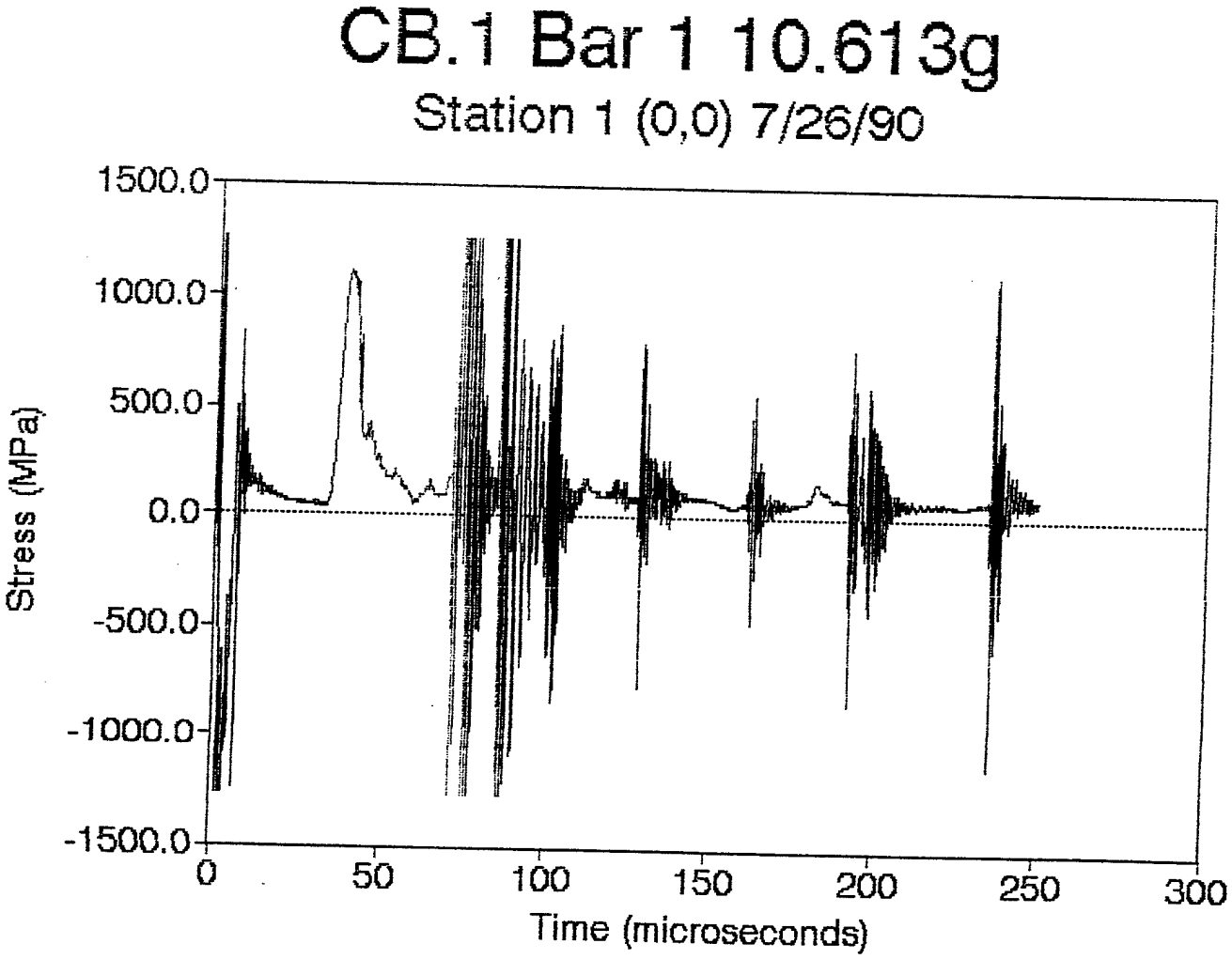
CB.1 Bar 1 10.613g
Station 1 (0,0) 7/26/90
1500.0
1000.0
500.0
0.0
-500.0
-1000.0
-1500.0
Stress (MPa)
0
50
100
150
200
250
300
Time (microseconds)

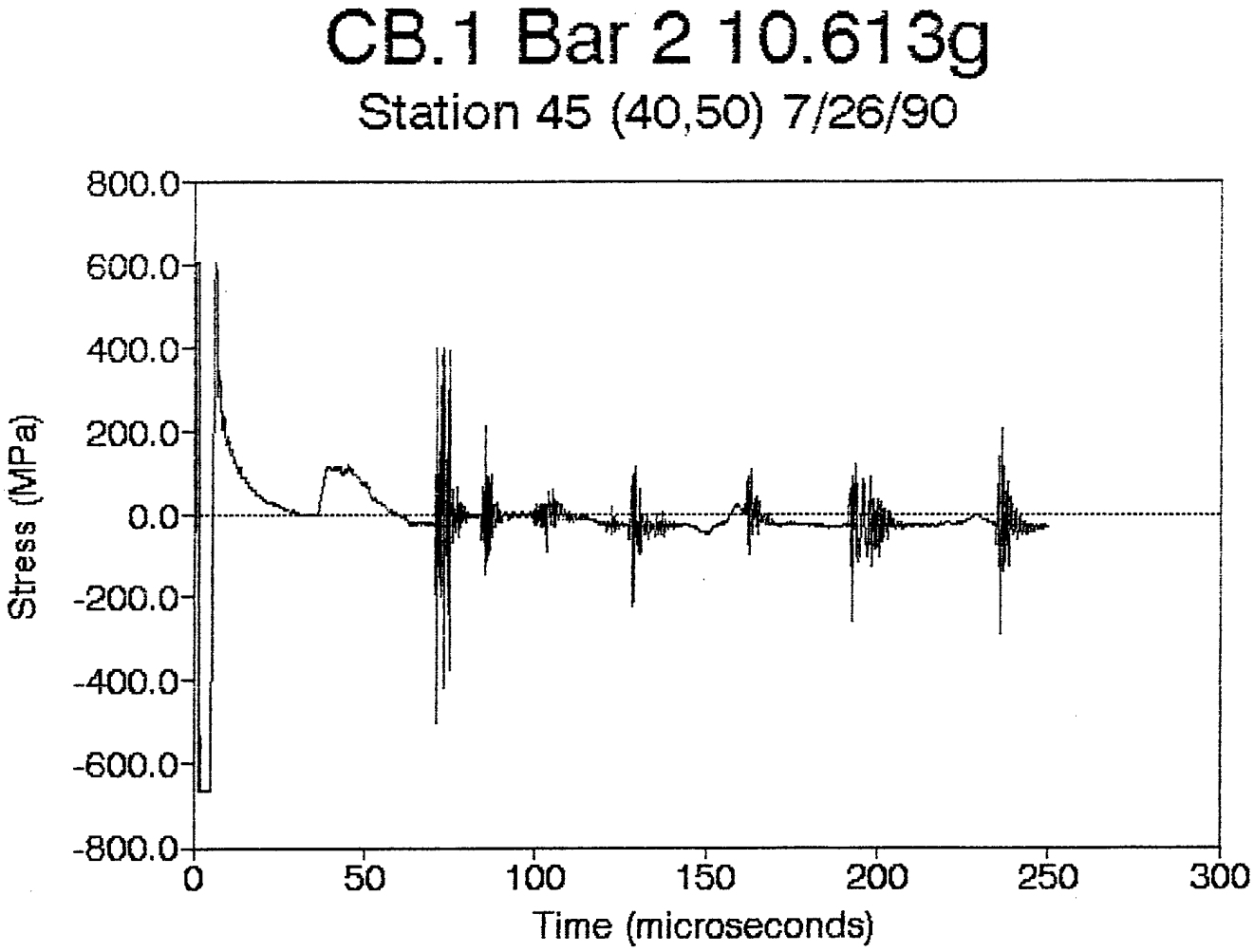
CB.1 Bar 2 10.613g
Station 45 (40,50) 7/26/90
800.0
600.0
400.0
200.0
0.0
-200.0
-400.0
-600.0
-800.0
Stress (MPa)
0
50
100
150
200
250
300
Time (microseconds)

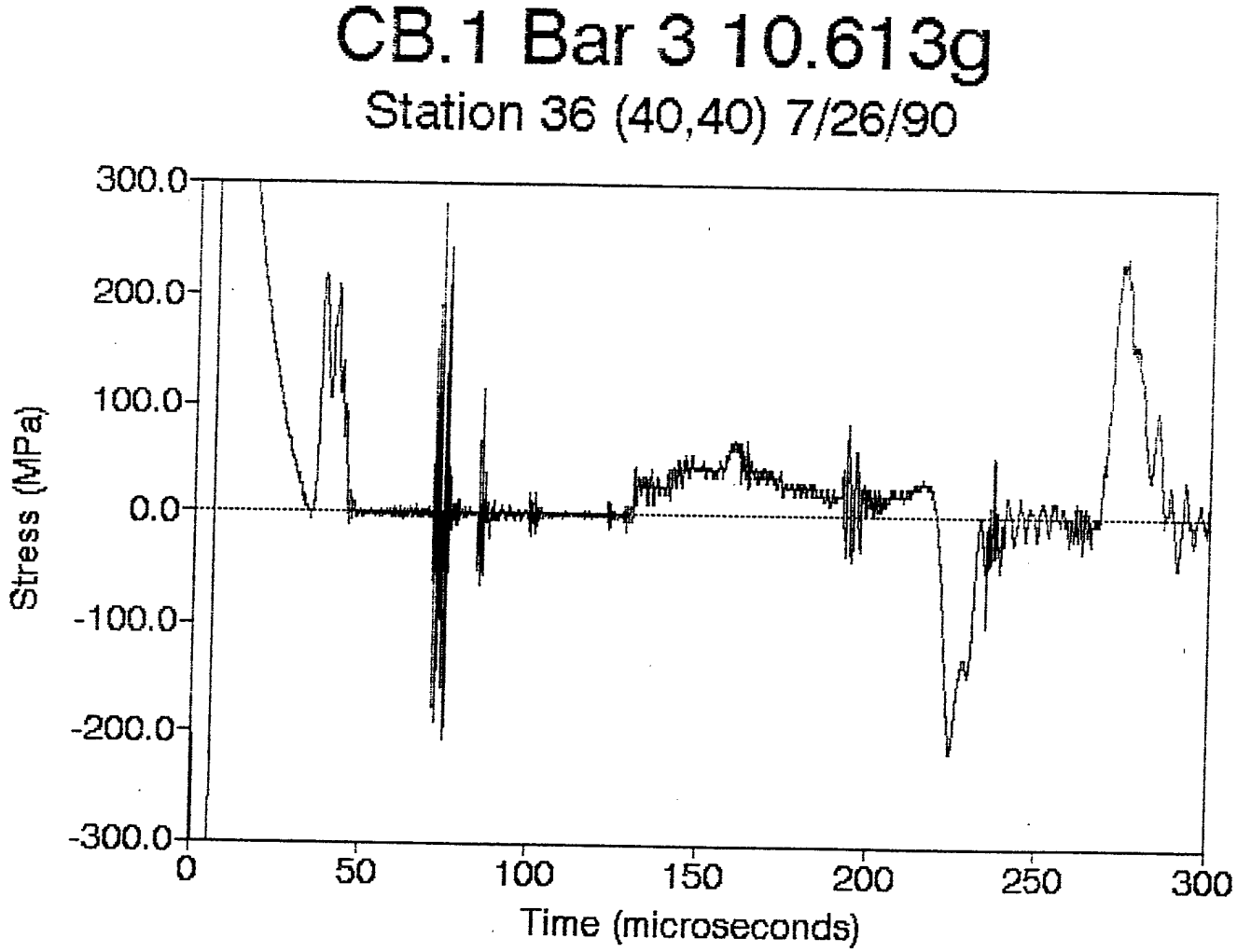
CB.1 Bar 3 10.613g
Station 36 (40,40) 7/26/90
300.0
200.0
100.0
0.0
-100.0
-200.0
-300.0
Stress (MPa)
0
50
100
150
200
250
300
Time (microseconds)

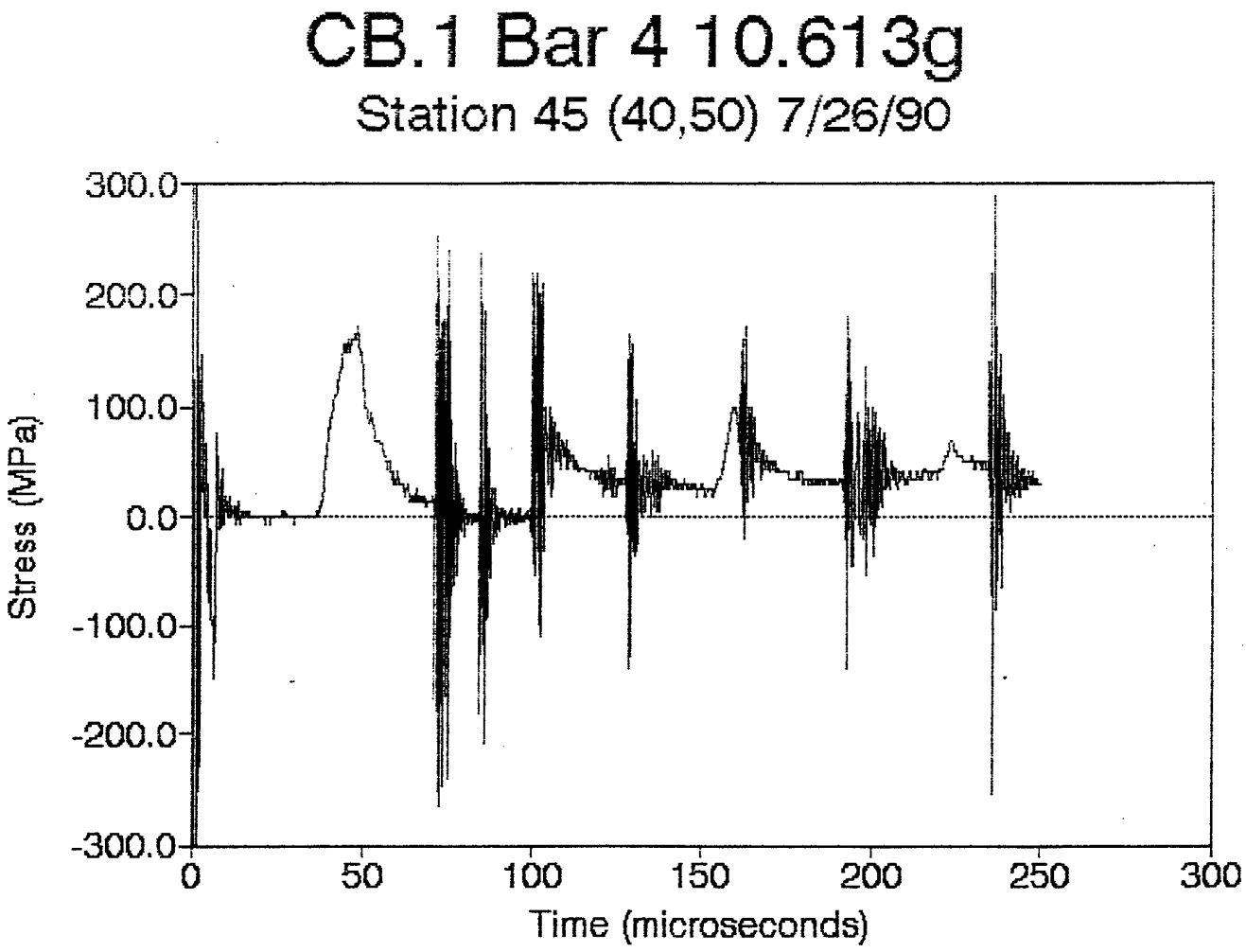
CB.1 Bar 4 10.613g
Station 45 (40,50) 7/26/90
300.0
200.0
100.0
0.0
-100.0
-200.0
-300.0
Stress (MPa)
0
50
100
150
200
250
300
Time (microseconds)

CB.1 Resister 10.613g

Station 36 (40,40) 7/26/90

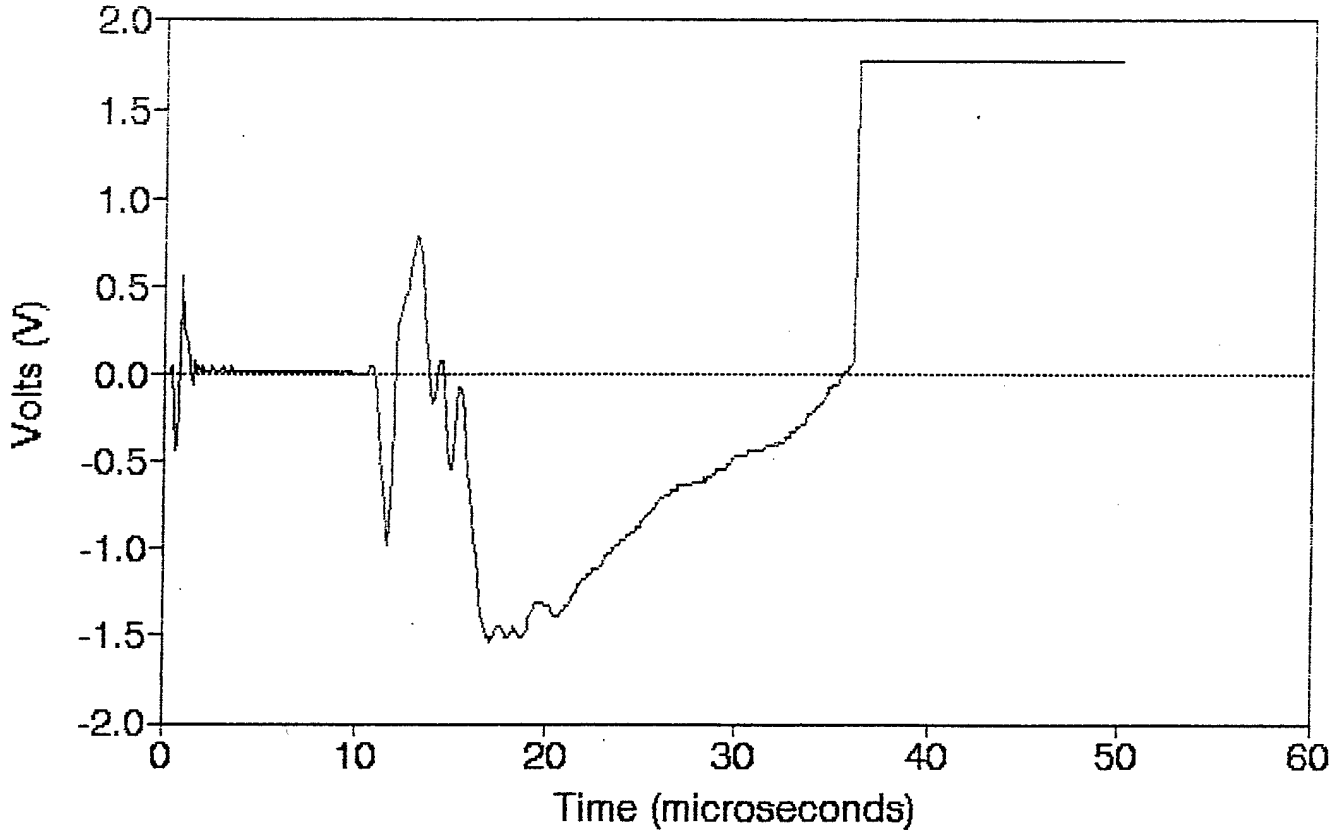

CB.2 470 Ohm Resistor 10.610g

Station 36 (40,40) 7/26/90

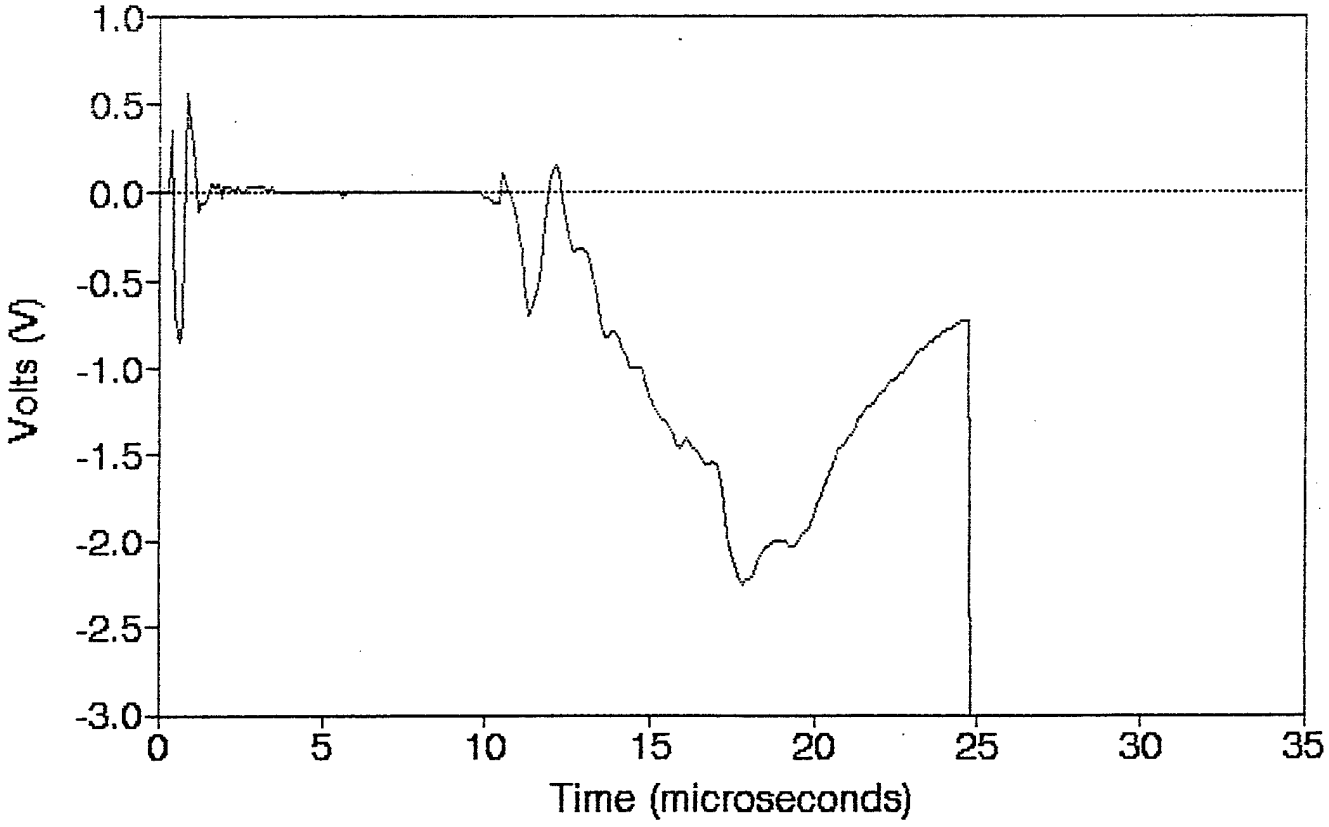

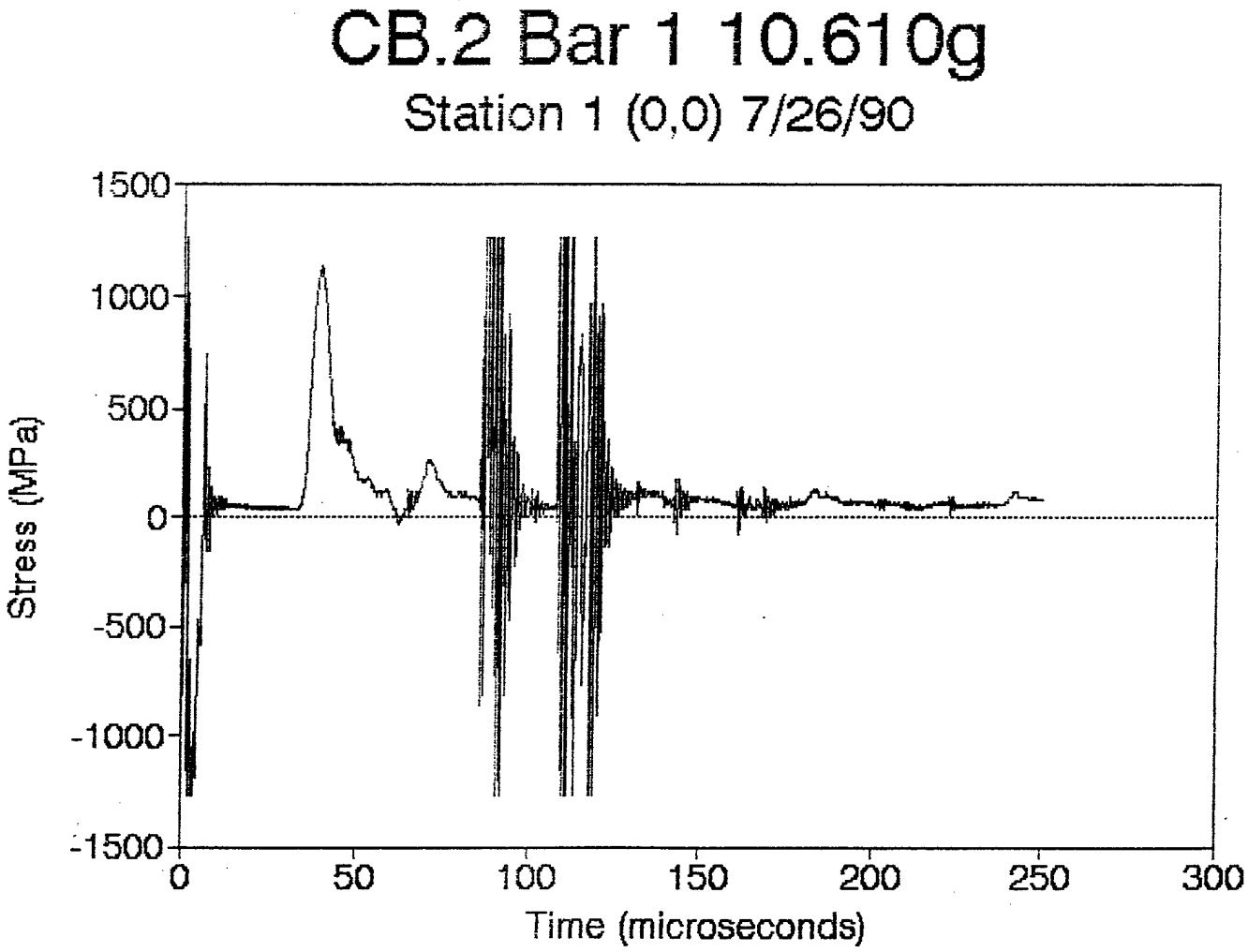
CB.2 Bar 1 10.610g
Station 1 (0,0) 7/26/90
1500
1000
500
0
-500
-1000
-1500
Stress (MPa)
0
50
100
150
200
250
300
Time (microseconds)

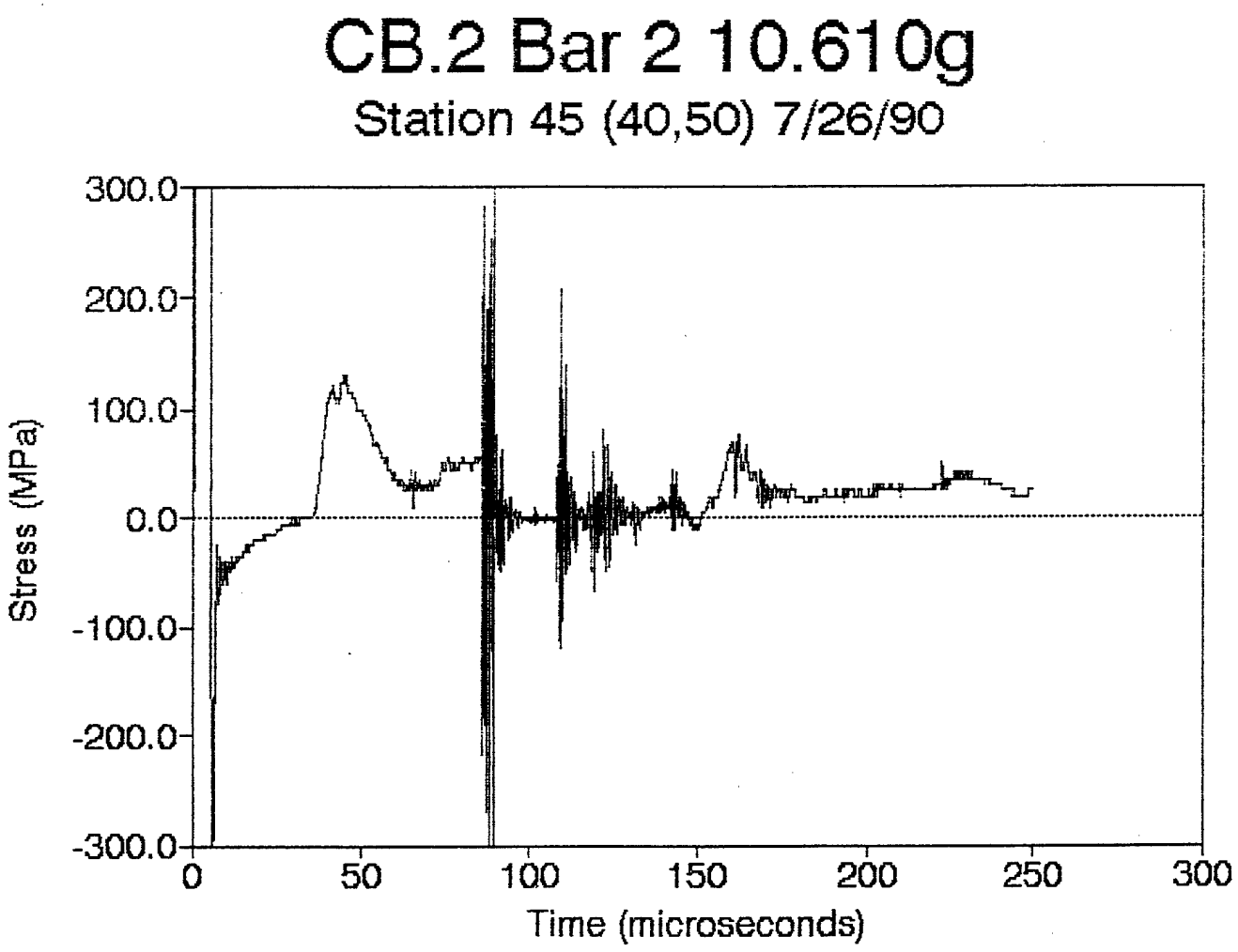
CB.2 Bar 2 10.610g
Station 45 (40,50) 7/26/90
300.0
200.0
100.0
0.0
-100.0
-200.0
-300.0
Stress (MPa)
0
50
100
150
200
250
300
Time (microseconds)

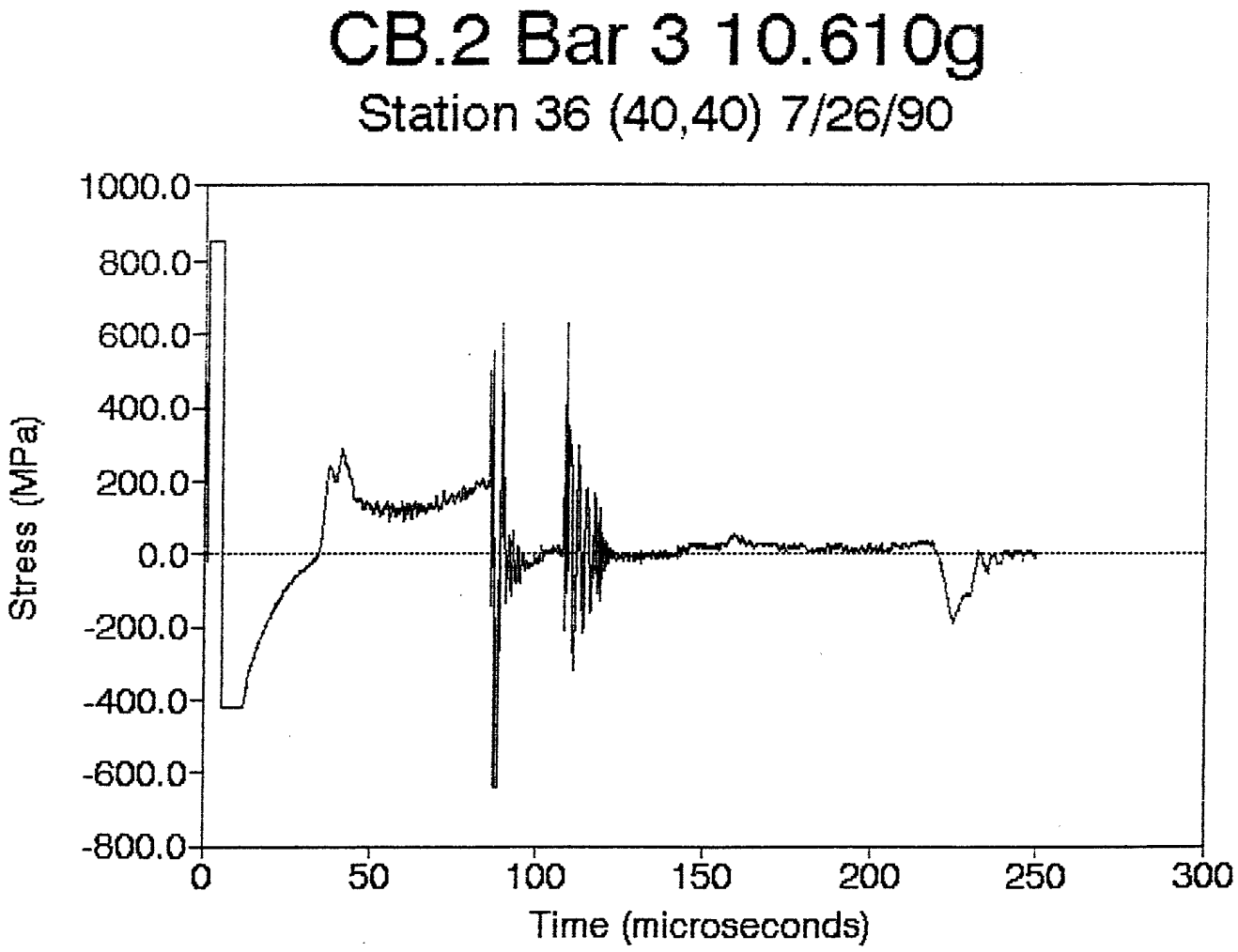
CB.2 Bar 3 10.610g
Station 36 (40,40) 7/26/90
1000.0
800.0
600.0
400.0
200.0
0.0
-200.0
-400.0
-600.0
-800.0
Stress (MPa)
0
50
100
150
200
250
300
Time (microseconds)

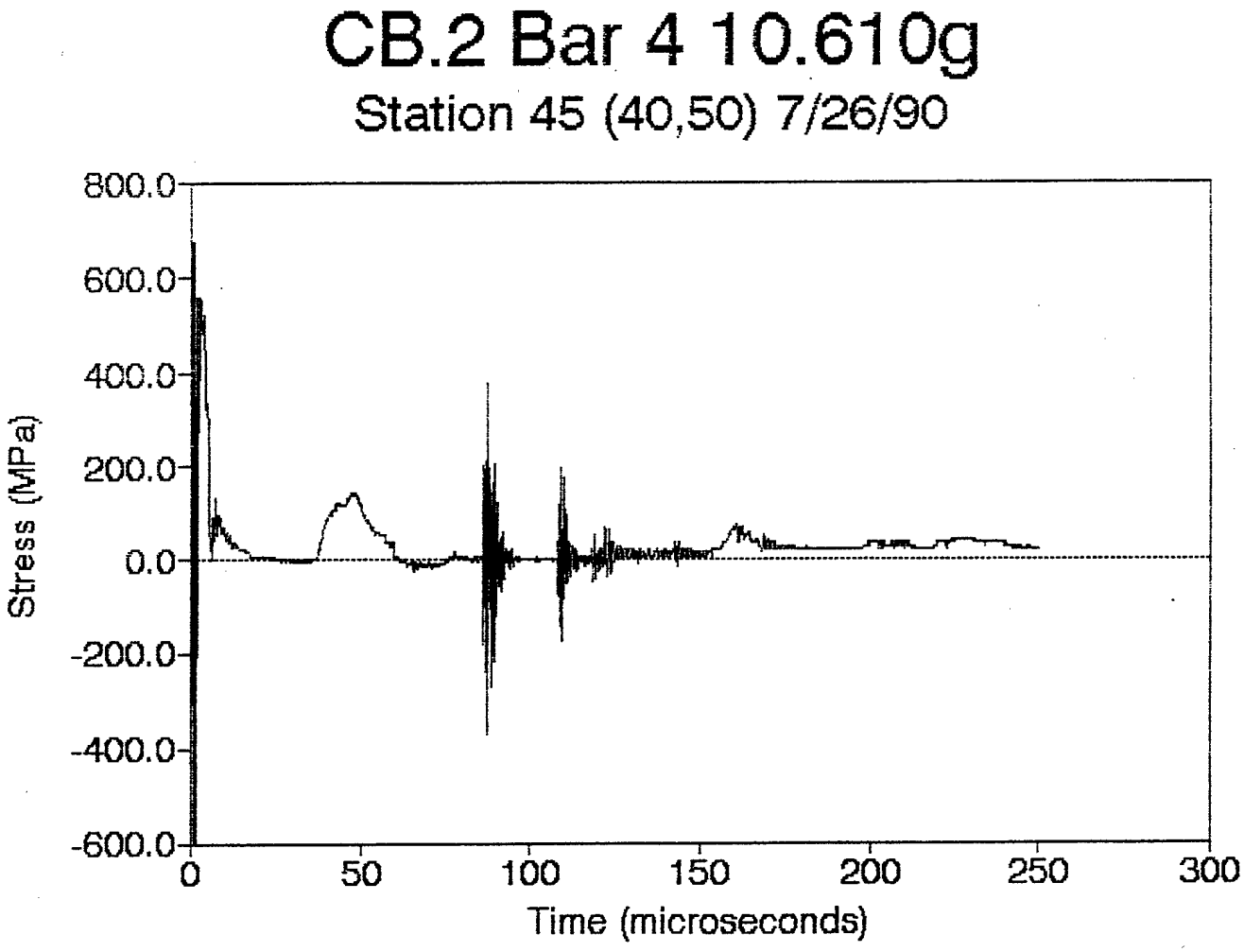
CB.2 Bar 4 10.610g
Station 45 (40,50) 7/26/90
800.0
600.0
400.0
200.0
0.0
-200.0
-400.0
-600.0
Stress (MPa)
0
50
100
150
200
250
300
Time (microseconds)

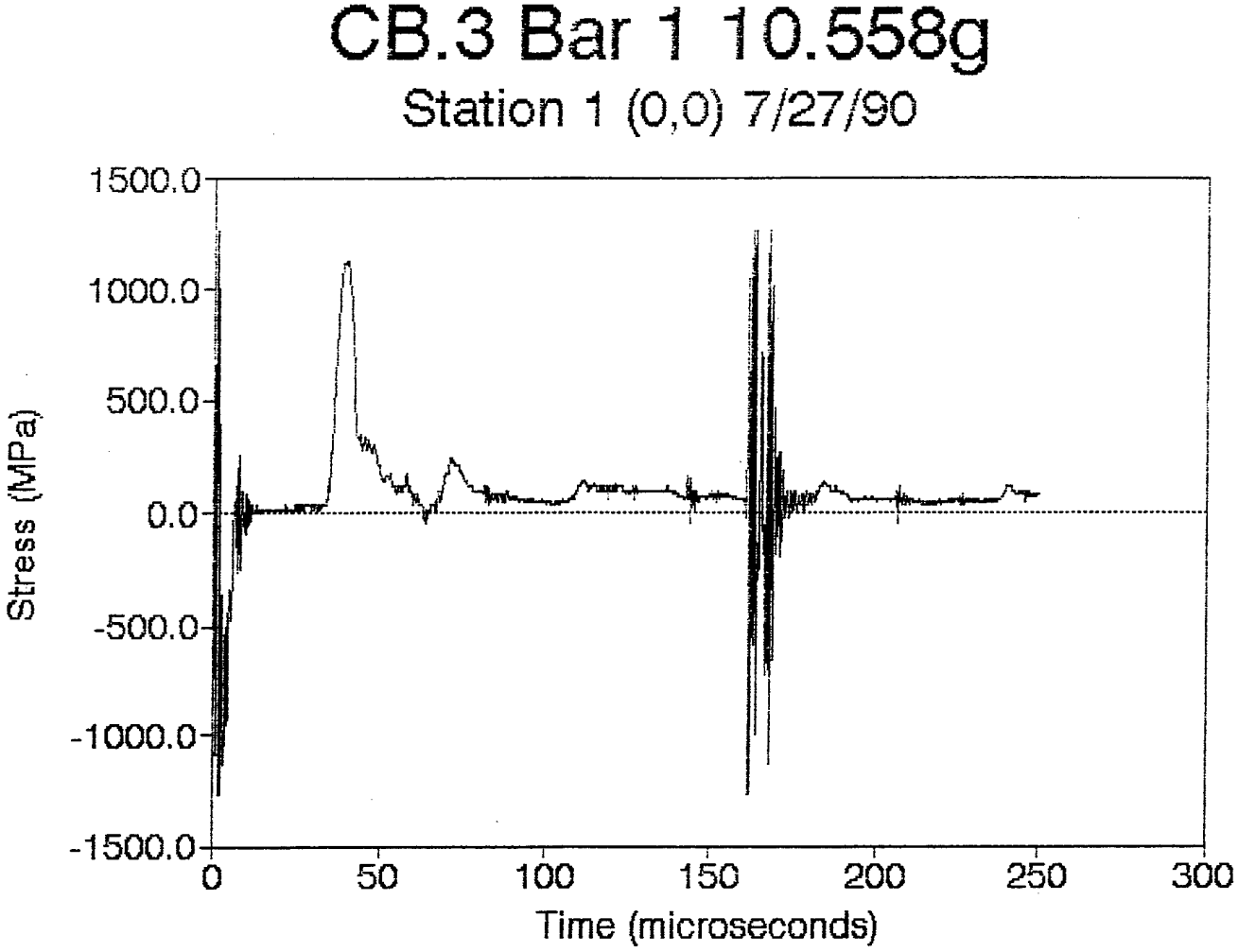
CB.3 Bar 1 10.558g
Station 1 (0,0) 7/27/90
1500.0
1000.0
500.0
0.0
-500.0
-1000.0
-1500.0
Stress (MPa)
0
50
100
150
200
250
300
Time (microseconds)

CB.3 Bar 2 10.558g

Station 45 (40,50) 7/27/90

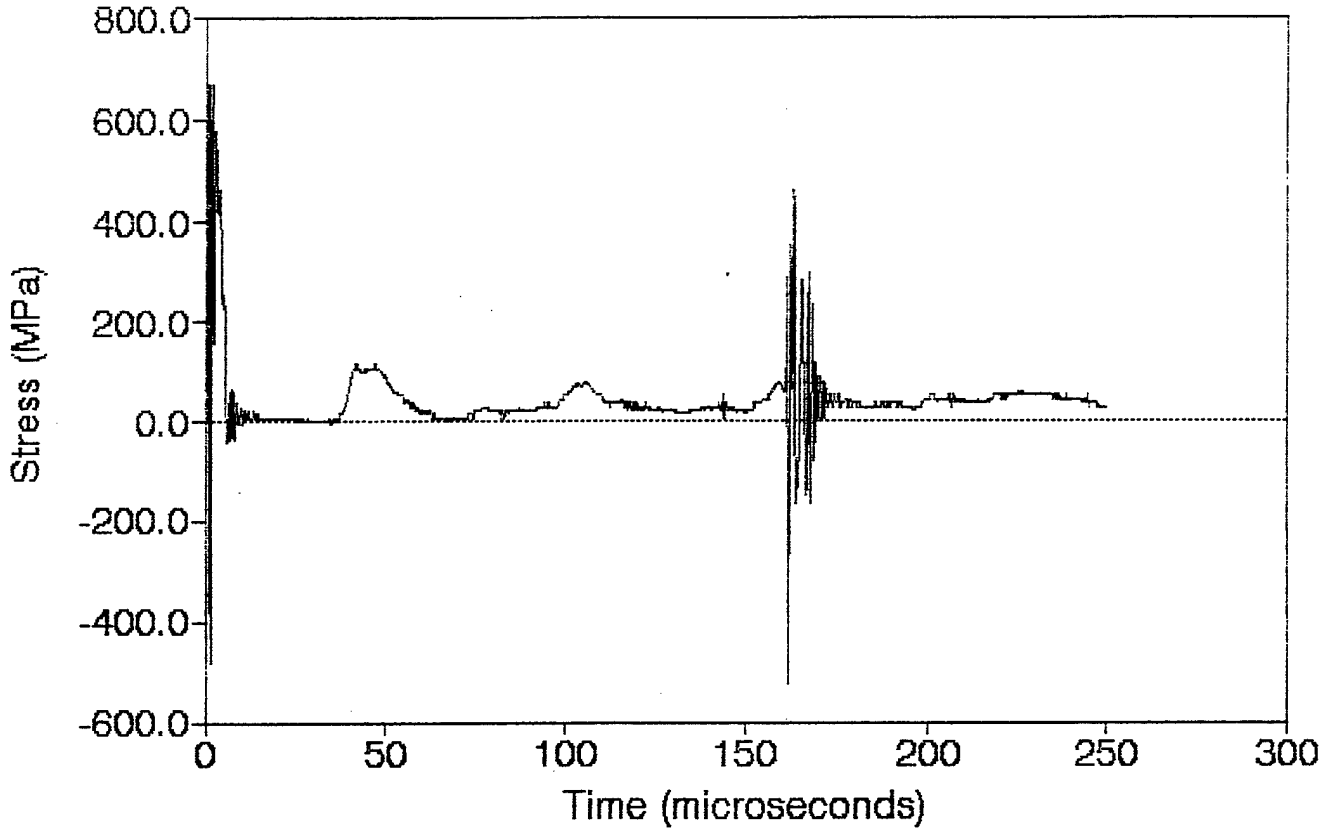

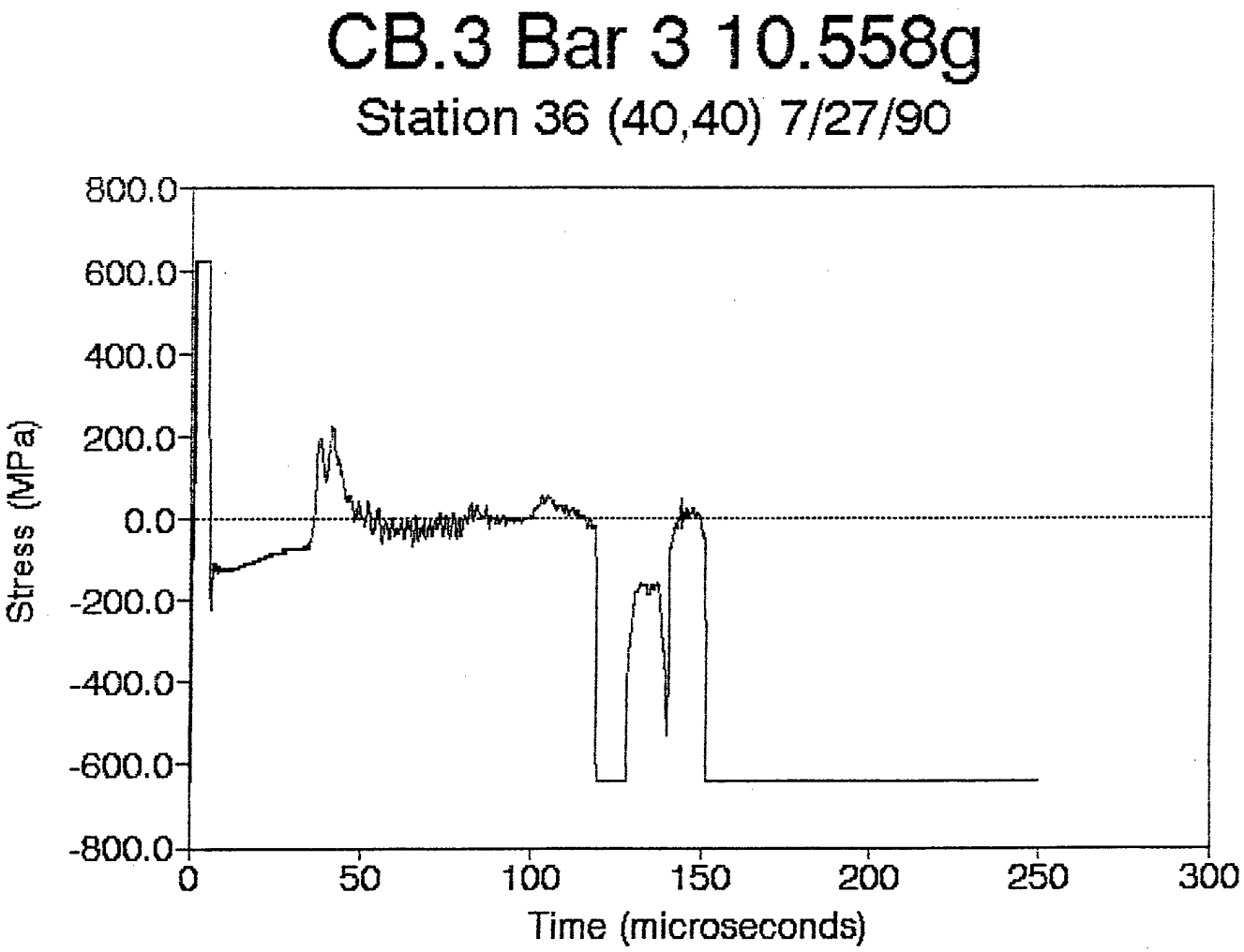
CB.3 Bar 3 10.558g
Station 36 (40,40) 7/27/90
800.0
600.0
400.0
200.0
0.0
-200.0
-400.0
-600.0
-800.0
Stress (MPa)
0
50
100
150
200
250
300
Time (microseconds)

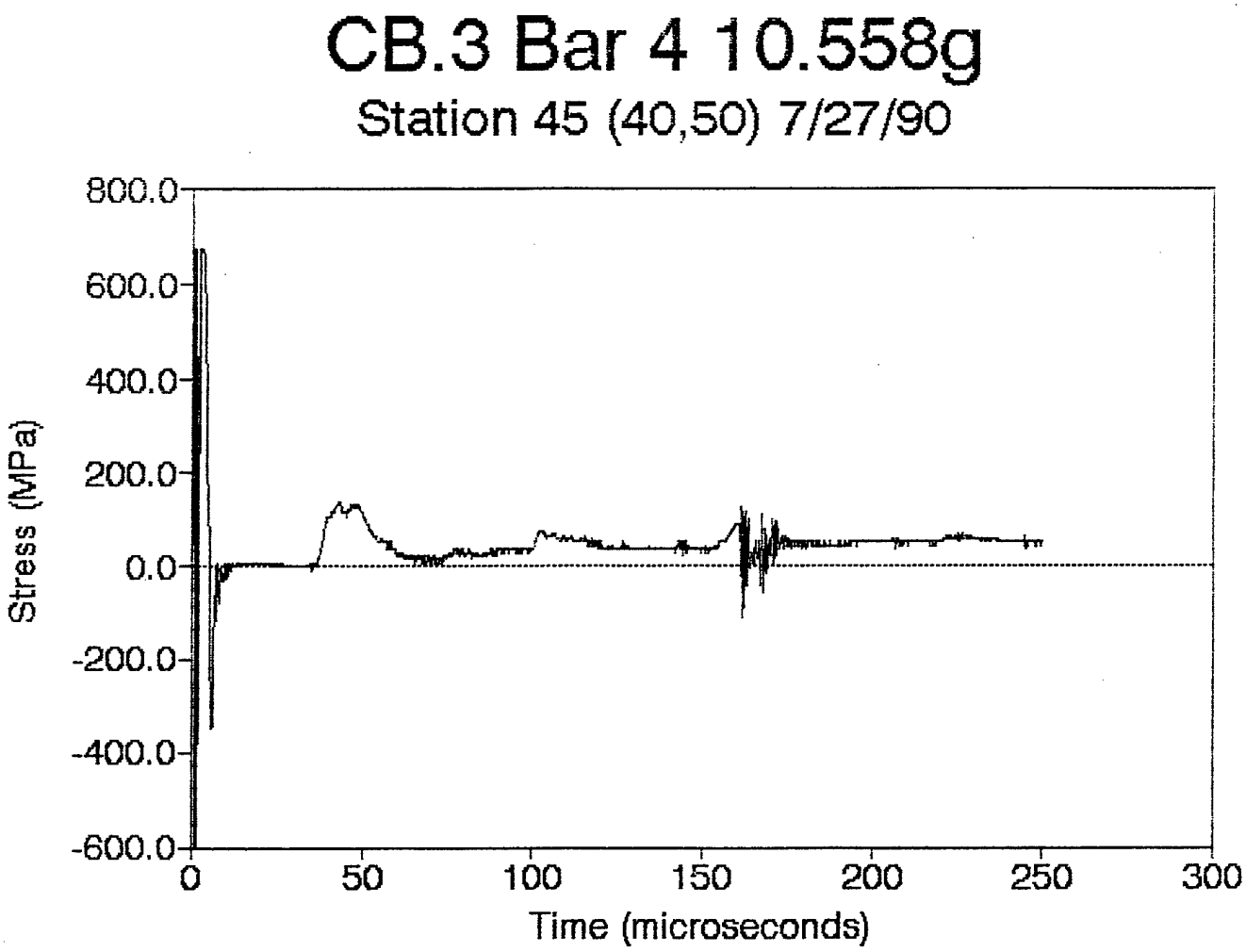
CB.3 Bar 4 10.558g
Station 45 (40,50) 7/27/90
800.0
600.0
400.0
200.0
0.0
-200.0
-400.0
-600.0
Stress (MPa)
0
50
100
150
200
250
300
Time (microseconds)

CB.3 470 Ohm Resistor 10.558g

Station 36 (40,40) 7/27/90

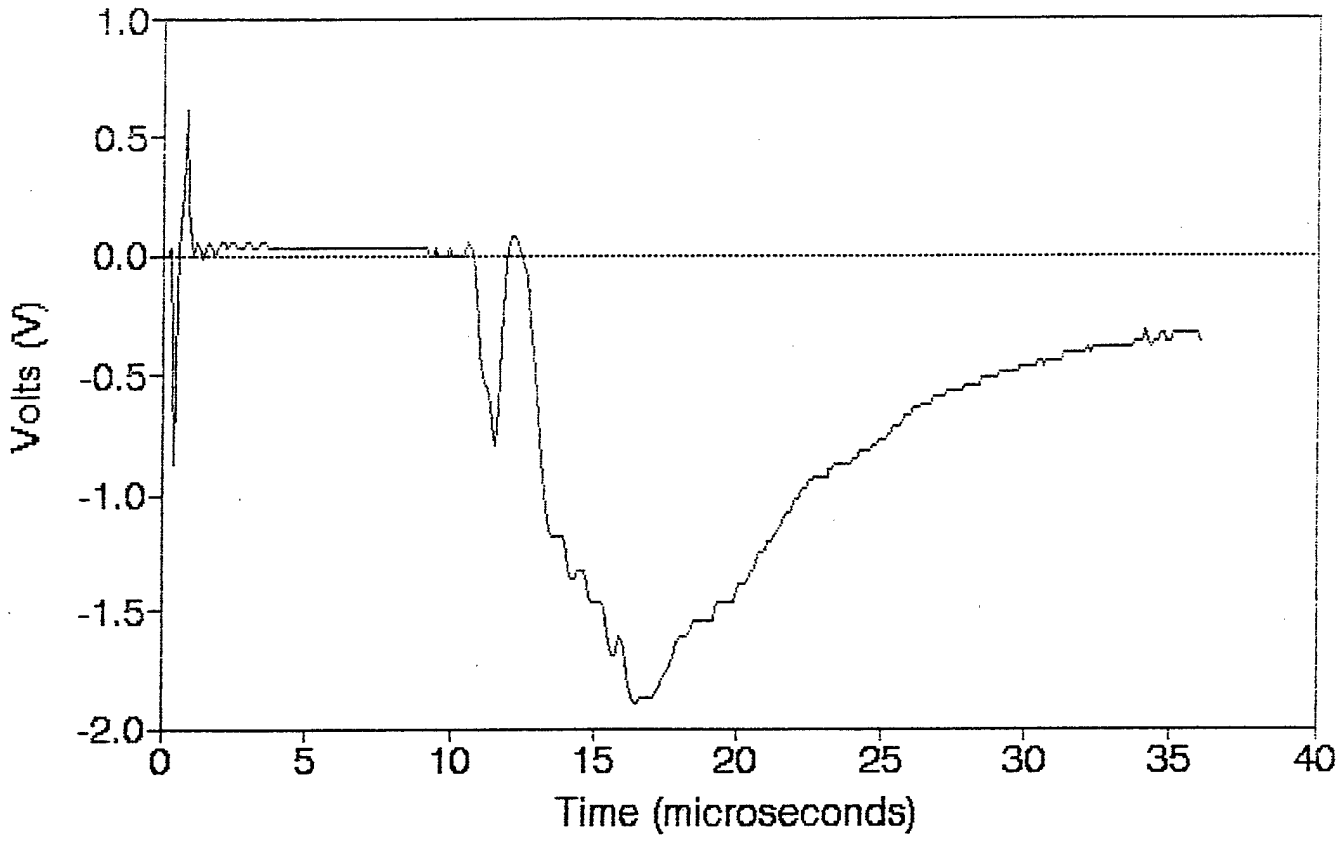

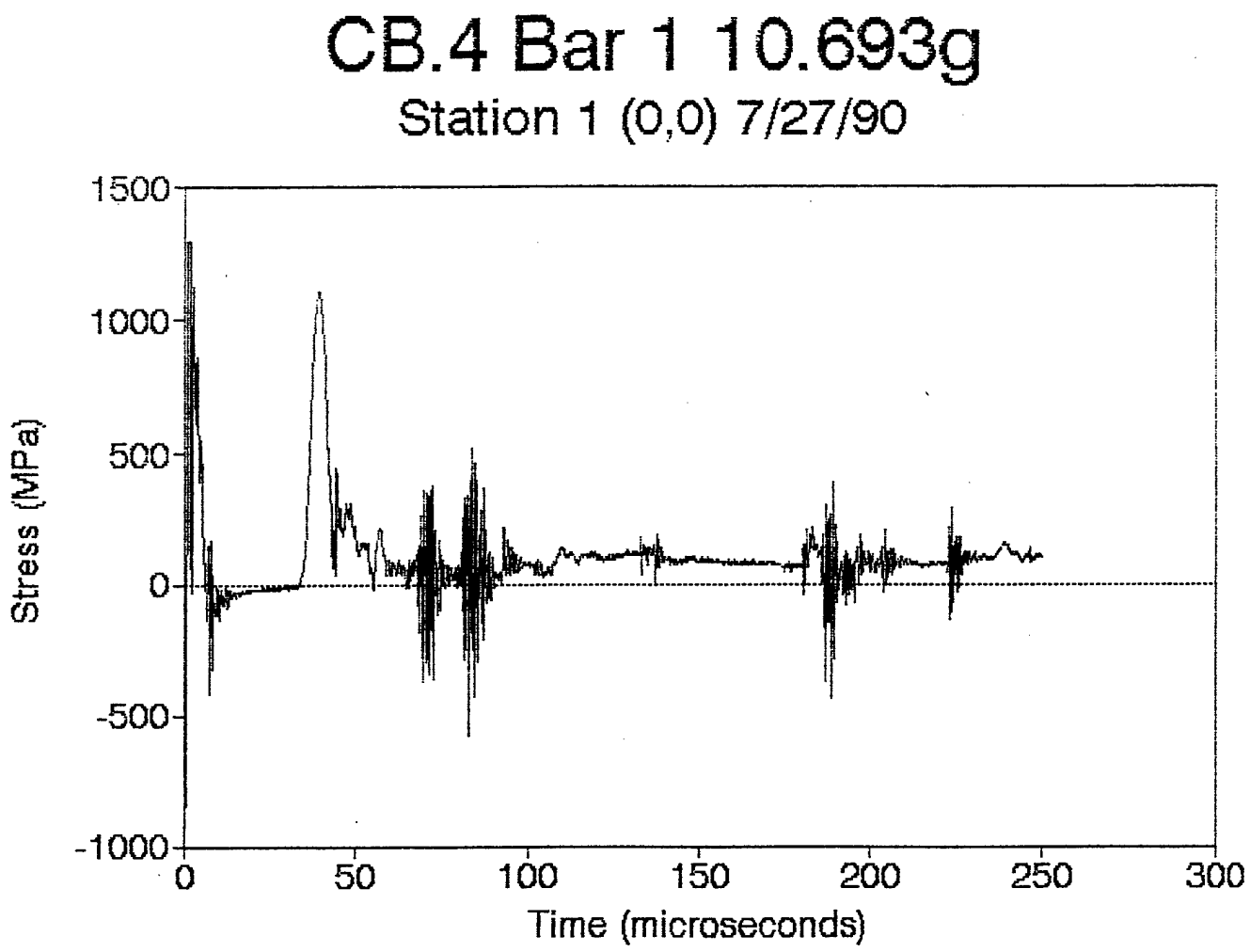
CB.4 Bar 1 10.693g
Station 1 (0,0) 7/27/90
1500
1000
500
0
-500
-1000
Stress (MPa)
0
50
100
150
200
250
300
Time (microseconds)

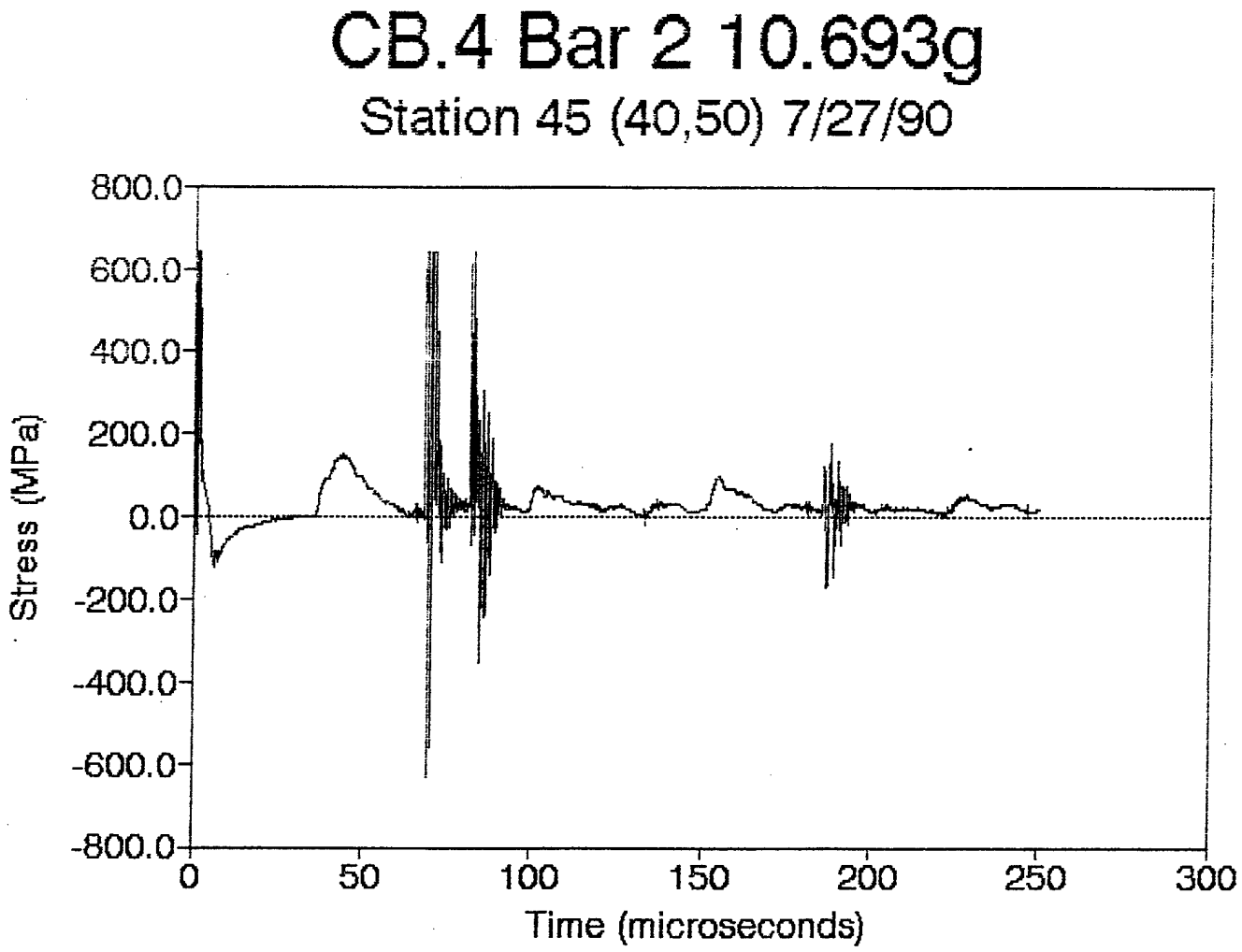
CB.4 Bar 2 10.693g
Station 45 (40,50) 7/27/90
800.0
600.0
400.0
200.0
0.0
-200.0
-400.0
-600.0
-800.0
Stress (MPa)
0
50
100
150
200
250
300
Time (microseconds)

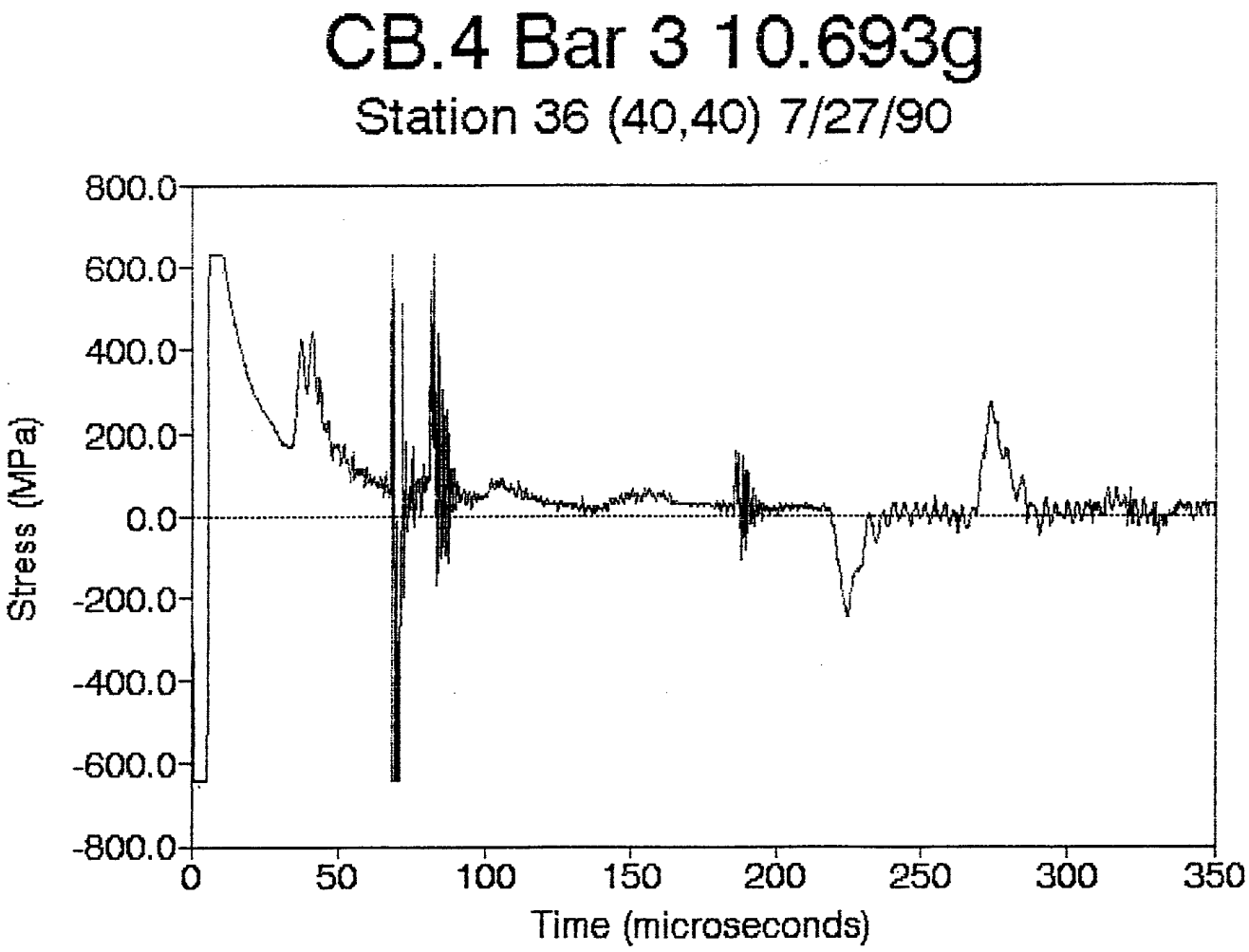
CB.4 Bar 3 10.693g
Station 36 (40,40) 7/27/90
800.0
600.0
400.0
200.0
0.0
-200.0
-400.0
-600.0
-800.0
Stress (MPa)
0
50
100
150
200
250
300
350
Time (microseconds)

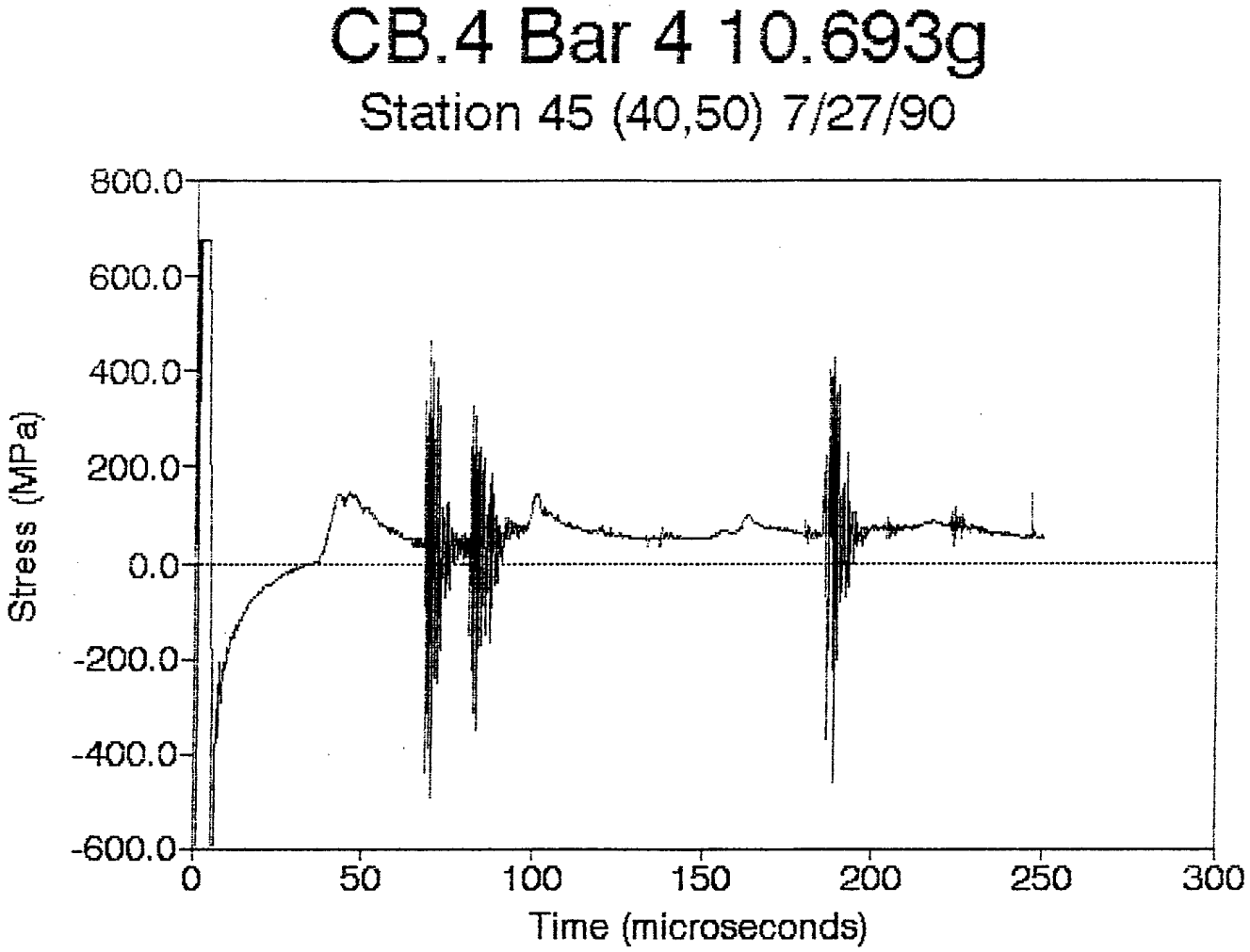
CB.4 Bar 4 10.693g
Station 45 (40,50) 7/27/90
800.0
600.0
400.0
200.0
0.0
-200.0
-400.0
-600.0
Stress (MPa)
0
50
100
150
200
250
300
Time (microseconds)

CB.5 470 Ohm Resistor 10.609g

Station 36 (40,40) 9/20/90

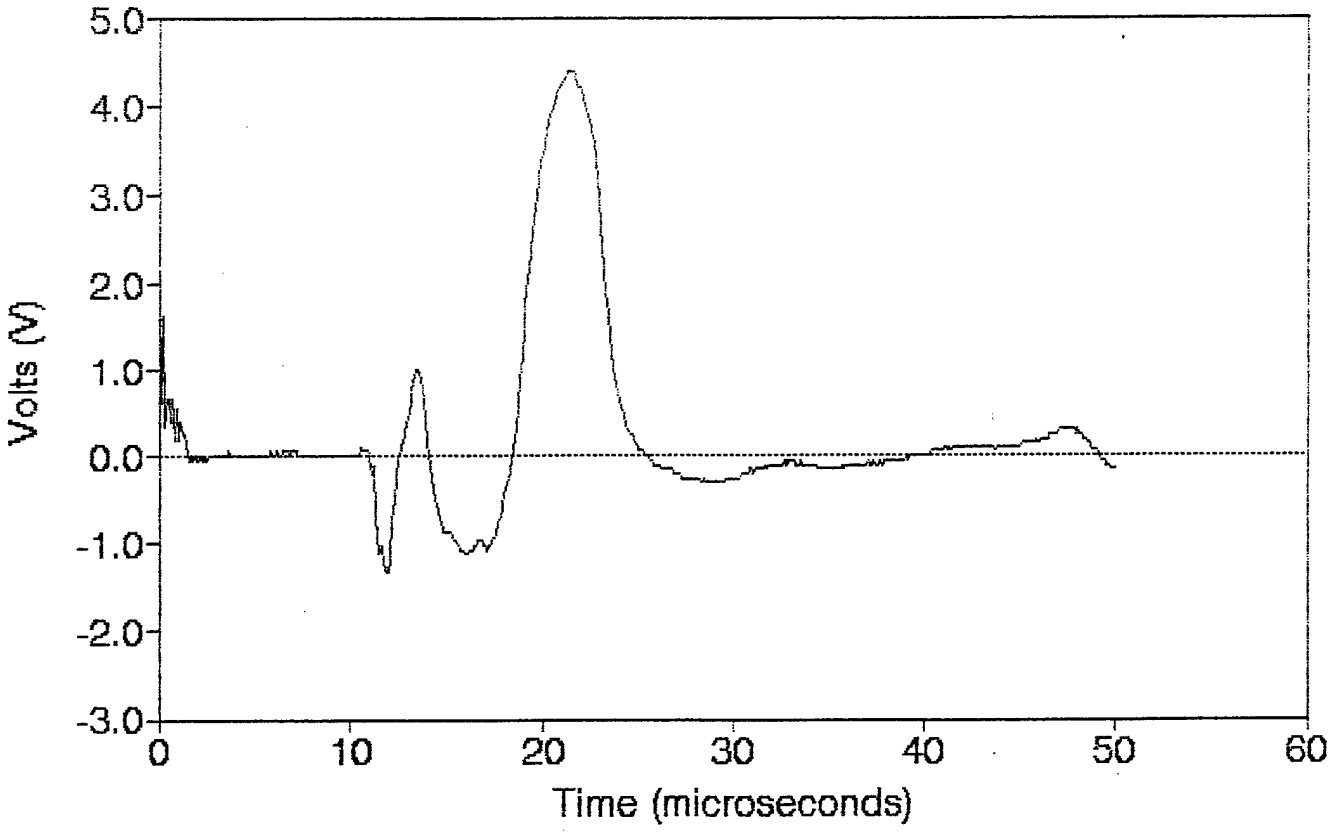

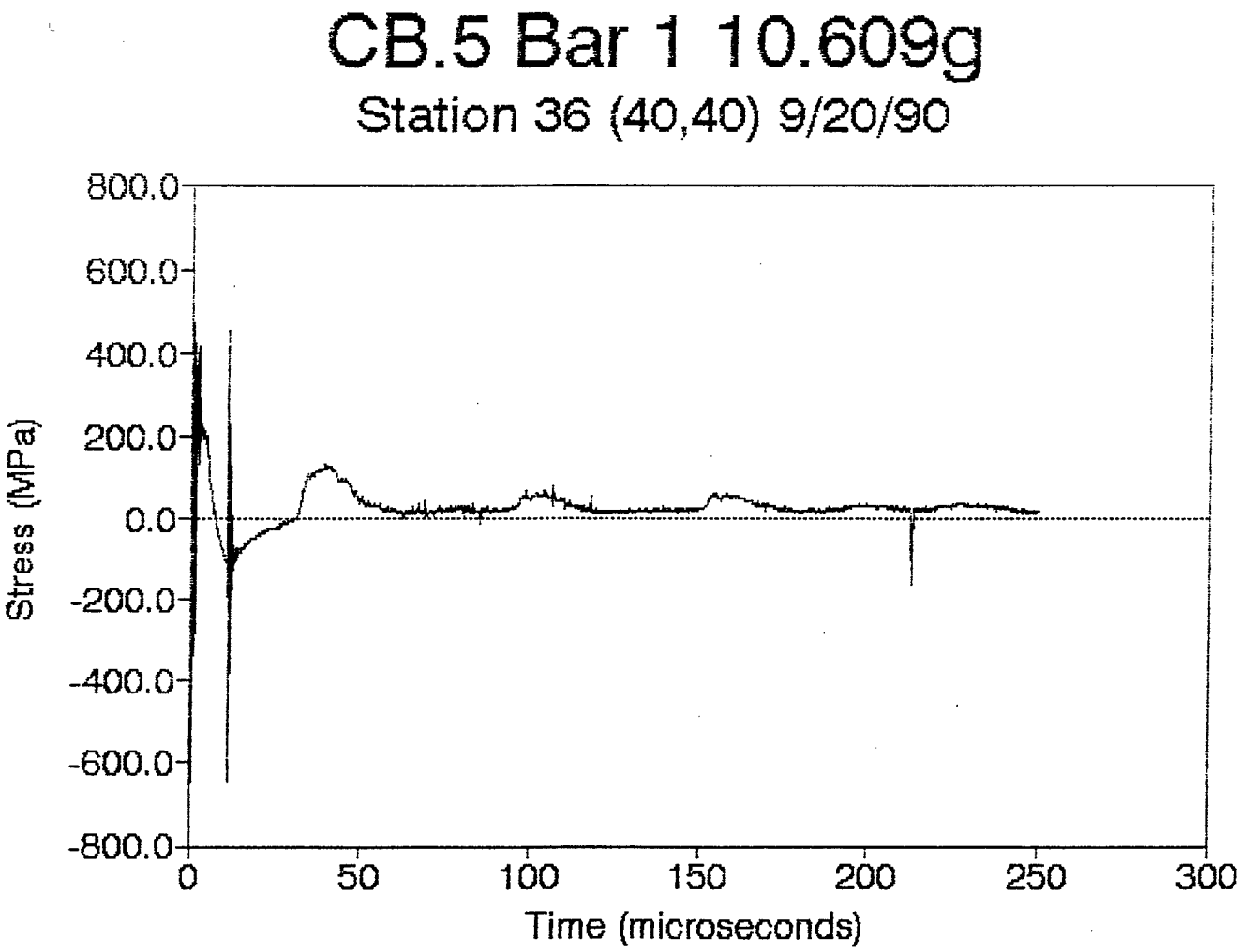
CB.5 Bar 1 10.609g
Station 36 (40,40) 9/20/90
800.0
600.0
400.0
200.0
0.0
-200.0
-400.0
-600.0
-800.0
Stress (MPa)
0
50
100
150
200
250
300
Time (microseconds)

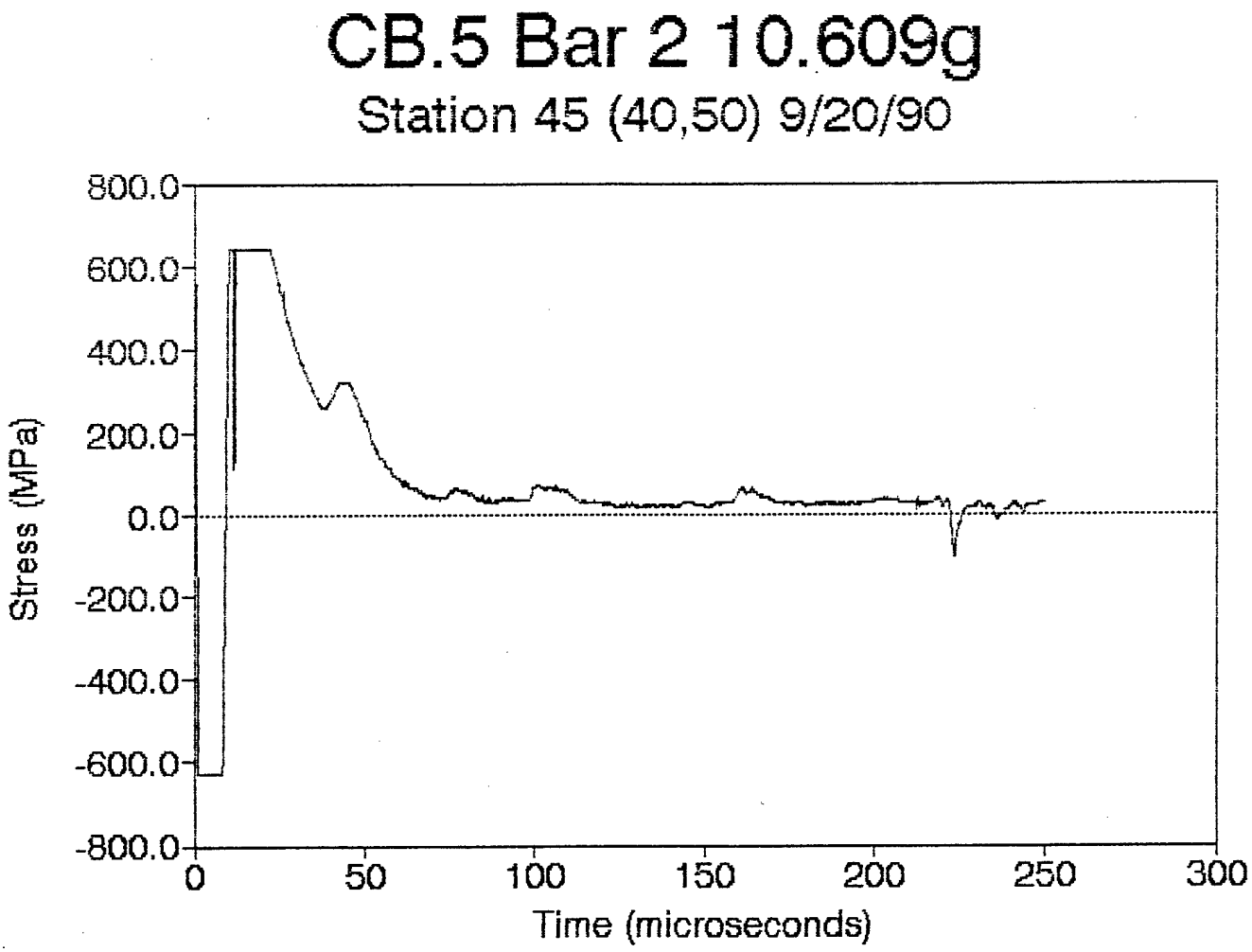
CB.5 Bar 2 10.609g
Station 45 (40,50) 9/20/90
800.0
600.0
400.0
200.0
0.0
-200.0
-400.0
-600.0
-800.0
Stress (MPa)
0
50
100
150
200
250
300
Time (microseconds)

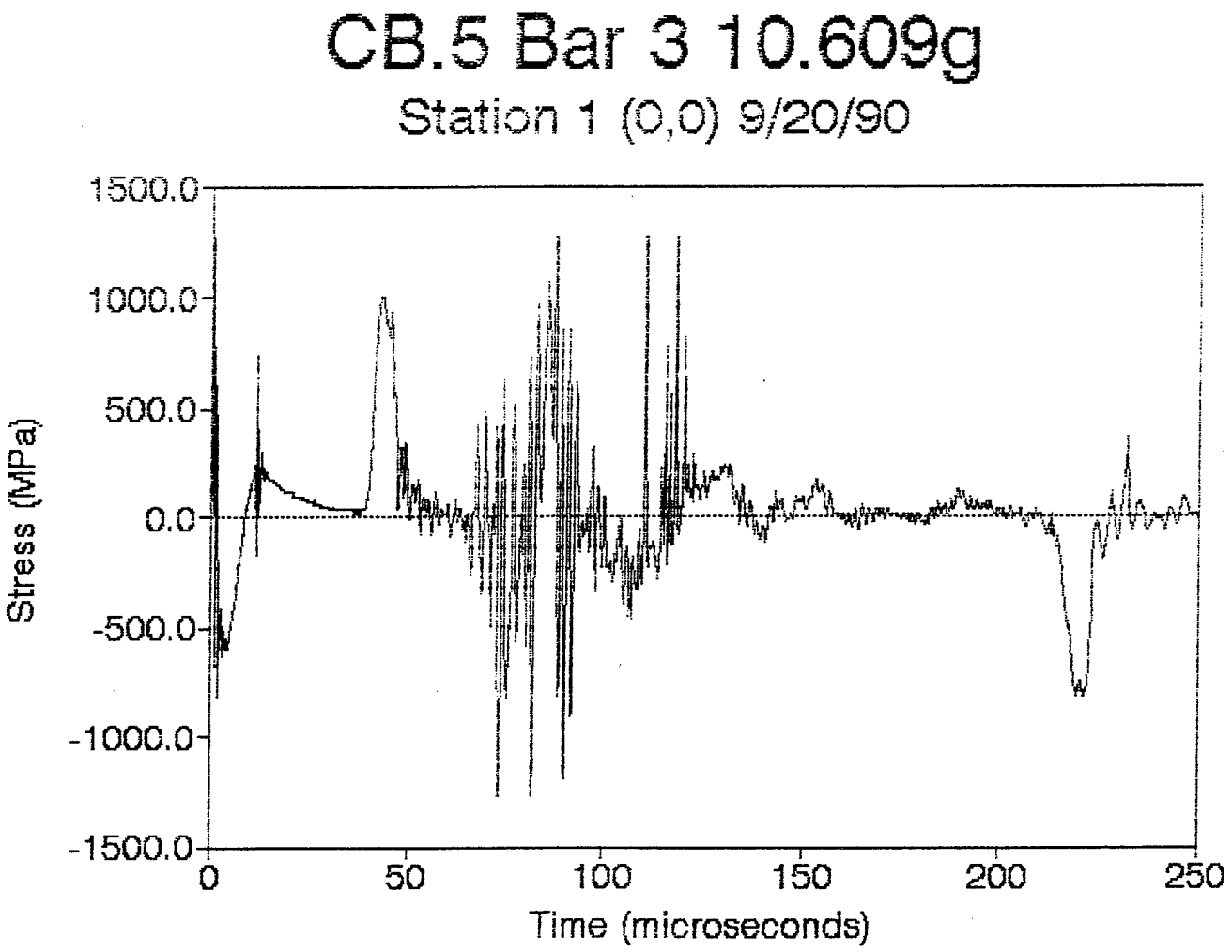
CB.5 Bar 3 10.609g
Station 1 (0,0) 9/20/90
1500.0
1000.0
500.0
0.0
-500.0
-1000.0
-1500.0
Stress (MPa)
0
50
100
150
200
250
Time (microseconds)

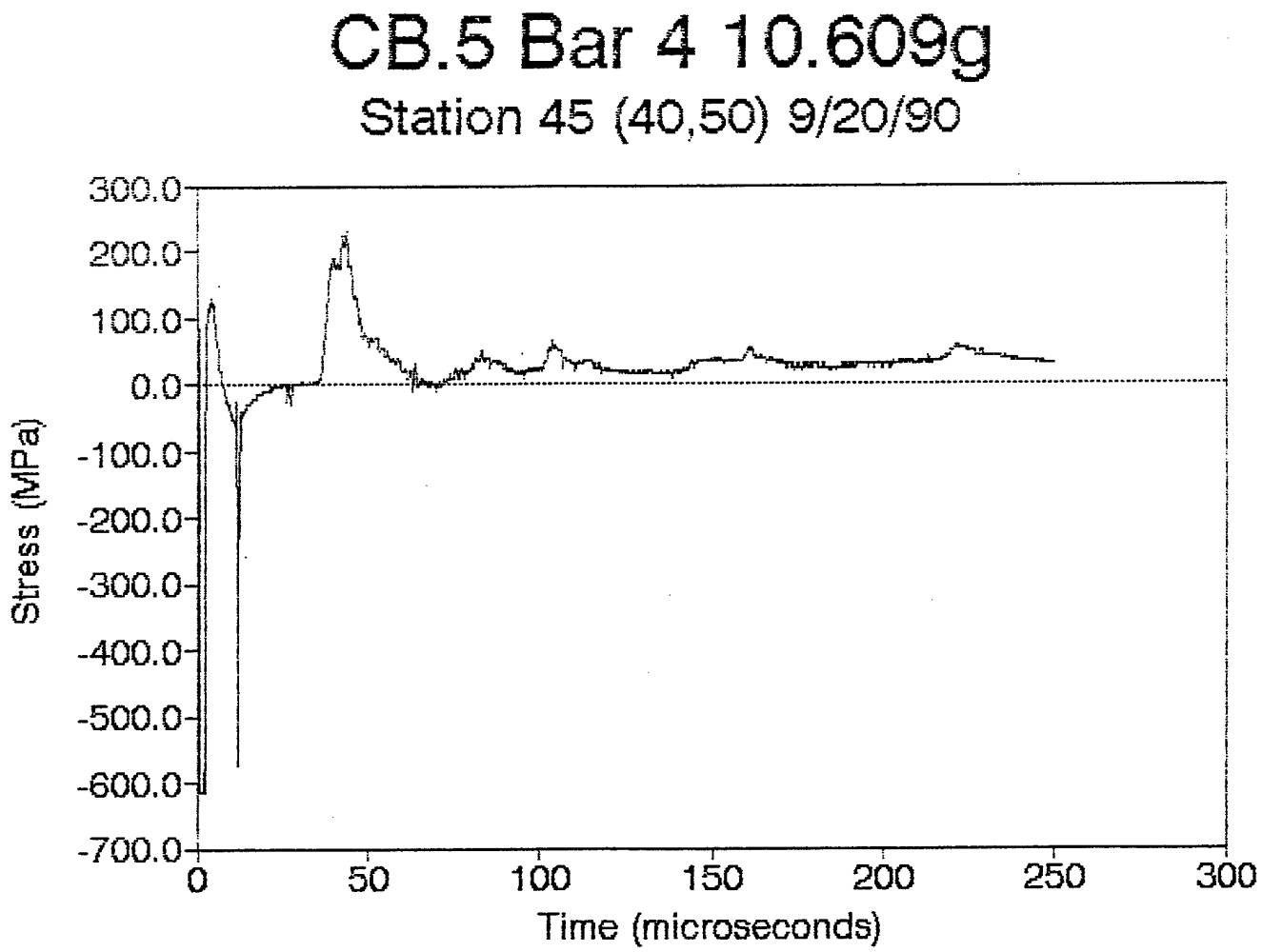
CB.5 Bar 4 10.609g
Station 45 (40,50) 9/20/90
300.0
200.0
100.0
0.0
-100.0
-200.0
-300.0
-400.0
-500.0
-600.0
-700.0
Stress (MPa)
0
50
100
150
200
250
300
Time (microseconds)

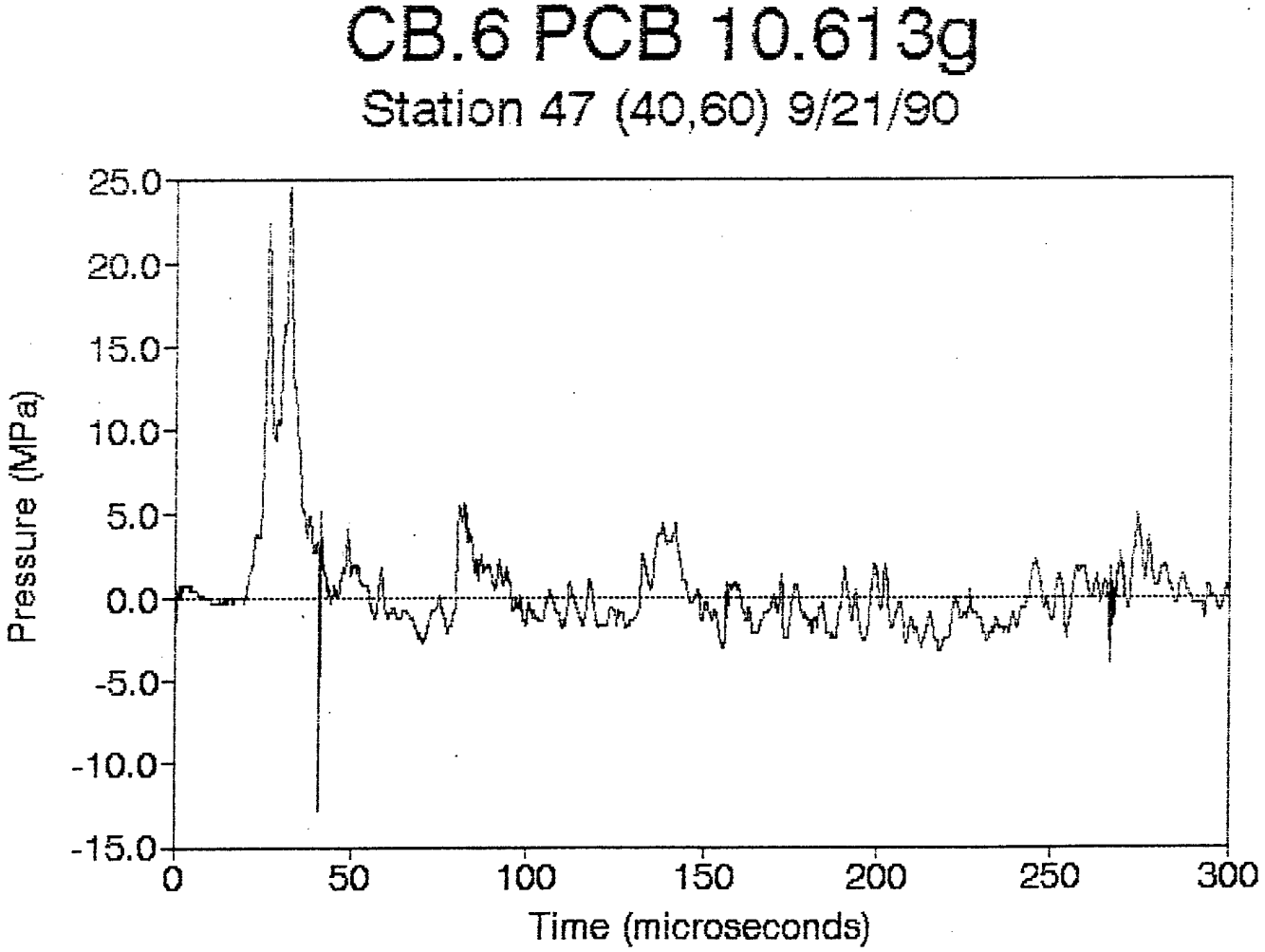
CB.6 PCB 10.613g
Station 47 (40,60) 9/21/90
25.0
20.0
15.0
10.0
5.0
0.0
-5.0
-10.0
-15.0
Pressure (MPa)
0
50
100
150
200
250
300
Time (microseconds)

CB.6 470 Ohm Resistor 10.613g

Station 36 (40,40) 9/21/90

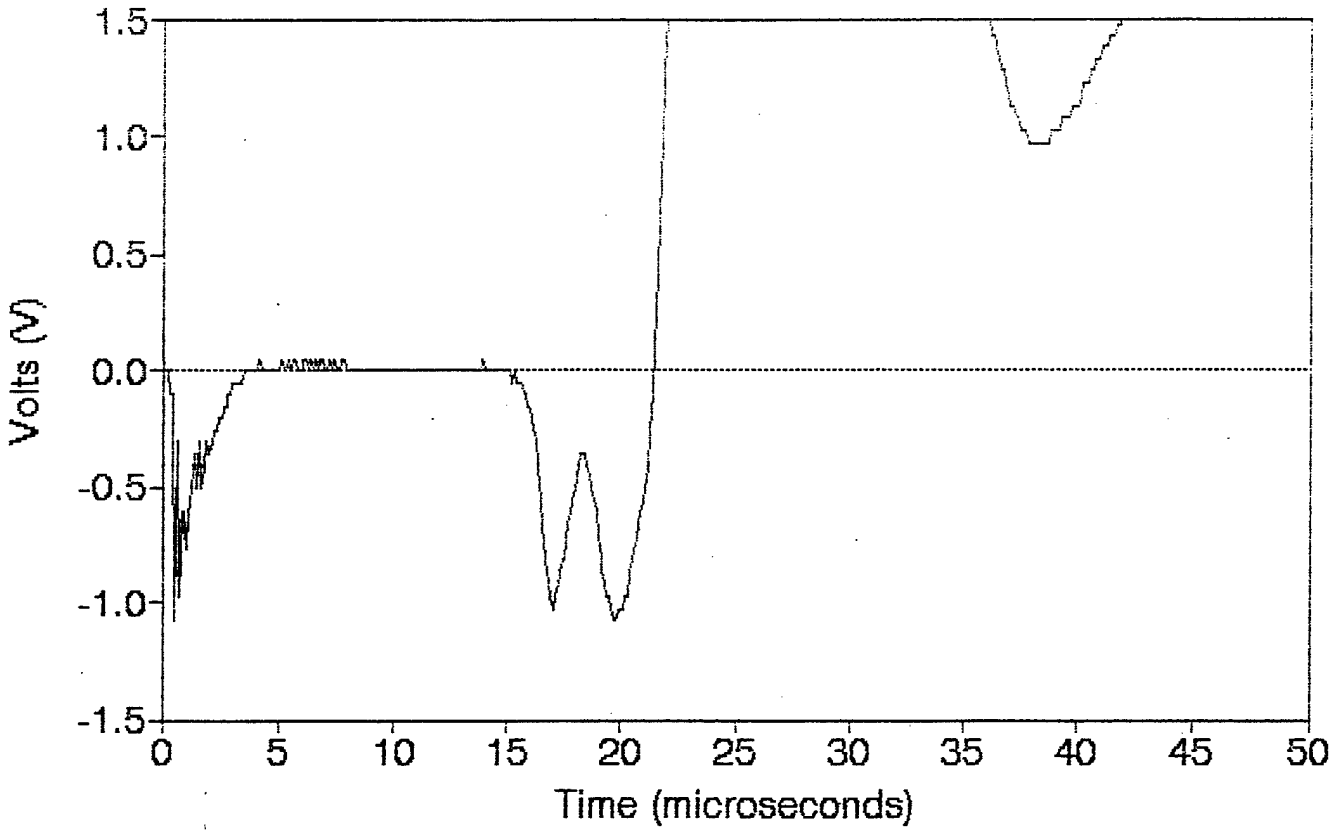

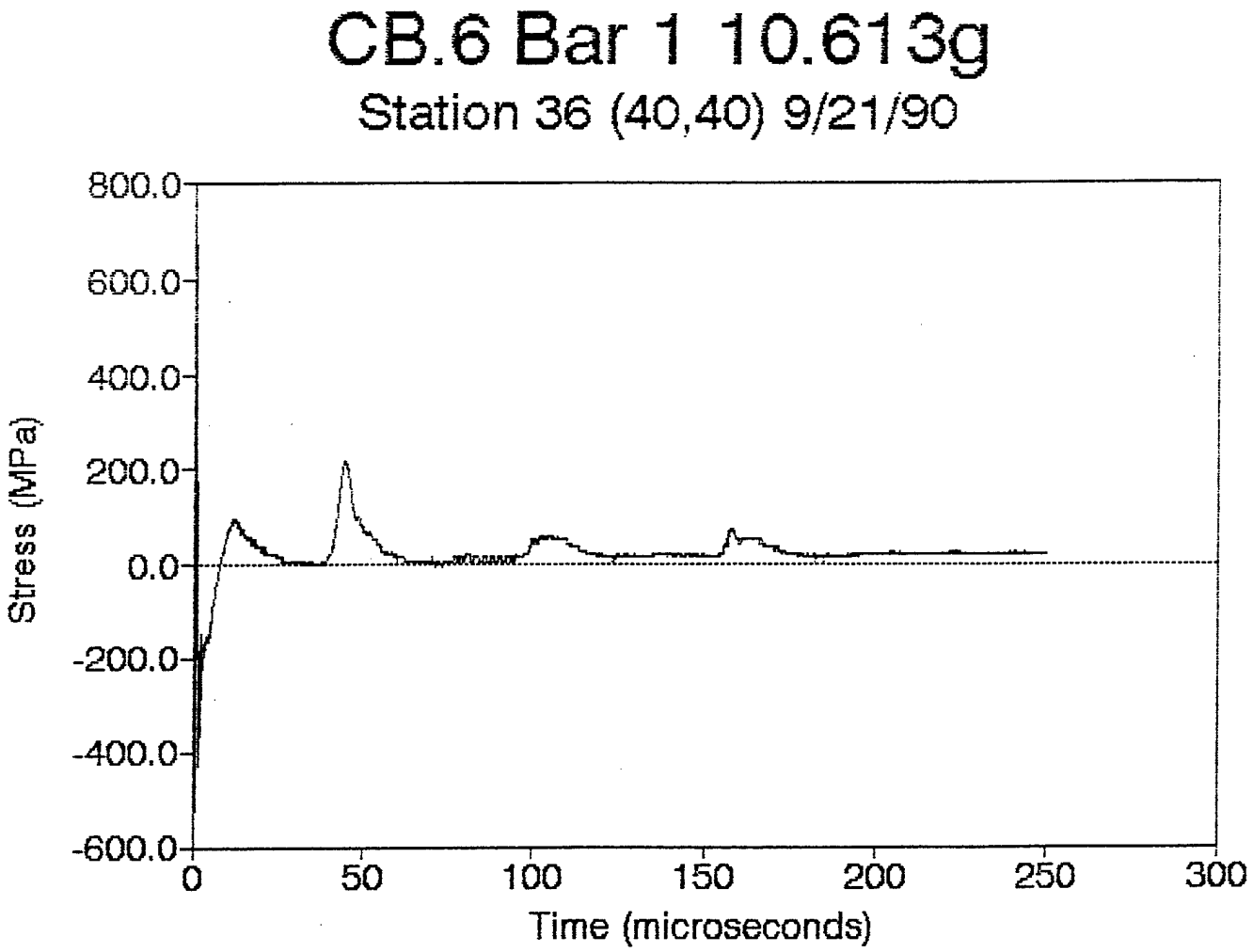
CB.6 Bar 1 10.613g
Station 36 (40,40) 9/21/90
800.0
600.0
400.0
200.0
0.0
-200.0
-400.0
-600.0
Stress (MPa)
0
50
100
150
200
250
300
Time (microseconds)

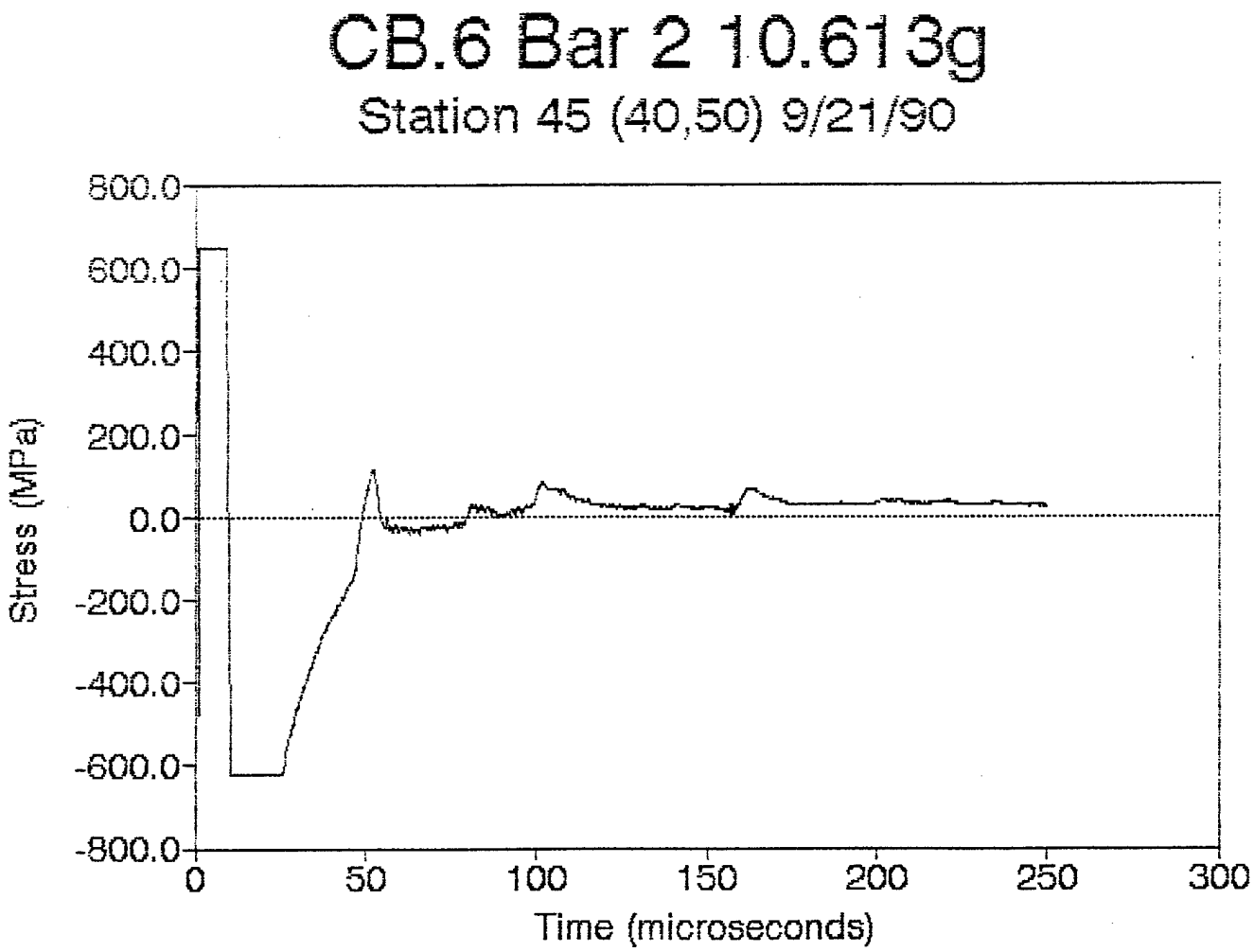
CB.6 Bar 2 10.613g
Station 45 (40,50) 9/21/90
800.0
600.0
400.0
200.0
0.0
-200.0
-400.0
-600.0
-800.0
Stress (MPa)
0
50
100
150
200
250
300
Time (microseconds)

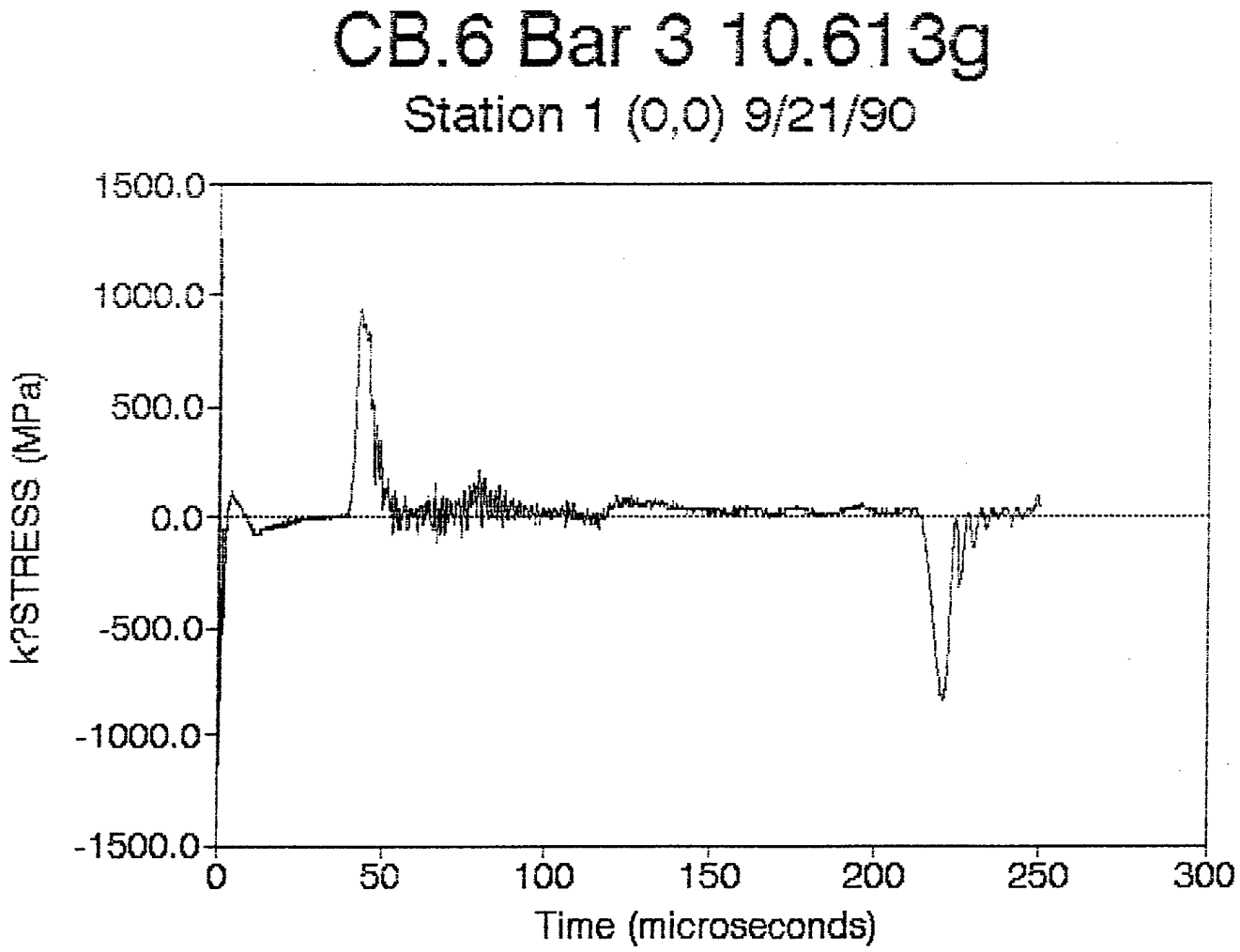
CB.6 Bar 3 10.613g
Station 1 (0,0) 9/21/90
1500.0
1000.0
500.0
0.0
-500.0
-1000.0
-1500.0
K?STRESS (MPa)
0
50
100
150
200
250
300
Time (microseconds)

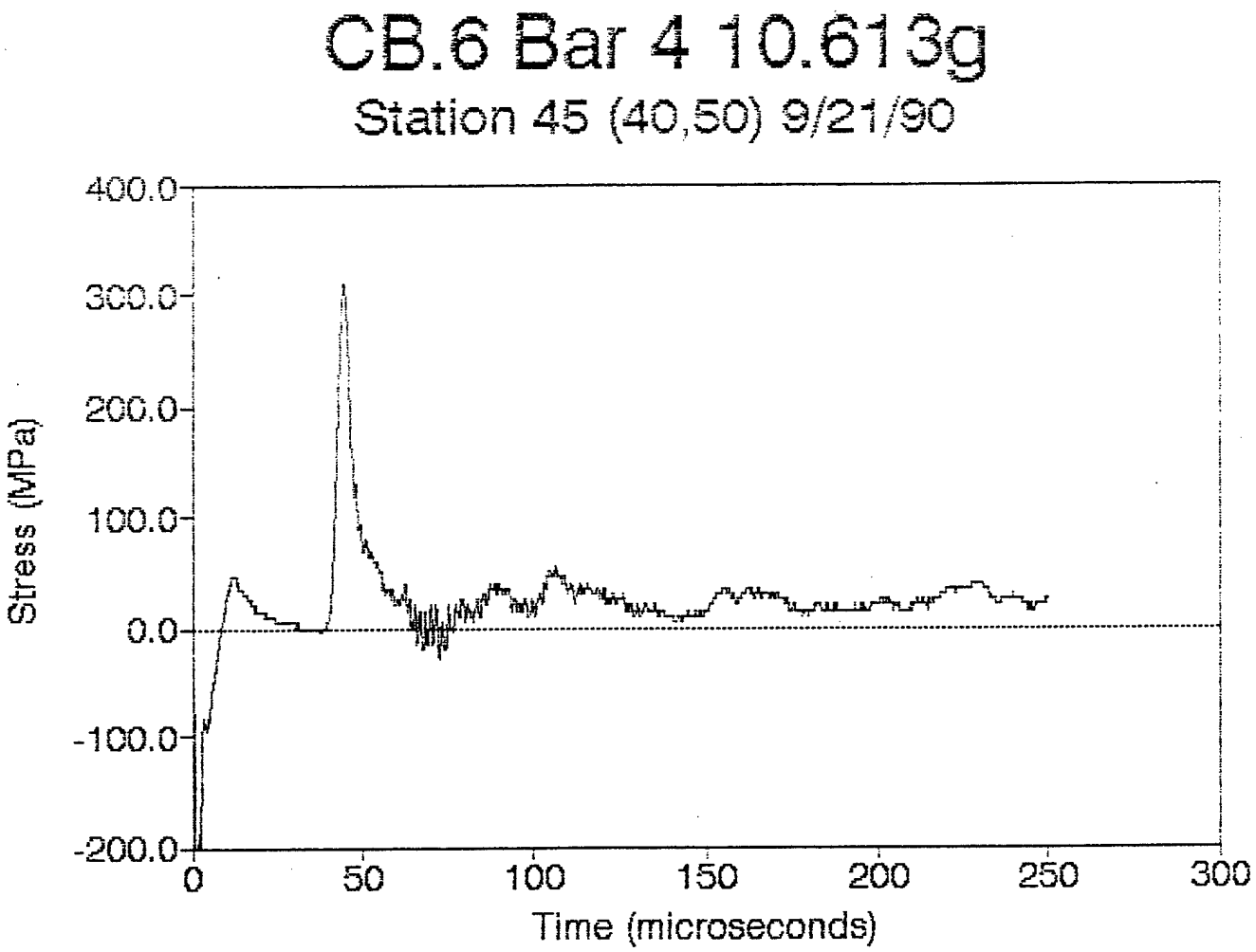
CB.6 Bar 4 10.613g
Station 45 (40,50) 9/21/90
400.0
300.0
200.0
100.0
0.0
-100.0
-200.0
Stress (MPa)
0
50
100
150
200
250
300
Time (microseconds)

LX.1 470 Ohm Resistor 11.330g

Station 36 (40,40) 7/24/90

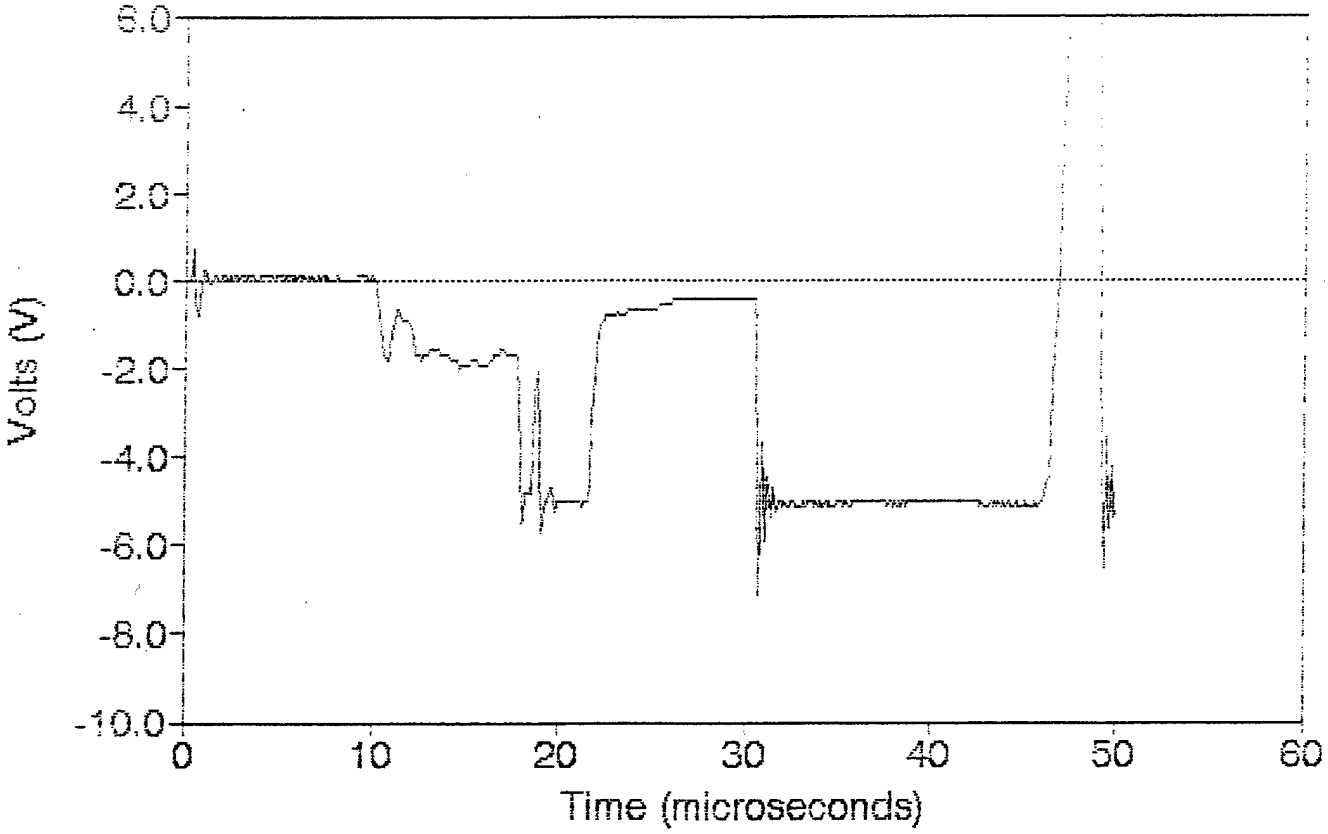

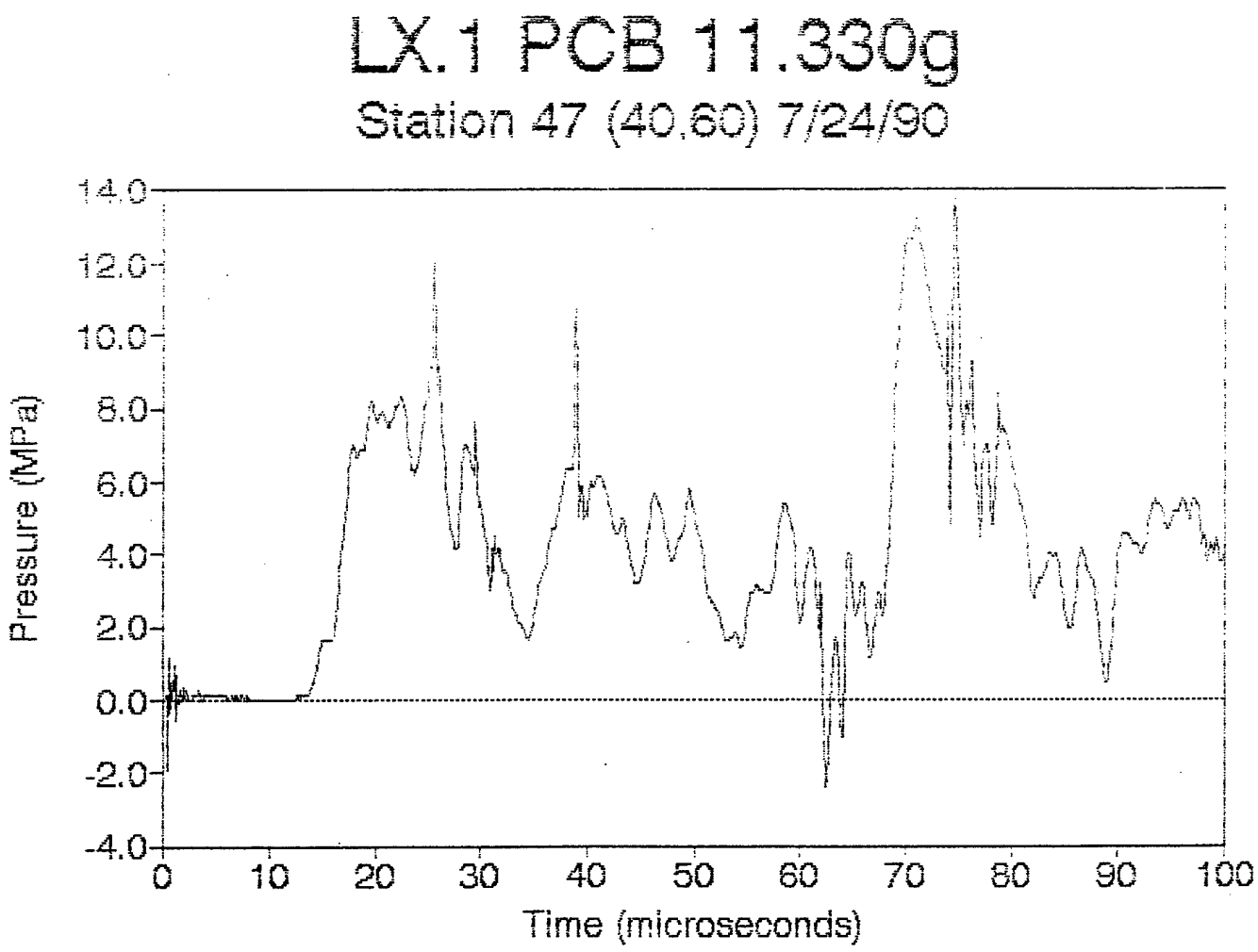
LX.1 PCB 11.330g
Station 47 (40,60) 7/24/90
Pressure (MPa)
14.0
12.0
10.0
8.0
6.0
4.0
2.0
0.0
-2.0
-4.0
0
10
20
30
40
50
60
70
80
90
100
Time (microseconds)

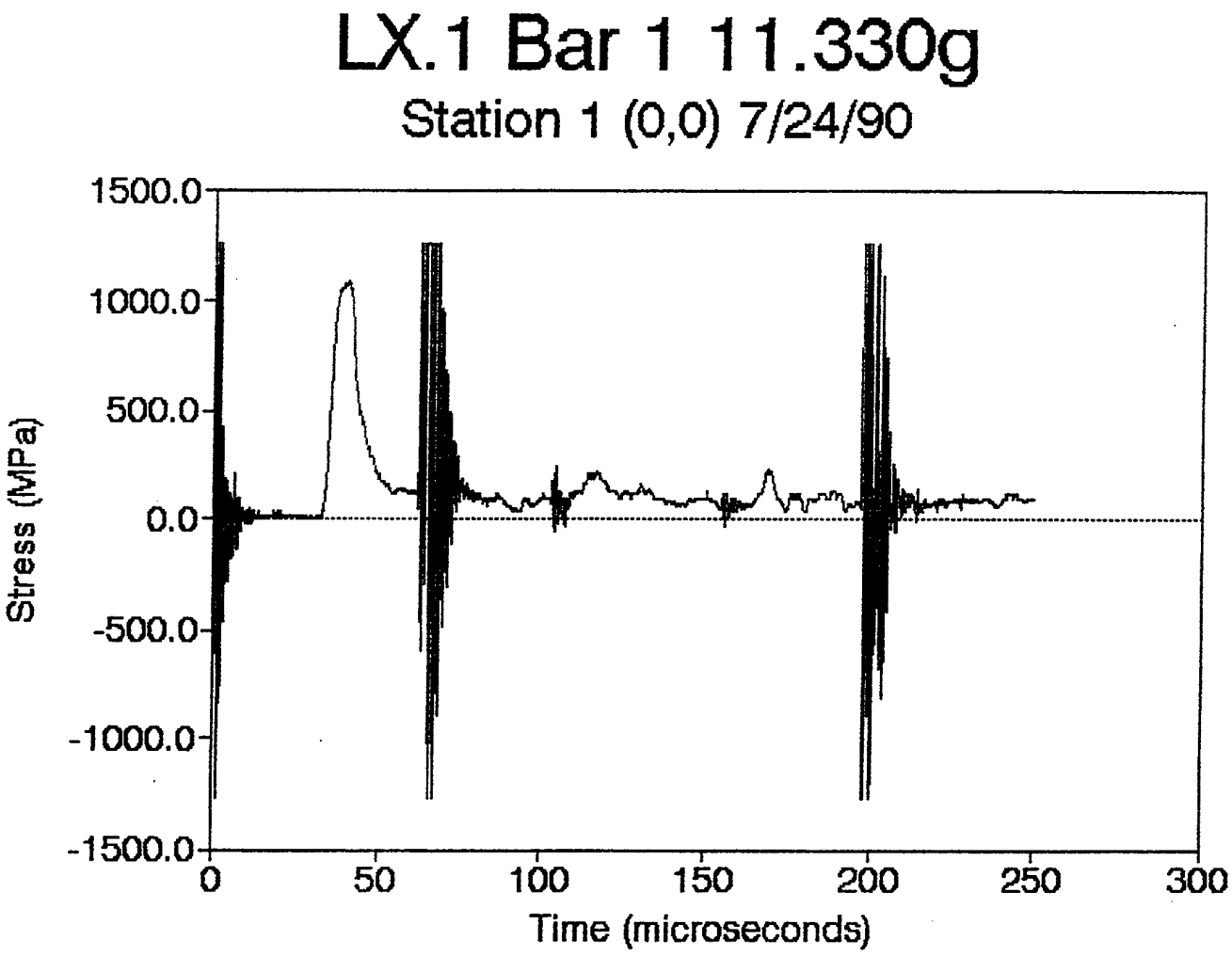
LX.1 Bar 1 11.330g
Station 1 (0,0) 7/24/90
1500.0
1000.0
500.0
0.0
-500.0
-1000.0
-1500.0
Stress (MPa)
0
50
100
150
200
250
300
Time (microseconds)

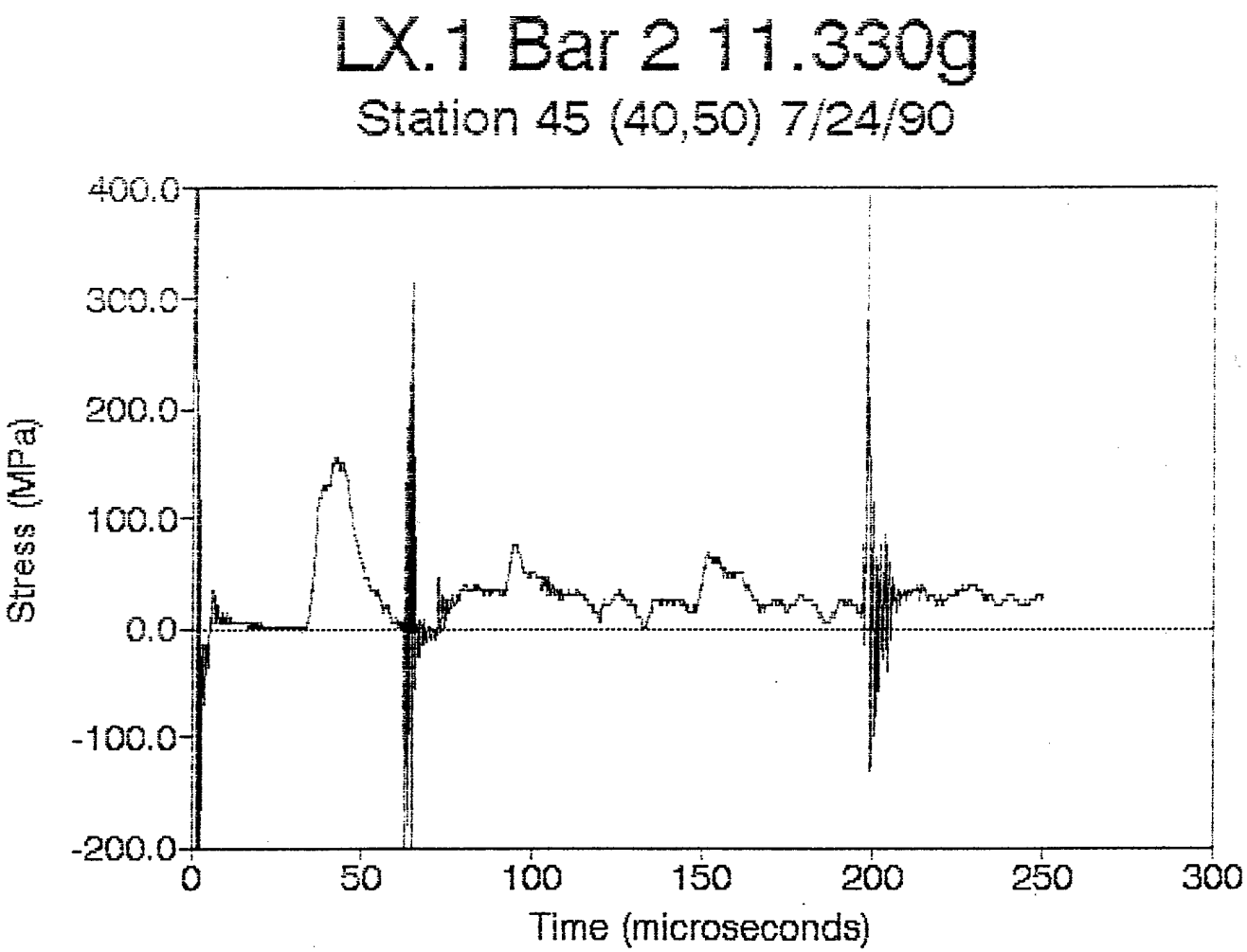
LX.1 Bar 2 11.330g
Station 45 (40,50) 7/24/90
Stress (MPa)
400.0
300.0
200.0
100.0
0.0
-100.0
-200.0
0
50
100
150
200
250
300
Time (microseconds)

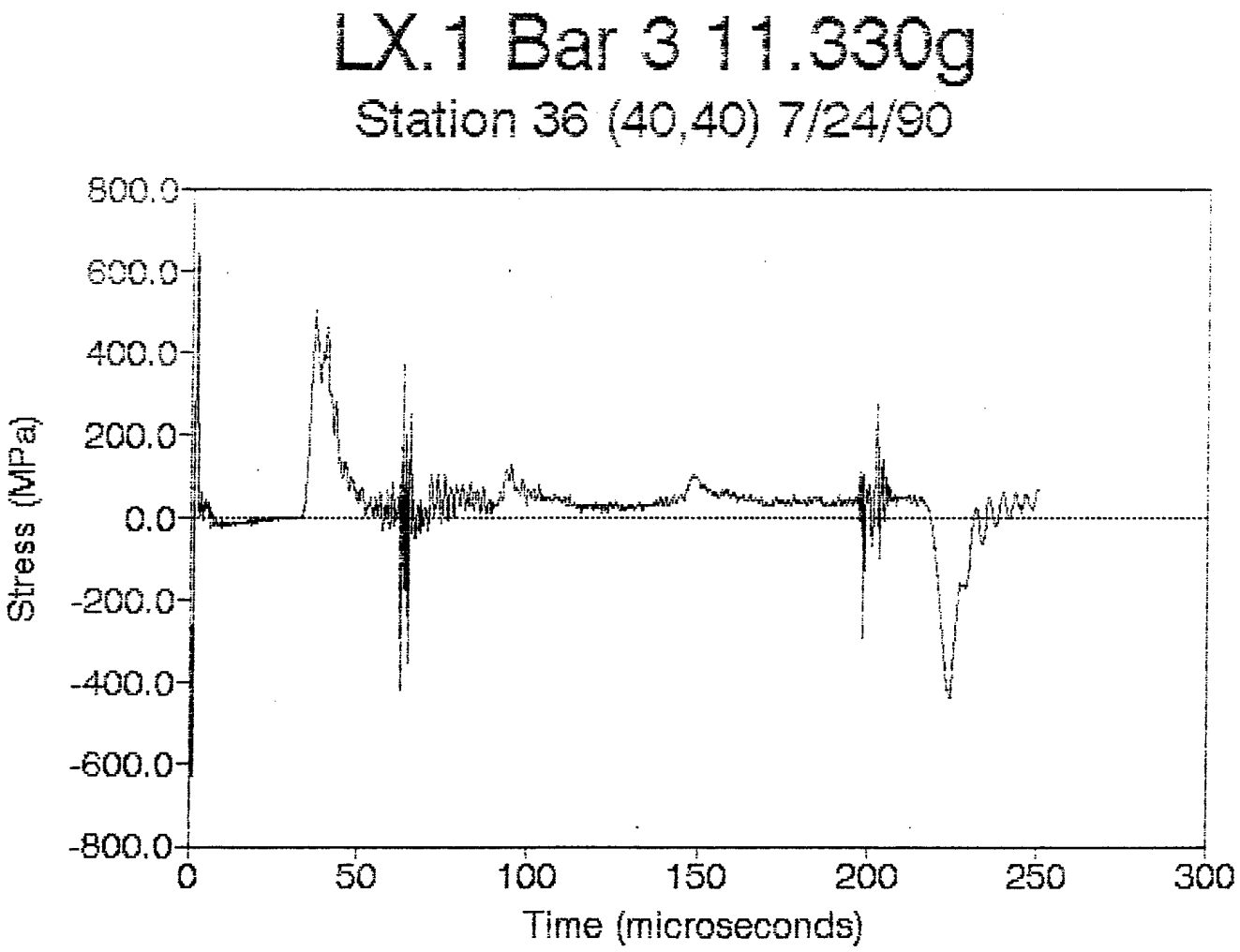
LX.1 Bar 3 11.330g
Station 36 (40,40) 7/24/90
800.0
600.0
400.0
200.0
0.0
-200.0
-400.0
-600.0
-800.0
Stress (MPa)
0
50
100
150
200
250
300
Time (microseconds)

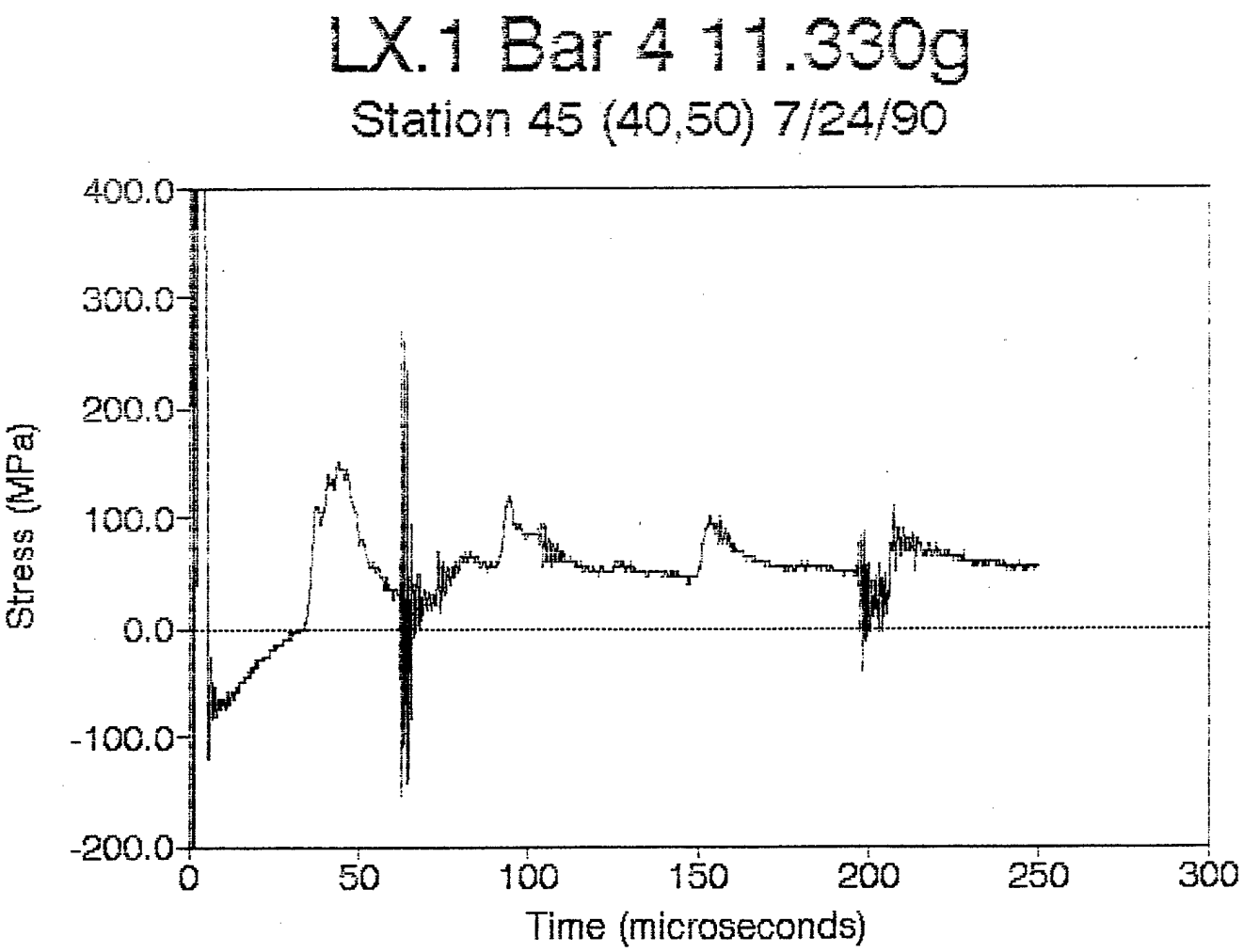
LX.1 Bar 4 11.330g
Station 45 (40,50) 7/24/90
400.0
300.0
200.0
100.0
0.0
-100.0
-200.0
Stress (MPa)
0
50
100
150
200
250
300
Time (microseconds)

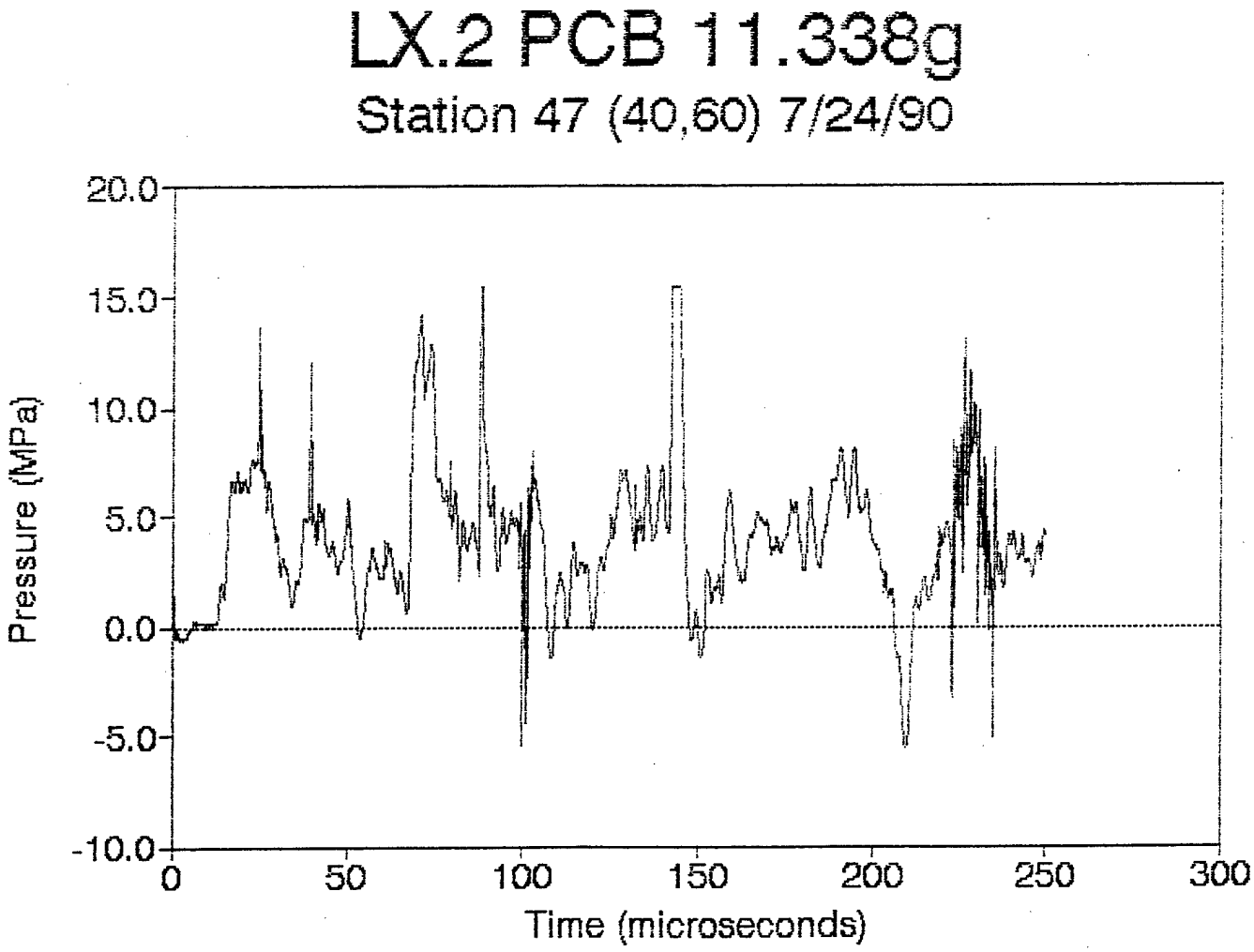
LX.2 PCB 11.338g
Station 47 (40,60) 7/24/90
20.0
15.0
10.0
5.0
0.0
-5.0
-10.0
Pressure (MPa)
0
50
100
150
200
250
300
Time (microseconds)

LX.2 470 Ohm Resistor 11.338g

Station 36 (40,40) 7/24/90

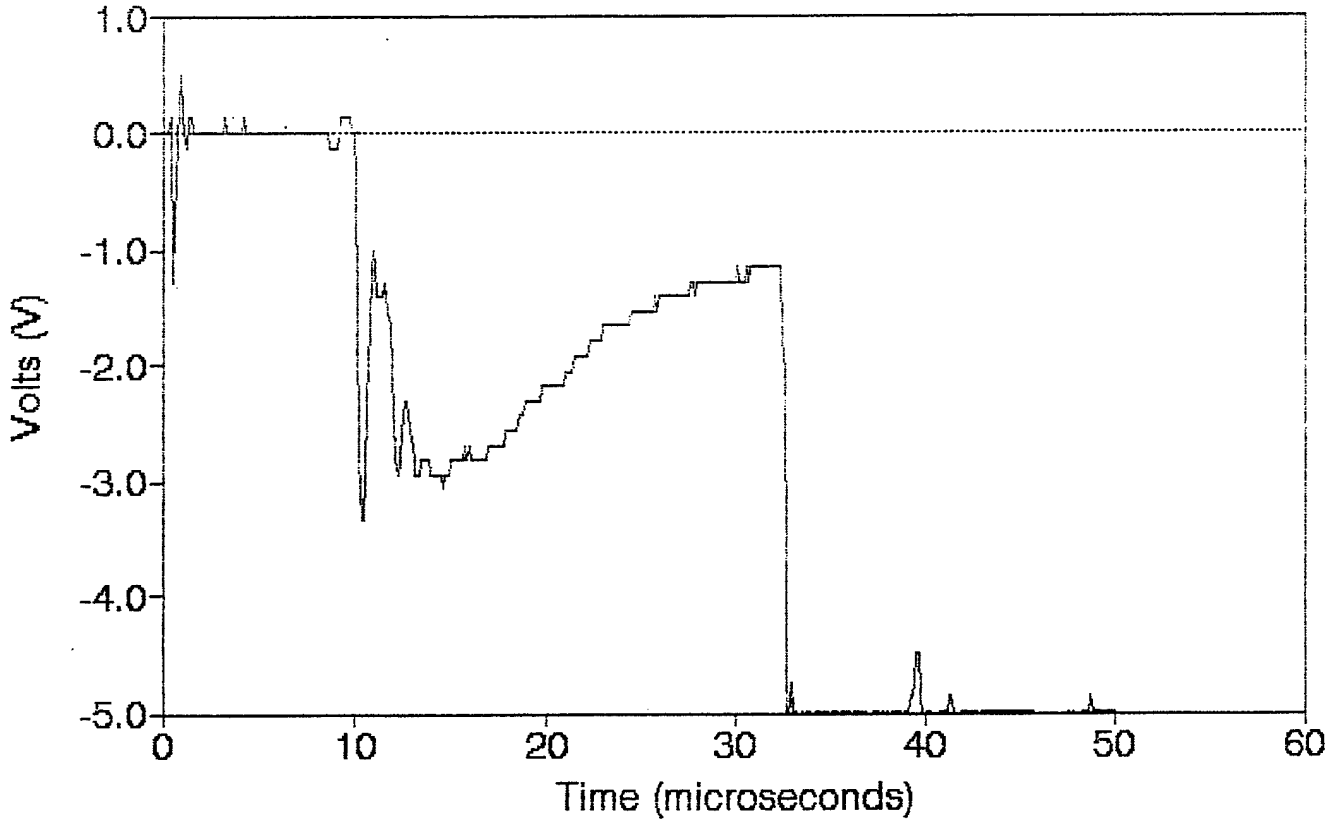

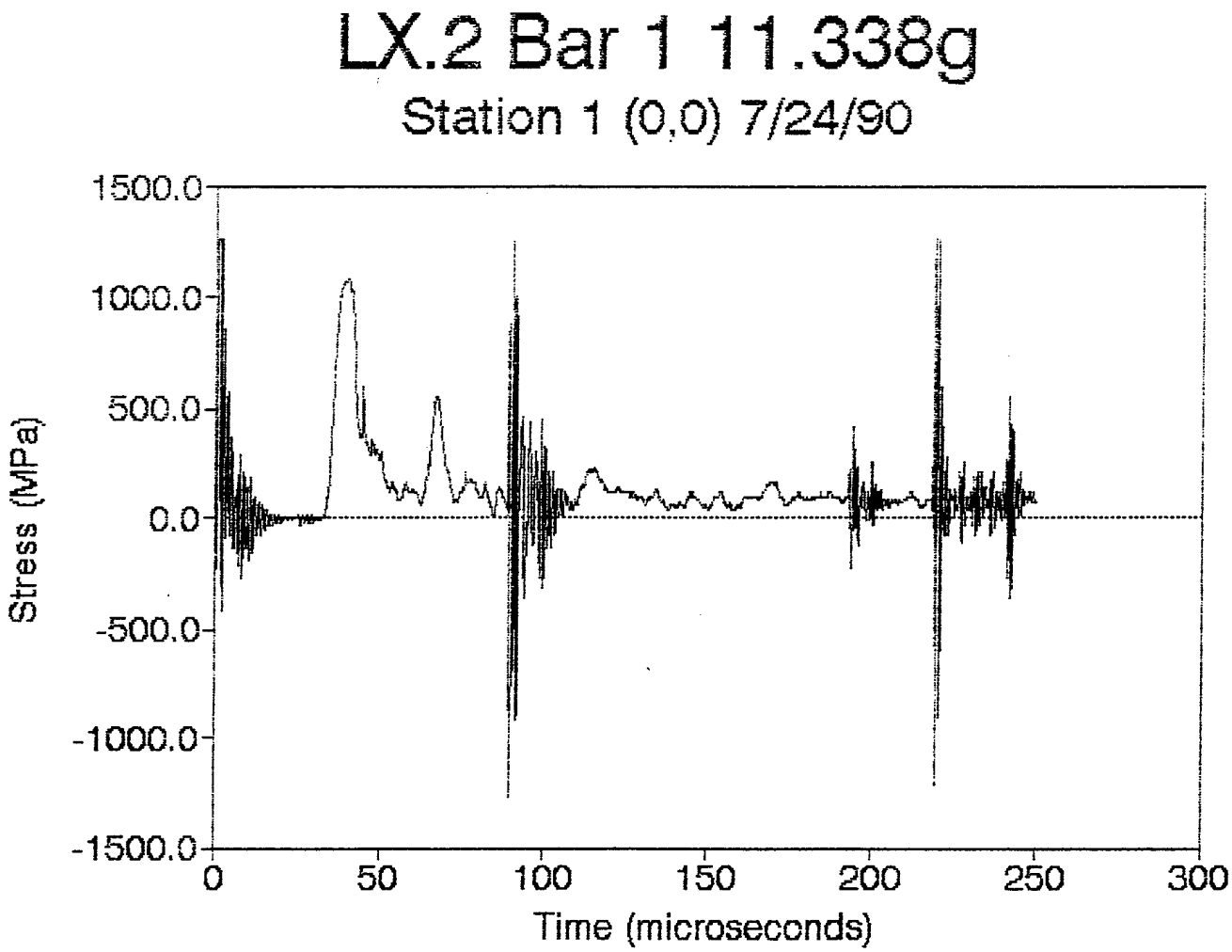
LX.2 Bar 1 11.338g
Station 1 (0,0) 7/24/90
1500.0
1000.0
500.0
0.0
-500.0
-1000.0
-1500.0
Stress (MPa)
0
50
100
150
200
250
300
Time (microseconds)

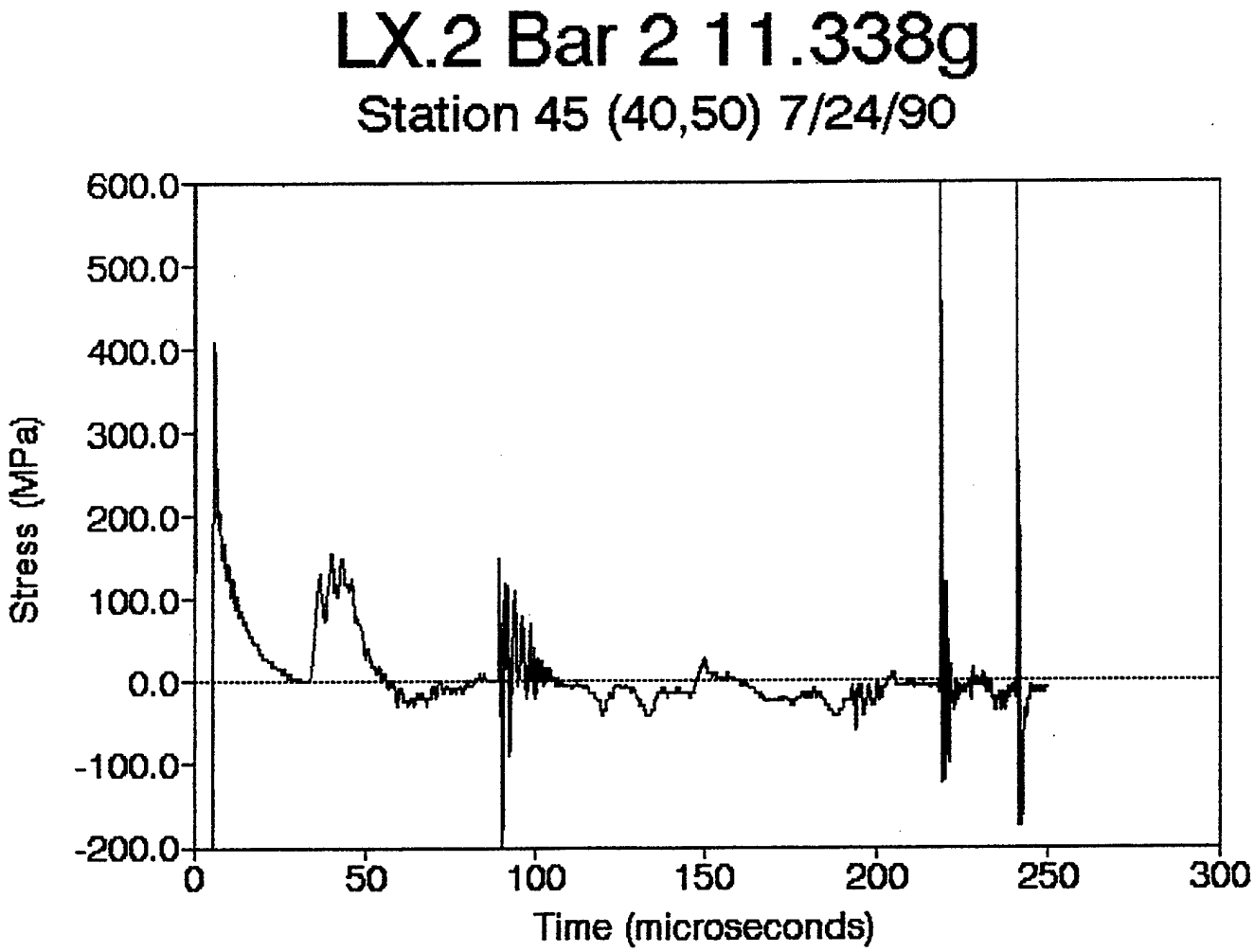
LX.2 Bar 2 11.338g
Station 45 (40,50) 7/24/90
600.0
500.0
400.0
300.0
200.0
100.0
0.0
-100.0
-200.0
Stress (MPa)
0
50
100
150
200
250
300
Time (microseconds)

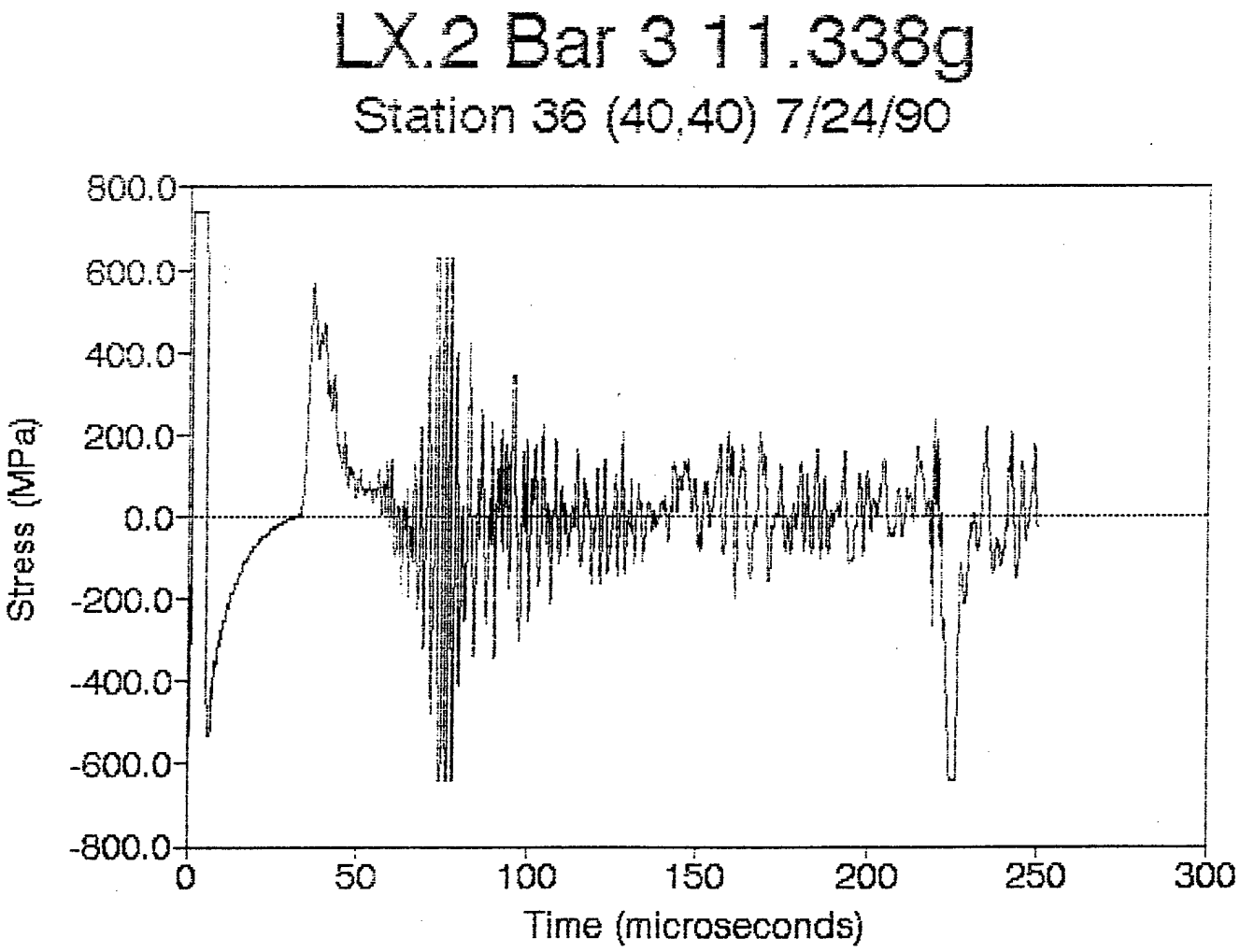
LX.2 Bar 3 11.338g
Station 36 (40,40) 7/24/90
800.0
600.0
400.0
200.0
0.0
-200.0
-400.0
-600.0
-800.0
Stress (MPa)
0
50
100
150
200
250
300
Time (microseconds)

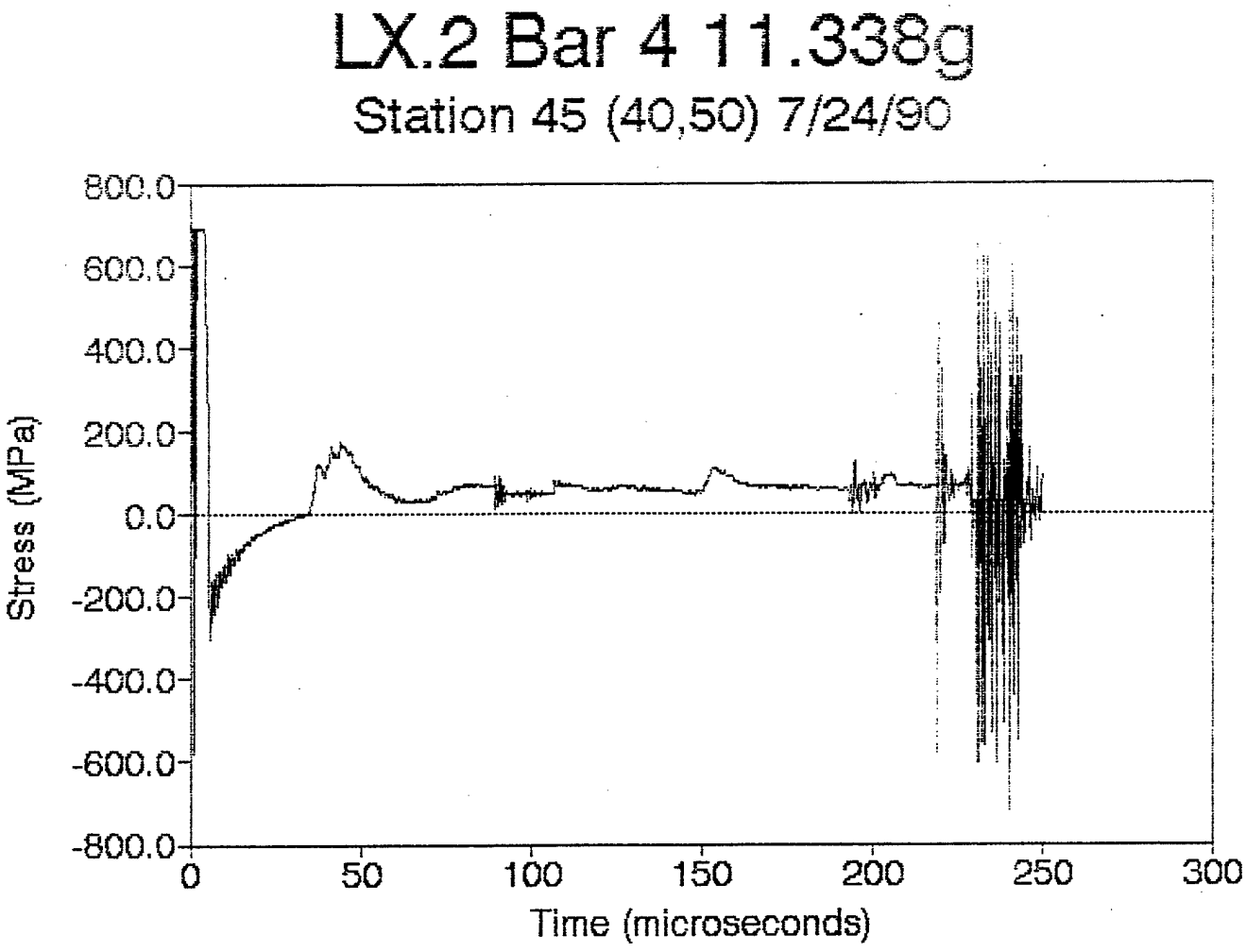
LX.2 Bar 4 11.338g
Station 45 (40,50) 7/24/90
800.0
600.0
400.0
200.0
0.0
-200.0
-400.0
-600.0
-800.0
Stress (MPa)
0
50
100
150
200
250
300
Time (microseconds)

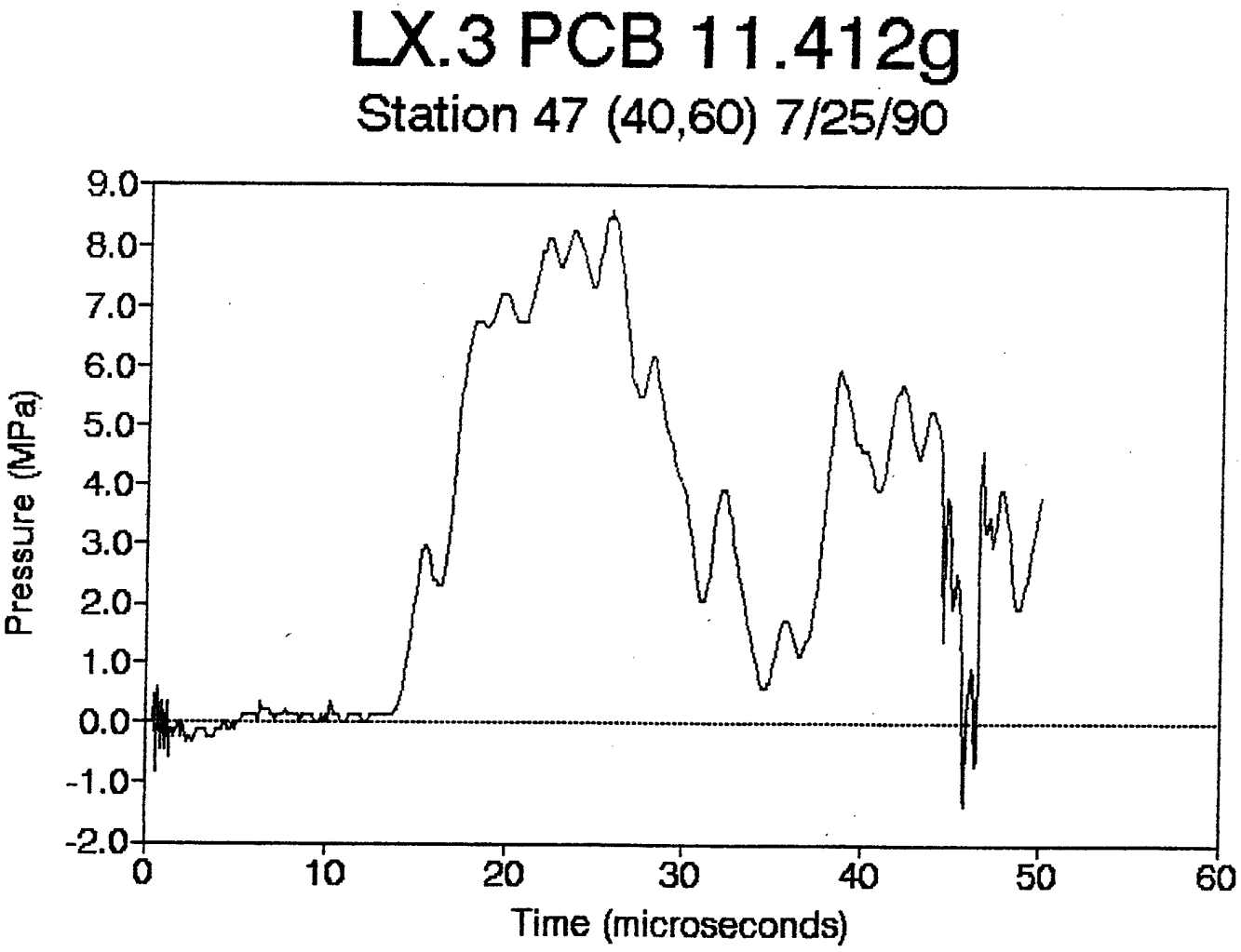
LX.3 PCB 11.412g
Station 47 (40,60) 7/25/90
Pressure (MPa)
9.0
8.0
7.0
6.0
5.0
4.0
3.0
2.0
1.0
0.0
-1.0
-2.0
0
10
20
30
40
50
60
Time (microseconds)

LX.3 470 Ohm Resistor 11.412g

Station 36 (40,40) 7/25/90

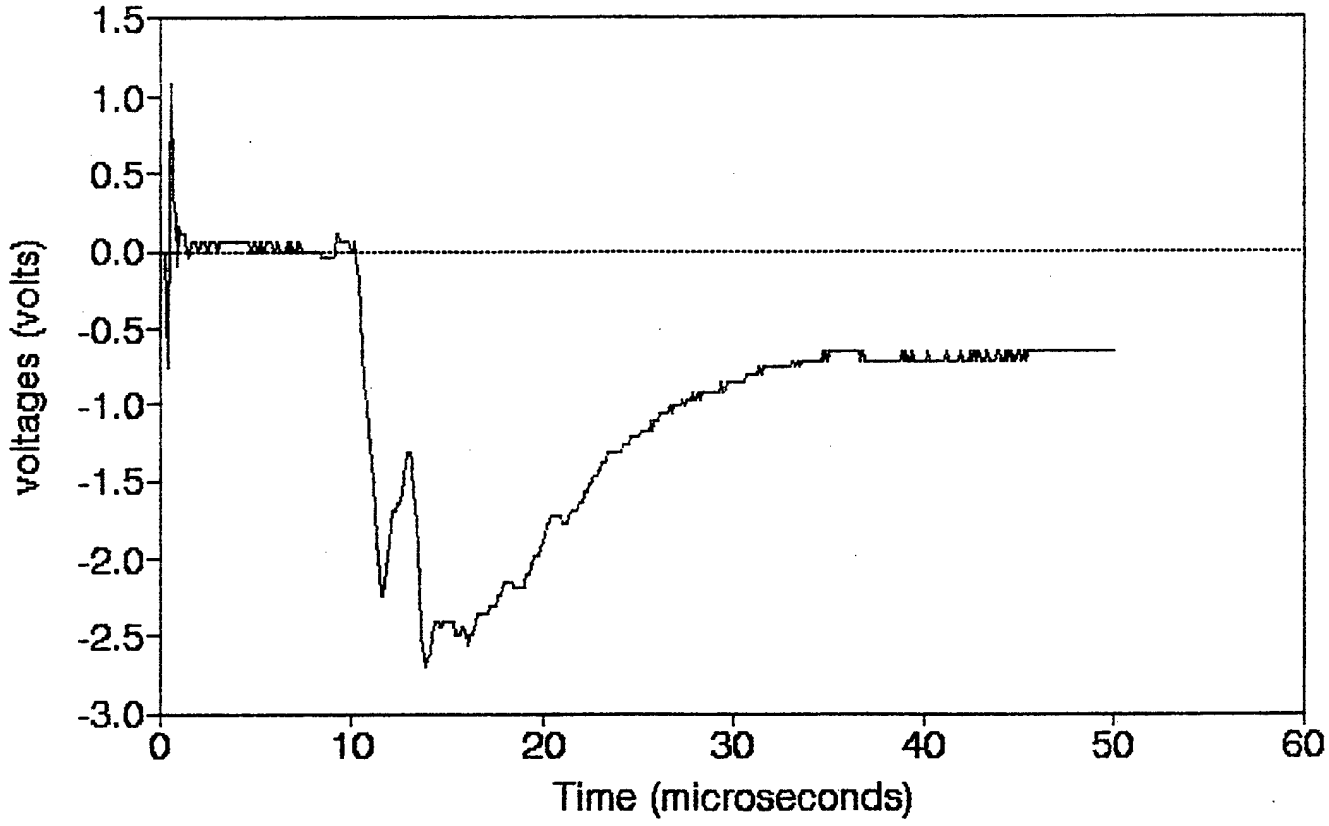

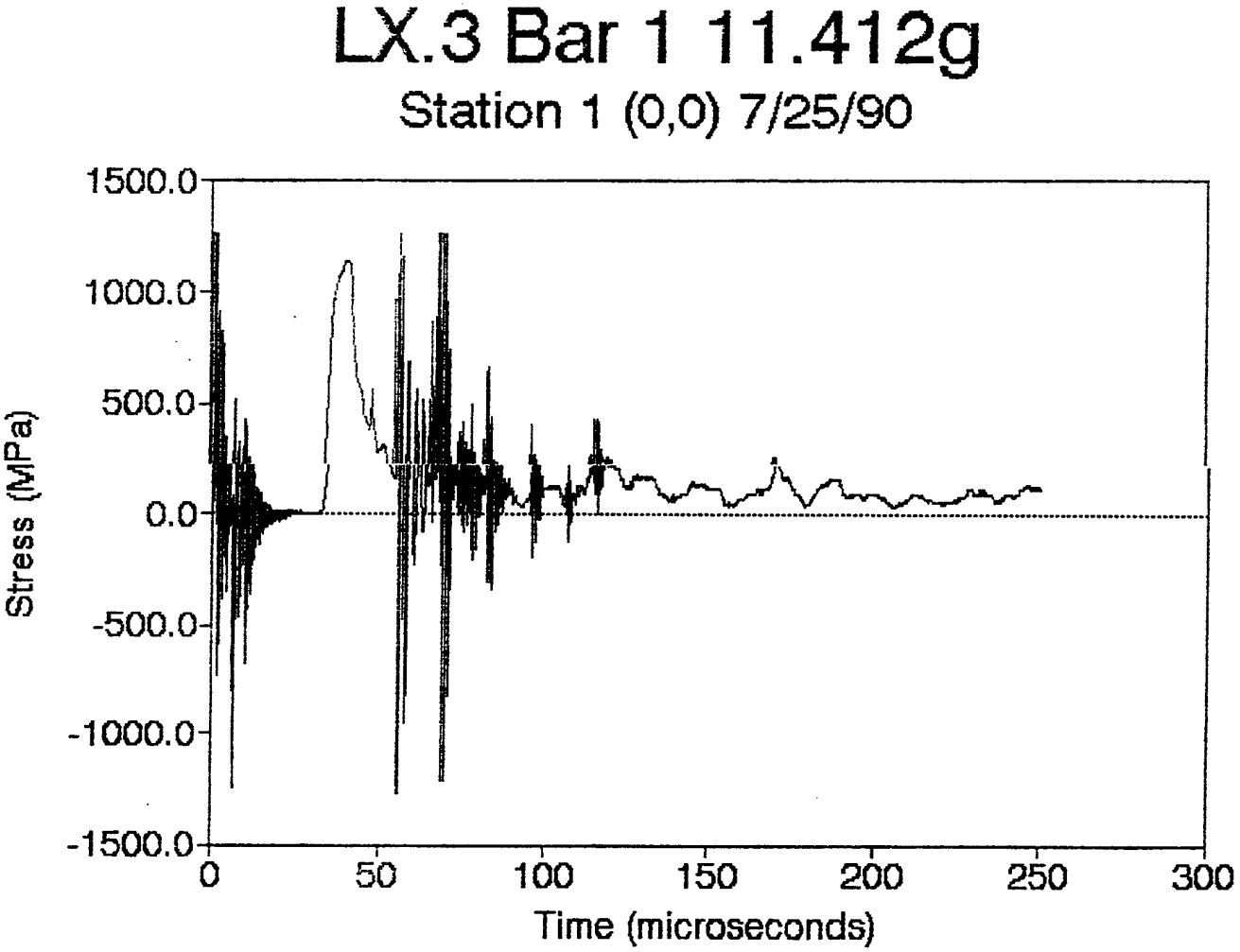
LX.3 Bar 1 11.412g
Station 1 (0,0) 7/25/90
1500.0
1000.0
500.0
0.0
-500.0
-1000.0
-1500.0
Stress (MPa)
0
50
100
150
200
250
300
Time (microseconds)

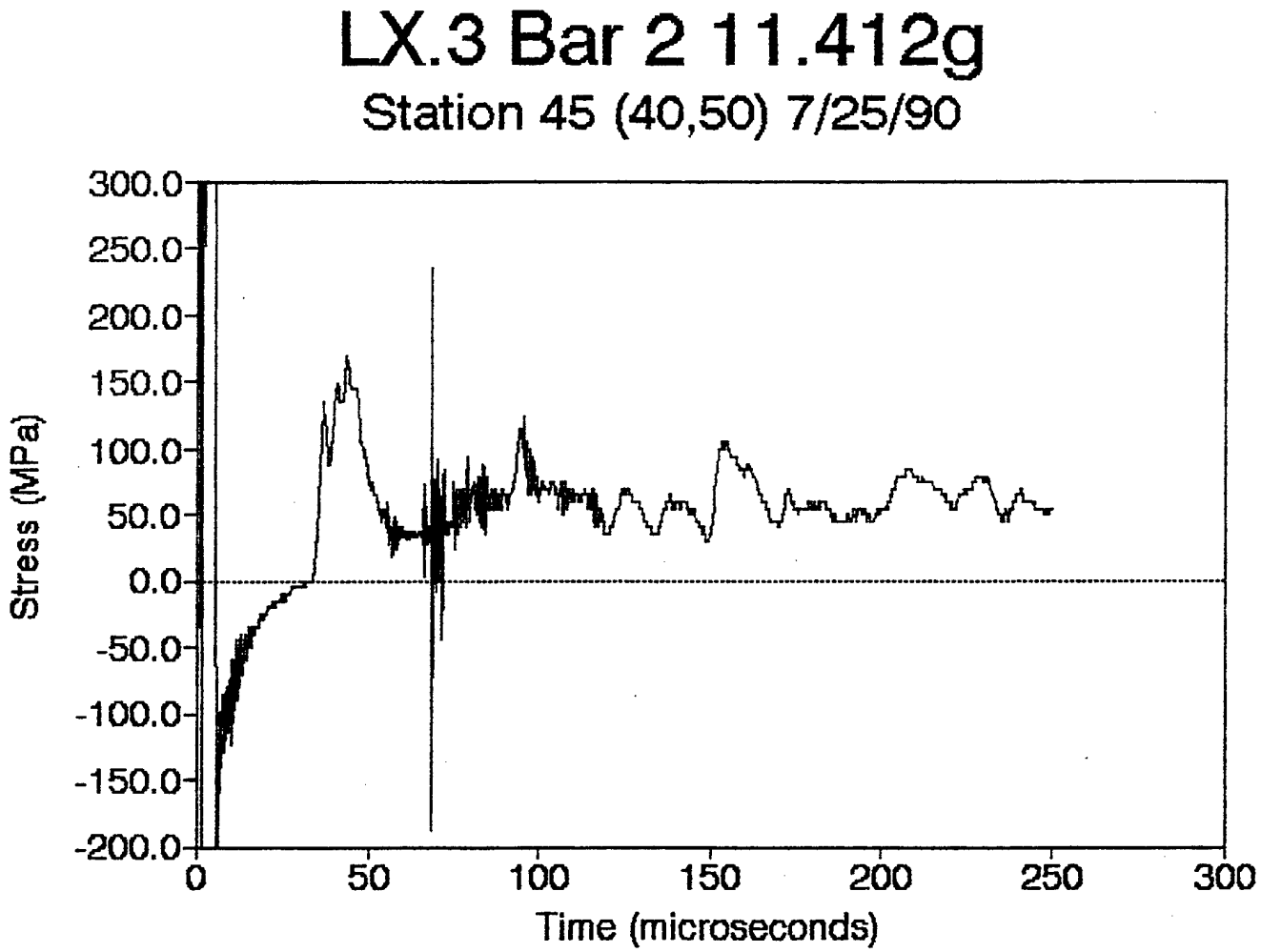
LX.3 Bar 2 11.412g
Station 45 (40,50) 7/25/90
300.0
250.0
200.0
150.0
100.0
50.0
0.0
-50.0
-100.0
-150.0
-200.0
Stress (MPa)
0
50
100
150
200
250
300
Time (microseconds)

LX.3 Bar 3 11.412g

Station 36 (40,40) 7/25/90

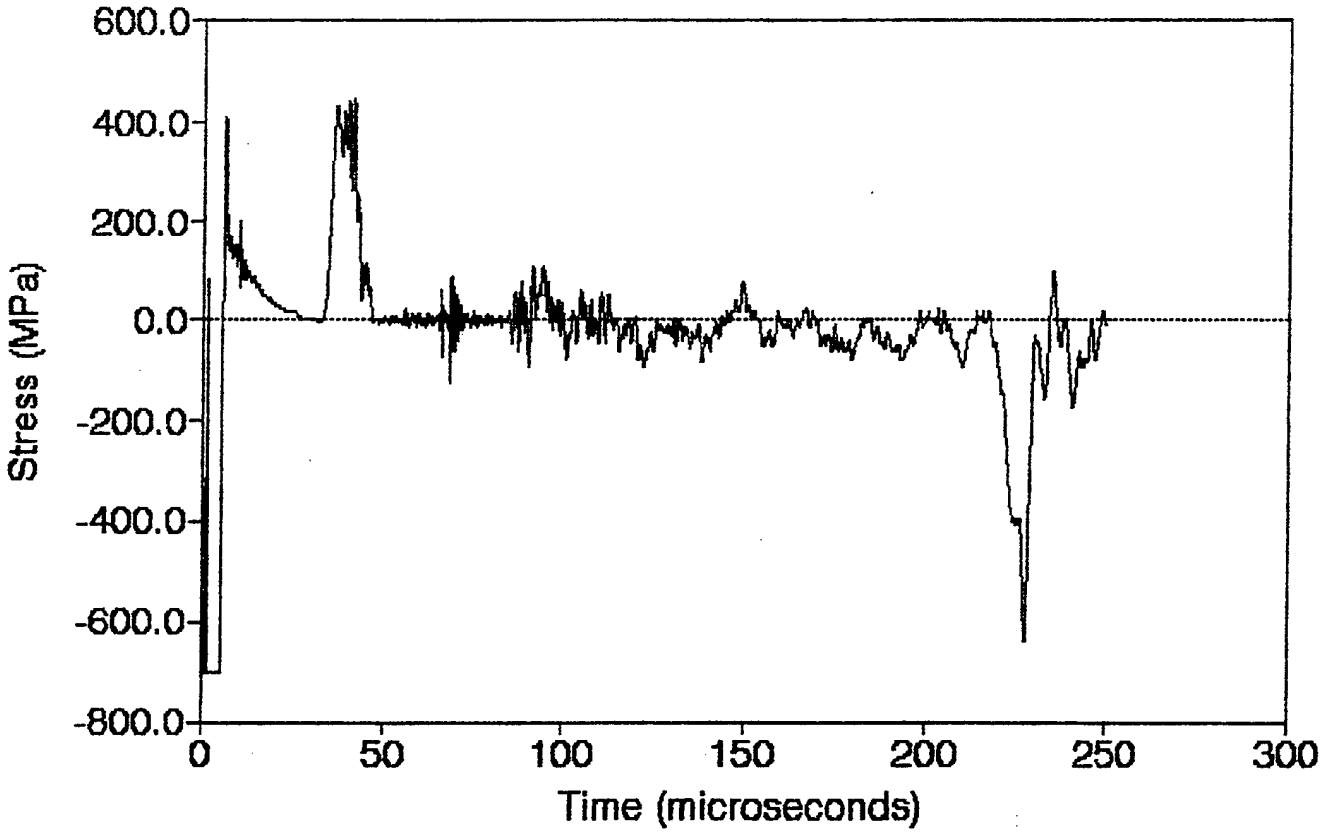

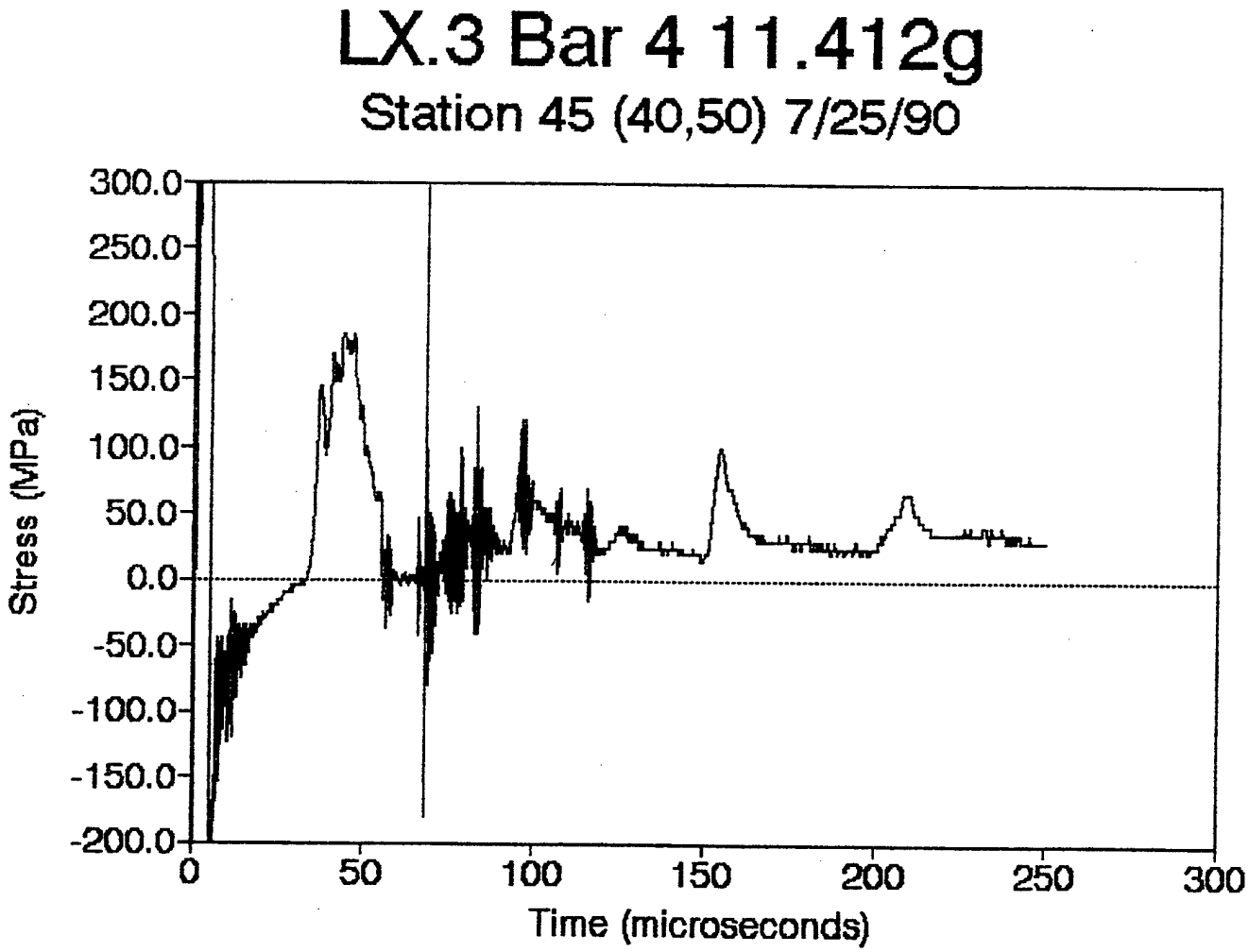
LX.3 Bar 4 11.412g
Station 45 (40,50) 7/25/90
300.0
250.0
200.0
150.0
100.0
50.0
0.0
-50.0
-100.0
-150.0
-200.0
Stress (MPa)
0
50
100
150
200
250
300
Time (microseconds)

LX.4 470 Ohm Resistor 11.392g

Station 36 (40,40) 7/25/90

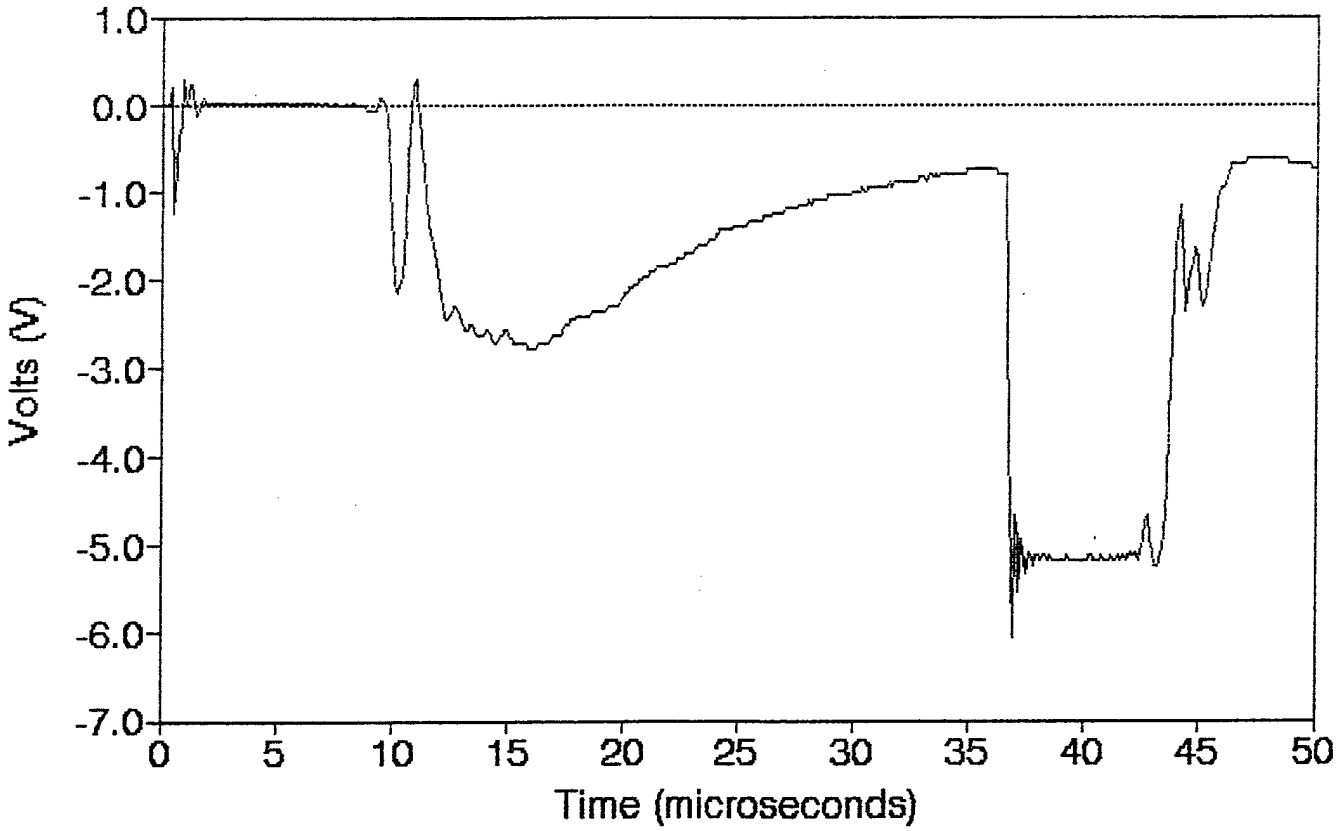

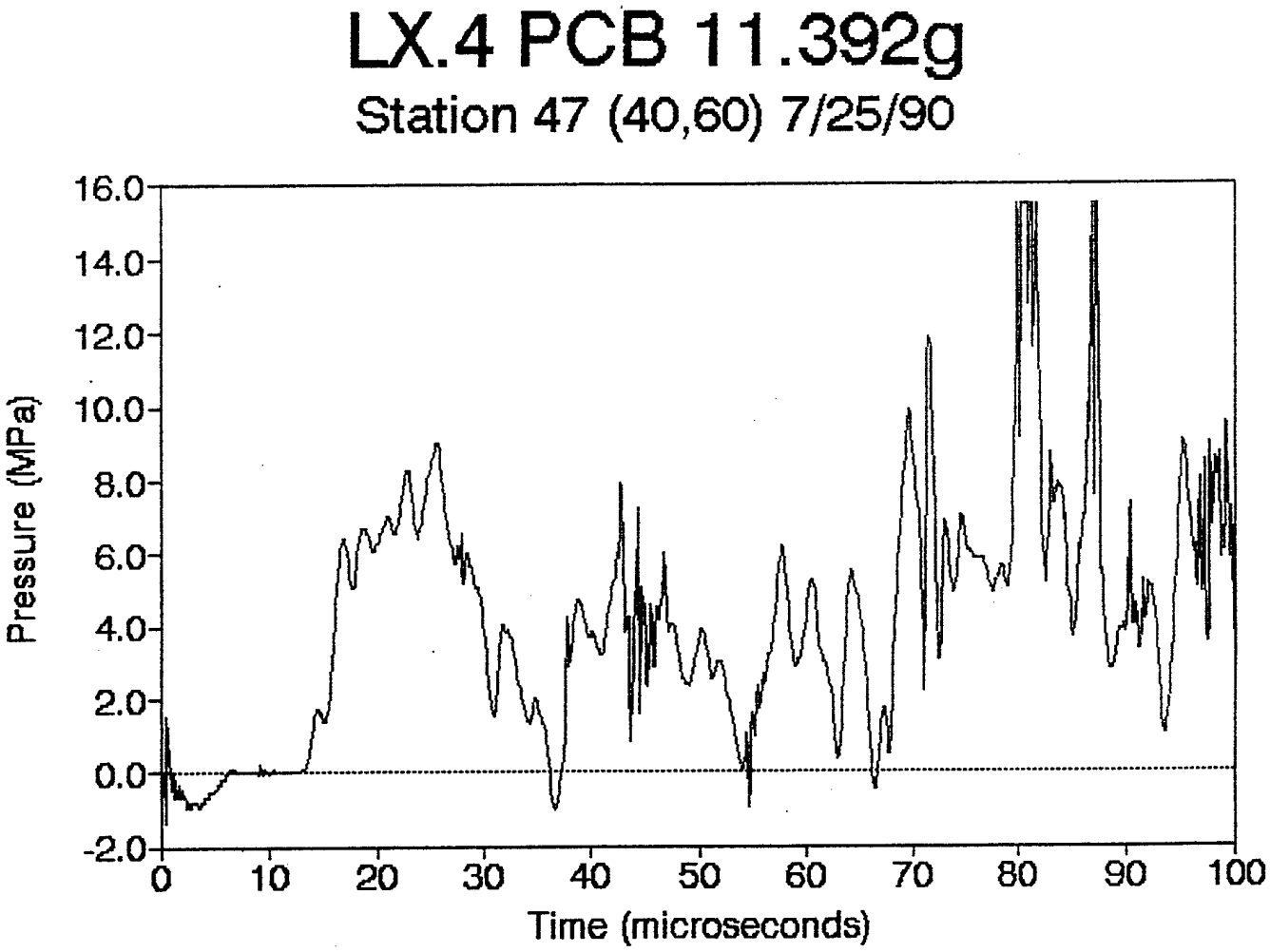
LX.4 PCB 11.392g
Station 47 (40,60) 7/25/90
Pressure (MPa)
16.0
14.0
12.0
10.0
8.0
6.0
4.0
2.0
0.0
-2.0
0
10
20
30
40
50
60
70
80
90
100
Time (microseconds)

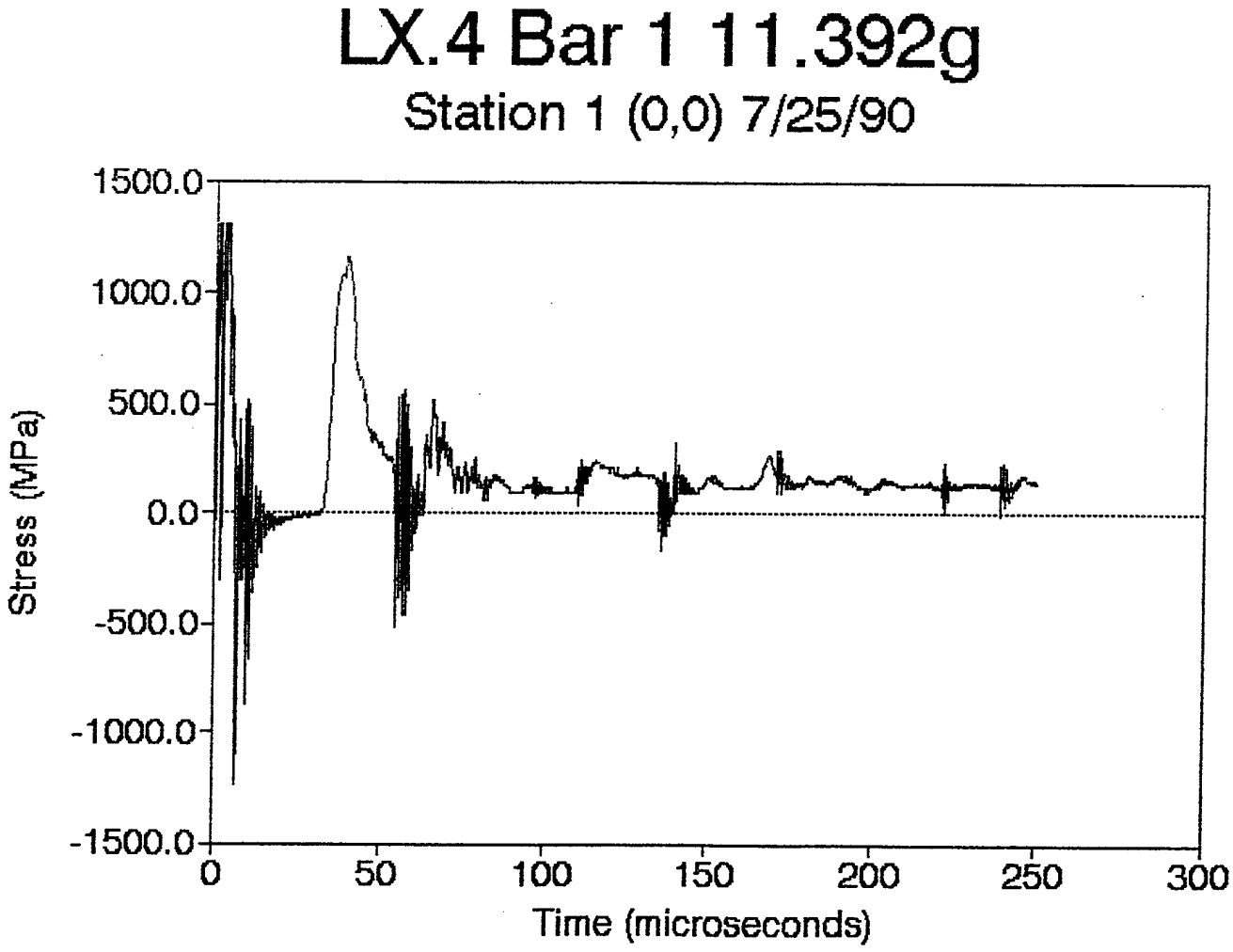
LX.4 Bar 1 11.392g
Station 1 (0,0) 7/25/90
1500.0
1000.0
500.0
0.0
-500.0
-1000.0
-1500.0
Stress (MPa)
0
50
100
150
200
250
300
Time (microseconds)

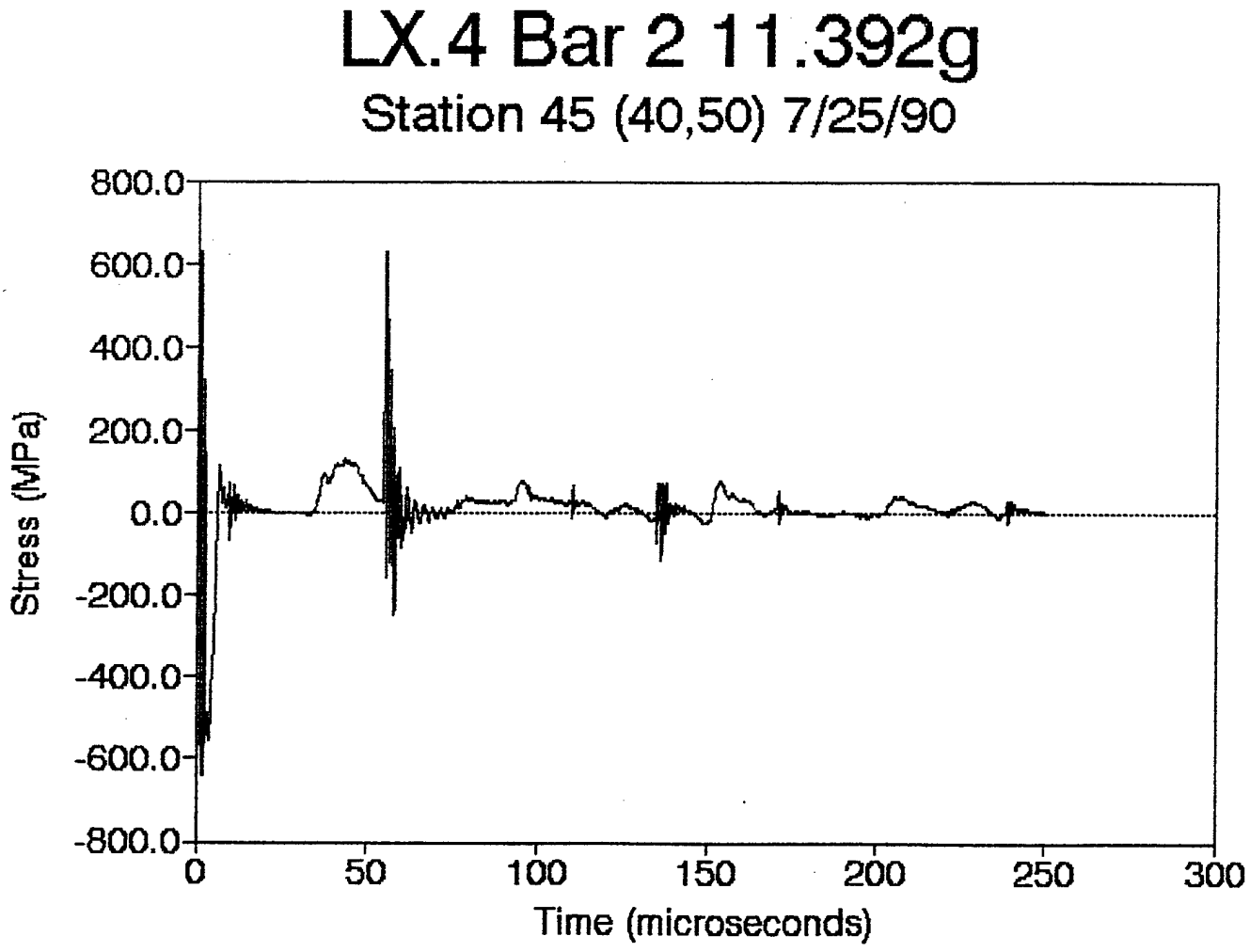
LX.4 Bar 2 11.392g
Station 45 (40,50) 7/25/90
800.0
600.0
400.0
200.0
0.0
-200.0
-400.0
-600.0
-800.0
Stress (MPa)
0
50
100
150
200
250
300
Time (microseconds)

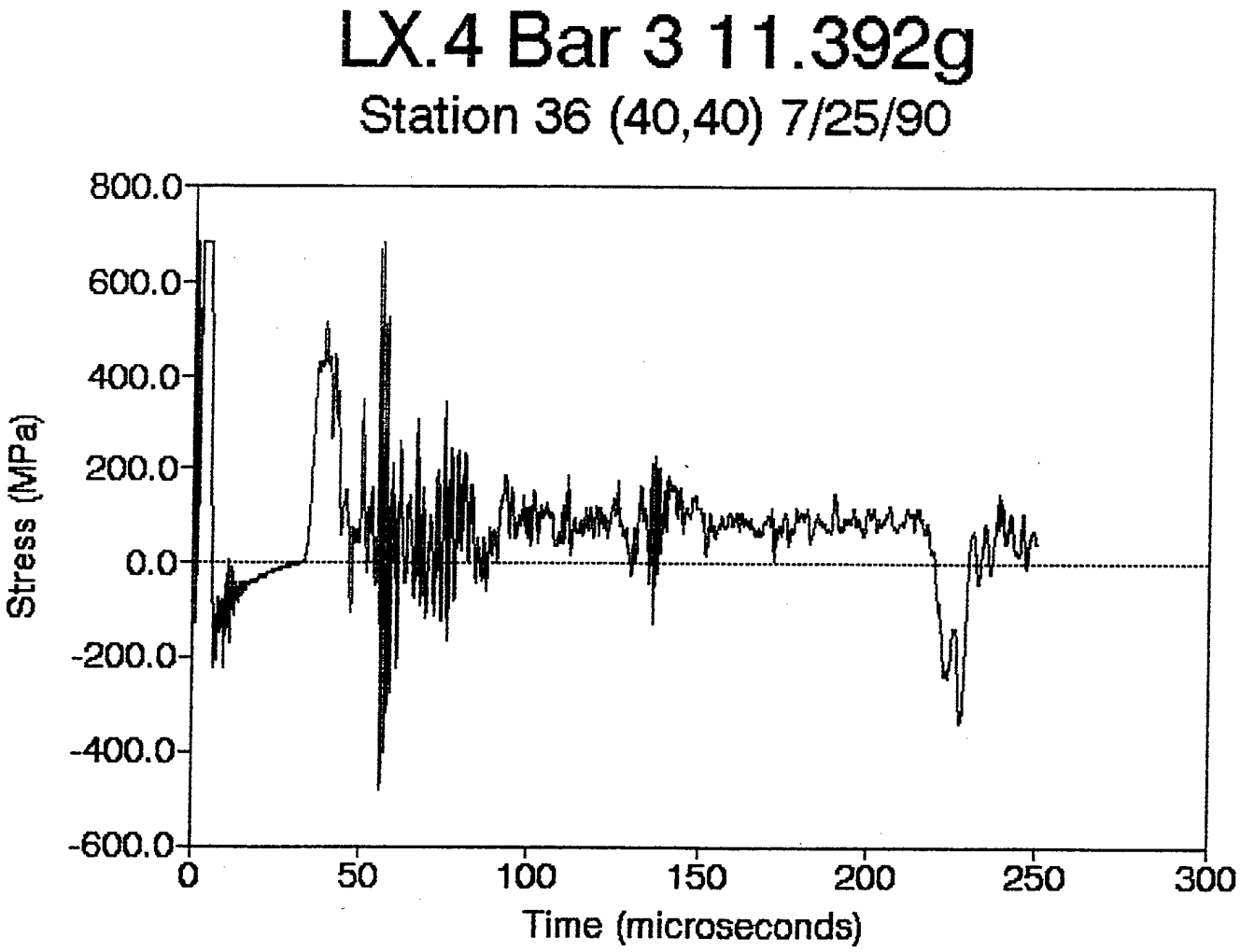
LX.4 Bar 3 11.392g
Station 36 (40,40) 7/25/90
800.0
600.0
400.0
200.0
0.0
-200.0
-400.0
-600.0
Stress (MPa)
0
50
100
150
200
250
300
Time (microseconds)

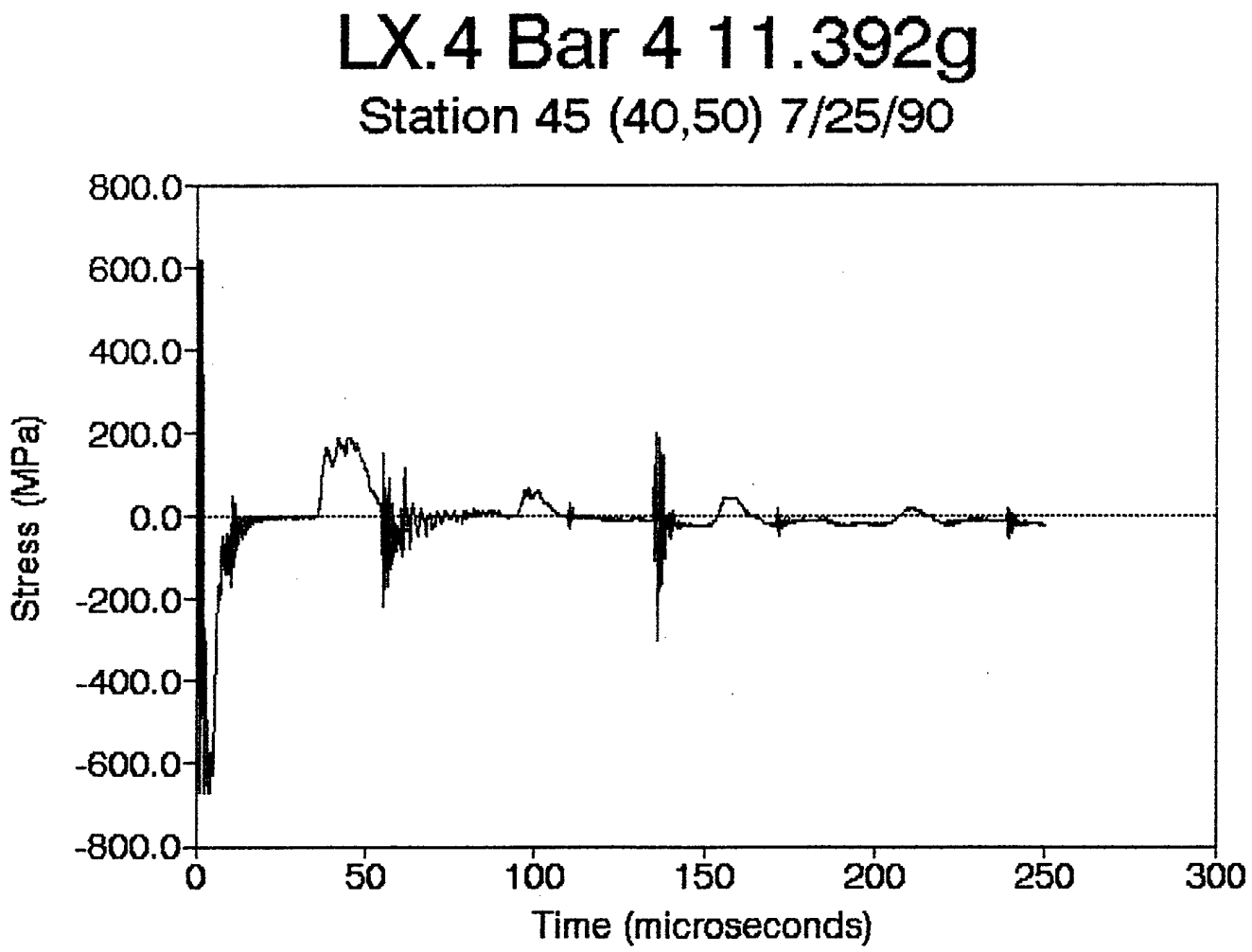
LX.4 Bar 4 11.392g
Station 45 (40,50) 7/25/90
800.0
600.0
400.0
200.0
0.0
-200.0
-400.0
-600.0
-800.0
Stress (MPa)
0
50
100
150
200
250
300
Time (microseconds)

LX.5 470 Ohm Resistor 11.304g

Station 36 (40,40) 9/4/90

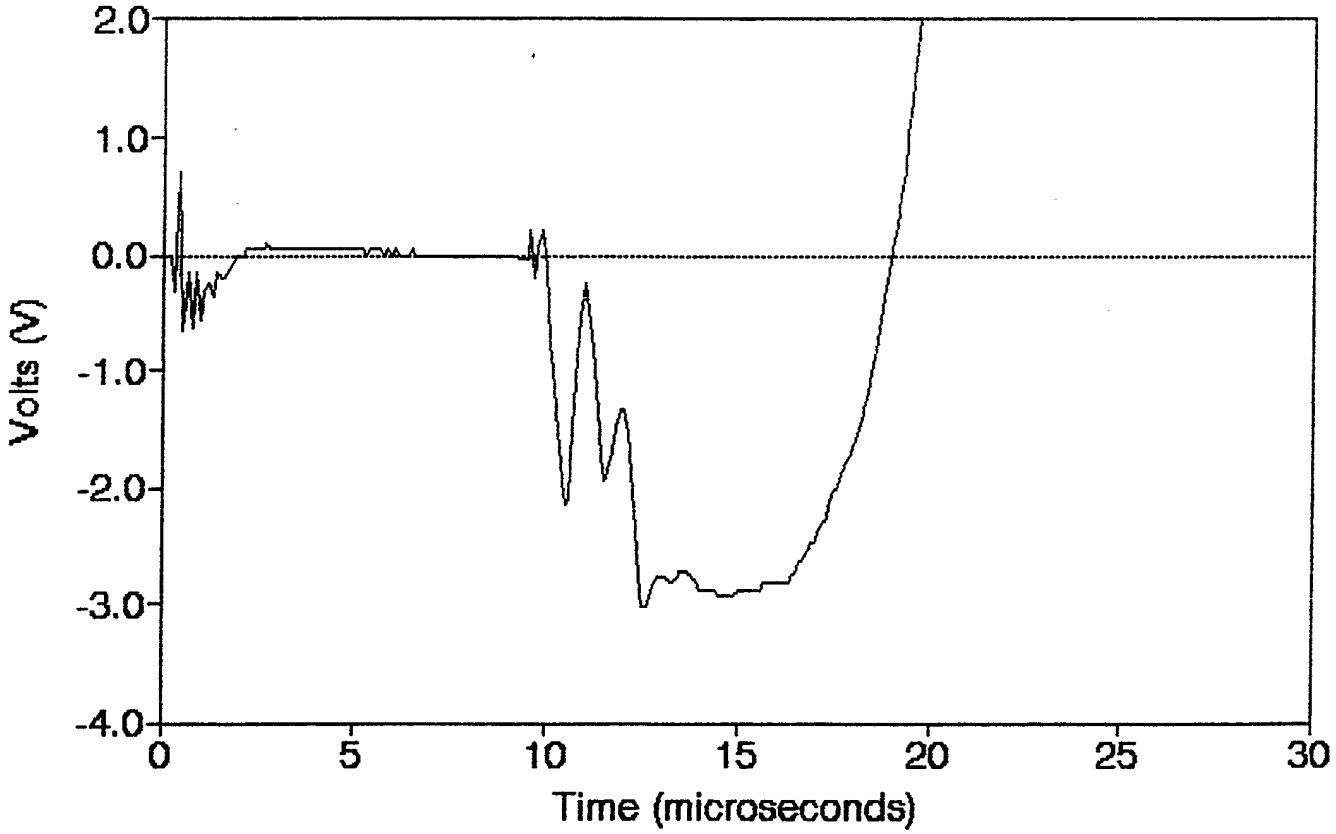

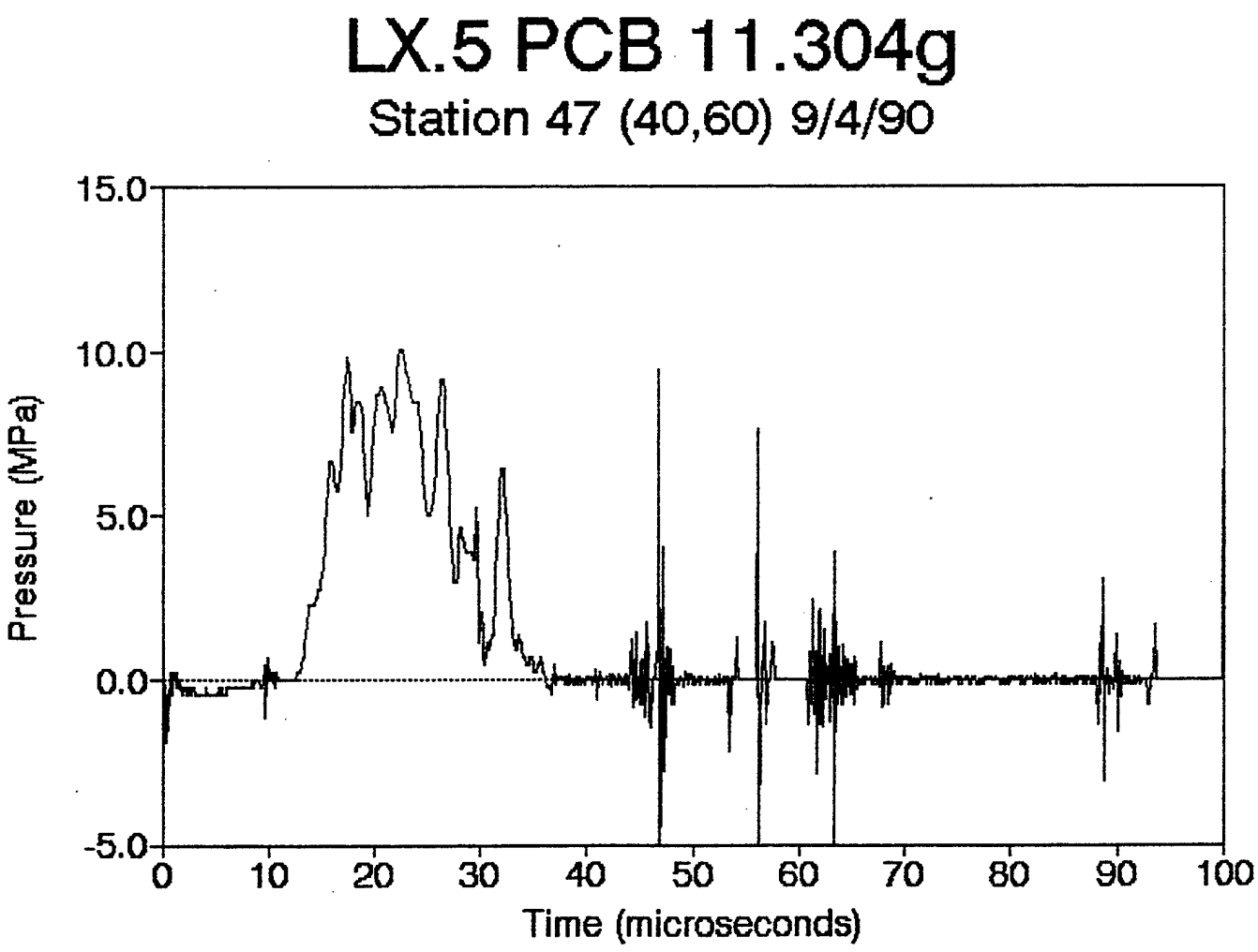
LX.5 PCB 11.304g
Station 47 (40,60) 9/4/90
15.0
10.0
5.0
0.0
-5.0
Pressure (MPa)
0
10
20
30
40
50
60
70
80
90
100
Time (microseconds)

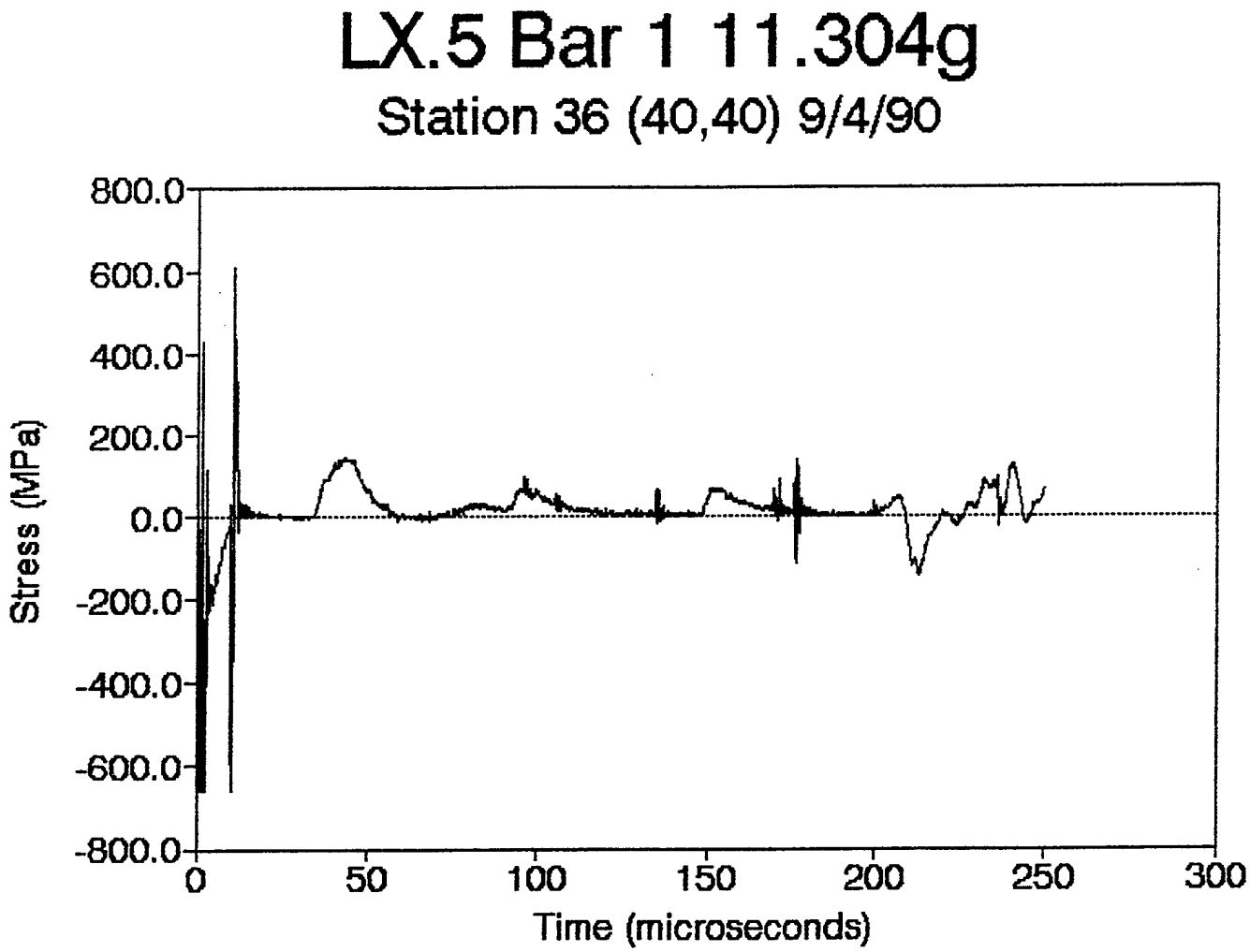
LX.5 Bar 1 11.304g
Station 36 (40,40) 9/4/90
800.0
600.0
400.0
200.0
0.0
-200.0
-400.0
-600.0
-800.0
Stress (MPa)
0
50
100
150
200
250
300
Time (microseconds)

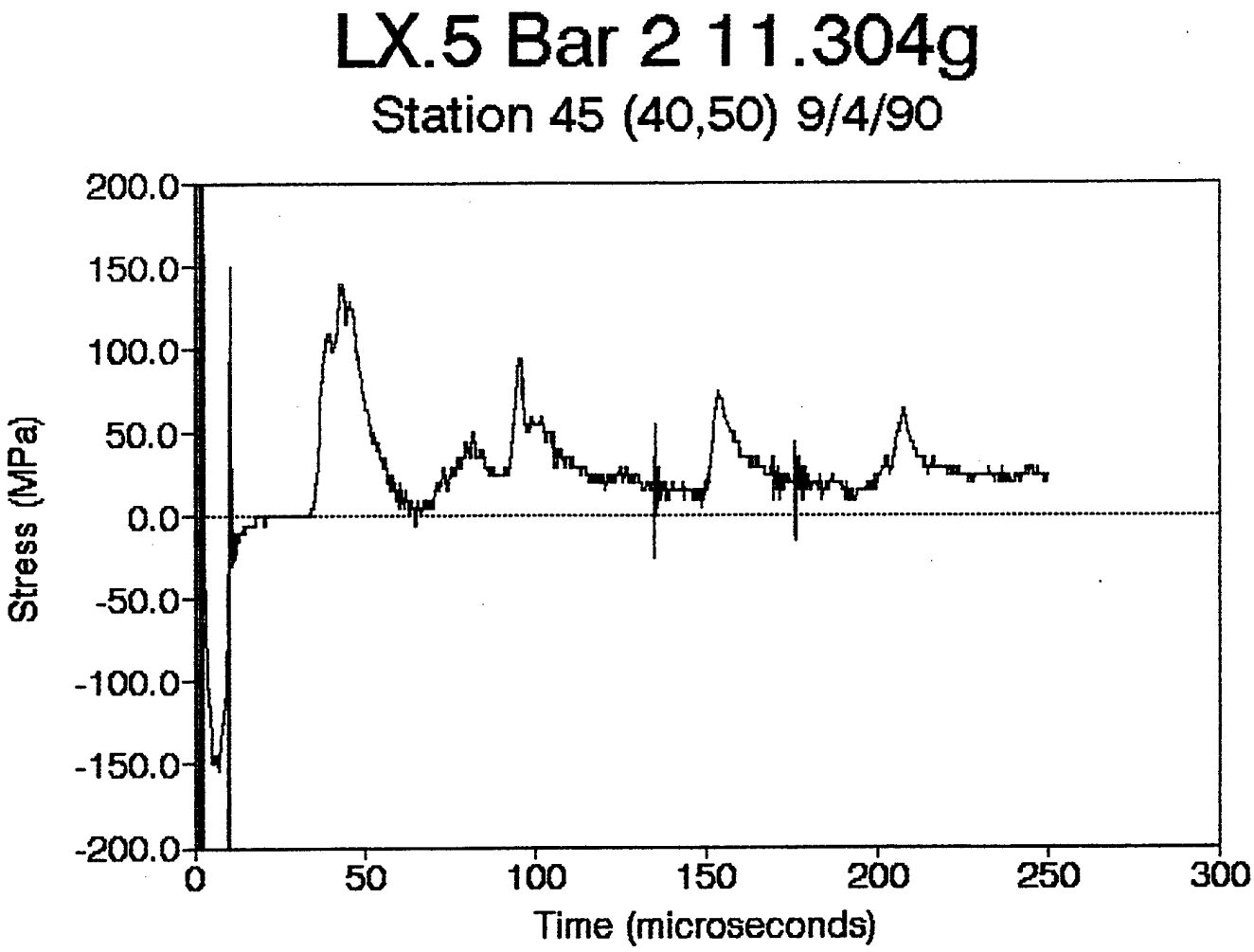
LX.5 Bar 2 11.304g
Station 45 (40,50) 9/4/90
200.0
150.0
100.0
50.0
0.0
-50.0
-100.0
-150.0
-200.0
Stress (MPa)
0
50
100
150
200
250
300
Time (microseconds)

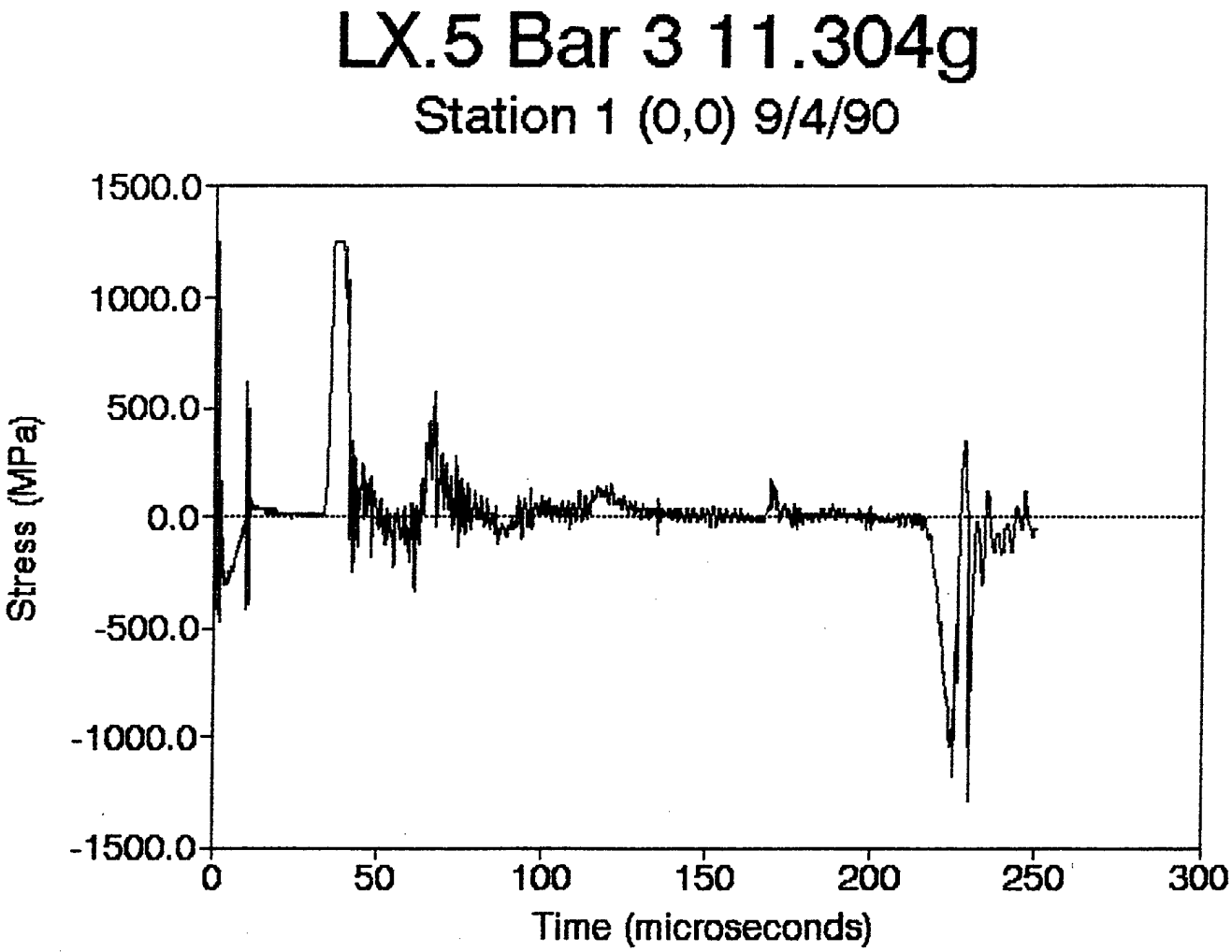
LX.5 Bar 3 11.304g
Station 1 (0,0) 9/4/90
1500.0
1000.0
500.0
0.0
-500.0
-1000.0
-1500.0
Stress (MPa)
0
50
100
150
200
250
300
Time (microseconds)

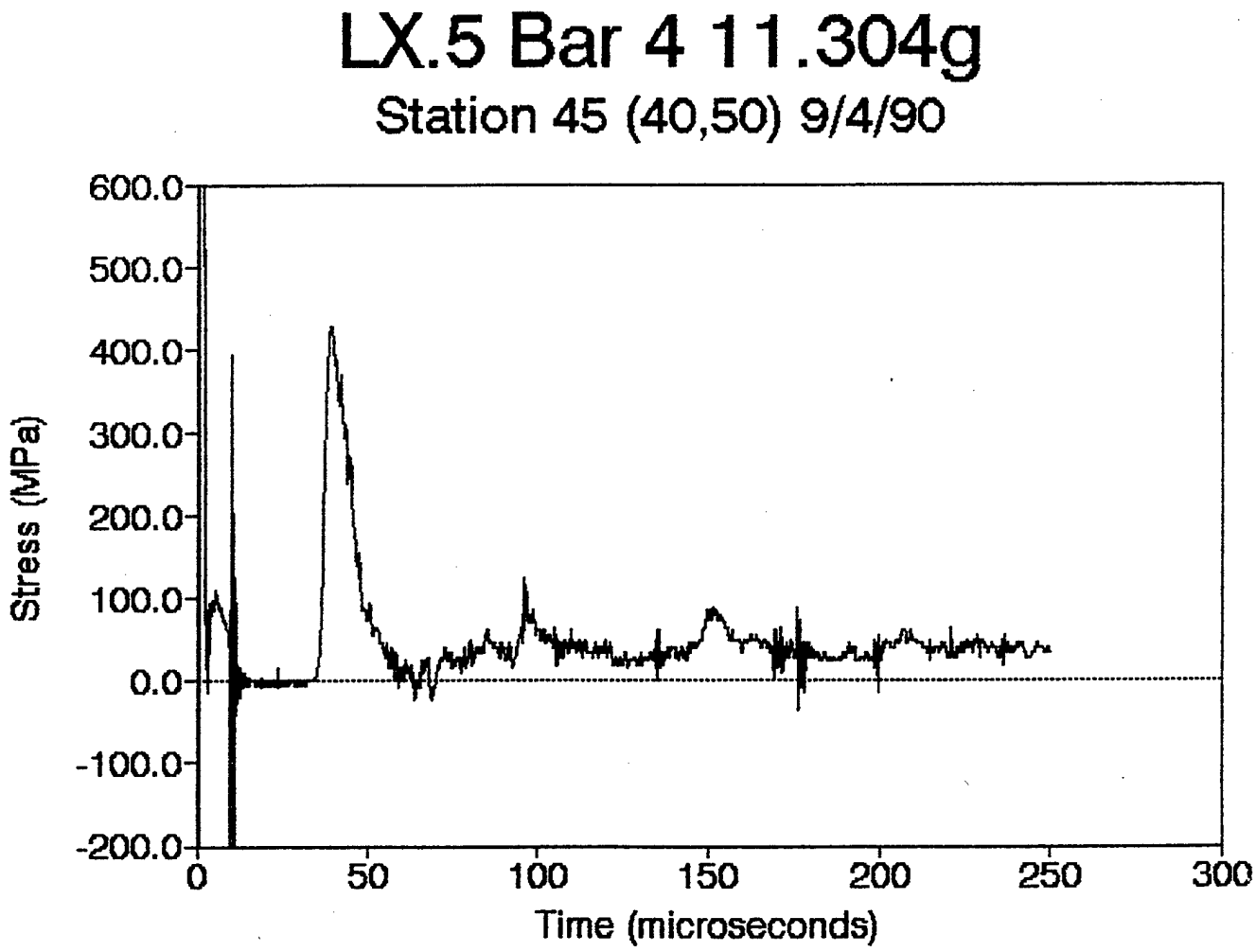
LX.5 Bar 4 11.304g
Station 45 (40,50) 9/4/90
600.0
500.0
400.0
300.0
200.0
100.0
0.0
-100.0
-200.0
Stress (MPa)
0
50
100
150
200
250
300
Time (microseconds)

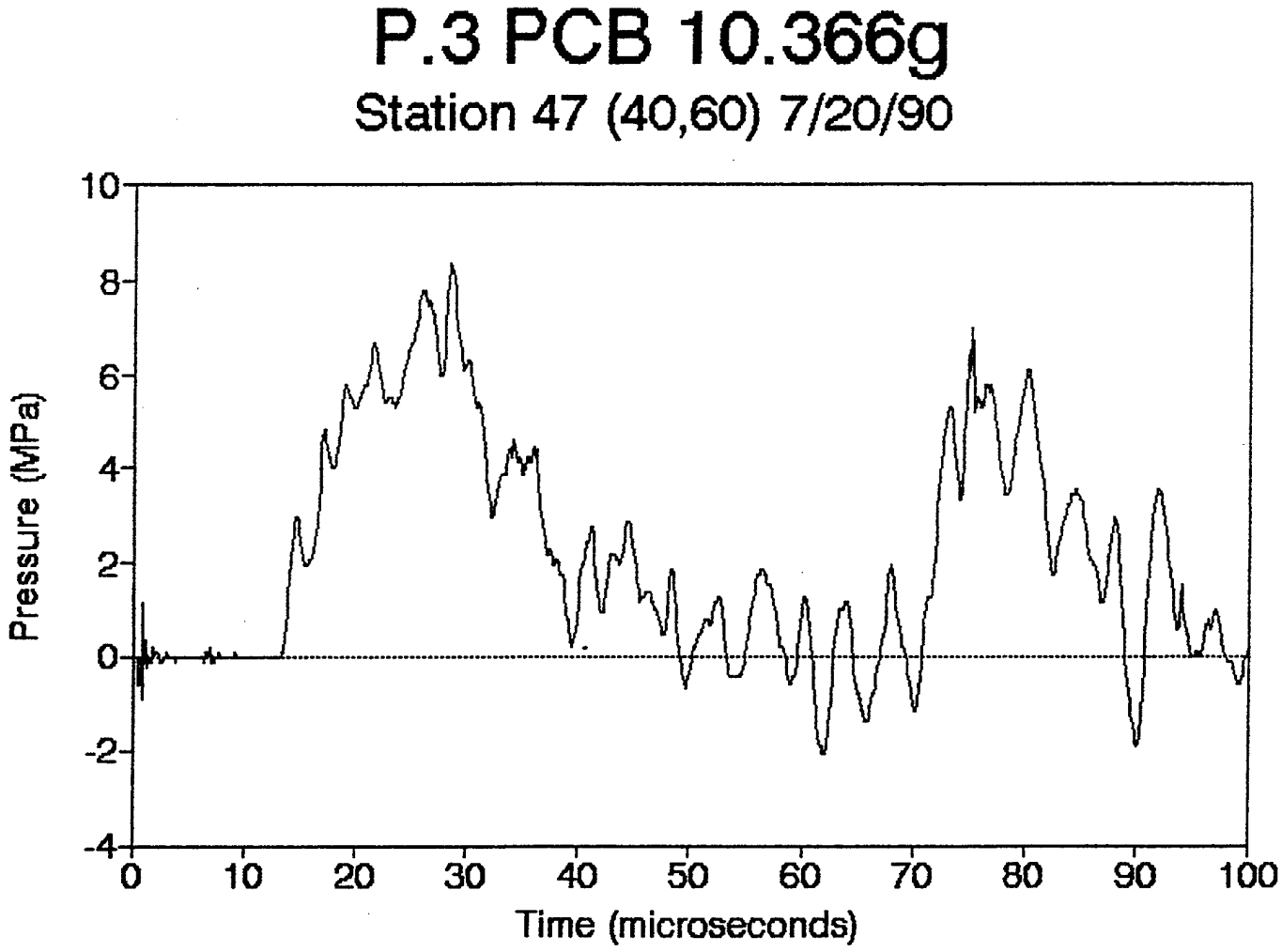
P.3 PCB 10.366g
Station 47 (40,60) 7/20/90
Pressure (MPa)
10
8
6
4
2
0
-2
-4
0
10
20
30
40
50
60
70
80
90
100
Time (microseconds)

P.3 470 Ohm Resistor 10.366g

Station 36 (40,40) 7/20/90

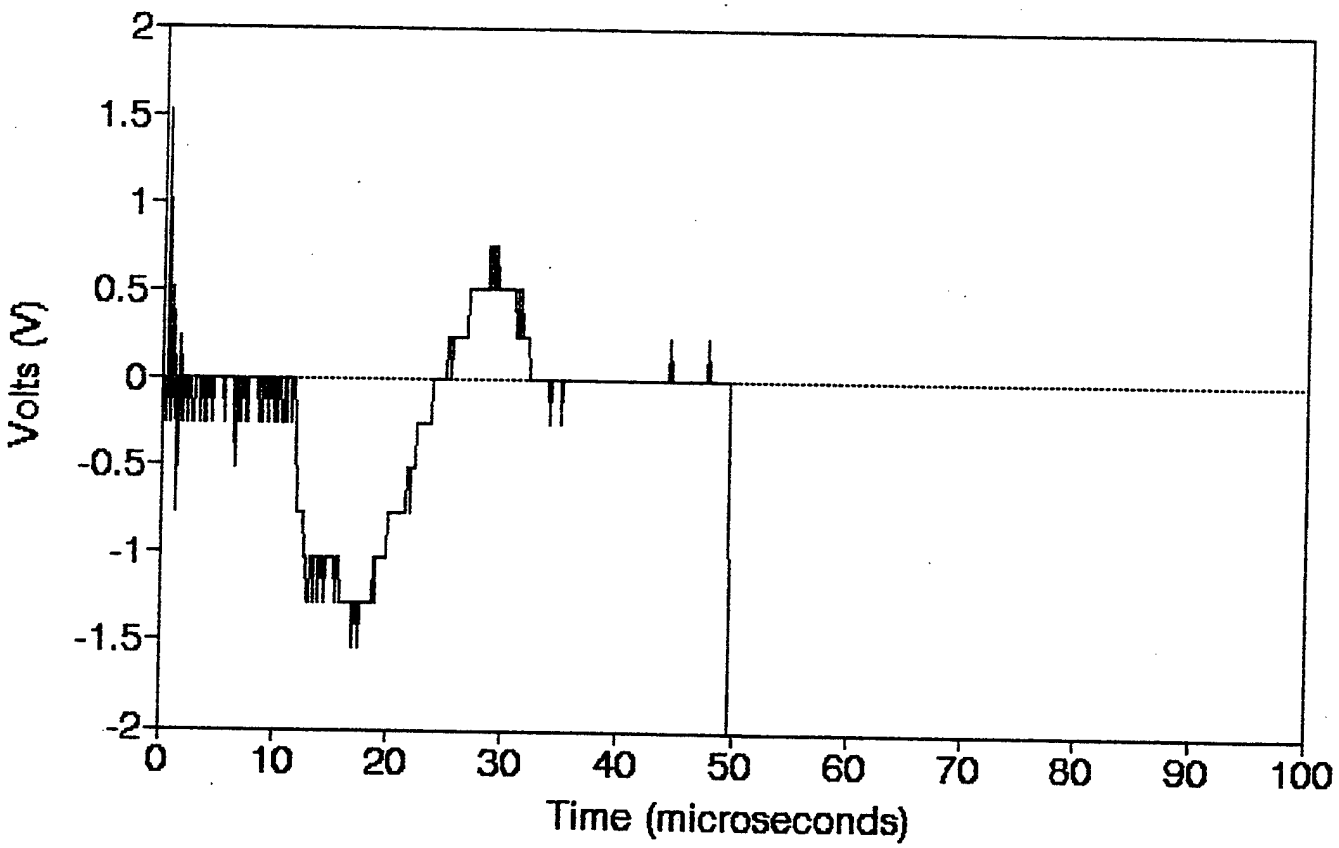

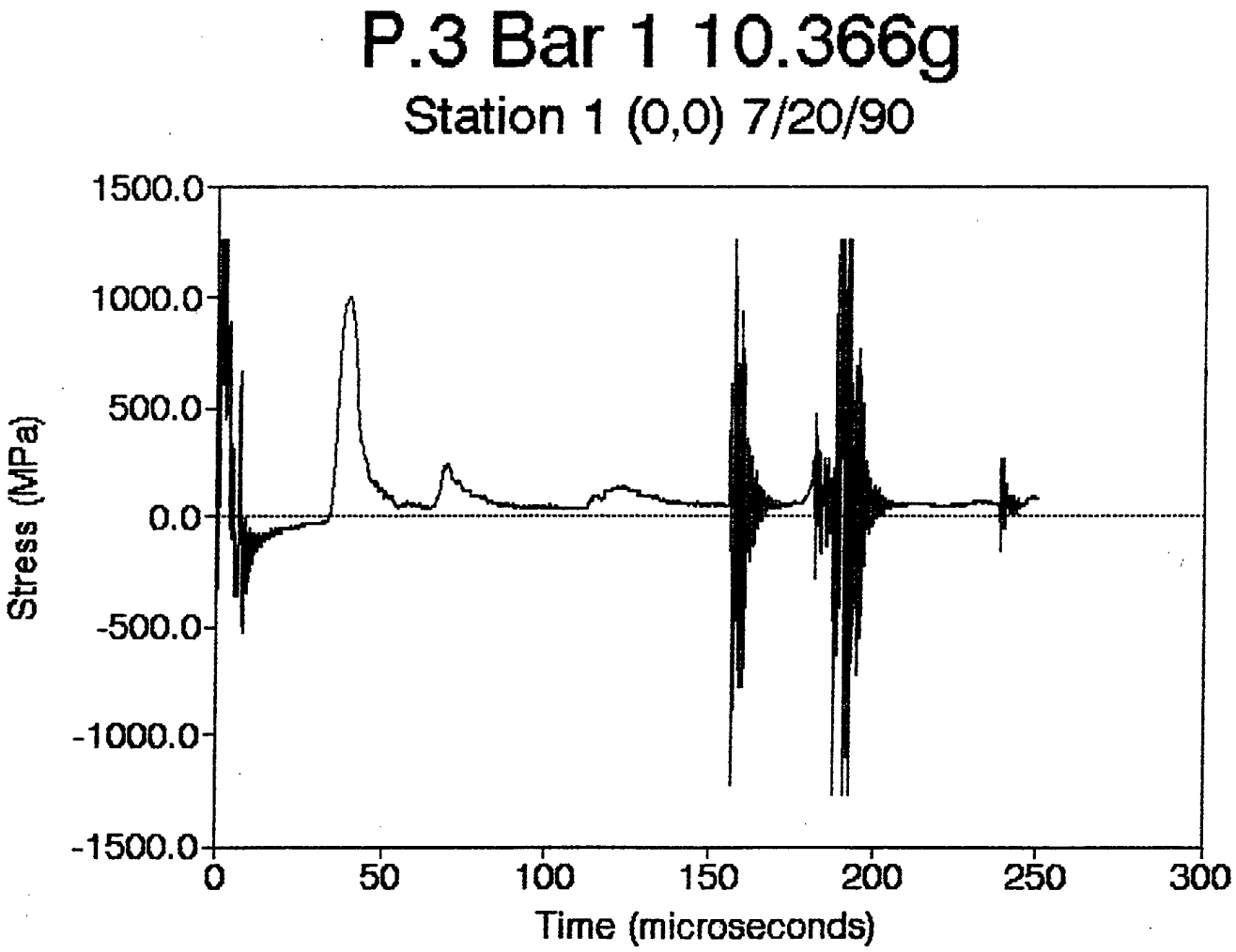
P.3 Bar 1 10.366g
Station 1 (0,0) 7/20/90
1500.0
1000.0
500.0
0.0
-500.0
-1000.0
-1500.0
Stress (MPa)
0
50
100
150
200
250
300
Time (microseconds)

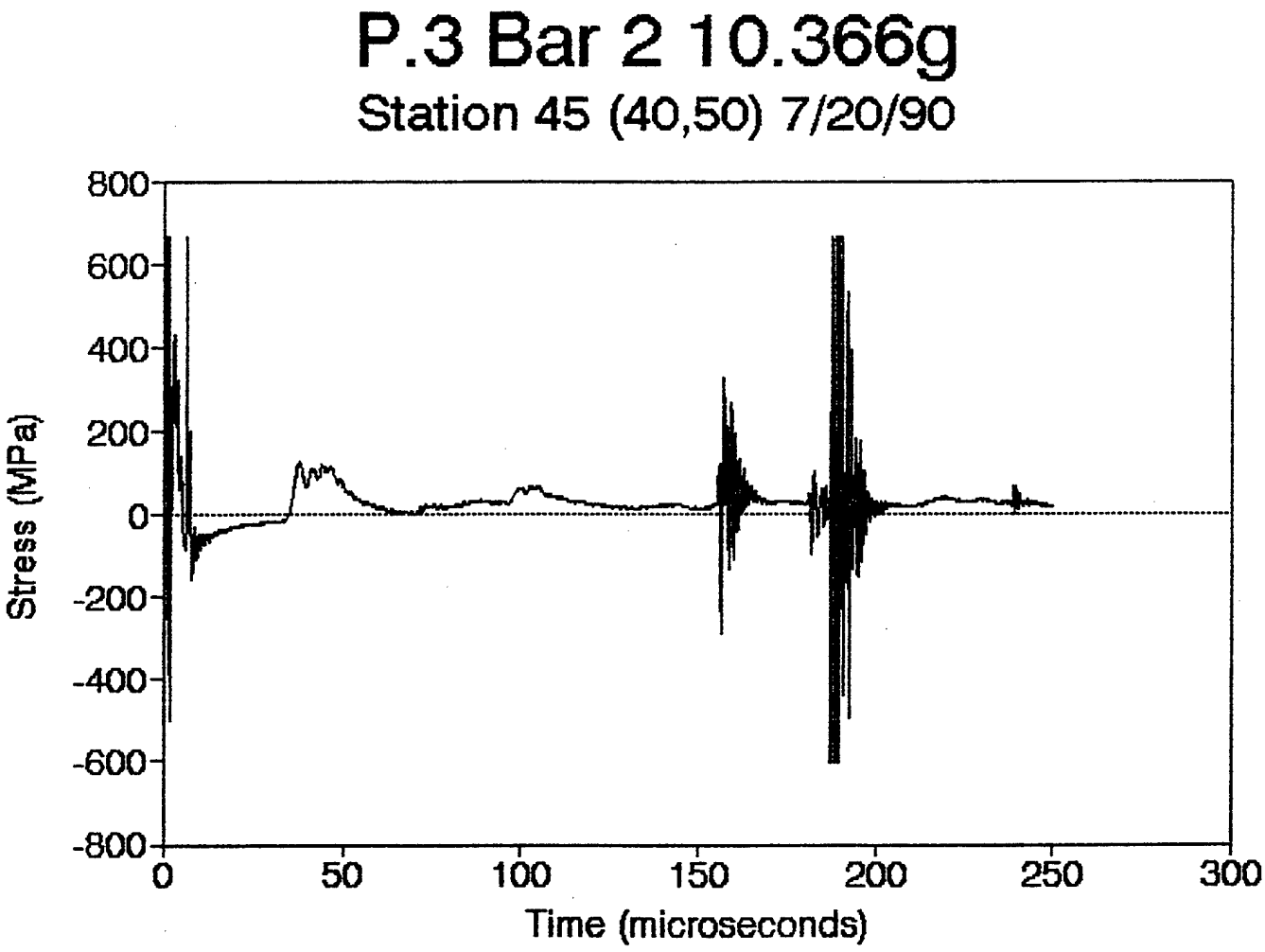
P.3 Bar 2 10.366g
Station 45 (40,50) 7/20/90
800
600
400
200
0
-200
-400
-600
-800
Stress (MPa)
0
50
100
150
200
250
300
Time (microseconds)

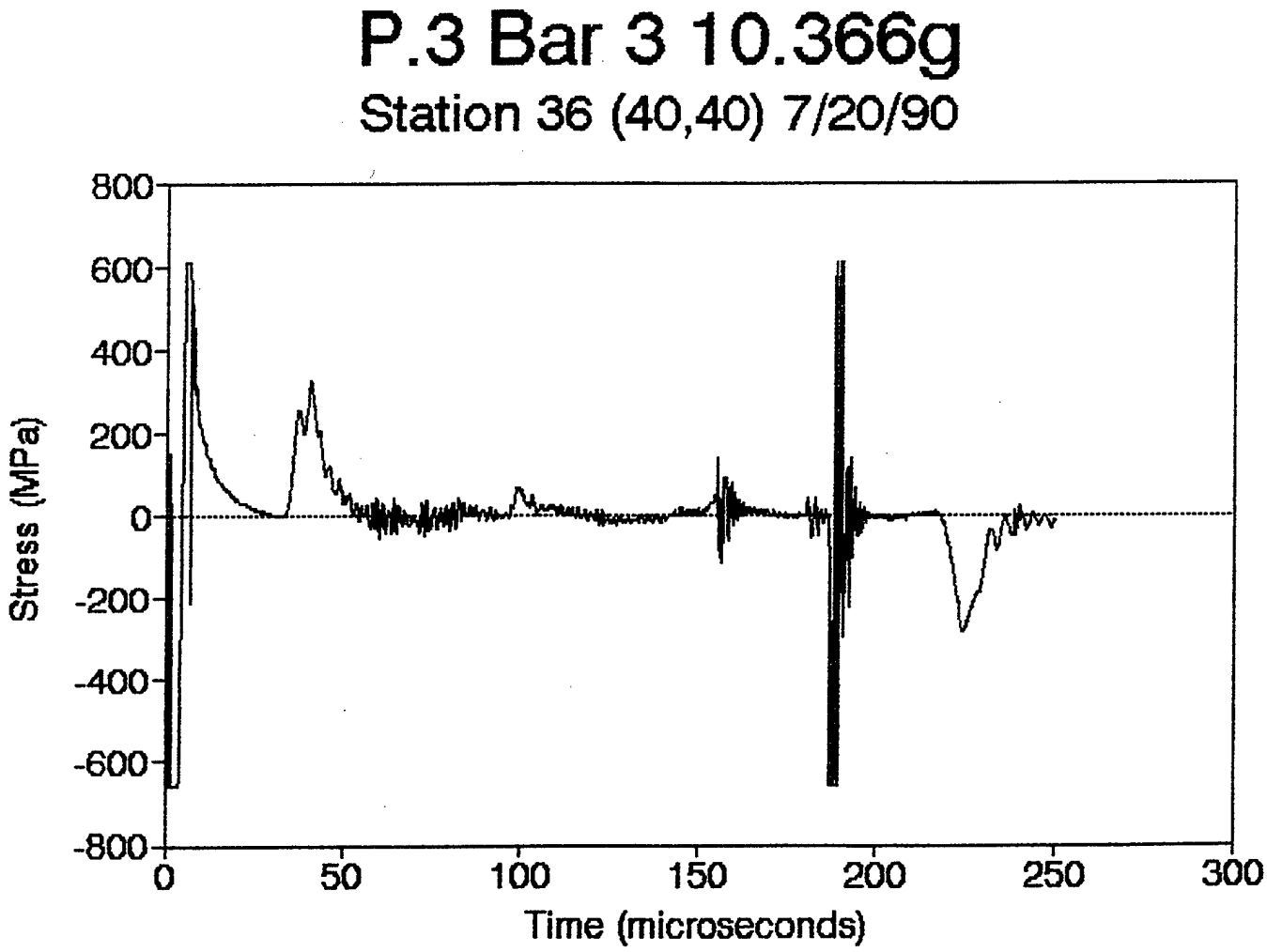
P.3 Bar 3 10.366g
Station 36 (40,40) 7/20/90
800
600
400
200
0
-200
-400
-600
-800
Stress (MPa)
0
50
100
150
200
250
300
Time (microseconds)

P.4 470 Ohm Resistor 10.402g

Station 36 (40,40) 7/23/90

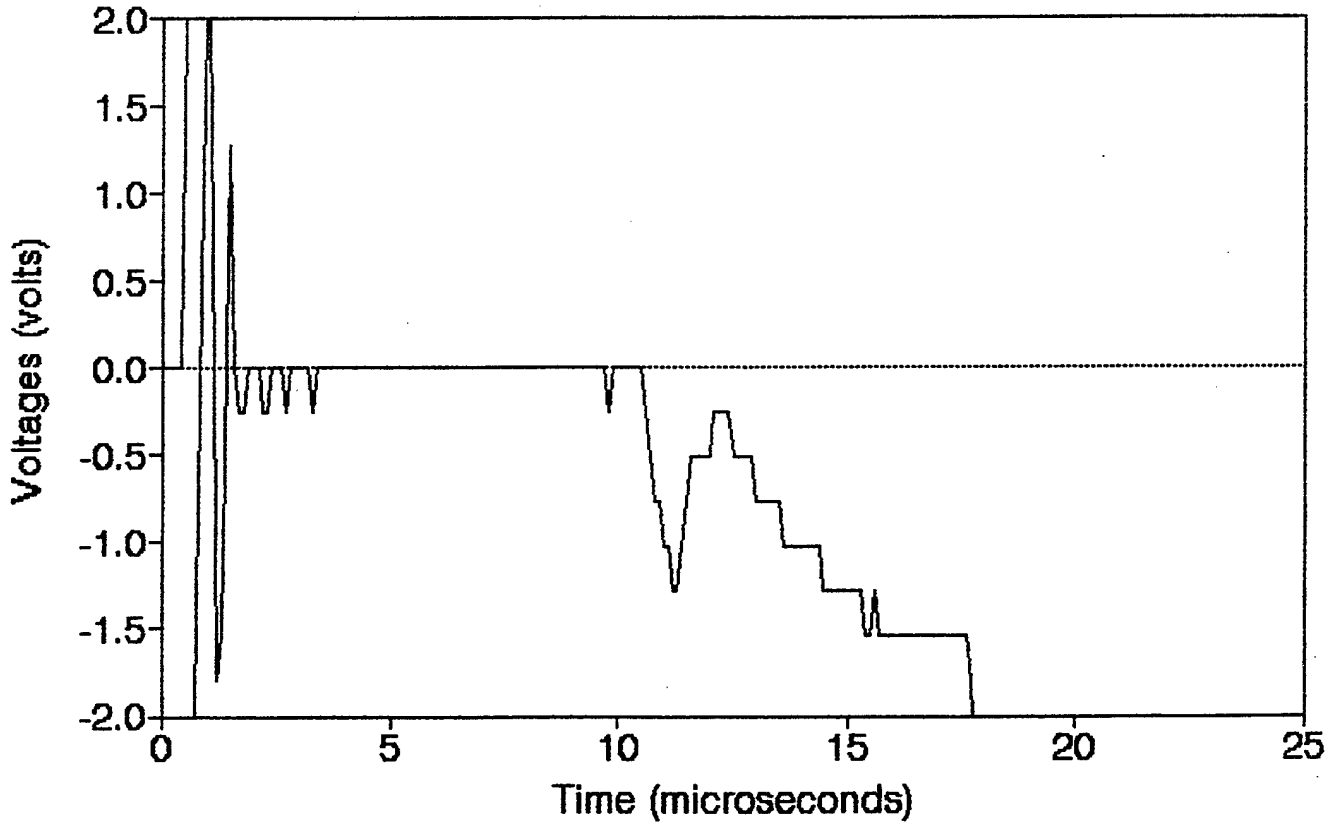

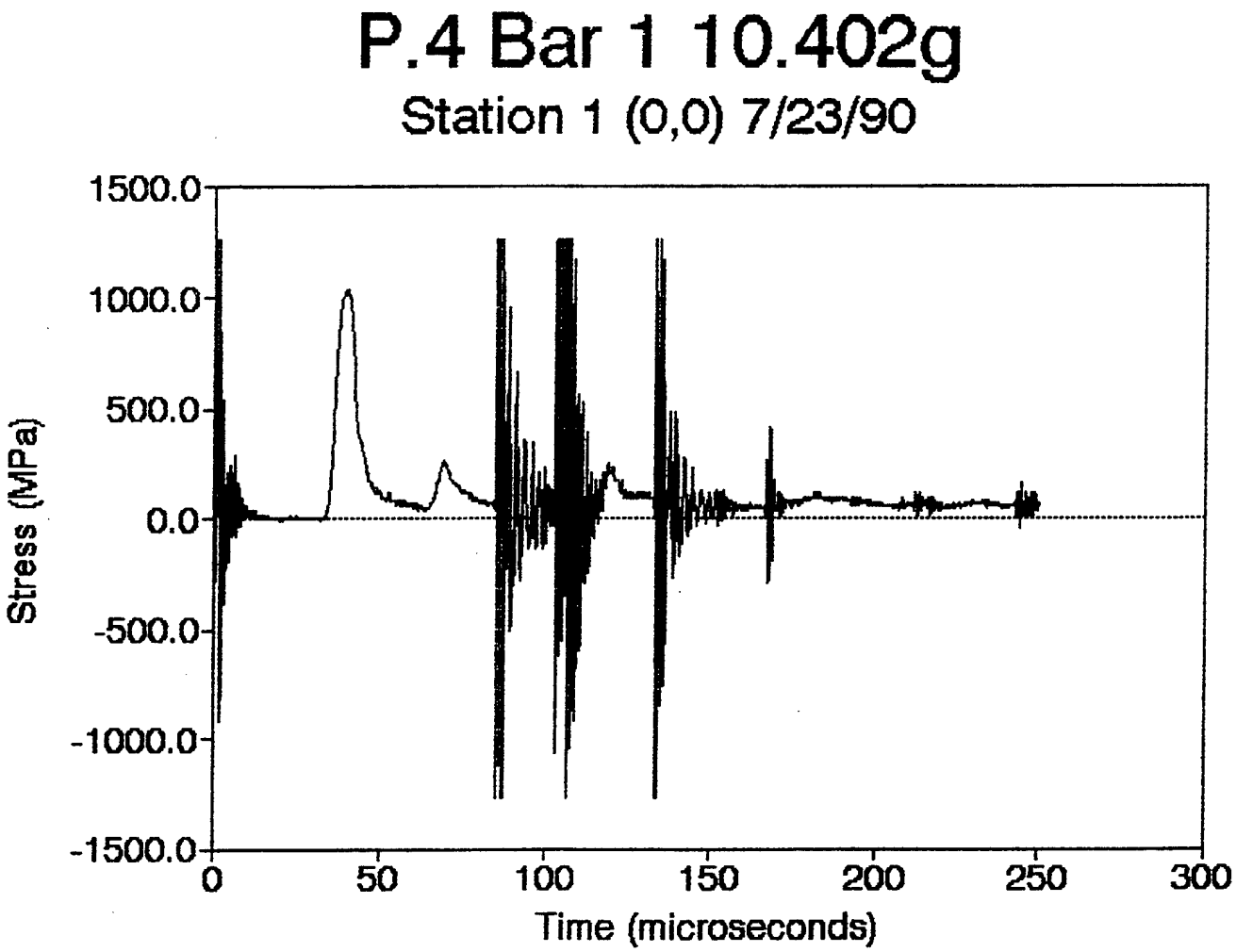
P.4 Bar 1 10.402g
Station 1 (0,0) 7/23/90
1500.0
1000.0
500.0
0.0
-500.0
-1000.0
-1500.0
Stress (MPa)
0
50
100
150
200
250
300
Time (microseconds)

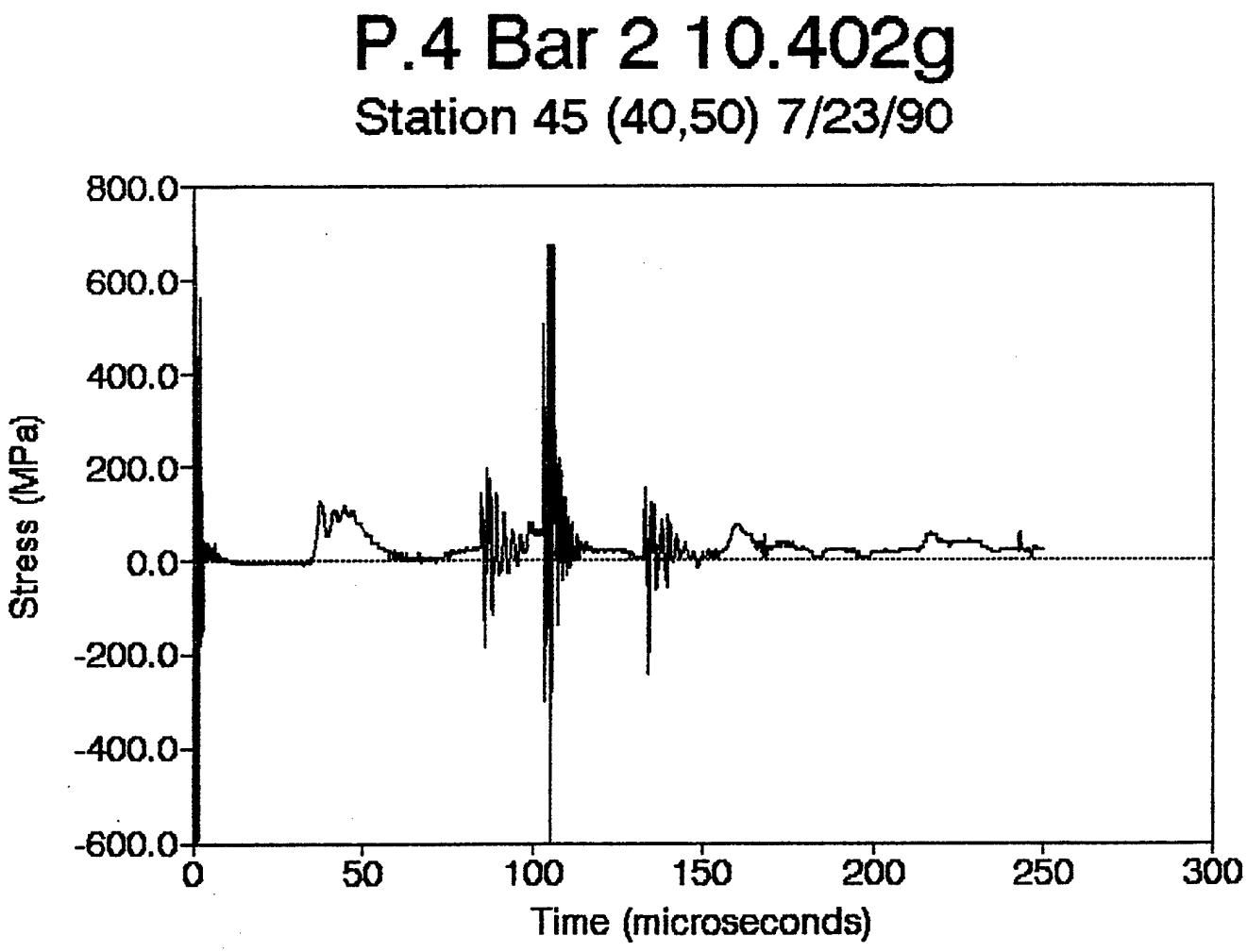
P.4 Bar 2 10.402g
Station 45 (40,50) 7/23/90
800.0
600.0
400.0
200.0
0.0
-200.0
-400.0
-600.0
Stress (MPa)
0
50
100
150
200
250
300
Time (microseconds)

P.4 Bar 3 10.402g

Station 36 (40,40) 7/23/90

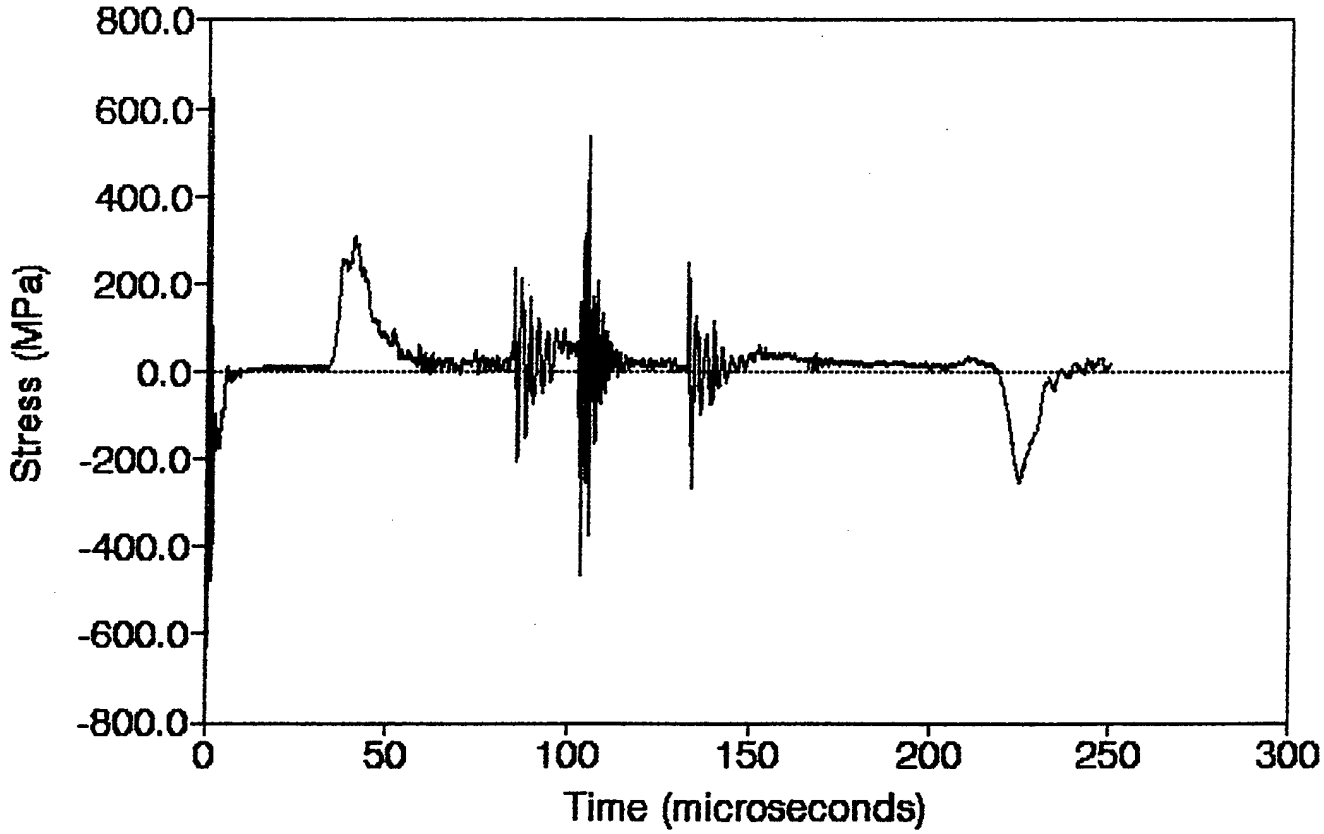

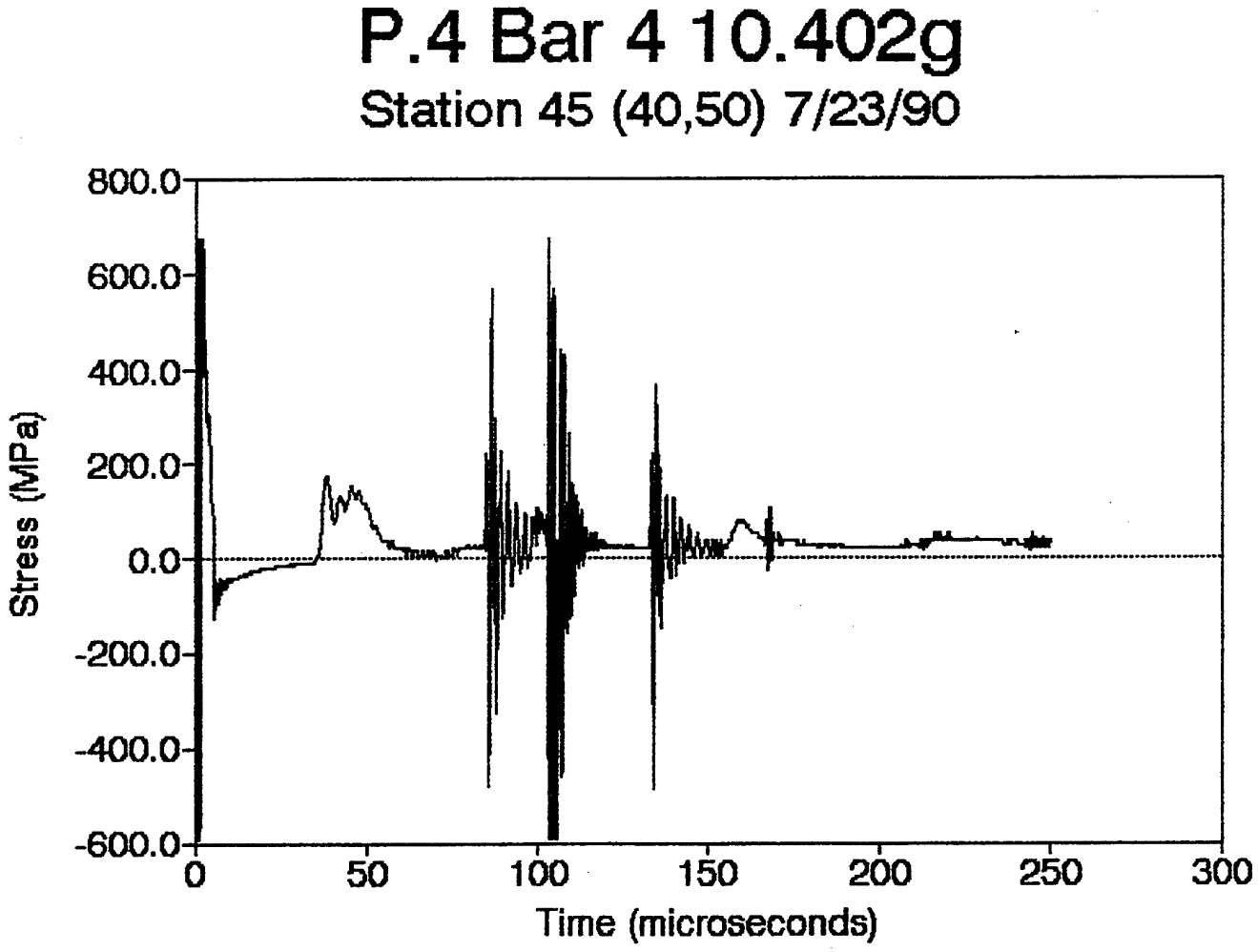
P.4 Bar 4 10.402g
Station 45 (40,50) 7/23/90
800.0
600.0
400.0
200.0
0.0
-200.0
-400.0
-600.0
Stress (MPa)
0
50
100
150
200
250
300
Time (microseconds)

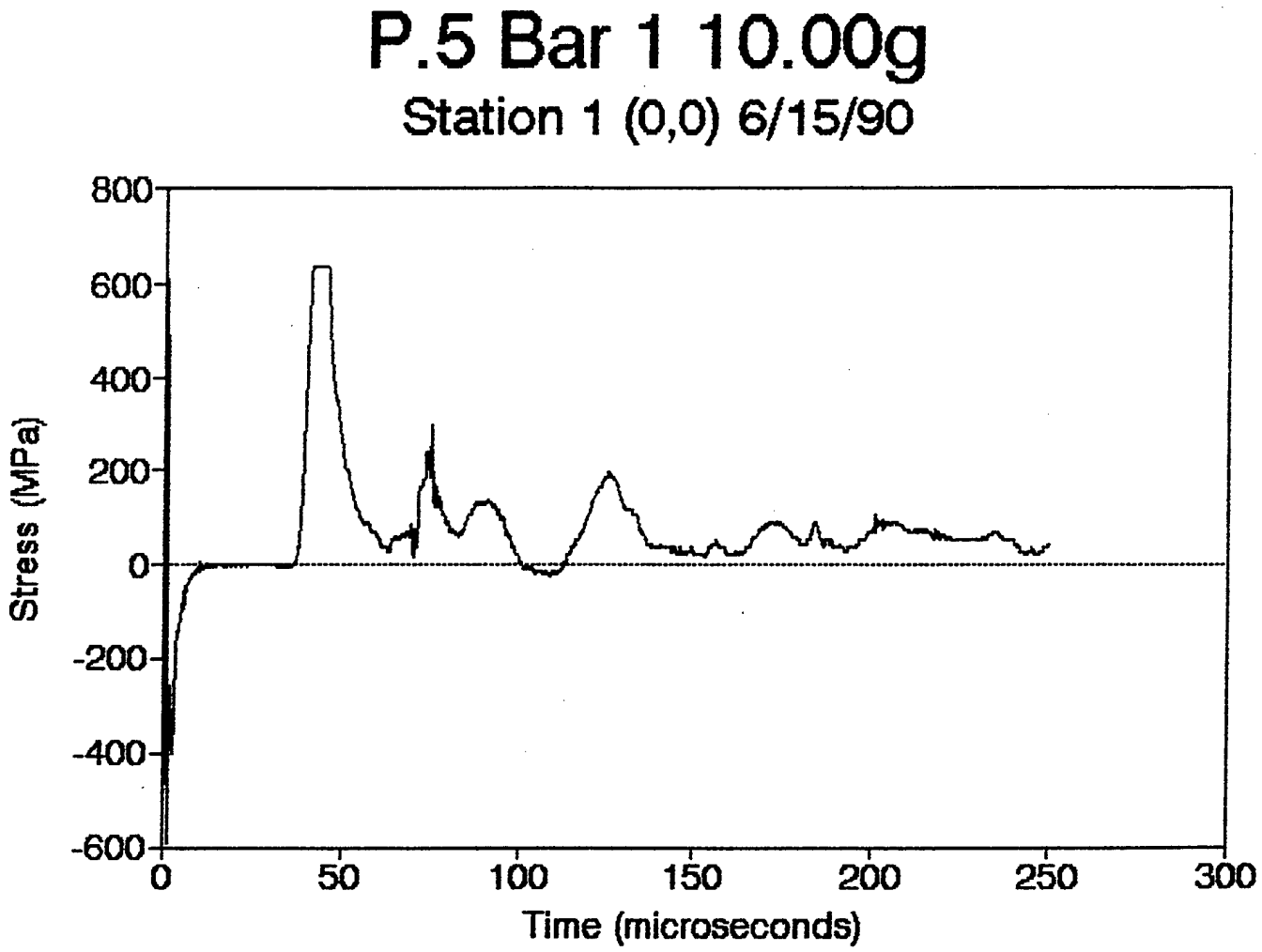
P.5 Bar 1 10.00g
Station 1 (0,0) 6/15/90
800
600
400
200
0
-200
-400
-600
Stress (MPa)
0
50
100
150
200
250
300
Time (microseconds)

P.5 Bar 2 10.00g

Station 45 (40,50) 6/15/90

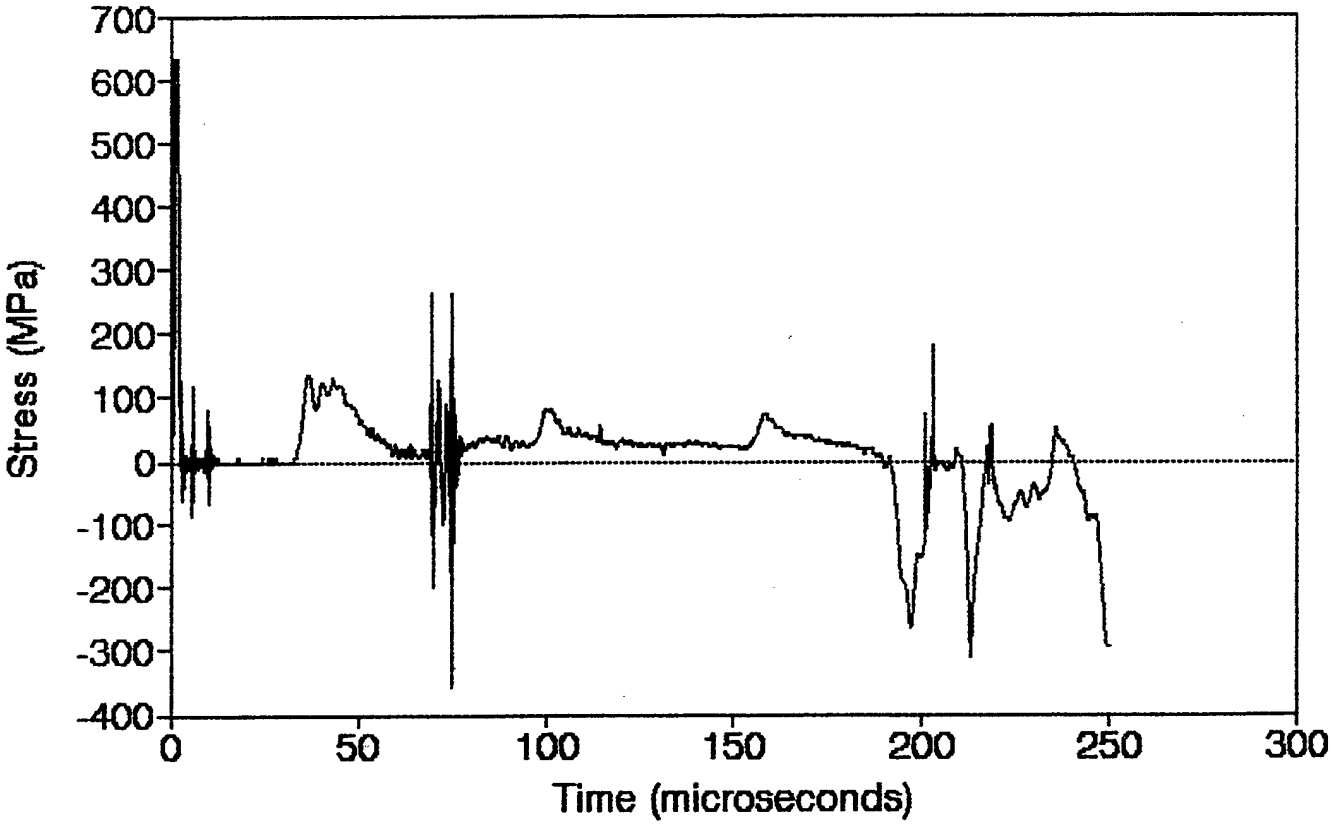

P.5 Bar 3 10.00g

Station 36 (40,40) 6/15/90

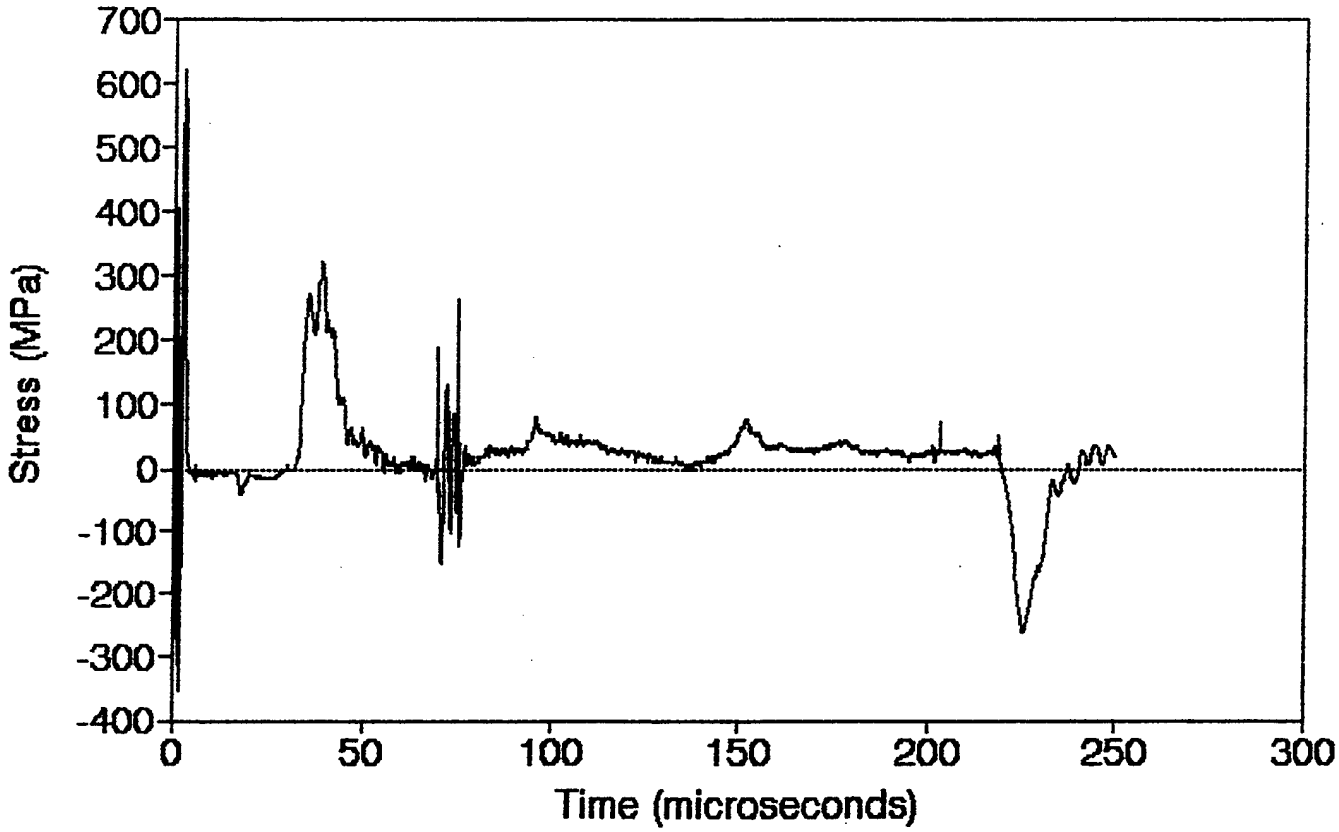

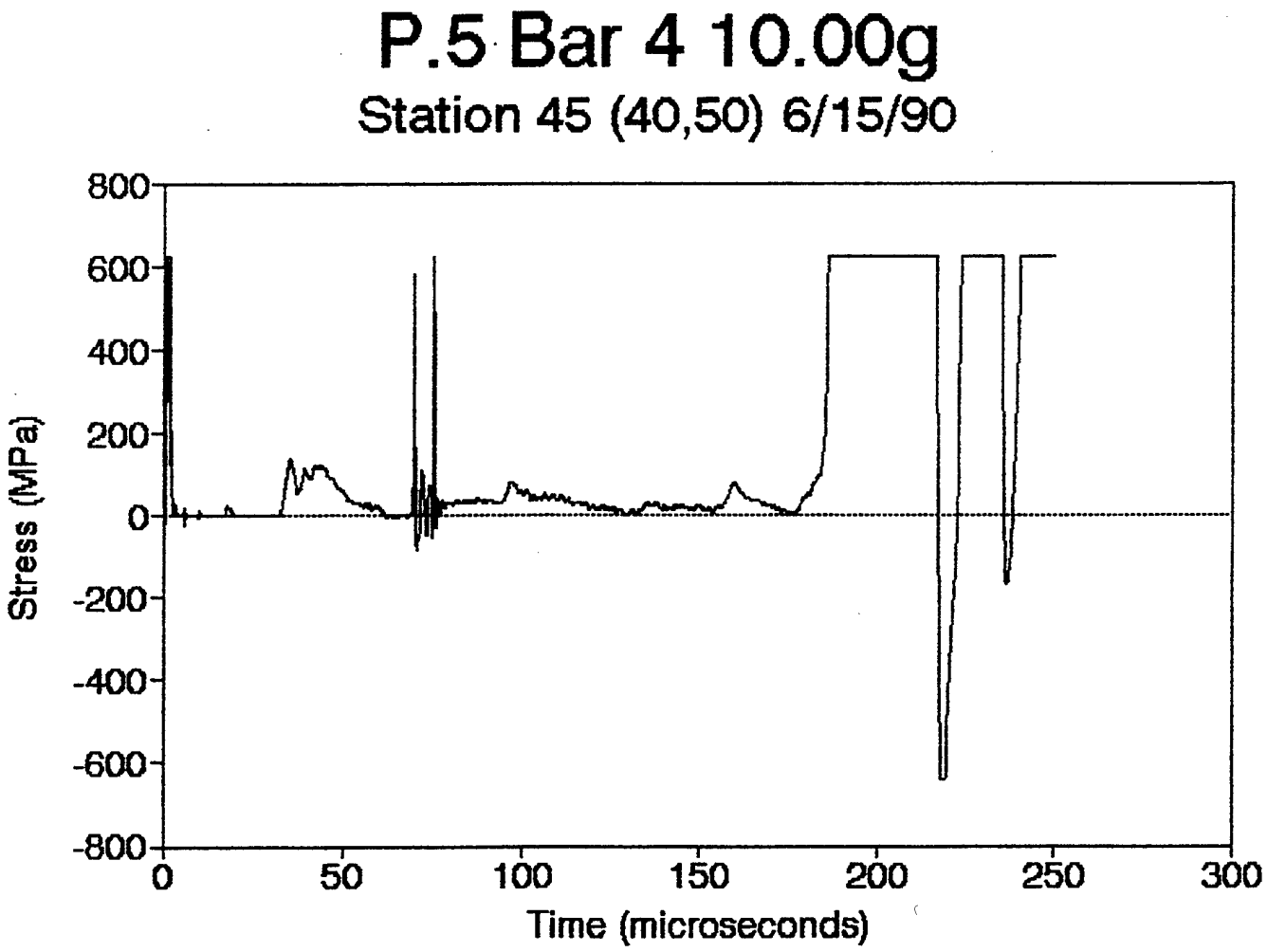
P.5 Bar 4 10.00g
Station 45 (40,50) 6/15/90
800
600
400
200
0
-200
-400
-600
-800
Stress (MPa)
0
50
100
150
200
250
300
Time (microseconds)

P.6 470 Ohm Resistor 10.278g

Station 36 (40,40) 7/19/90

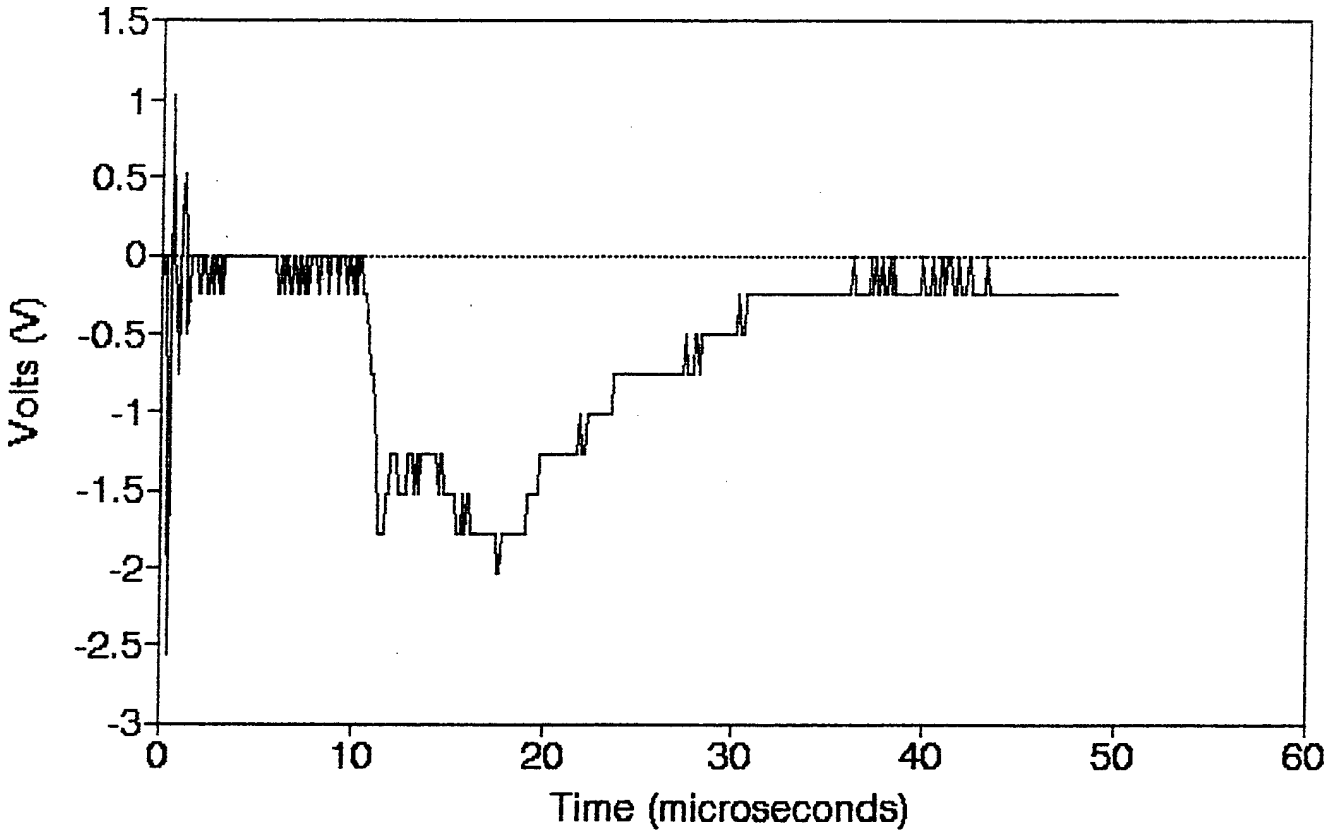

P.6 PCB 10.278g

Station 47 (40,60) 7/19/90

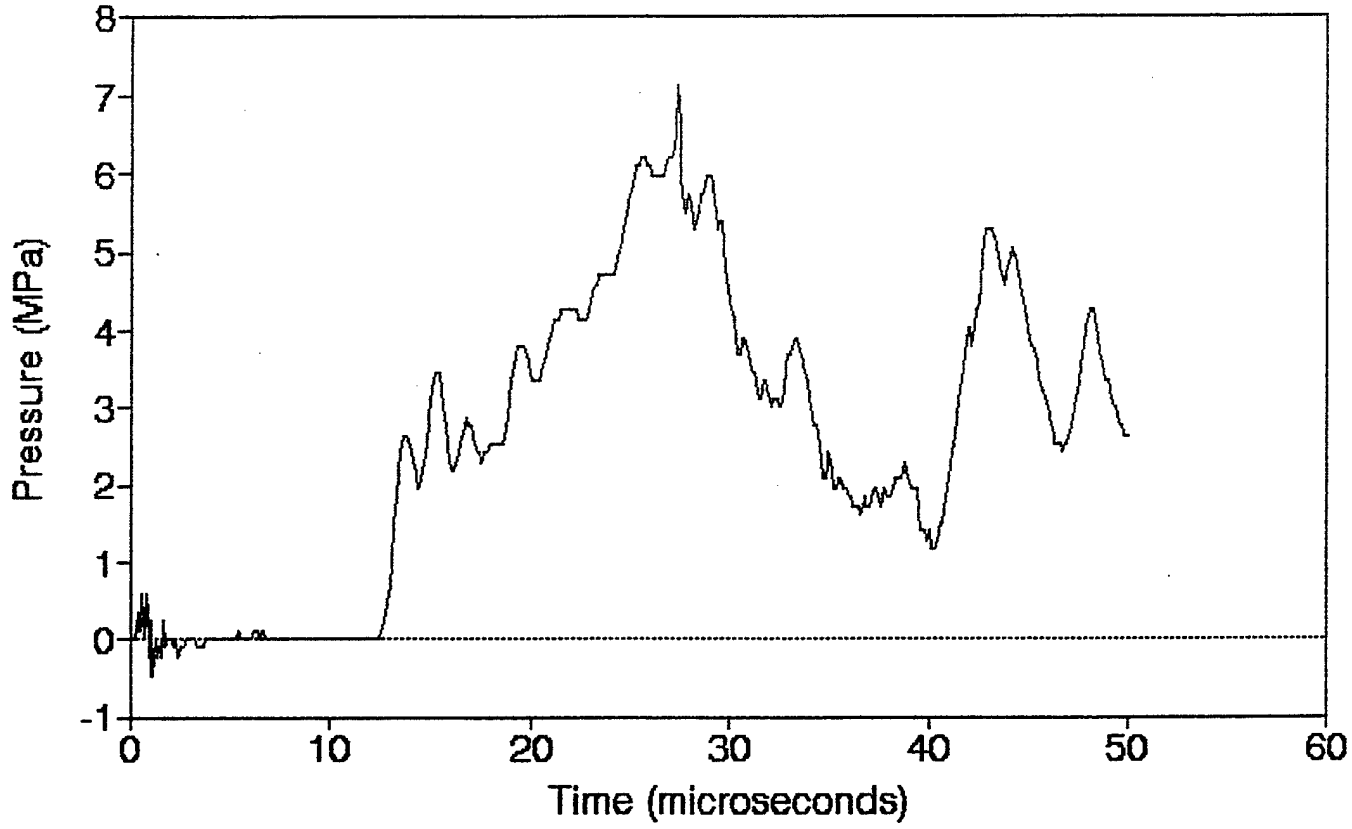

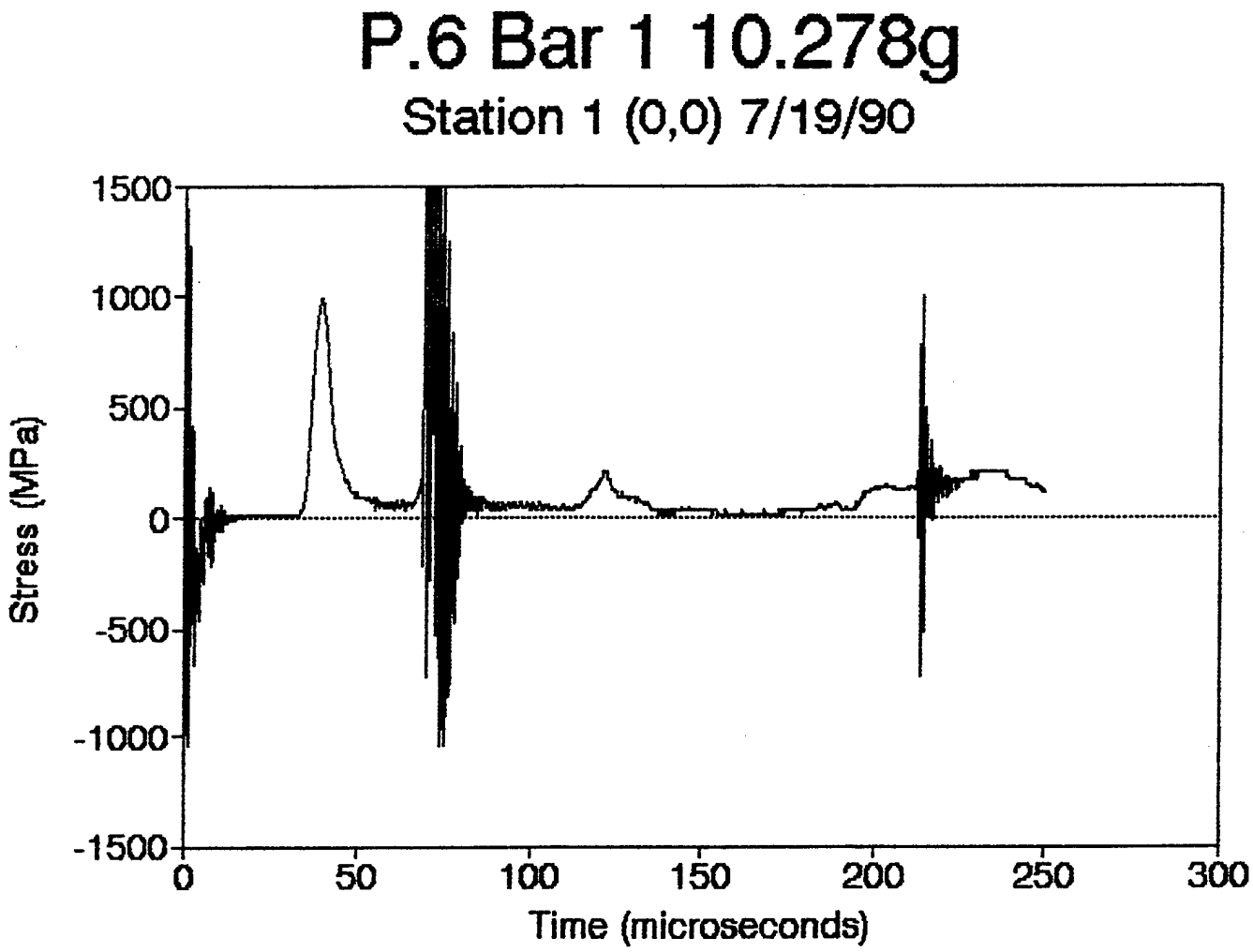
P.6 Bar 1 10.278g
Station 1 (0,0) 7/19/90
Stress (MPa)
1500
1000
500
0
-500
-1000
-1500
0
50
100
150
200
250
300
Time (microseconds)

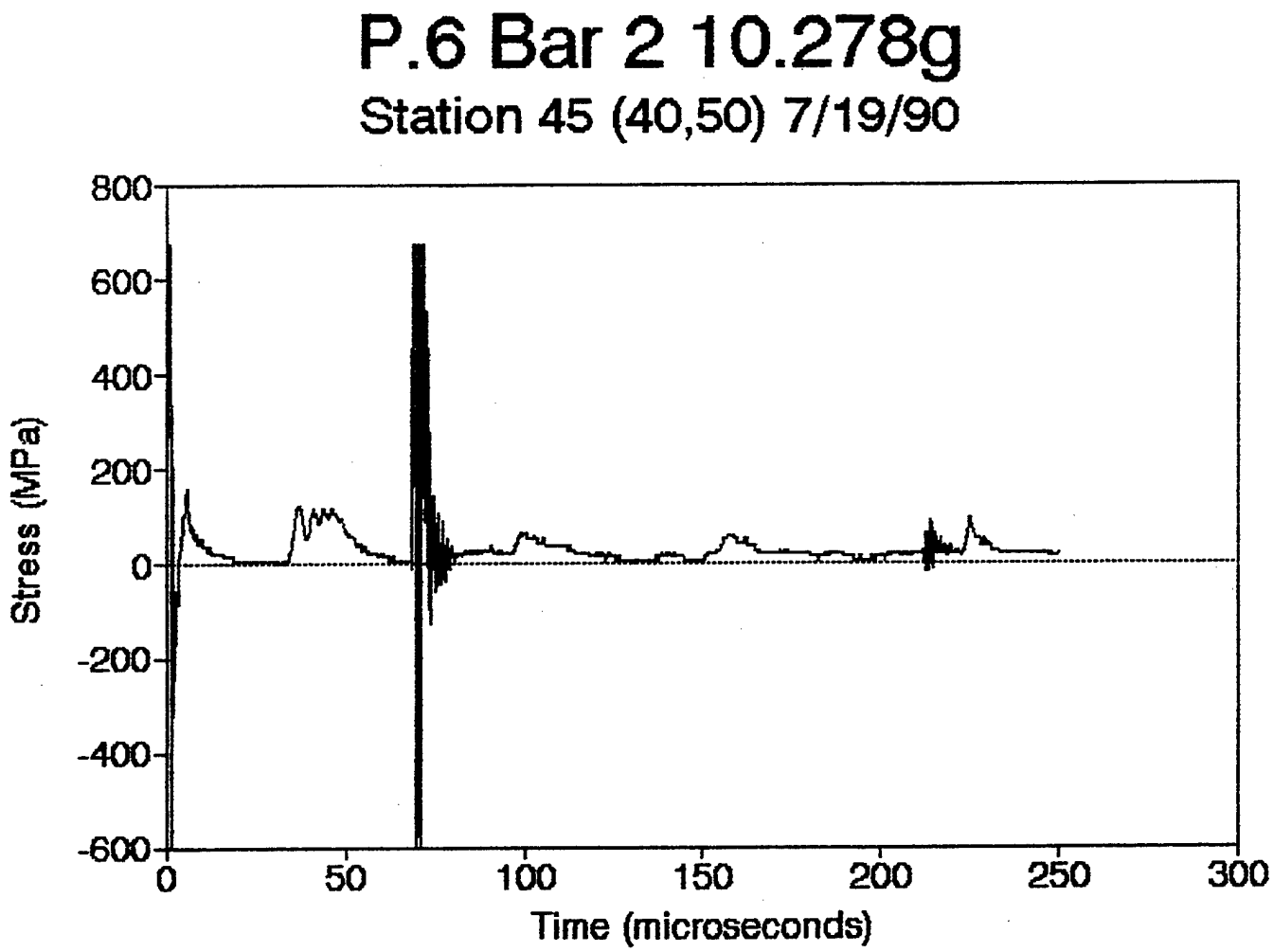
P.6 Bar 2 10.278g
Station 45 (40,50) 7/19/90
800
600
400
200
0
-200
-400
-600
Stress (MPa)
0
50
100
150
200
250
300
Time (microseconds)

P.6 Bar 3 10.278g

Station 36 (40,40) 7/19/90

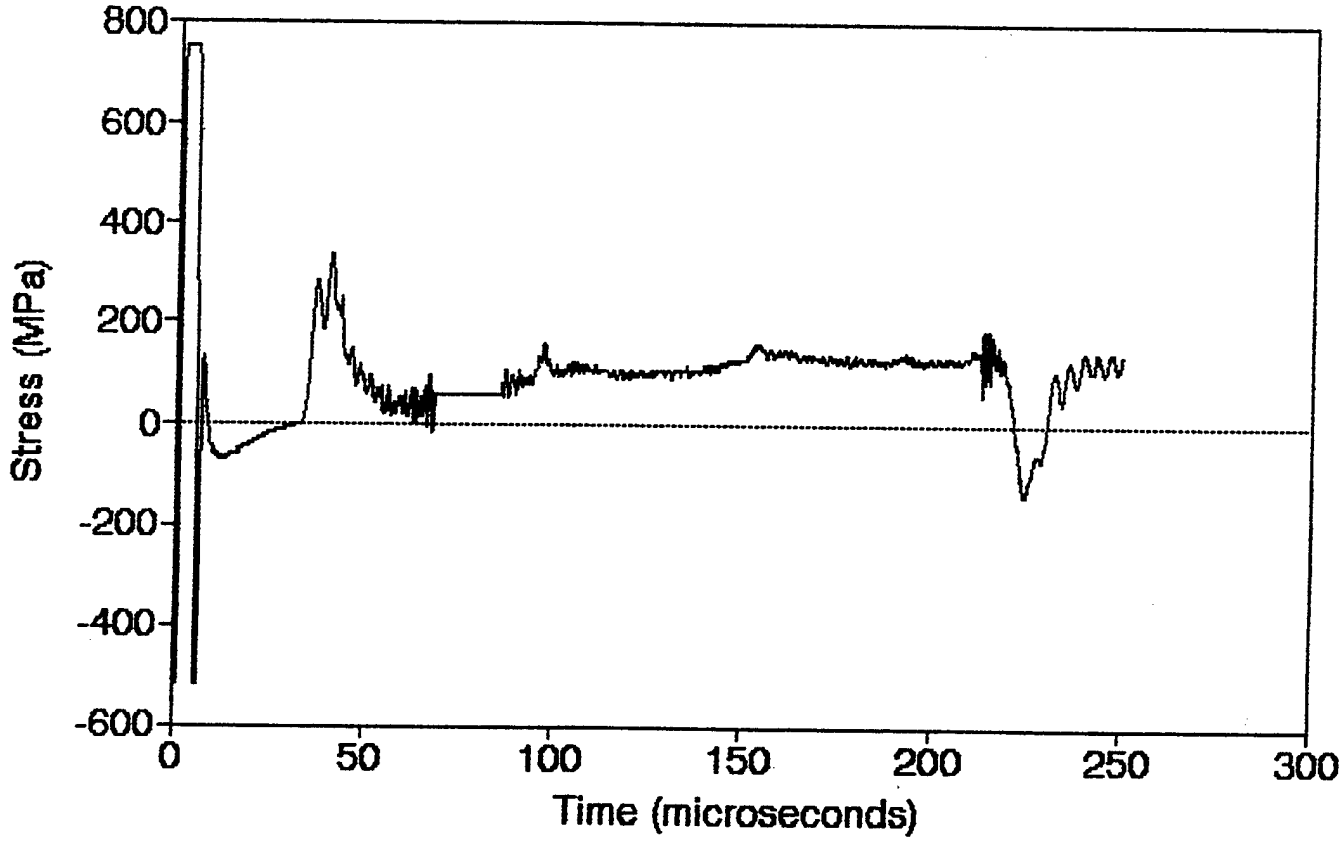

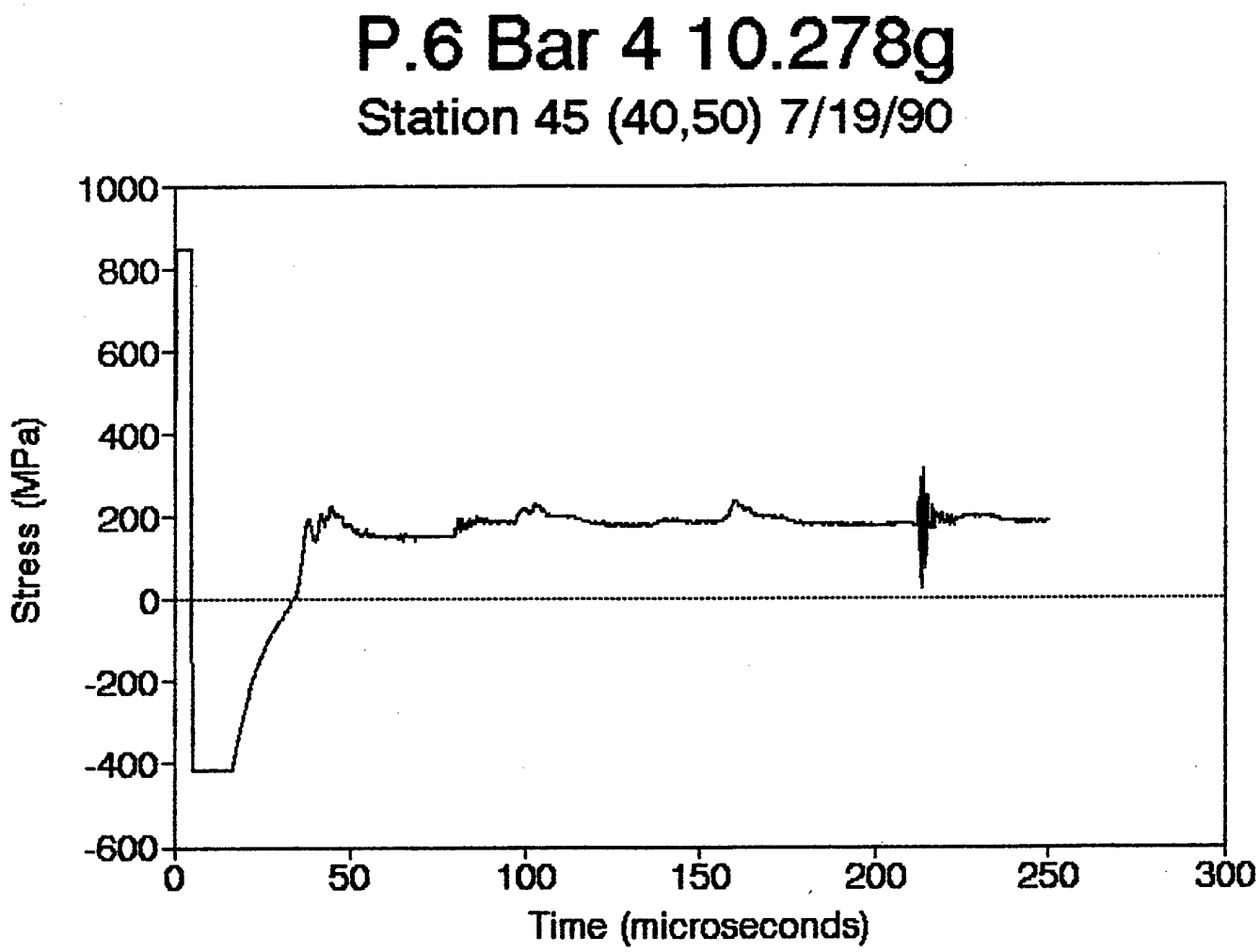
P.6 Bar 4 10.278g
Station 45 (40,50) 7/19/90
1000
800
600
400
200
0
-200
-400
-600
Stress (MPa)
0
50
100
150
200
250
300
Time (microseconds)

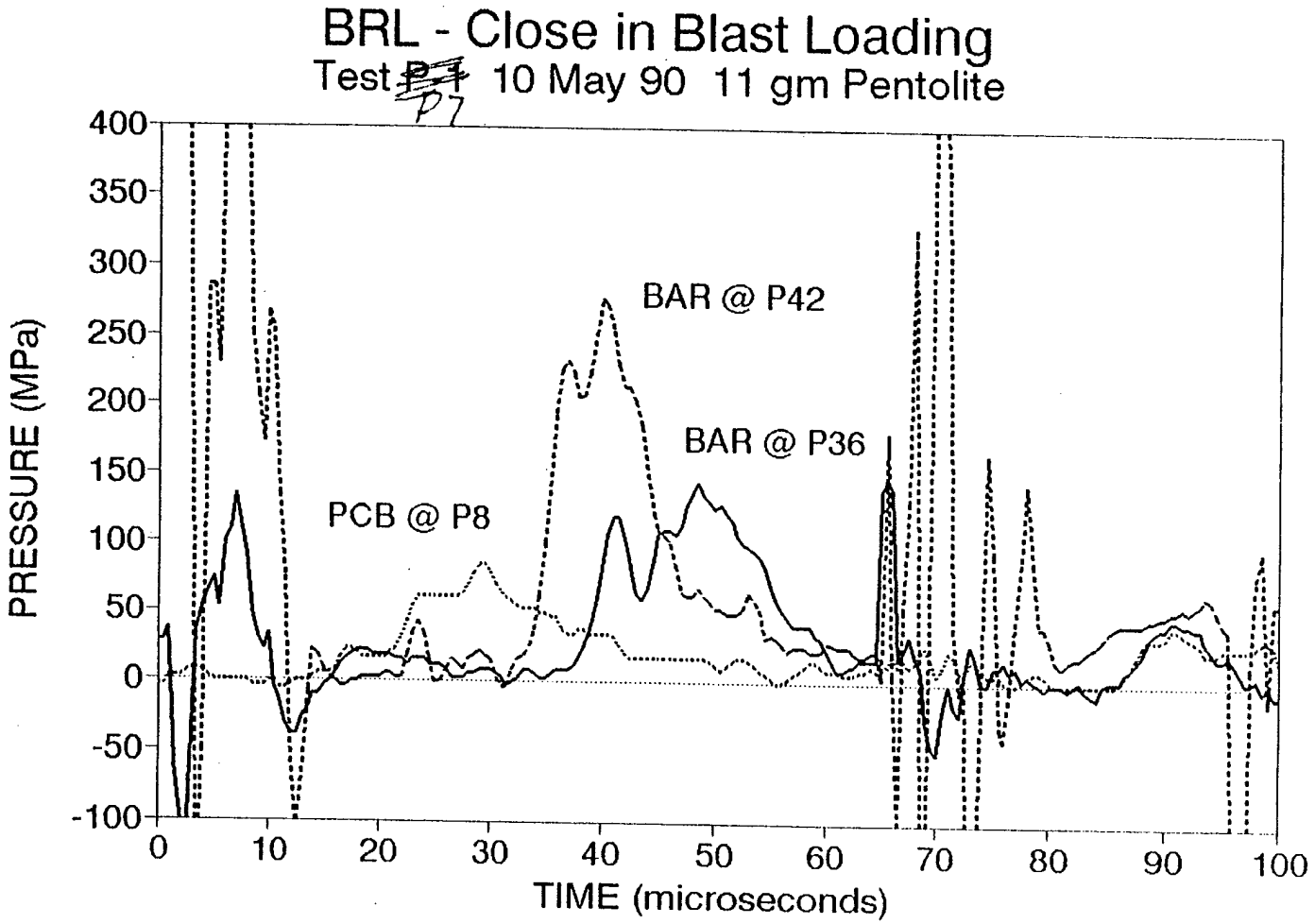
BRL - Close in Blast Loading
Test P7 10 May 90 11 gm Pentolite
PRESSURE (MPa)
400
350
300
250
200
150
100
50
0
-50
-100
0
10
20
30
40
50
60
70
80
90
100
TIME (microseconds)
BAR @ P42
BAR @ P36
PCB @ P8

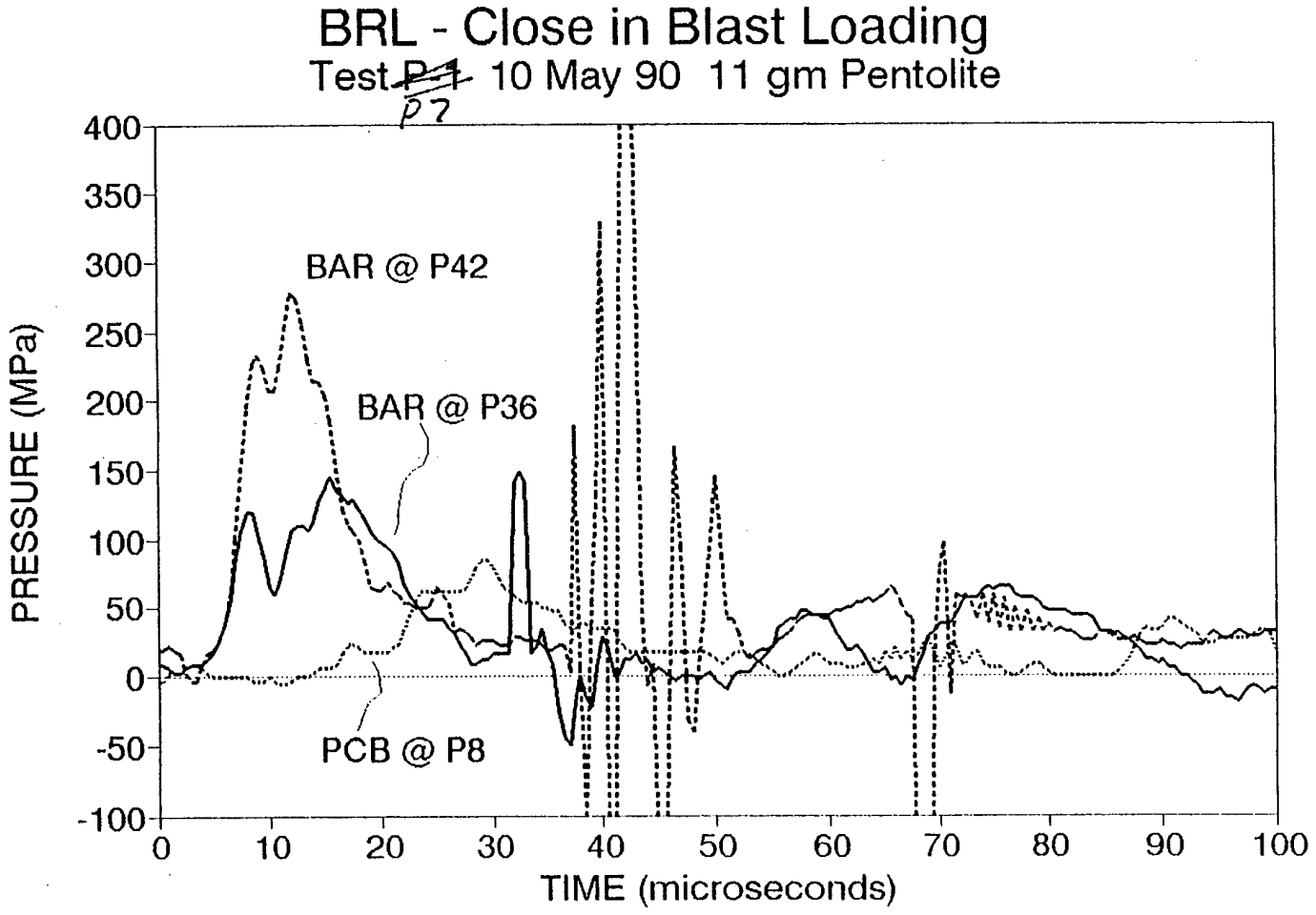
BRL - Close in Blast Loading
Test P7 10 May 90 11 gm Pentolite
PRESSURE (MPa)
TIME (microseconds)
BAR @ P42
BAR @ P36
PCB @ P8
400
350
300
250
200
150
100
50
0
-50
-100
0
10
20
30
40
50
60
70
80
90
100

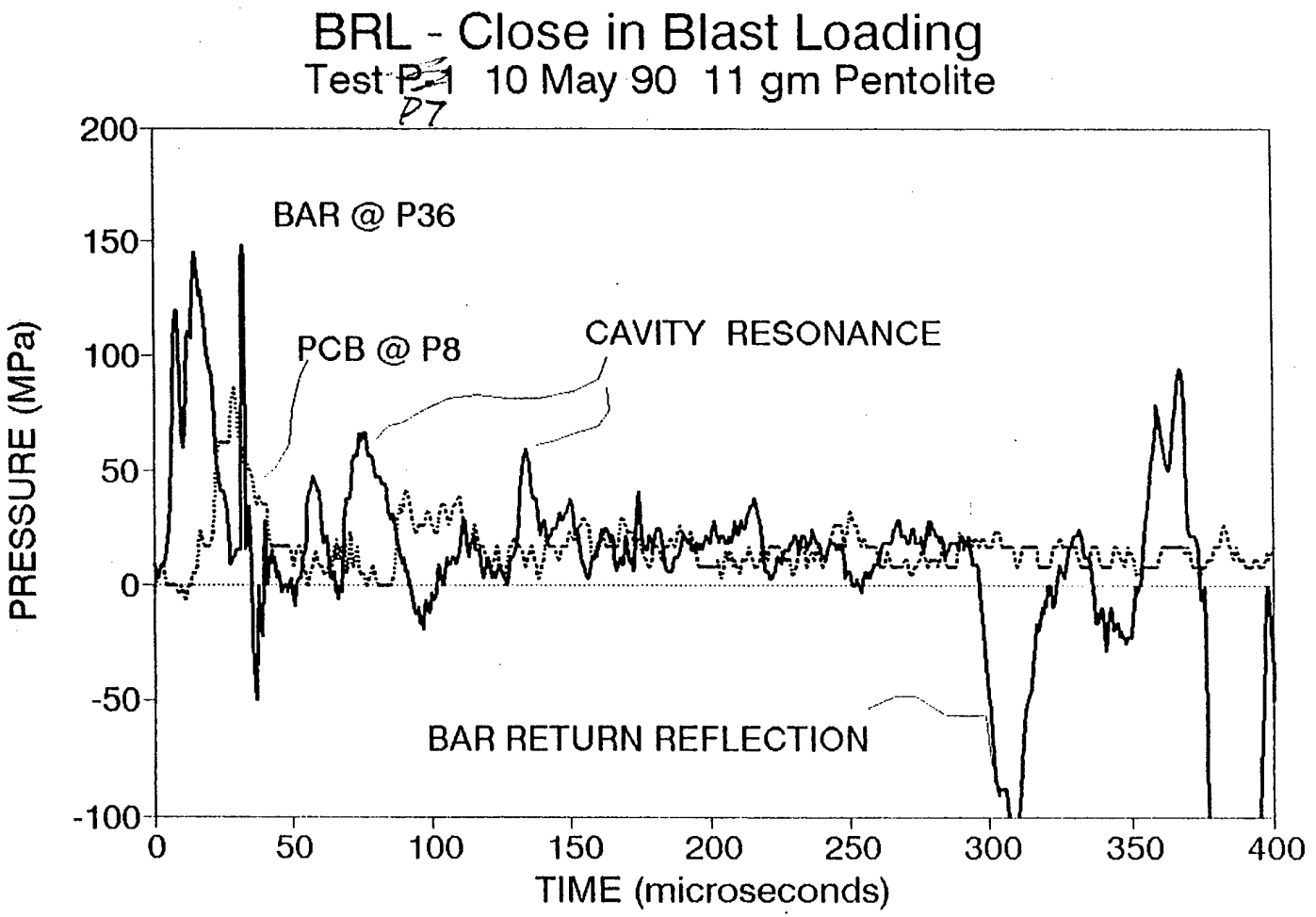
BRL - Close in Blast Loading
Test P-1 10 May 90 11 gm Pentolite
P7
BAR @ P36
PCB @ P8
CAVITY RESONANCE
BAR RETURN REFLECTION
PRESSURE (MPa)
TIME (microseconds)
200
150
100
50
0
-50
-100
0
50
100
150
200
250
300
350
400

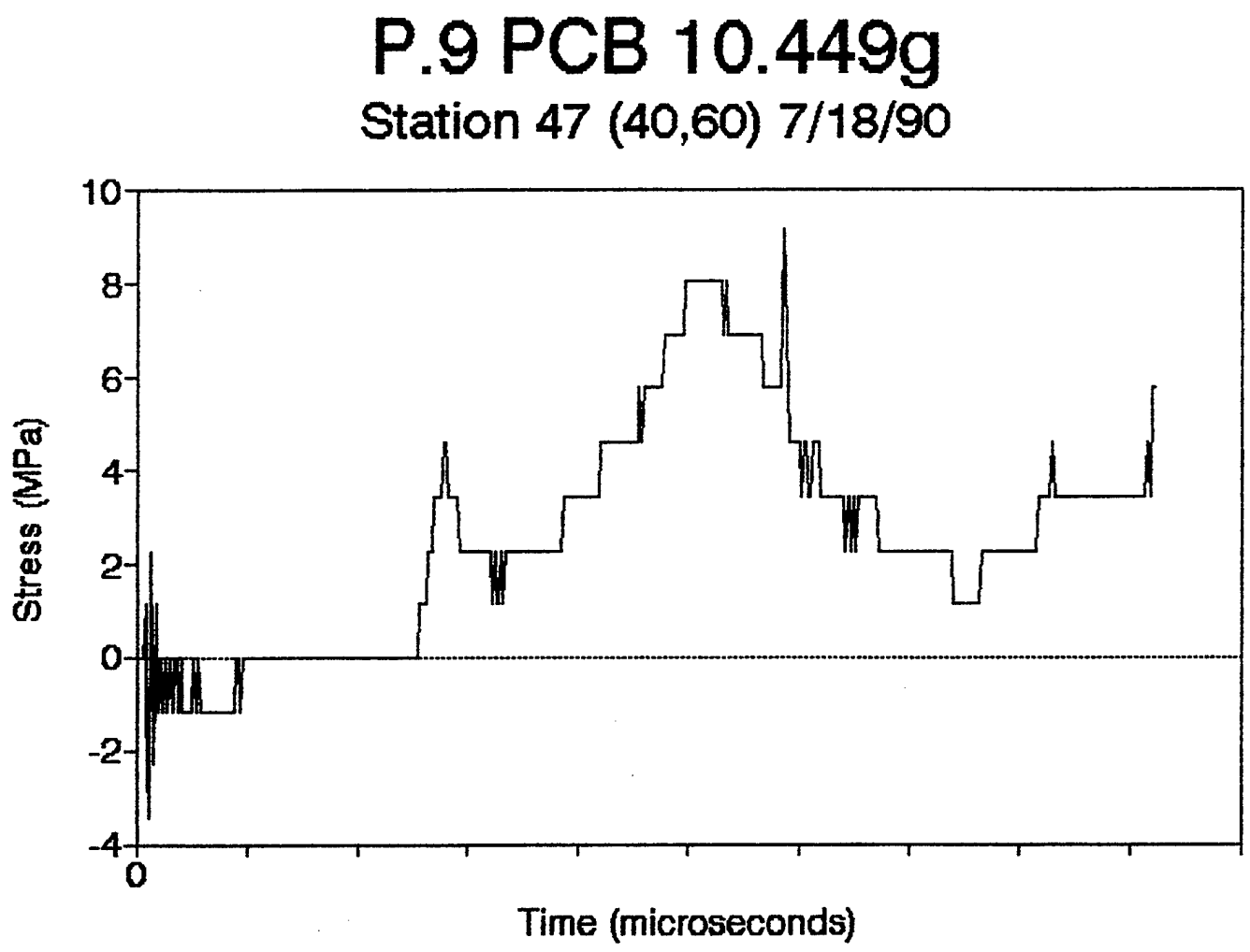
P.9 PCB 10.449g
Station 47 (40,60) 7/18/90
10
8
6
4
2
0
-2
-4
Stress (MPa)
0
Time (microseconds)

P.9 470 Ohm Resistor 10.449g

Station 36 (40,40) 7/18/90

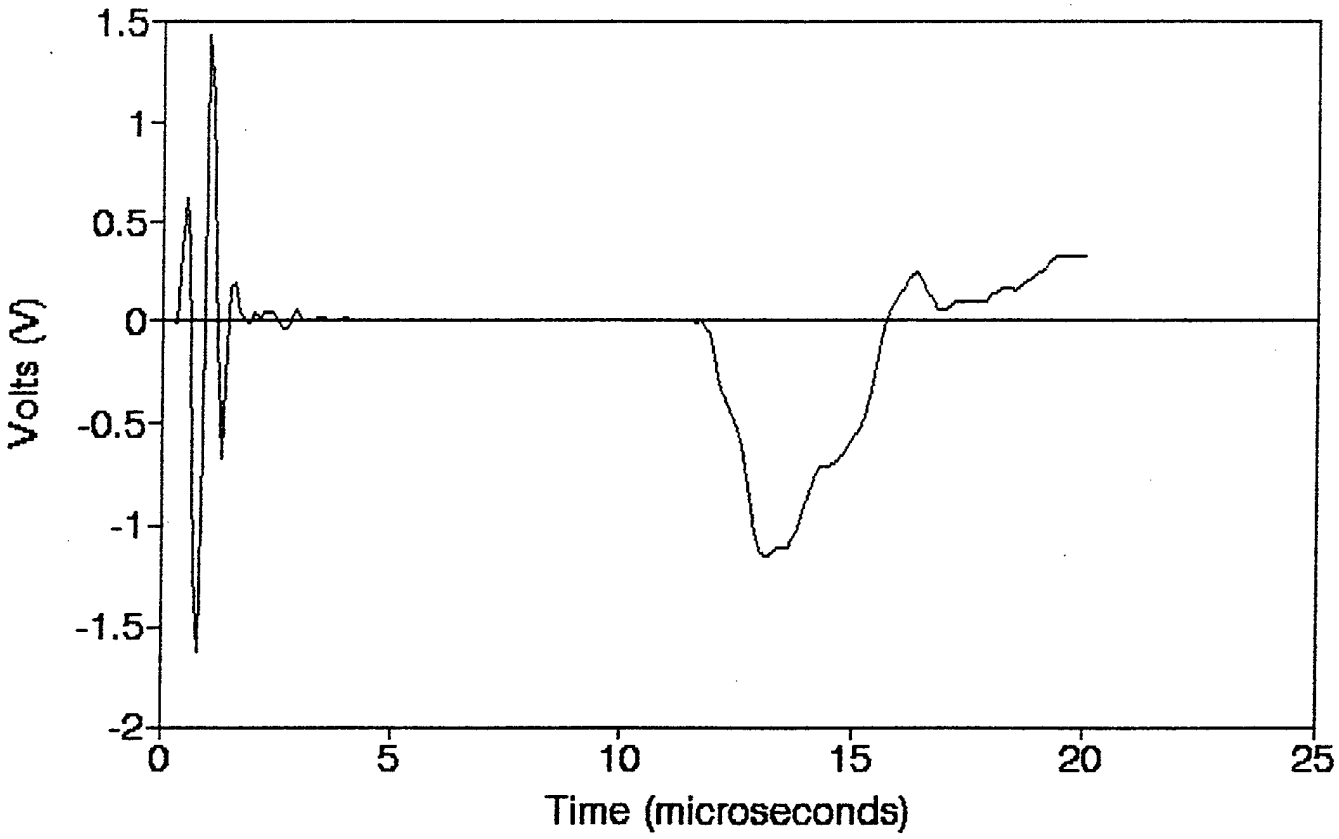

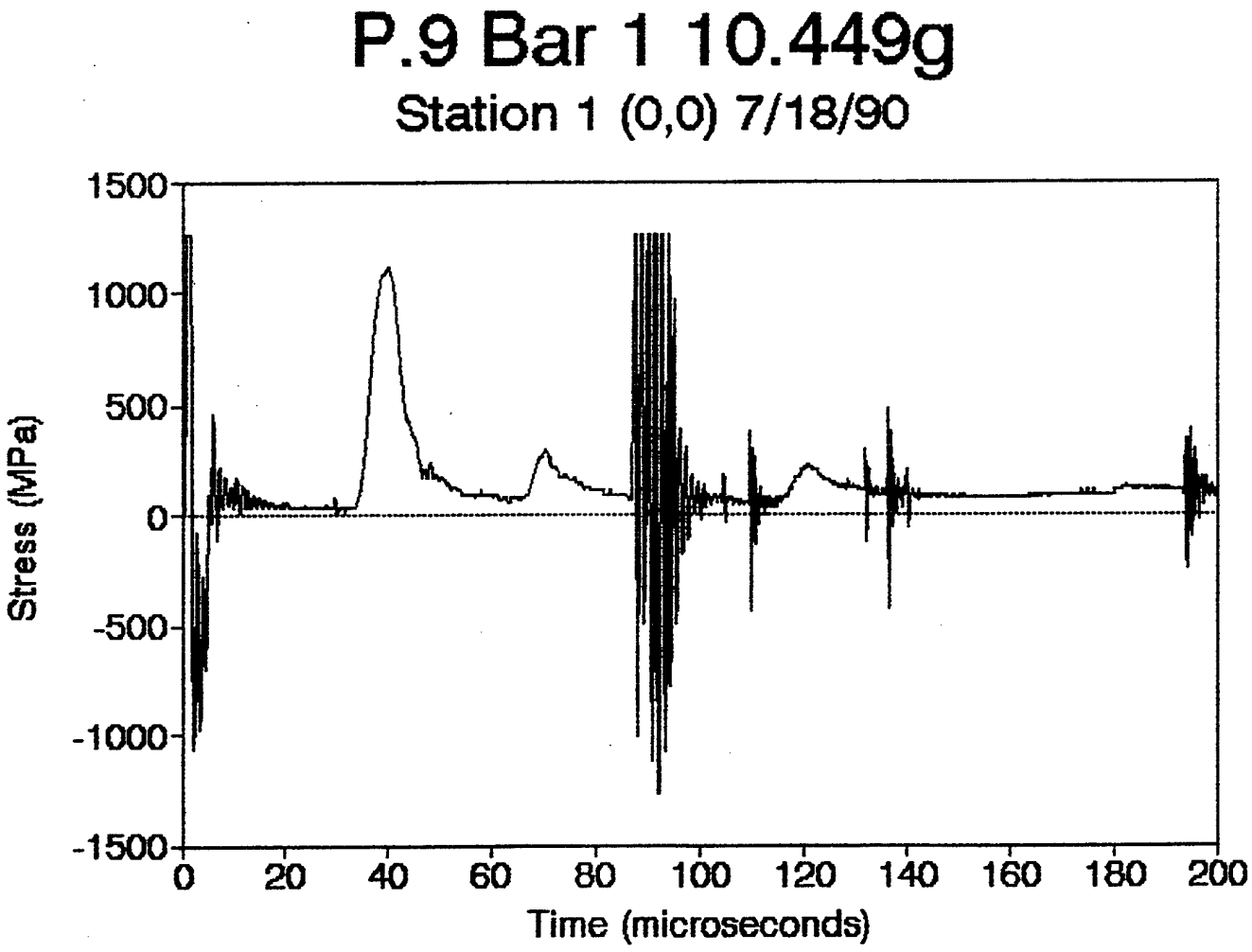
P.9 Bar 1 10.449g
Station 1 (0,0) 7/18/90
Stress (MPa)
1500
1000
500
0
-500
-1000
-1500
0
20
40
60
80
100
120
140
160
180
200
Time (microseconds)

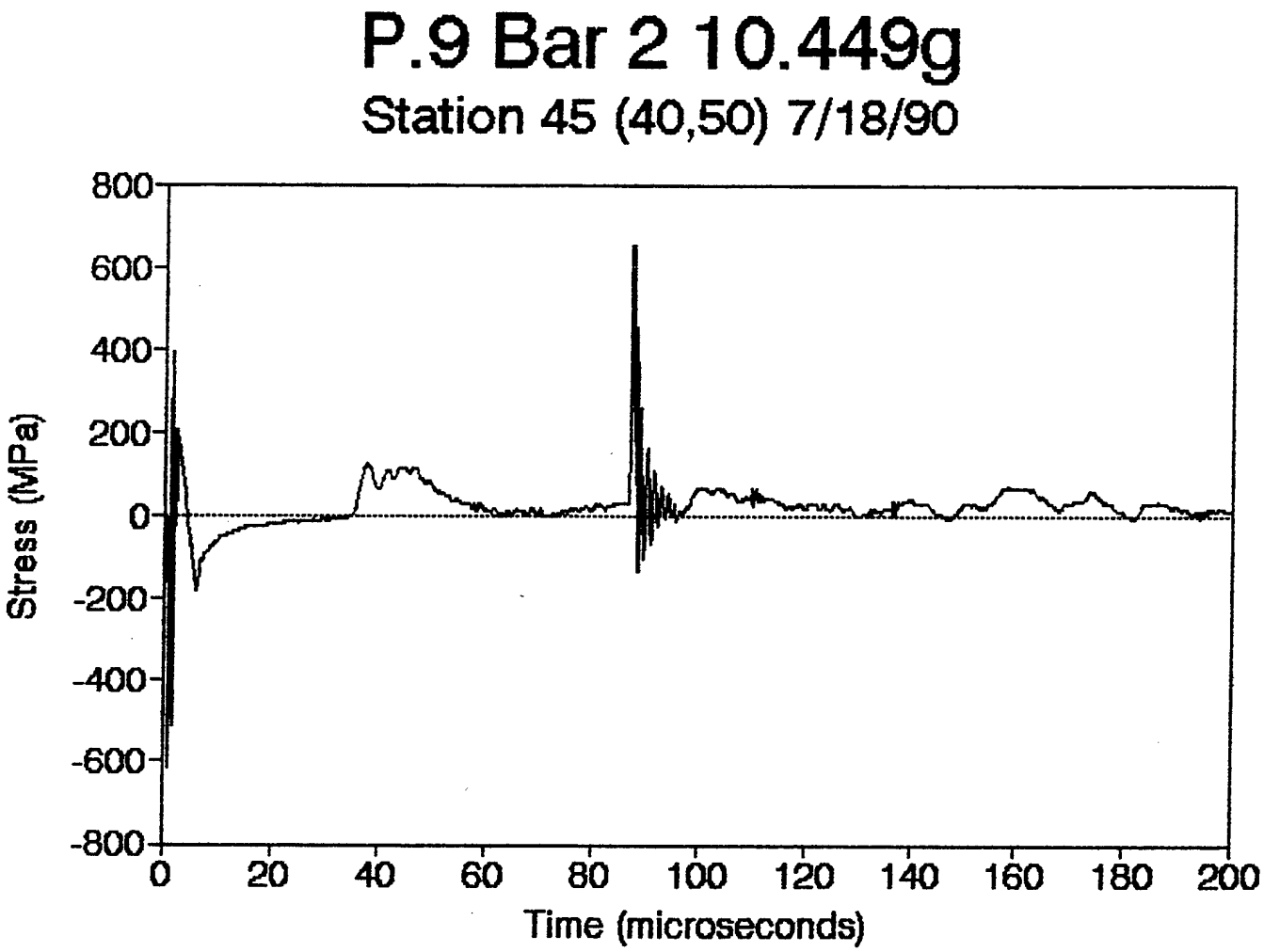
P.9 Bar 2 10.449g
Station 45 (40,50) 7/18/90
800
600
400
200
0
-200
-400
-600
-800
Stress (MPa)
0
20
40
60
80
100
120
140
160
180
200
Time (microseconds)

P.9 Bar 3 10.449g

Station 36 (40,40) 7/18/90

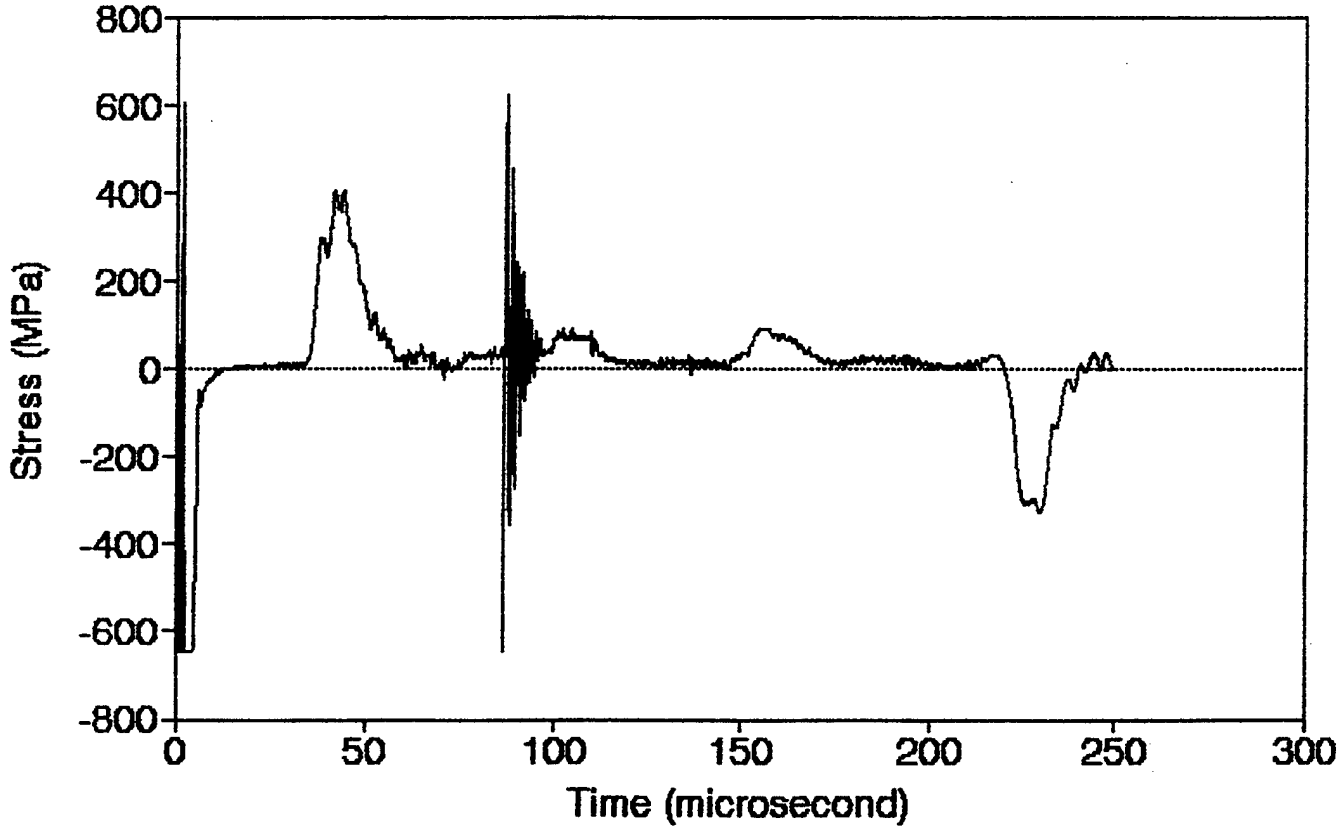

P.9 Bar 4 10.449g

Station 45 (40,50) 7/18/90

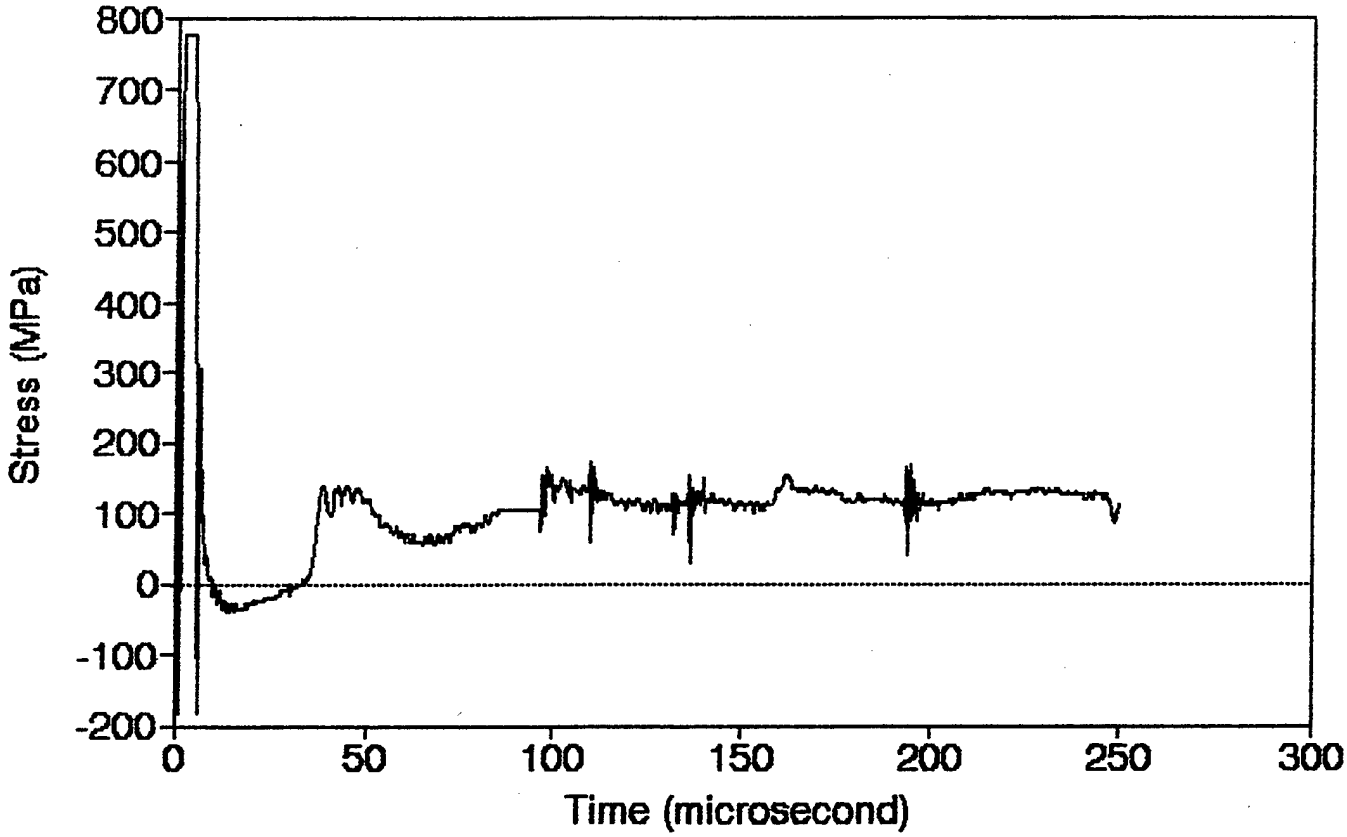

NO. OF COPIES	ORGANIZATION
2	DEFENSE TECHNICAL INFO CTR ATTN DTIC DDA 8725 JOHN J KINGMAN RD STE 0944 FT BELVOIR VA 22060-6218
1	DIRECTOR US ARMY RESEARCH LAB ATTN AMSRL OP SD TA 2800 POWDER MILL RD ADELPHI MD 20783-1145
3	DIRECTOR US ARMY RESEARCH LAB ATTN AMSRL OP SD TL 2800 POWDER MILL RD ADELPHI MD 20783-1145
1	DIRECTOR US ARMY RESEARCH LAB ATTN AMSRL OP SD TP 2800 POWDER MILL RD ADELPHI MD 20783-1145
	ABERDEEN PROVING GROUND
2	DIR USARL ATTN AMSRL OP AP L (305)

NO. OF COPIES	ORGANIZATION
2	HQDA ATTN SARD TR MS K KOMINOS DR R CHAIT PENTAGON WASHINGTON DC 20310-0103
2	HQDA ATTN SARD TT DR F MILTON C NASH PENTAGON WASHINGTON DC 20310-0103
2	FED EMERGENCY MGT AGCY ATTN PUBLIC RELATIONS OFC TECH LIB WASHINGTON DC 20472
1	CHAIRMAN DOD EXPLSVS SAFETY BD ROOM 856 C HOFFMAN BLDG 1 2461 EISENHOWER AVENUE ALEXANDRIA VA 22331-0600
1	DIR OF DEFNS RSRCH AND ENGRNG ATTN DD TWP WASHINGTON DC 20301
1	DEFNS INTELLIGENCY AGCY ATTN DT 2 WPNS & SYS DIV WASHINGTON DC 20301
1	ASSIST SECRETARY OF DEFNS ATOMIC ENERGY ATTN DOCUMENT CONTROL WASHINGTON DC 20301
5	DEFNS SPEC WEAPONS AGCY ATTN CSTI TECH LIB ESA W SUMMA E SEIDEN WEP T KENNEDY M FRANKEL 6801 TELEGRAPH RD ALEXANDRIA VA 22310-3398
1	CHAIRMAN JOINT CHIEFS OF STAFF ATTN J5 R&D DIVISION WASHINGTON DC 20301

NO. OF COPIES	ORGANIZATION
2	DA DCSOPS ATTN TECH LIB DIR OF CHEM & NUC OPS WASHINGTON DC 20310
4	COMMANDER FIELD COMMAND DSWA ATTN FCTTIS E L MARTINEZ FCTOSL F MOYNIHAN FCTIH H ROSS FCTIH W BRENNAN KIRTLAND AFB NM 87115
1	US ARMY RSRCH DEVELOPMENT & STANDARDIZATION GRP UK ATTN ROY E REICHENBACH PSC 802 BOX 15 FPO AE 09499-1500
10	CENTRAL INTEL AGENCY DIR DB STANDARD ATTN GE 47 HQ WASHINGTON DC 20505
1	DIRECTOR DARPA ATTN TECH LIB 3701 NORTH FAIRFAX DR ARLINGTON VA 22203-1714
2	COMMANDER US ARMY NRDEC ATTN AMSNA D D SIELING STRNC UE J CALLIGEROS NATICK MA 01762
2	COMMANDER US ARMY CECOM ATTN AMSEL RD AMSEL RO TPPO P FT MONMOUTH NJ 07703-5301
1	COMMANDER US ARMY CECOM R&D TECH LIB ATTN ASQNC ELC IS L R MYER CTR FT MONMOUTH NJ 07703-5000
1	MIT ATTN TECH LIB CAMBRIDGE MA 02139

NO. OF COPIES	ORGANIZATION
1	COMMANDER US ARMY NGIC ATTN RSRCH & DATA BR 220 7TH STREET NE CHARLOTTESVILLE VA 22901-5396
1	COMMANDER US ARMY ARDEC ATTN AMSTA AR FSM W MR BARBER BLDG 94 PICATINNY ARSENAL NJ 07806-5000
1	US ARMY TRAC FT LEE ATTN ATRC L MR CAMERON FORT LEE VA 23801-6140
1	US ARMY MISSILE & SPACE INTELLIGENCE CTR ATTN AIAMS YDL REDSTONE ARSENAL AL 35898-5500
1	COMDG OFFICER CODE L51 NAVAL CIVIL ENGRNG LAB ATTN J TANCRETO PORT HUENEME CA 93043-5003
2	COMMANDER US ARMY STRTGC DEFNS CMD ATTN CSSD H MPL TECH LIB CSSD H XM DR DAVIES PO BOX 1500 HUNTSVILLE AL 35807
2	COMMANDER US ARMY CORPS OF ENGNRS WATERWAYS EXPRMNT STATION ATTN CEWES SS R J WATT CEWES TL TECH LIB PO BOX 631 VICKSBURG MS 39180-0631
1	COMMANDER US ARMY ENGINEER DIVISION ATTN HNDED FD PO BOX 1500 HUNTSVILLE AL 35807

NO. OF COPIES	ORGANIZATION
3	COMMANDER US ARMY NUC & CHEML AGCY 7150 HELLER LOOP STE 101 SPRINGFIELD VA 22150-3198
1	COMMANDER US ARMY CORPS OF ENGNRS FT WORTH DISTRICT ATTN CESWF PM J PO BOX 17300 FT WORTH TX 76102-0300
1	TRAC FLVN ATTN ATRC FT LEAVENWORTH KS 66027-5200
1	COMMANDER US ARMY RSRCH OFFICE ATTN SLCRO D PO BOX 12211 RSRCH TRIANGLE PARK NC 27709-2211
1	HQ TRAC RPD ATTN ATRC RPR RADDA FT MONROE VA 23651-5143
2	OFFICE OF NAVAL RSRCH ATTN DR A FAULSTICK CODE 23 800 N QUINCY STREET ARLINGTON VA 22217
1	TRAC WSMR ATTN ATRC WC KIRBY WSMR NM 88002-5502
2	COMMANDER US ARMY WSMR ATTN STEWS NED DR MEASON STEWS DATTS O R L PENNY WSMR NM 88002-5158
2	CHIEF OF NAVAL OPS DEPARTMENT OF THE NAVY ATTN OP 03EG OP 985F WASHINGTON DC 20350

NO. OF COPIES	ORGANIZATION
1	COMMANDER DAVID TAYLOR RSRCH CTR ATTN CODE 522 TECH INFO CTR BETHESDA MD 20084-5000
1	OFFCR IN CHARGE CODE L31 CIVIL ENGRNG LAB NAVAL CNSTRCTN BATTLN CTR ATTN TECH LIB PORT HUENEME CA 93041
1	COMMANDING OFFICER WHITE OAK WARFARE CTR ATTN CODE WA501 NNPO SILVER SPRING MD 20902-5000
1	COMMANDER CODE 533 NAVAL WEAPONS CTR ATTN TECH LIB CHINA LAKE CA 93555-6001
1	COMMANDER DAHLGREN DIVISION NAVAL SURFACE WARFARE CTR ATTN CODE E23 LIB DAHLGREN VA 22448-5000
1	COMMANDER NAVAL RSRCH LAB ATTN CODE 2027 TECH LIB WASHINGTON DC 20375
1	OFFICER IN CHARGE WHITE OAK WARFARE CTR DETACHMENT ATTN CODE E232 TECH LIB 10901 NEW HAMPSHIRE AVE SILVER SPRING MD 20903-5000
1	AL LSCF ATTN J LEVINE EDWARDS AFB CA 93523-5000
1	COMMANDER NAVAL WPNS EVALUATION FAC ATTN DOCUMENT CONTROL KIRTLAND AFB NM 87117

NO. OF COPIES	ORGANIZATION
2	COMMANDER US ARMY NRDEC ATTN SSCNC YSD J ROACH SSCNC WST A MURPHY KANSAS ST NATICK MA 10760-5018
1	RADC EMTLD DOCUMENT LIB GRIFFISS AFB NY 13441
1	AEDC ATTN R MCAMIS MAIL STOP 980 ARNOLD AFB TN 37389
1	OLAC PL TSTL ATTN D SHIPLETT EDWARDS AFB CA 93523-5000
1	AFIT ENY ATTN LTC HASEN PHD WP AFB OH 45433-6583
2	AIR FORCE ARMAMENT LAB ATTN AFATL DOIL AFATL DLYV EGLIN AFB FL 32542-5000
1	IDAHO NATL ENGRNG LAB ATTN SPEC PRGMS J PATTON 2151 NORTH BLVD MS 2802 IDAHO FALLS ID 83415
3	PHILLIPS LAB AFWL ATTN NTE NTED NTES KIRTLAND AFB NM 87117-6008
1	LAWRENCE LIVERMORE NATL LAB ATTN TECH INFO DEPT L 3 PO BOX 808 LIVERMORE CA 94550
1	AFIT ATTN TECH LIB BLDG 640 B WP AFB OH 45433

NO. OF COPIES	ORGANIZATION
1	NASA ATTN SCI & TECH INFO FAC PO BOX 8757 BWI AIRPORT BALTIMORE MD 21240
1	FTD NIIS WP AFB OH 45433
3	KAMAN SCIENCES CORP ATTN LIB P A ELLIS F H SHELTON PO BOX 7463 COLORADO SPRINGS CO 80933-7463
4	IDAHO NATL ENGRNG LAB EG&G IDAHO INC ATTN R GUENZLER MS 3505 R HOLMAN MS 3510 R A BERRY W C REED PO BOX 1625 IDAHO FALLS ID 83415
3	SANDIA NATL LABS ATTN DOC CONTROL 3141 D GARDNER DIV 1421 J MCGLAUN DIV 1541 PO BOX 5800 ALBUQUERQUE NM 87185-5800
1	LOS ALAMOS NATL LAB REPORT COLLECTION RESEARCH LIB MS P362 PO BOX 7113 LOS ALAMOS NM 87544-7113
1	SANDIA NATL LABS LIVERMORE LAB ATTN DOC CNTRL FOR TECH LIB PO BOX 969 LIVERMORE CA 94550
1	NASA AMES RSRCH CTR APPLIED COMPTNL AERO BR ATTN DR T HOLTZ MS 202 14 MOFFETT FIELD CA 94035

NO. OF COPIES	ORGANIZATION
1	NASA LANGLEY RSRCH CTR ATTN TECH LIB HAMPTON VA 23665
2	APPLIED RSRCH ASSOC INC ATTN J KEEFER N H ETHRIDGE PO BOX 548 ABERDEEN MD 21001
4	APPLIED RSRCH ASSOC INC ATTN C NEEDHAM J CREPEAU S HIKIKA R NEWELL 4300 SAN MATEO BLVD ALBUQUERQUE NM 87110
1	ADA TECHNOLOGIES INC ATTN JAMES R BUTZ HONEYWELL CTR STE 110 304 INVERNESS WAY SOUTH ENGLEWOOD CO 80112
1	CARPENTER RSRCH CORP ATTN H JERRY CARPENTER 27520 HAWTHORNE BLVD SUITE 263 ROLLING HILLS ESTATES CA 90274
1	AEROSPACE CORP ATTN TECH INFO SERVICES PO BOX 92957 LOS ANGELES CA 90009
1	THE BOEING COMPANY ATTN AEROSPACE LIB PO BOX 3707 SEATTLE WA 98124
2	FMC CORP ADVANCED SYSTEMS CTR ATTN J DROTLEFF C KREBS MDP 95 BOX 58123 2890 DE LA CRUZ BLVD SANTA CLARA CA 95052

NO. OF COPIES	ORGANIZATION
1	SVERDRUP TECHNOLOGY INC SVERDRUP CORP AEDC ATTN BD HEIKKINEN MS 900 ARNOLD AFB TN 37389-9998
2	DYNAMICS TECHNOLOGY INC ATTN D T HOVE G P MASON 21311 HAWTHORNE BLVD STE 300 TORRANCE CA 90503
1	KTECH CORP ATTN DR E GAFFNEY 901 PENNSYLVANIA AVE NE ALBUQUERQUE NM 87111
1	EATON CORP DEFNS VALVE & ACTUATOR DIV ATTN J WADA 2338 ALASKA AVE EL SEGUNDO CA 90245-4896
2	MCDONNELL DOUGLAS ASTRONAUTICS CORP ATTN ROBERT W HALPRIN K A HEINLY 5301 BOLSA AVENUE HUNTINGTON BEACH CA 92647
4	KAMAN AVIDYNE ATTN R RUETENIK S CRISCIONE R MILLIGAN T STAGLIANO 83 SECOND AVENUE NORTHWEST INDUSTRIAL PARK BURLINGTON MA 01830
1	MDA ENGRNG INC ATTN DR DALE ANDERSON 500 EAST BORDER STREET SUITE 401 ARLINGTON TX 07601
2	POINTWISE INC ATTN J CHAWNER J STEINBRENNER PO BOX 210698 BEDFORD TX 76095-7698

NO. OF COPIES	ORGANIZATION
2	PHYSICS INTRNTL CORP PO BOX 5010 SAN LEANDRO CA 94577-0599
2	KAMAN SCIENCES CORP ATTN DASIAC 2 CP 816 STATE ST SANTA BARBARA CA 93102-1479
1	LOGICON RDA ATTN G P GANONG PO BOX 9377 ALBUQUERQUE NM 87119
1	LOGICON RDA ATTN B LEE 6053 W CENTURY BLVD LOS ANGELES CA 90045
1	LOCKHEED MIS & SPACE CO ATTN J J MURPHY DEPT 81 11 BLDG 154 PO BOX 504 SUNNYVALE CA 94086
2	SCIENCE CTR ROCKWELL INTRNTL CORP ATTN DR S CHAKRAVARTHY DR D OTA 1049 CAMINO DOS RIOS THOUSAND OAKS CA 91358
1	METACOMP TECHNOLOGIES INC ATTN S CHAKRAVARTHY 650 WESTLAKE BLVD SUITE 203 WESTLAKE VILLAGE CA 91362
1	ORLANDO TECHNOLOGY INC ATTN D MATUSKA 60 SECOND ST BLDG 5 SHALIMAR FL 32579
4	S CUBED DIV OF MAXWELL LABS INC ATTN TECH LIB R DUFF K PYATT J BARTHEL PO BOX 1620 LA JOLLA CA 92037-1620

NO. OF COPIES	ORGANIZATION
1	SAIC ATTN J GUEST 2301 YALE BLVD SE SUITE E ALBUQUERQUE NM 87106
1	SUNBURST RECOVERY INC ATTN DR C YOUNG PO BOX 2129 STEAMBOAT SPRINGS CO 80477
1	SVERDRUP TECHNOLOGY INC ATTN RF STARR PO BOX 884 TULLAHOMA TN 37388
1	S CUBED DIV OF MAXWELL LABS INC ATTN JAMES SEVIER 2501 YALE BLVD SE ALBUQUERQUE NM 87106
3	SRI INTERNATIONAL ATTN DR GR ABRAHAMSON DR J GRAN DR B HOLMES 333 RAVENWOOD AVE MENLO PARK CA 94025
1	TRW BALLISTIC MISSILE DIV ATTN H KORMAN MAIL STATION 526 614 PO BOX 1310 SAN BERNADINO CA 92402
1	BATTELLE TWSTIAC 505 KING AVENUE COLUMBUS OH 43201-2693
1	THERMAL SCIENCE INC ATTN R FELDMAN 2200 CASSENS DR ST LOUIS MO 63026
2	DENVER RSRCH INSTITUTE ATTN J WISOTSKI TECH LIB PO BOX 10758 DENVER CO 80210

NO. OF COPIES	ORGANIZATION
1	STATE UNIV OF NEW YORK MCHNCL & AEROSPACE ENGRNG ATTN DR PEYMAN GIVI BUFFALO NY 14260
2	UNIV OF MARYLAND INST FOR ADV COMP STUDIES ATTN L DAVIS G SOBIESKI COLLEGE PARK MD 20742
1	CALIFORNIA INSTITUTE OF TECHNOLOGY ATTN T J AHRENS 1201 E CALIFORNIA BLVD PASADENA CA 91109
1	STANFORD UNIV ATTN DR D BERSHADER DURAND LABORATORY STANFORD CA 94305
1	UNIV OF MINNESOTA AHPCRC ATTN DR TAYFUN E TEZDUYAR 1100 WASHINGTON AVE SO MINNEAPOLIS MN 55415
3	SOUTHWEST RSRCH INSTITUTE ATTN DR C ANDERSON S MULLIN A B WENZEL PO DRAWER 28255 SAN ANTONIO TX 78228-0255

NO. OF
COPIES ORGANIZATION

ABERDEEN PROVING GROUND

1 CDR USATECOM
ATTN: AMSTE-TE-F, L TELETSKI

1 CDR USATHAMA
ATTN: AMSTH-TE
APG-EA

1 CDR USATC
ATTN: STEC-LI

27 DIR USARL
ATTN: AMSRL-SC-C, C NIETUBICZ
AMSRL-SC-CC,
C ELLIS
D HISLEY
P COLLINS
T KENDALL
R SHEROKE
AMSRL-SC-I, W STUREK
AMSRL-SC-S, R PEARSON
AMSRL-SL-CM, E FIORVANTE
AMSRL-WT-TB,
R FREY
J STARKENBERG
K BENJAMIN
W LAWRENCE
T DORSEY
R LOTTERO
J CONDON
L FERGUSON
C MERMAGEN
A MIHALCIN
P MULLER
R LOUCKS
S SCHRAML
J SULLIVAN
AMSRL-WT-PB,
P PLOSTINS
P WEIHNACHT
B GUIDOS
AMSRL-WT-TC, K KIMSEY

USER EVALUATION SHEET/CHANGE OF ADDRESS

This Laboratory undertakes a continuing effort to improve the quality of the reports it publishes. Your comments/answers to the items/questions below will aid us in our efforts.

1. ARL Report Number/Author ARL-CR-309 (Dick) Date of Report October 1996

2. Date Report Received _____

3. Does this report satisfy a need? (Comment on purpose, related project, or other area of interest for which the report will be used.) _____

4. Specifically, how is the report being used? (Information source, design data, procedure, source of ideas, etc.) _____

5. Has the information in this report led to any quantitative savings as far as man-hours or dollars saved, operating costs avoided, or efficiencies achieved, etc? If so, please elaborate. _____

6. General Comments. What do you think should be changed to improve future reports? (Indicate changes to organization, technical content, format, etc.) _____

CURRENT ADDRESS

_____
Organization

_____
Name

_____
Street or P.O. Box No.

_____
City, State, Zip Code

7. If indicating a Change of Address or Address Correction, please provide the Current or Correct address above and the Old or Incorrect address below.

OLD ADDRESS

_____
Organization

_____
Name

_____
Street or P.O. Box No.

_____
City, State, Zip Code

(Remove this sheet, fold as indicated, tape closed, and mail.)

(DO NOT STAPLE)

DEPARTMENT OF THE ARMY

OFFICIAL BUSINESS

NO POSTAGE
NECESSARY
IF MAILED
IN THE
UNITED STATES

BUSINESS REPLY MAIL
FIRST CLASS PERMIT NO 0001,APG,MD

POSTAGE WILL BE PAID BY ADDRESSEE

DIRECTOR
US ARMY RESEARCH LABORATORY
ATTN AMSRLWT TB
ABERDEEN PROVING GROUND MD 21005-5066